

Structural and kinetic characterisation of cardiomyopathy
associated mutations in troponin C

Thesis submitted for the degree of Doctor of Philosophy at the
University of Leicester

By

Khawla Abd Al-Kareem Kasar

Department of Molecular and cell Biology

College of Medicine, Biological sciences and Psychology

September 2017

Abstract

Cardiovascular diseases are the leading cause of illness and death worldwide. Many heart diseases are due to the impairment of cardiac regulatory mechanisms such as TnC Ca^{2+} -mediated regulation of cardiac muscle contraction. To date a number of Troponin C mutations have been linked to several cardiomyopathies diseases. In this thesis, we aimed to investigate the following troponin C mutations Y5H, A8V, A31S, E59D, D75Y, C84Y, D145E, and I148V which have been shown to cause familial hypertrophic (HCM) and dilated (DCM) cardiomyopathies. We used various structural, biochemical and kinetic methods to assess the impact of these mutations on troponin function and structure. Transient kinetics were used to assess the effect of these mutations on the equilibrium distribution and kinetics of transitions between different thin filament regulatory states. Overall, TnC mutations had little impact on the secondary structure of TnC however HSQC experiments revealed both local and long range structural changes. Our data revealed that cTnC mutations affected various interactions between thin filament components including the interaction of troponin complex with tropomyosin and actin-tropomyosin. More importantly all TnC mutations reduced the proportion of the thin filament in the blocked state and the rate constant of Ca^{2+} dissociation from thin filaments. These findings suggest that mutations in TnC have the potential to affect several allosteric transitions. Consequently, while changes in steps critical for muscle relaxation have been found, mutations in TnC have the potential to affect more than one step in the allosteric network of interactions involved in the regulation of muscle contraction.

Acknowledgements

First of all, I would like to express my deepest gratitude to my supervisor Dr Mohammed El-Mezgueldi for the opportunity to work in his lab, for his countless hours of guidance, for his encouragement throughout the research and writing of this thesis.

I would like to express my gratitude to my PhD committee Dr Sue Schackeleton and Prof Russell Wallis for their support. Also, I would like to thanks Dr Frederick Muskett for his help with the NMR experiments, Luca Mureddu, Geerten W. Vuister for their help with the NMR data analysis and Dr Jaswir Basran for her help with the ITC experiments.

Many thanks to all members of lab 2/11 in particular Saeed Asiri and Manaf Guma.

Thanks to all my friends. I am eternally grateful to my best friends Hanaa Al-Mahmmodi, Ibteehal Al-shemirty, Rusule Al-Rubbay, and Qais Ismael for pleasant time we spent together, the experience they selflessly shared with me, and they are forever families to me.

I cannot begin to think of how grateful I am to have such wonderful and understanding parents and families. Special thanks to my mother, my father, my brother Mohaned, my sister's khamail, Ebteehal, Hind, rasha, saja, Mariam and Linda.

Last but not least, I would like to thank Leicester University for hosting me and Al-Nahrain University (Iraq-Baghdad) for their generous financial support.

Khawla Kasar

Leicester university/England

September 2017

List of Abbreviations

ADP	Adenosine diphosphate
AP	Atrial Pressure
AV	Atrioventricular Valves
CD	Circular Dichroism
cTnC	Cardiac Troponin C
cTnI	Cardiac Troponin I
cTnT	Cardiac Troponin T
DCM	Dilated Cardiomyopathy
DNA	Deoxyribonucleic Acid
DTT	Dithiothreitol
EDTA	Ethylene diamine tetra-acetic acid
EGTA	Ethylene glycol tetra acetic acid
EDTA	Ethylene diamine tetra acetic acid
F-actin	Filamentous actin
G-actin	Globular actin
HCM	Hypertrophic Cardiomyopathy
IPTG	IsoPropyl-beta-d-ThioGalactopyranside
ITC	Isothermal titration calorimetry
K_B	Equilibrium constant between blocked and closed states
K_T	Equilibrium constant between closed and open states
LAP	Left Atrial Pressure
LV	Left Ventricle
LVP	Left Ventricular Pressure
MOPS	3-(n-Morpholino) Propane sulfonic Acid
NMR	Nuclear Magnetic Resonance
PBP	Phosphate binding protein

PCR	Polymerase Chain Reaction
PIA	N-(1-pyrenyl)-iodoacetamide
Pi	Inorganic phosphate
RyR	Ryandine Receptors
S1	Myosin subfragment1
SDS	Sodium Dodecyl Sulfate
Tm	Tropomyosin
Tn	Troponin

Units/Symbol

Units/Symbols

A	Absorbance
Å	Angstrom ($1\text{Å} = 1 \times 10^{-10}$)
bp	Bas pairs
g	gram
h	hour
kDa	Kilo dalton
l	liter
M	molar
min	minute
°C	Degrees Celsius
OD	Optical density
rpm	Revolutions per minute
s	second
EGF	Absorption
EMT	wavelength

Table of content

LIST OF ABBREVIATIONS	III
CHAPTER 1	1
INTRODUCTION	1
1.1 Human cardiac structure and function.....	2
1.1.1 Anatomy of the human heart.....	2
1.1.2 Function of the human heart	4
1.1.3 Calcium and Excitation-contraction coupling.....	6
1.2 Inherited Heart disease	8
1.2.1 Hypertrophic cardiomyopathy (HCM)	10
1.2.2 Dilated cardiomyopathy (DCM).....	13
1.3 How do mutations lead to cardiac remodeling?	14
1.4 Structure of the sarcomere	16
1.4.1 Thick filament (myosin)	18
1.4.2 Thin filament	21
1.4.2.1 Actin.....	21
1.4.2.2 Tropomyosin.....	24
1.4.2.3 The troponin complex.....	27
1.4.2.3.1 Troponin T (TnT)	29
1.4.2.3.2 Troponin I (TnI)	31
1.4.2.3.3 The calcium binding subunit troponin C (TnC).....	34
1.4.2.3.3.1 Troponin structure	35
1.4.2.3.3.2 Function of troponin C	37
1.5 The molecular basis of regulation of striated muscle contraction	40
1.5.1 The mechanism of striated muscle contraction	40
1.5.2 Regulation of muscle contraction.....	42
1.5.2.1 The role of calcium in the regulation.....	42
1.5.2.2 Thin filament switches between three different states.....	43
1.5.2.3 The role of troponin C in the contraction heart muscle	44
1.5.2.4 The role of TnC in the relaxation of the heart	46
1.6 TnC mutations	47
1.6.1 Y5H	49
1.6.2 A8V	50
1.6.3 A31S.....	51
1.6.4 E59D	52
1.6.5 D75Y	53
1.6.6 C84Y.....	55
1.6.7 D145E	56
1.6.8 I148V	58
1.7 Aim of study	58
CHAPTER 2	61
2.1 Design the mutations	62
2.1.1 Primer Design	62
2.1.2 PCR	62
2.1.3 Transformation.....	62
2.1.4 Plasmid Mini Preps.....	63
2.2 Protein purification from tissues.....	63
2.2.1 Cardiac myosin preparation	63

2.2.2	Preparation of sheep cardiac muscle acetone powder	64
2.2.3	Cardiac F-actin preparation	65
2.2.3.1	Preparation of N-(1-pyrenyl)-iodoacetamide-labelled cardiac F-actin	65
2.2.4	Preparation of cardiac troponin complex.....	66
2.2.5	Preparation of cardiac tropomyosin (cTm)	67
2.3	Expression and purification of human troponin complex	68
2.3.1	Purification of troponin T (TnT) and troponin I (TI).....	68
2.3.2	Purification of troponin C (TnC).....	69
2.3.3	Reconstitution of troponin complex	69
2.4	General assays	70
2.4.1	The Actomyosin ATPase assay.....	70
2.4.2	Determination of the secondary structure of cTnC mutants by Circular Dichroism	71
2.4.3	Isothermal titration calorimetry (ITC)	72
2.5	Transient State Kinetic Measurements	73
2.5.1	Kinetics of Myosin subfragment-1 (S1) Binding to PIA-actin thin filament was used to determine the equilibrium constant between thin filament blocked and closed states	73
2.5.2	Calcium Dissociation Kinetics Measurements	74
2.6	NMR Spectroscopy	75
2.6.1	Preparation of minimal media.....	75
2.6.2	Expression of troponin C ¹⁵ N	75
CHAPTER 3 PURIFICATION AND RECONSTITUTION OF CARDIOMYOPATHY ASSOCIATED TROPONIN C MUTANTS INTO A STABLE AND FUNCTIONAL TROPONIN ITC TERNARY COMPLEX.77		
3.1	Introduction.....	78
3.2	Results	79
3.2.1	Mutagenesis	79
3.2.2	Test expression.....	80
3.2.3	Reconstitution of Troponin complex.....	81
3.2.4	Circular Dichroism of TnC mutations.....	86
3.2.4.1	Effect of troponin C mutations on the secondary structure of troponin C.....	86
3.2.4.2	Effect of TnC mutations on the secondary structure of troponin complex	90
3.2.5	Effect of hcTnC mutations on the activation and inhibition of the actomyosin ATPase by the troponin complex.....	94
3.3	Discussion	98
3.3.1	The effect of HCM and DCM on the secondary structure	99
3.3.1.1	The effect of HCM and DCM on the secondary structure of TnC	99
3.3.1.2	The effect of the HCM and DCM on the structure of troponin complex.....	100
3.3.2	The effect of the TnC mutations on the steady state actomyosin ATPase.....	101
CHAPTER 4 103		
4.1	Introduction.....	104
4.2	Result.....	106
4.2.1	Impact of HCM and DCM cTnC mutations on the kinetics of calcium dissociation.	106
4.2.1.1	Effect of TnC mutations on the thin filament-switch between blocked and closed states	113
4.2.2	Effect of TnC mutations on Troponin binding to tropomyosin and actin-tropomyosin.	117
4.2.2.1	Effect of TnC mutations on the TnC-TnI binding.....	117
4.2.2.2	Effect of TnC mutations on the troponin tropomyosin binding.....	122
4.2.2.3	Effect of TnC mutations on the binding of troponin complex to thin filaments.....	126
4.3	Discussion	130
4.3.1	Cardiac troponin C mutations alter the Ca ²⁺ binding affinity.	131

4.3.2 Impact of TnC mutations on the transition between the blocked and closed state	132
4.3.3 cTnC mutations affect the binding between TnC and the partners	134
CHAPTER 5	136
5.1 Introduction.....	137
5.2 Results	139
5.2.1 Preparation of NMR sample	139
5.2.2 Effect of the cTnC mutations on the troponin C structure	140
5.2.2.1 HSQC experiment.....	140
5.2.2.2 Mutations located in N-helix	141
5.2.2.3 Mutations located in the Ca ²⁺ binding sites.....	146
5.2.2.4 Flexible linker mutation	152
5.2.2.5 Mutations located in Ca ²⁺ and Mg ²⁺ binding sites.....	155
5.3 Discussion.....	159
CHAPTER 6 GENERAL DISCUSSION.....	162
6.1 Introduction.....	163
6.2 Investigation of the effects of troponin C mutations on the structure of troponin C and the troponin complex.....	164
6.3 Effect of troponin C mutations on the interaction between the components of the thin filament macromolecular complex.	165
6.4 Effect of mutations on the kinetics of Ca ²⁺ dissociation and the transition between the blocked and closed states.	166
6.5 Conclusion	168

List of Figures

Figure 1.1 Internal View of human heart	3
Figure1.2: Cardiac cell types.....	4
Figure 1. 3: Diagram of the heart during the diastole and systole phases of the cardiac cycle.	5
Figure1.4: Structures involved in Ca ²⁺ cycling.	8
Figure 1.5: Three major patterns of ventricular remodelling.....	10
Figure 1. 6: The hypertrophic hear.....	12
Figure 1.7: Dilated heart.....	14
Figure 1. 8: Structure of sarcomere.	18
Figure1.9: Structure of myosin.....	20
Figure1.10: Thin filament structure.	22
Figure 1. 11: Structure of G-actin.	23
Figure 1.12: Micrograph of actin filaments.....	24
Figure1.13: crystal structure of tropomyosin.....	26
Figure 1.14: Space-filling model of cardiac troponin complex.....	28
Figure 1.15: The interaction between the components of cardiac thin(A) filament and structure of troponin complex (B).....	29
Figure 1. 16: The position of cTnl in the crystal structure of troponin complex.	33
Figure 1. 17: A ribbon digram of the TnC structure.....	35
Figure 1.18: Troponin C structure.	37
Figure 1. 19: Ribbon structure of troponin (A) and conformational change of troponin during the contractions of muscle (B).....	39
Figure 1. 20: Schematic diagram of the McKillop-Geeves three-state regulatory model of the thin filament.	44

Figure 1.21: A diagram illustrating the various steps in thin filament cooperative allosteric activation that could be affected by TnC mutations.....	48
Figure 1. 22: Location of cTnC mutations in the 3D structure of troponin C	49
Figure 3.1: Agarose gel of the products of a PCR reaction using the various hcTnC clones.....	80
Figure 3.2: Test expressions.	81
Figure 3.3: TnT purification.	82
Figure 3.4: TnI Purification.	83
Figure 3.5: TnC purification.	84
Figure 3.6: Size exclusion chromatography of the reconstituted troponin complex.	85
Figure 3.7: Characterization of secondary structure TnC DCM mutants by circular dichroism.	87
Figure 3.8: Characterization of secondary structure of TnC HCM mutants by circular dichroism.	87
Figure 3.9: Thermal denaturation of TnC WT, HCM, and DCM mutations.....	89
Figure 3.10: Characterization of secondary structure of TnC WT and DCM mutates reconstituted in troponin complex.	91
Figure 3.11: Characterization of secondary structure of TnC WT and HCM mutations reconstituted in troponin complex.	91
Figure 3.12: CD measurements of the thermal denaturation of TnC WT and DCM mutants reconstituted in troponin complex.	92
Figure 3.13: First-derivative profiles for CD data measurements of thermal denaturation of TnC WT and HCM mutants reconstituted in troponin complex.....	93
Figure 3.14: Effect of the HCM and DCM cTnC mutations on the ability of the troponin complex to activate the Actin-Tm activated Myosi-S1 ATPase in presence of Ca ²⁺	95
Figure 3.15: Effect of the HCM and DCM cTnC mutations on the ability of the troponin complex to inhibit the Actin-Tm activated Myosin-S1 ATPase in absence of Ca ²⁺	96
Figure 3.16: The maximal activation and inhibition obtained for each troponin complex obtained by reconstitution with each hcTnC mutant.	97
Figure 4.1: Characterization of the Ca ²⁺ dissociation rate from troponin C.	108
Figure 4.2: Characterization of the Ca ²⁺ dissociation from troponin complex.	109
Figure 4.3: Characterization of the Ca ²⁺ dissociation rates from thin filament.....	110
Figure 4.4: Characterization of the Ca ²⁺ dissociation from thin filament in presence of S1.	111
Figure 4.5: Ca ²⁺ dissociation fluorescence obtains by Quoin-2.	112
Figure 4.6: Ca ²⁺ dissociation fluorescence obtains by Quoin-2.	112
Figure 4.7: Ca ²⁺ dissociation fluorescence obtains by Quoin-2.	112
Figure 4.8: Determination of KB of HCM and DCM cTnC mutations reconstituted in troponin complex.	115
Figure 4.9: Comparison of thin filament switching parameter KB of cTnC mutations.	116
Figure 4.10: TnC binding to TnI by isothermal titration calorimetry(ITC). Titration of Troponin C WT with troponin I in presence 1mM CaCl ₂	119
Figure 4.11: TnC binding to TnI by isothermal titration calorimetry (ITC).....	119
Figure 4.12: TnC binding to TnI by isothermal titration calorimetry(ITC).	120
Figure 4.13: TnC binding to TnI by isothermal titration calorimetry (ITC).....	121
Figure 4.14: Troponin complex binding to Tropomyosin by isothermal titration calorimetry(ITC).	123
Figure 4.15 Troponin complex binding to Tropomyosin by isothermal titration calorimetry(ITC):	123
Figure 4.16: Troponin complex binding to Tropomyosin by isothermal titration calorimetry(ITC).	124
Figure 4.17: Troponin complex binding to Tropomyosin by isothermal titration calorimetry(ITC).	125
Figure 4.18 Troponin complex binding to actin-Tm thin filament by isothermal titration calorimetry (ITC).127	
Figure 4.19: Troponin complex binding to actin-Tm thin filament by isothermal titration calorimetry (ITC).	127
Figure 4.20 Troponin complex binding to actin-Tm thin filament by isothermal titration calorimetry (ITC).128	
Figure 4.21: Troponin complex binding to actin.Tm thin filament by isothermal titration calorimetry (ITC).	128
Figure 5.1: size exclusion chromatography of cardiac troponin C.	139
Figure 5.2: 2D ¹ H- ¹⁵ N HSQC NMR spectra of cardiac TnC WT.	141
Figure 5.3: Location of Y5H and A8V in the structure of hcTnC.	142

Figure 5.4: 2D ^1H - ^{15}N HSQC NMR spectra of cardiac TnC-Y5H.	142
Figure 5.5: Chemical shift differences between TnC-Y5H and TnC-WT.....	143
Figure 5.6: Mapping Chemical Shift Perturbations induced by Y5H mutation in hcTnC	143
Figure 5.7: 2D ^1H - ^{15}N HSQC NMR spectra of cardiac TnC-A8V.	144
Figure 5.8: Mapping of TnC-A8V on the TnC-WT	145
Figure 5.9: Mapping Chemical Shift Perturbations induced by A8V mutation in hcTnC	145
Figure 5.10: Location of A31S, E59D and D75Y in the structure of hcTnC.	146
Figure 5.11: 2D ^1H - ^{15}N HSQC NMR spectra of cardiac TnC-A31S.	147
Figure 5.12: Mapping of TnC-A31S on the TnC-WT.....	147
Figure 5.13: Mapping Chemical Shift Perturbations induced by A31S mutation in hcTnC	148
Figure 5.14: 2D ^1H - ^{15}N HSQC NMR spectra of cardiac TnC-E59D.	149
Figure 5.15: Mapping of TnC-E59D on the TnC-WT	149
Figure 5.16: Mapping Chemical Shift Perturbations induced by E59D mutation in hcTnC	150
Figure 5.17: 2D ^1H - ^{15}N HSQC NMR spectra of cardiac TnC-D75Y.	151
Figure 5.18: Mapping of TnC-D75Y on the TnC-WT	151
Figure 5.19: Mapping Chemical Shift Perturbations induced by D75Y mutation in hcTnC	152
Figure 5.20: Location of C84Y in the structure of hcTnC.....	153
Figure 5.21: 2D ^1H - ^{15}N HSQC NMR spectra of cardiac TnC-C84Y.	153
Figure 5.22: Mapping of TnC-C84Y on the TnC-WT.....	154
Figure 5.23: Mapping Chemical Shift Perturbations induced by C84Y mutation in hcTnC	154
Figure 5.24: Location of D145E and I148V in the structure of hcTnC.	155
Figure 5.25: 2D ^1H - ^{15}N HSQC NMR spectra of cardiac TnC-D145E.	156
Figure 5.26: Mapping of TnC-D145E on the TnC-WT	156
Figure 5.27: Mapping Chemical Shift Perturbations induced by D145E mutation in hcTnC	157
Figure 5.28: 2D ^1H - ^{15}N HSQC NMR spectra of cardiac TnC-I148V.	158
Figure 5.29: Mapping of TnC-I148V on the TnC-WT.....	158
Figure 5.30: Mapping Chemical Shift Perturbations induced by I148V mutation in hcTnC.	159
Figure 5.31: Sum of the residues with a Delta shifts above the threshold of 0.1ppm.	161

List of tables

Table 3.1 Melting point temperature(mid-point) of troponin C mutants in isolated troponin C.	88
Error! Bookmark not defined.	
Table 3.2: Melting point temperature(mid-point) of troponin C mutants reconstituted in troponin complex	93
Table 3.3: Maximal and activation and inhibition.	97
Table 4.1: The rate of Ca^{2+} dissociation.....	107
Table 4.2: a Summary of K_b values for thin filaments reconstituted with hcTnC mutants.....	116
Table 4.3: Binding parameters between troponin C WT and HCM and DCM mutations and cTnl.	121
Table 4.4: Binding parameters of troponin to tropomyosin.	125
Table 4.5: Binding parameters of troponin to thin filament	129

Chapter 1

Introduction

1.1 Human cardiac structure and function.

1.1.1 Anatomy of the human heart.

The heart is a hollow organ consisting of four chambers: the right atrium, the left atrium, the right ventricle and the left ventricle (figure 1.1). It functions as a circulatory pump which provide oxygen and nutrients to the various body tissues by circulating the blood throughout the body. Structurally, the heart muscle is inhomogeneous. The atria are smaller than the ventricles and have thinner, less muscular walls than the ventricles. The size of the two sides of the heart is different because the function of each side is different. The chambers on the right side are smaller than the chambers in the left side because the right side of the heart maintains pulmonary circulation to the nearby lungs while the left side of the heart pumps blood all the way to the extremities of the body in the systemic circulatory loop. Functionally, the right ventricle is responsible to send blood to the lungs to be re-oxygenated. The blood in the lungs returns to the heart through the pulmonary veins. From the pulmonary veins, blood enters the heart again in the left atrium. Immediately, after the left atrium is filled with re-oxygenated blood, the blood is pushed into the left ventricle (LV) then the left ventricle pump drives the blood to the rest of the body, as show in figure 1.1.

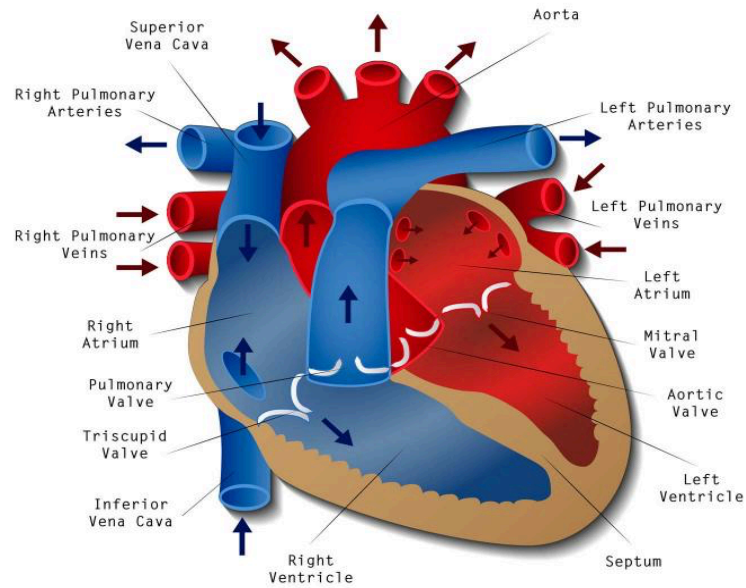


Figure 1.1 Internal View of the human heart.

In the fetal heart, progenitor cells differentiate into a primitive tubular heart that forms the adult heart. The adult heart consists of several cell types, maintaining structural, mechanical, electrical and functional integrity of the heart. As shown in figure 1.2, these cells are Endothelial cells which form the inner lining of cardiac blood vessels, fibroblasts forming extracellular matrix, which provides mechanical support to the heart, Atrial cardiomyocytes which contribute to the contraction of the atrium, Conduction cells which create electrical impulses for cardiac contractility, Ventricular cardiomyocytes are involved in contractility of the ventricles, and finally the smooth muscle cells which contribute to vasculatures (Moretti *et al.*, 2006). Recently it has been established that the upregulation of fetal genes can be used as a marker of pathological remodelling of the heart (Nandi & Mishra, 2015). However, to date the role of genetic reprogramming in cardiac remodelling (inherited Heart disease) remains poorly understood.

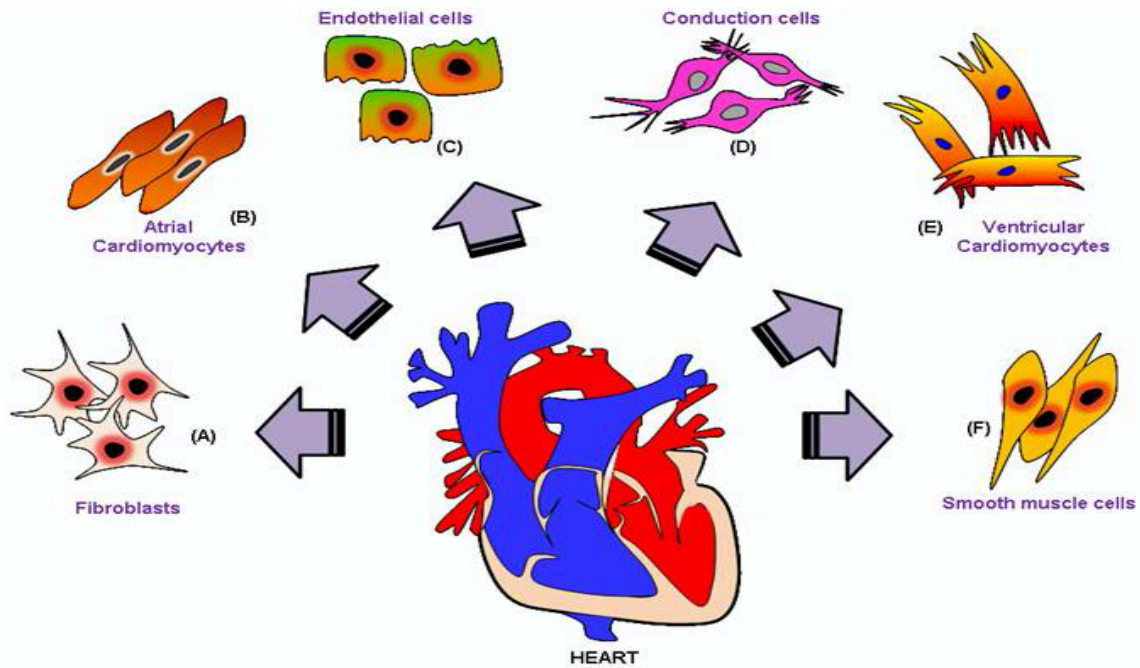


Figure 1.2: Cardiac cell types.

Schematic presentation of various cardiac cell types. (A) Fibroblasts (B) Atrial (C) Endothelial cells (D) Conduction cells (E) Ventricular (F) Smooth muscle cells (Nandi & Mishra, 2015).

1.1.2 Function of the human heart

The human heart beats nonstop about 3 billion times throughout an average human life span by repeated rhythmic contractions. These repeating contractions are controlled by a series of electrical impulses that travel through cardiac pacemaker cells. The pacemaker of the heart is the starting of the conduction system of the heart. It is a small bundle of cells known as the sinoatrial (SA) node and located in the wall of the right atrium inferior to the superior vena cava. The SA node is responsible for controlling the pace of the heart as a whole and promptly signals the atria to contract. The SA node send the signal to another mass of conductive tissue known as the atrioventricular (AV) node which is situated in the lower right atrium. The impulse travels from SA node to the AV node within 50 ms. This slow conduction through the AV node causes the atria to contract before the ventricles.

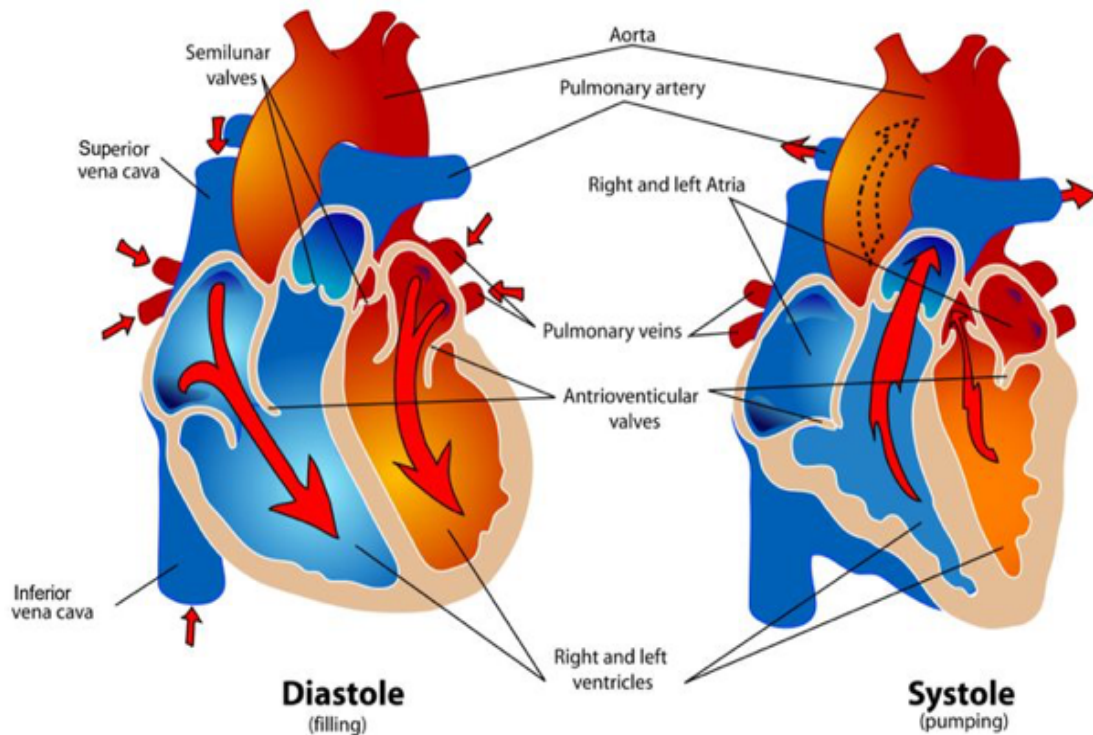


Figure 1.3: Diagram of the heart during the diastole and systole phases of the cardiac cycle.

The cardiac cycle begins with atrial systole and progresses to ventricular systole, atrial diastole, and ventricular diastole, when the cycle begins again. <https://fthmb.tqn.com>

An illustration of the phases of the cardiac cycle is shown figure 1.3. The cardiac cycle is the sequence of events that occurs when the human heart beats. It starts with contraction of the atria and ends with ventricular relaxation. This cycle includes two phases named: the systole and the diastole. The Systole is the time when the heart undergoes contraction to pumps blood into circulation while the diastole is the time when the heart undergoes relaxation to fill the chambers with blood. Thus, one cardiac cycle is completed when the heart chambers fill with blood and blood is then pumped out of the heart. Both the atria and ventricles undergo systole and diastole. This mechanism

has to be regulated and coordinated to ensure blood is pumped efficiently to the body. Disorders of the heart's cycle can cause problems with the heart's ability to function effectively. The key mechanism that control the alternating contractions and relaxations of the heart is a transient binding of Ca^{2+} to a complex of protein, troponin ITC and a series of structural changes that spreads throughout the contractile apparatus (described in more detail later).

1.1.3 Calcium and Excitation-contraction coupling

Excitation-contraction coupling (E-C) is the process responsible for the regulation of the heart on a beat to beat basis (Bers, 2002) . Contraction of the myocyte is initiated by the depolarization of the cell electrically. The depolarization is produced by the action potential due to the rapid opening of Na^+ channels in the T-tubules and leads to the opening of the voltage sensitive Ca^{2+} channel $I_{\text{Ca, L}}$ (Bers, 2002). The resulting entry of a small amount of Ca^{2+} ($\sim 10 \mu\text{M}$) leads to the binding of Ca^{2+} to ryanodine receptors (RyRs) on the sarcoplasmic reticulum (SR)(L. M. Delbridge *et al.*, 1996). This binding of the extracellular Ca^{2+} to the RyRs results in a substantial Ca^{2+} release from the SR during a process known as calcium induced calcium release (CICR) in a region of the muscle cell, called the transverse-tubule as shown in Figure 1.4. This large amount of Ca^{2+} is required to increase the free intracellular concentration from the diastolic level of 100 nM to a systolic level of 600 nM because of the high Ca^{2+} buffering capacity of the myocyte (MB Cannell *et al.*, 1995) . The magnitude of the rise of $[\text{Ca}^{2+}]$ depends on the degree to which the SR is filled with Ca^{2+} , which is dependent upon the duration between contractions, (Pinali *et al.*, 2013) the extent of Ca^{2+} binding to various Ca^{2+} protein buffers and uptake into organelles including mitochondria (Eisner *et al.*, 2017) . In fact, free Ca^{2+} accounts for as little as 1% of the total intracellular Ca^{2+} and the majority of Ca^{2+} is bound to

intracellular Ca^{2+} buffers. In cardiac myocytes, Ca^{2+} is buffered predominantly by SERCA2a and myofibrillar TnC and to a less extent by membrane phospholipids, myosin light chains and phosphocreatine in the cytoplasm and parvalbumin, and calsequestrin in the SR. The binding of Ca^{2+} to troponin C in thin filament is an important physiological regulator of contraction and will be discussed in more detail later. This binding leads to conformational changes in the thin filament macromolecular complex and results in cardiac muscle contraction. Conversely, the reuptake of calcium into the SR is mediated by the SR calcium ATPase or eject out of the myocyte by the sodium–calcium exchanger and plasmalemmal Ca^{2+} ATPase. Consequently, the conformational changes of the thin filaments back to the original state as a result of the decrease in the Ca^{2+} concentration and this lead to dissociation of actin-myosin and then relaxation of the heart muscle.

In general, the events that occur during the E–C coupling process are now well established (Eisner *et al.*, 2017). This process results in a Ca^{2+} transient that depends not only on a combination of the properties of Ca^{2+} channels and transporters but also on their precise location and spatial arrangement. In addition, the Ca^{2+} transient can be modulated by various physiological factors to increase or decrease the magnitude of the cardiac contraction.

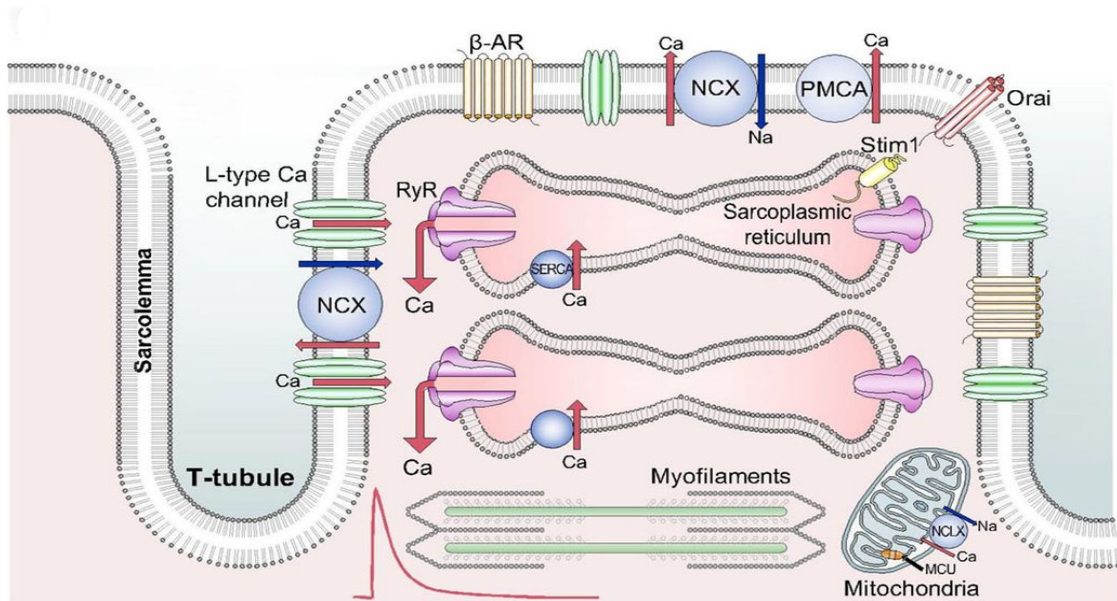


Figure 1.4: Cardiac cellular structures involved in Ca^{2+} cycling.

The figure shows surface membrane, transverse tubule, sarcoplasmic reticulum (SR), and mitochondria, as well as the various channels and transporters mentioned in the text. Calcium enters the cell through the L-type calcium channel (LTCC). This calcium binds to troponin C resulting in activation of contractile proteins. The muscle relaxes when calcium is removed into the sarcoplasmic reticulum by sarcoplasmic reticulum calcium pump (Eisner *et al.*, 2017) .

1.2 Inherited Heart disease

According to the British Heart Foundation, over 600,000 people in the UK are carrying a faulty gene that puts them at a high risk of developing a coronary heart disease or a cardiomyopathy. Cardiomyopathies are fundamental defects of cardiac muscle associated with abnormalities of cardiac wall thickness, chamber size, contraction, relaxation, conduction, and rhythm. The abnormality in genes can be one of the most common risk factor for familial hypertrophic and dilated cardiomyopathies (Ashrafian & Watkins, 2007). To date, many studies established that the mutations in genes encoding sarcomeric proteins have been implicated in the development of familial hypertrophic (HCM) and dilated cardiomyopathies (DCM). Thus, genetic factors can result in changes of the structure of the human heart which are caused by chronic alterations in loading

conditions by a mechanism that result in remodelling of the heart and that remains to be elucidated (Opie *et al.*, 2006).

Remodelling of the human heart can be defined as changes in gene expression, and/or molecular, cellular and interstitial changes that are different clinically from the changes in size, shape and function of the heart produced by cardiac injury. The remodelling process can be influenced by hemodynamic load, neurohormonal activation. Additionally, cardiac remodelling is characterised by three characteristics. Firstly, an increase in the thickness of the chamber's walls, which is due to an increase in the pressure load. Secondly, an irregular hypertrophy due to changes in the volume load which influence cardiomyocyte length. Finally, the last stage of remodelling is due to an increase in the left ventricle volume due to changes in both pressure and volume loads as a result of myocardial infarction (figure 1.5) (Opie *et al.*, 2006) . Although there are many components involved in the remodelling process such as the interstitium, fibroblasts, collagen and coronary vasculature the major cardiac cell involved in the remodelling process is the cardiomyocyte.

There are four major classes of cardiomyopathies. hypertrophic (HCM), dilated (DCM), restrictive (RCM), and arrhythmogenic right ventricular (ARV) cardiomyopathies. These cardiomyopathies are associated with cardiac failure and dysfunction that can lead to cardiovascular morbidity and mortality. Unravelling the genotype-phenotype relationship might provide an essential clue to understanding the disease and help to find the proper treatment (Arad *et al.*, 2002). Here we aimed to investigate the effects of six HCM and six DCM mutations in the cardiac TnC gene to understand how regulation of cardiac contractility is altered.

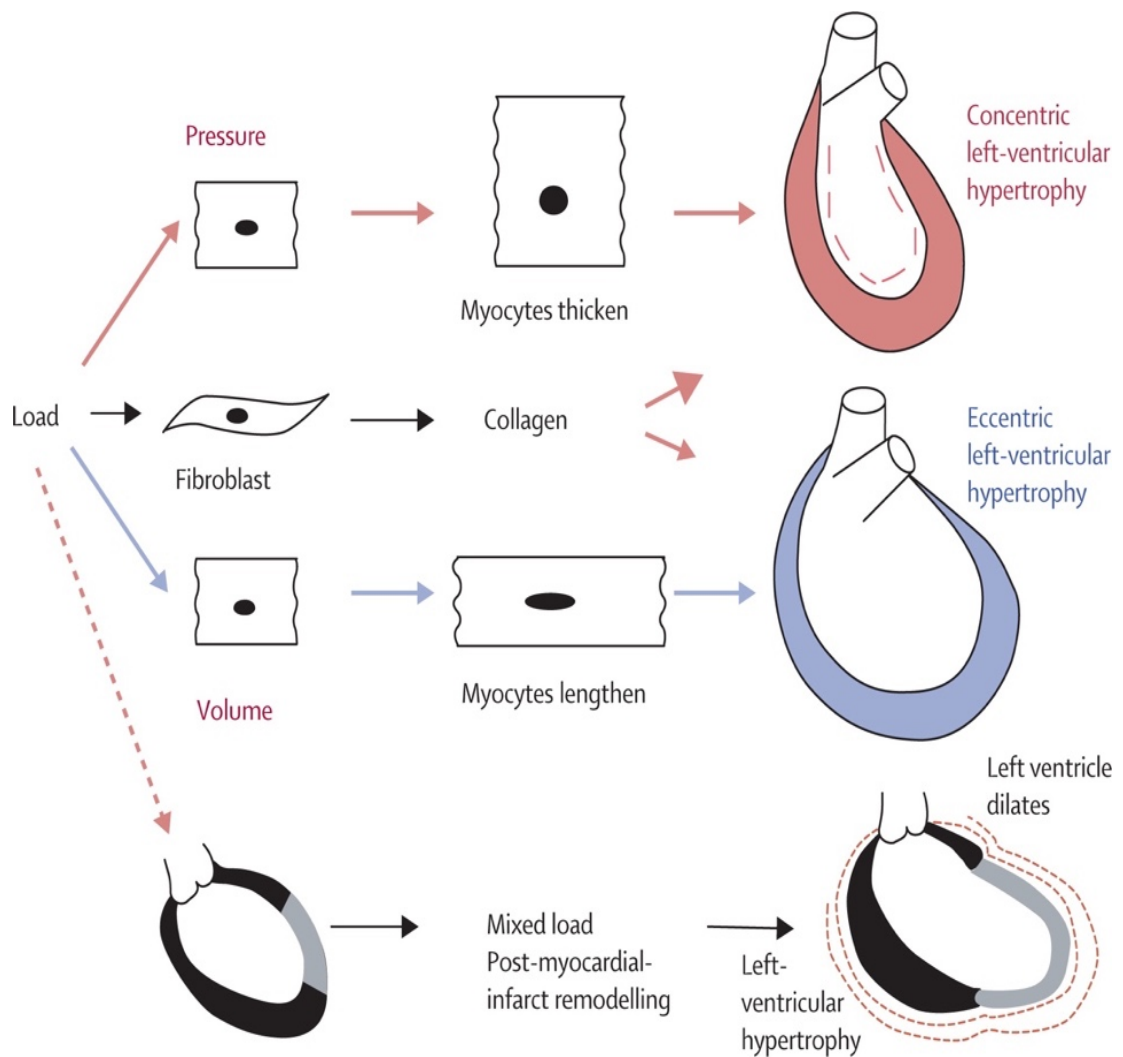


Figure 1.5: Three major patterns of ventricular remodelling.

The patterns display changes in the ventricular architecture that take place during remodelling. The top of the diagram shows concentric left-ventricular hypertrophy because of an increase in cardiomyocyte thickness as a result of increased pressure load (Left ventricle growing inwards represented by dotted). The middle part of the diagram displays eccentric hypertrophy due to cardiomyocyte lengthening as a result of change in the volume load. The final change is post-infarct, when the stretched and dilated infarcted tissue increases the left-ventricular volume with a combined volume and pressure load on the non-infarcted zones (combined effects of concentric and eccentric hypertrophy represented by dotted lines)(Opie *et al.*, 2006b) .

1.2.1 Hypertrophic cardiomyopathy (HCM)

Hypertrophic cardiomyopathy HCM is the major cause of sudden cardiac death in the young (Harada & Morimoto, 2004). It is an inherited cardiac disorder and it is the most

common type with estimated prevalence of 1:500 (0.2 % in the population)(Tardiff, 2005). Genetic studies have established that over 75% of HCM patients screened for protein mutations displayed mutations in 10 different sarcomeric genes (Richard *et al.*, 2003), including those encoding proteins of the troponin complex (Marian, 2008). HCM is generally characterized by left ventricular wall (LVW) thickening causing left ventricular hypertrophy (figure 1.6). The normal thickness of LVW is 12 mm or less. In HCM patients LVW thickness is in general >15 mm and can reach up to 50 mm in extreme hypertrophy cases (Maron *et al.*, 1995). This thickening makes it harder for human heart to pump blood out of heart and around the body. Finally histological examination showed that the observed cardiac hypertrophy was due to cardiomyocyte hypertrophy (that is a substantial increase in the size of cardiomyocytes). Furthermore, cardiomyocytes are normally arranged in a parallel manner. In HCM patients, cellular disarray within the myocardium and interstitial fibrosis are common histopathological features features (Cirino & Ho, 1993).

Patients with hypertrophic cardiomyopathy have a variable presentation including shortness of breath, chest pain, palpitations, light headedness and fainting. These conditions can develop as a result of having HCM to abnormal heart rhythms, or arrhythmias, including heart block and endocarditis. This disease can present at any age. Also, few people do not present with any symptoms. A few patients die suddenly without any previous symptoms.

Although there is a substantial amount of studies that have been carried out in order to understand how sarcomeric protein mutations would lead to hypertrophic cardiomyopathy; the full biochemical, molecular and cellular changes triggered by

sarcomeric protein gene mutations that lead to HCM remain unclear. The mechanism linking changes in the gene and protein to the observed cellular and whole organ changes remain incompletely defined. Bonne et al suggested that the amount of functional protein could be reduced (haploinsufficiency) by gene mutations that inactivate an allele, or alternatively by creating a mutant protein that either interferes with normal function (dominant negative) or assumes a new function (Bonne *et al.*, 1998). Thus, this reduction in the amount of functional protein could result in an imbalance in the stoichiometry of thick to thin filament components leading to sarcomeric functional and structural changes. Other evidence from Biophysical studies showed that HCM mutant proteins alter thin and thick filaments biochemical properties in the sarcomere. Interestingly several studies demonstrated an increase in calcium sensitivity resulting in a proportional increase in tension generation and ATPase activity at a given calcium concentration in HCM mutations affecting myosin, troponin T, C, and I or myosin light chain proteins. In other word, the cardiac sarcomeric mutations could change the function of the sarcomere by changing the amount of force generated by cardiomyocyte.

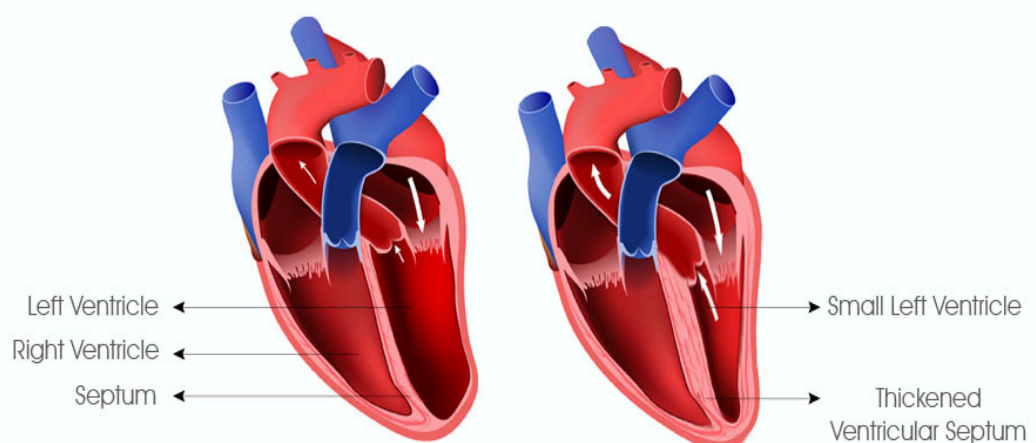


Figure 1.6: The hypertrophic heart.

The figure shows the normal heart versus a hypertrophic cardiomyopathy (HCM) heart..

www.medinda.net

1.2.2 Dilated cardiomyopathy (DCM)

Dilated cardiomyopathy DCM is considered as a major cause for morbidity and mortality among cardiovascular diseases (Mestroni et al., 1999). However, the disease prevalence is not as high as in HCM (1:5000). According to the American Heart Association up to one-third of DCM patients inherit the disease from their parents. DCM can be defined as a heart disease which is characterized by an enlargement of the left ventricle (figure 1.7) and impaired contraction of left or left and right ventricles (Harada & Morimoto, 2004; Tsien, 1983). Frequently, the disease starts in the left ventricle and then often spreads to the right ventricle and then to the atria. Thus, the heart muscle becomes stretched and thin and the heart is unable to pump blood around the human body efficiently.

The most common symptoms of DCM include shortness of breath, fatigue and swelling of the ankles, feet, legs, abdomen and veins in the neck. DCM also can lead to heart valve problems, arrhythmias (irregular heartbeats) and blood clots in the heart.

In term of Pathophysiological mechanisms, it was hypothesised that DCM would impair cardiac function and lead to remodelling of the heart because of the defective force transmission (Kamisago et al., 2000). The intracellular scaffolding supplied by cytoskeletal proteins (such as desmin and dystrophin), is essential for force transmission from the sarcomere to the extracellular matrix; and it is fundamental for the protection of myocytes from extrinsic mechanical stress. Defects in these cytoskeletal proteins have been suggested to lead to DCM by reducing force transmission and/or resistance to mechanical stress (Franz et al., 2001). Another hypothesis suggested that specific mutations in the mitochondrial DNA which are believed to alter the energy production could lead to DCM (Franz et al., 2001). Finally, several mutations have been identified in

cardiac contractile and regulatory proteins and are thought to cause DCM by affecting the amount or kinetics of force production. As mentioned previously, here we aimed to investigate the effect of eight mutations (4 associated with HCM and 4 associated with DCM) in the Ca^{2+} regulatory subunit cardiac troponin C (cTnC), which is an essential part of the sarcomere, on the dynamics of thin filament.

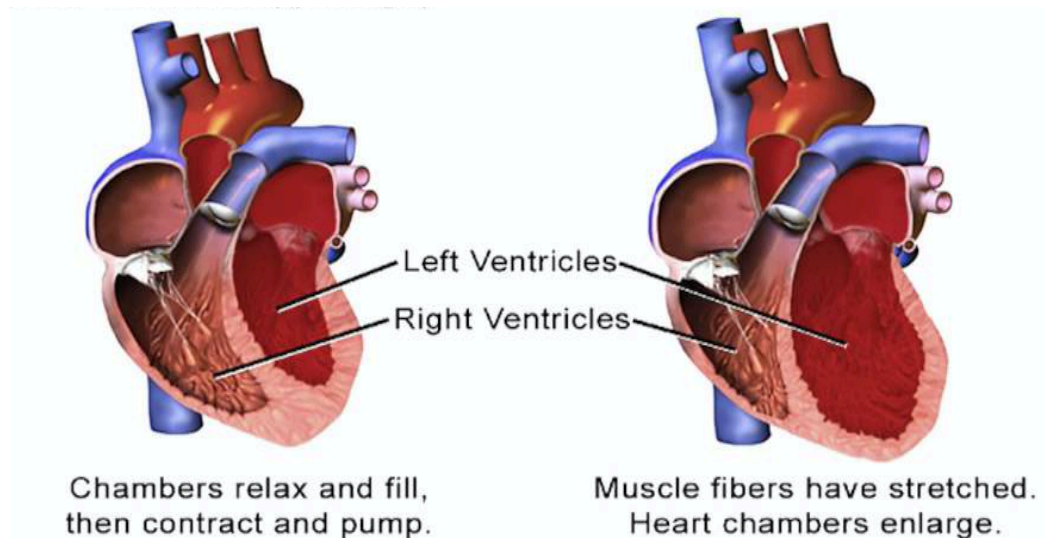


Figure 1.7: An illustration of a dilated heart.

The figure shows the normal heart versus heart with dilated cardiomyopathy. Left ventricular remodelling manifested as gradual increase in the left ventricular www.medinda.net

1.3 How do mutations lead to cardiac remodeling?

Cardiac remodeling is a process that involves multiple progressive alterations of subcellular components, including myofibrillar protein composition, sarcoplasmic reticulum, mitochondria, nuclei, cell membranes and the extracellular matrix. These changes contribute to the altered contractile performance of the heart (Machackova *et al.*, 2006). The fundamental function of heart cells is to generate contractile force by the sarcomere, the basic unite of cardiac muscle, and its transmission to the extracellular matrix. Abnormal function in any component induces cardiac remodeling (hypertrophy or

dilation). The structural changes induced by the mutations could affect the processes of sarcomere and myofibril formations. These processes are tightly regulated and coordinated. The result of several studies suggested that most mutated sarcomeric proteins incorporate into their myofibrils (Becker *et al.*, 1997). On the other hand, recent studies showed that there is a significant relationship between the deregulation of protein degradation (Protein degradation is an essential mechanism for maintaining normal cardiac muscle function) pathways with the pathogenesis of multiple forms of heart disease. Given the fundamental importance of the sarcomere for cardiac function it is not surprising that it possesses a strict system for the controlled degradation of proteins (Lyon *et al.*, 2013). The fundamental question is how the mutation can act leading to HCM and DCM disease or cardiac remodelling. These diseases related cellular and organ changes reflect complex qualitative and quantitative changes in the contractile machinery, gene expression, cellular signalling, subcellular organelles and myocardial metabolism (Machackova *et al.*, 2006b).

HCM and DCM are caused by single-point mutations in the genes that encode contractile proteins. These contractile proteins form crossbridges to generate force and contraction and include myosin, actin, troponin subunits, tropomyosin and myosin-binding protein C (MyBPC). The evidence accumulated from many studies suggest that the sarcomeric proteins mutations could lead to a depressed contractile function and this could trigger compensatory hypertrophy (Lankford *et al.*, 1995; Watkins *et al.*, 1996). Many studies have investigated on changes in Ca^{2+} sensitivity, a parameter believed to play a central role in the mechanism leading to HCM. Altered Ca^{2+} sensitization could lead to Ca^{2+} trapping and altered Ca^{2+} fluxes during excitation- contraction coupling (Ashrafian *et al.*, 2011). Publications that concentrate on Ca^{2+} sensitivity, which is altered in the

hypertrophic heart showed that mutations in different genes of myofilament proteins increase Ca^{2+} sensitivity and this could lead to cellular changes, such as intracellular Ca^{2+} handling, sarcoplasmic reticulum Ca^{2+} reuptake and phosphorylation of some proteins, probably contributing to several of the manifestations of the disease (Robinson *et al.*, 2002; Guinto *et al.*, 2009). Additionally, several investigators have report that the difference in responsiveness of Ca^{2+} in the heart failure does not reflect substantial differences in the protein isoform composition, but also demonstrates a change in the endogenous phosphorylation status of thin and thick filament proteins (Suematsu *et al.*, 2001; van der Velden *et al.*, 2003a; van der Velden *et al.*, 2003b). Such an alteration may be determined by the presence of different amounts of kinases, such as the cyclic AMP-dependent protein kinase A (PKA), protein kinase C (PKC) and myosin light chain kinase (MLCK), as well as phosphatases, in the cardiomyopathies. All these facts support that genetic factors play a fundamental role in the pathogenesis of many cardiovascular disorders, and thus, studying the effects of the mutations associated with cardiomyopathies, at the molecular level, is considered a pre-requisite to understand the biochemical basis of the remodelling observed in these cardiovascular diseases.

1.4 Structure of the sarcomere

The heart is a pump made of muscle. Contraction of the heart is due to contractions of millions of cardiac cells called cardiomyocytes. Contraction of cardiomyocytes is achieved by contraction of small units called sarcomeres.

A sarcomere is the basic unit of a muscle and repeating this unit forms Myofibrils, which under the microscope show alternating dark and light bands. Sarcomeres are composed of long, fibrous proteins that slide past each other when the muscles contract and relax.

Figure 1.8 show the structure of a sarcomere. The major components of the sarcomere are: The Z-disc (a complex macromolecular structure made principally of alpha actinin), the thick filament (made primarily of myosin), the thin filament (actin, the troponin complex, and tropomyosin), the M line (M protein and myomesin), and titin (Bonnemann & Laing, 2004). It also contains myosin-binding protein C, which binds at one end to the thick filament and the other to actin (Gregorio & Antin, 2000).

The proteins which form the sarcomeres are unique in many of their functional and architectural features. These dynamic proteins network equip the sarcomeres with mechanical stability, elasticity, spatial organisation and long-rang communication capacity (Otterbein *et al.*, 2001). One of the main property of the sarcomere is the paracrystalline lattice. This lattice formed by the noticeable axial and transverse order of actin and myosin filaments. For this reason, the axial distance of actin and myosin filament is fine tuned to produce appropriate contractions and relaxations. This distance has to be kept constant during the stresses and strains of contraction and relaxation. Thus, the motor function of the sarcomeres depends crucially on completely regular, parallel and repetitive array of actin and myosin. The function of the sarcomeric proteins of the thin filament, the thick filaments and the Z-disk can be modified through protein isoforms or post-translational modifications and their alterations by various factors could be the main reason in many cardiac diseases.

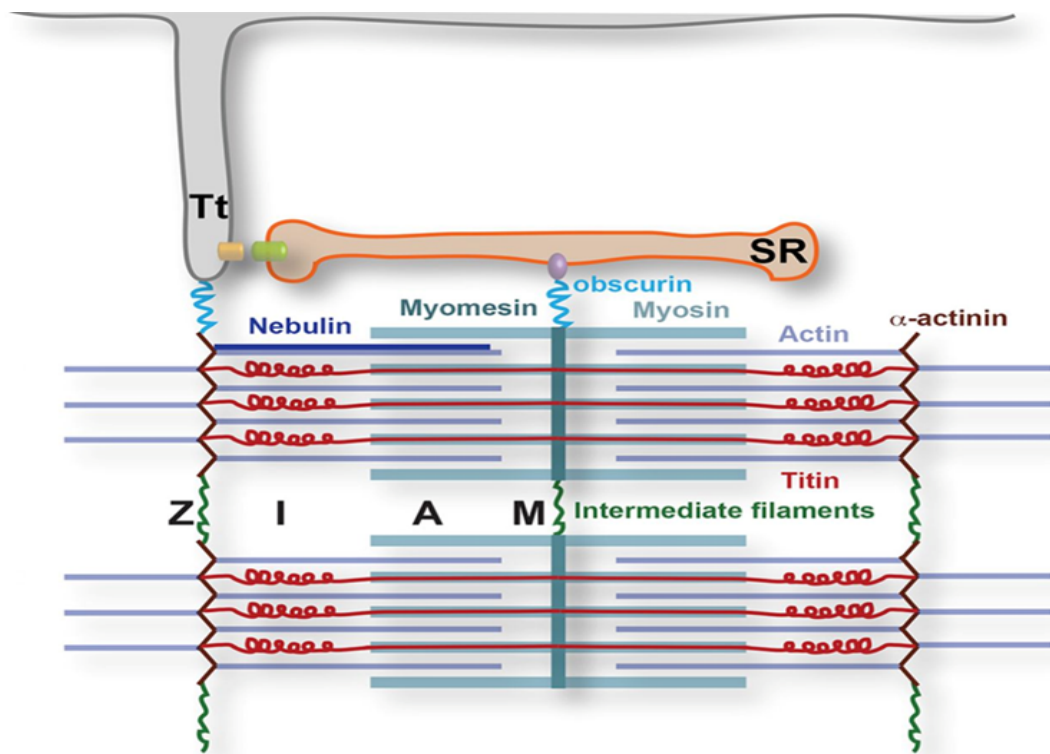


Figure 1.8: Structure of sarcomere.

Basic structure of the sarcomere showing some links between membranes and sarcomeres

1.4.1 Thick filament (myosin)

Myosin is the main component of thick filaments and it is responsible for producing force and muscle contraction. It is a large super-family of motor proteins. So far more than 37 myosin's families have been identified. Myosin in muscle is responsible for force generation by coupling ATP hydrolysis to the interaction of myosin with actin filaments.

In term of structure and as illustrated in figure 1.9, panel A, myosin is composed of six polypeptide chains: four light chains and two heavy chains. The light chains comprise two regulatory light chain (RLC), each about 20 KDa, and two essential light chain (ELC), each about 17KDa. Both myosin light chains (MLCs), the RLC and ELC attach to their respective MHC motifs (Geeves & Lehrer, 1994). The two heavy chains are wrapped around each other to form a double helical structure. The heavy chain can be further subdivided into

three parts: subfragment 1 (S1), subfragment 2 (S2) and light meromyosin (LMM). The LMM is located at the C-terminal of the heavy chain and is 100% made of an α -helical coiled coil. The N-terminal part of myosin is made of a globular domain called the myosin head and represents the motor domain of the myosin. In addition, S1 includes two prominent segments the motor domain (NH₂-terminal catalytic domain), which contain the actin-binding sites and the ATPase catalytic site and the neck region formed by a prolonged alpha-helix (the tail), to which are bound the essential and regulatory light chains (Ivan *et al.*,) (figure 1.9, panel B). This region was later named the lever arm and is linked to the actin and nucleotide binding sites by a region named the converter domain (Figure 1.9). Overall, this part of myosin (S1) holds all of the motor functions of myosin (the ability to hydrolyse ATP, produce motility and force).

Contraction of the heart muscle is triggered by calcium binding to the actin-containing thin filament (thin filament will be discussed in detail in the next section). This binding lead to changes in thin filament structure and allows myosin heads or motor domains from the thick filaments to bind to actin in the thin filament. Although the contraction of heart is triggered by calcium binding to the troponin C in thin filaments it is also modulated by structural changes in the myosin. Recently it has been demonstrated that contraction of the heart muscle is modulated by structural changes in the myosin-containing thick filaments (Thomas *et al.*, 2016). This study showed that cRLC phosphorylation generates a structural signal that it transmitted between myosin molecules in thick filaments and from the thick to thin filament, altering their calcium sensitivity (calcium sensitivity will be discussed later). The impact of cRLC phosphorylation on thick filament structure and its calcium sensitivity were emulated by increasing sarcomere length or by deletion the N terminus of the cRLC. Changes in the thick filament

structure were highly cooperative with respect to either calcium concentration or extent of cRLC (Kampourakis *et al.*, 2016)

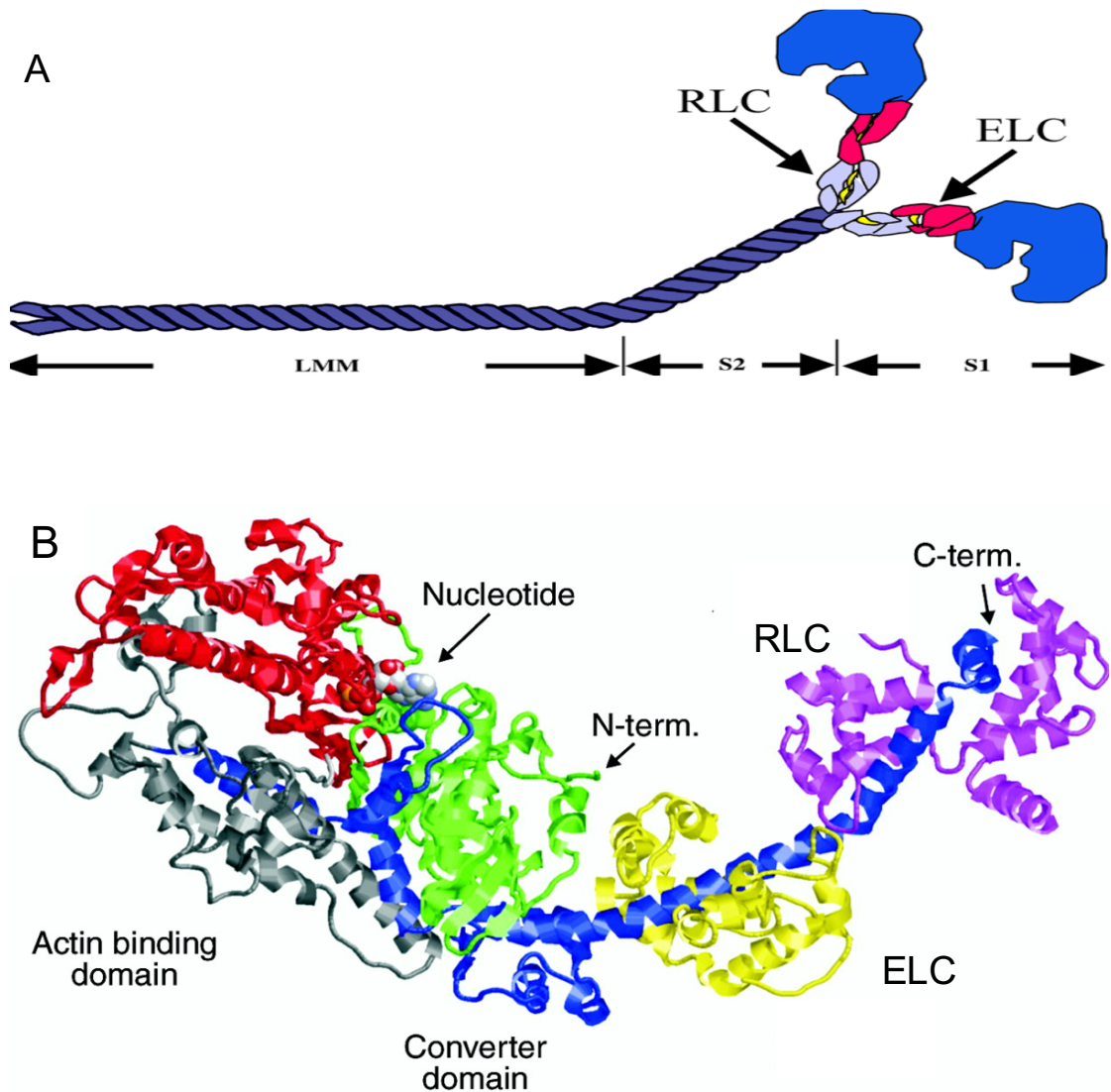


Figure 1.9: Structure of myosin.

Panel (A) shows myosin structure which formed from tail domain (a hexameric protein consisting of two myosin heavy chain polypeptides that self-associate via an alpha helical coiled-coil rod) and head domain. Panel (B) shows the atomic structure of myosin head. Each globular head domain is associated with two light chains the yellow display the Essential light chain (ELC), and the magenta display the Regulatory light chain (RLC). The green, red/grey, and blue segments represent the 25 kDa, 50 kDa, and 20 kDa segments of the heavy chain (Ruegg *et al.*, 2002).

1.4.2 Thin filament

1.4.2.1 Actin

Actin constitute an essential cytoskeletal protein in eukaryotic cells and was discovered in 1942 by Straub (Szent-Györgyi, 2004). It is a critical protein for many cell functions such as muscle contraction, cell division, cell migration, conservation of cell shape, and cell adhesion (Chaponnier & Gabbiani, 2004). There are six genes with each encoding a different actin isoform. α -smooth muscle actin (α -SMA) and γ -smooth muscle actin (γ -SMA) are expressed in smooth muscle cells while α -cardiac actin (α -CAA) and α -skeletal actin (α -SKA), are predominant in cardiac and skeletal muscles. The last two isoforms β -cytoplasmic (β -CYA) and γ -cytoplasmic actins (γ -CYA) are non-muscle isoforms (Perrin & Ervasti, 2010). Actin is a major compound of thin filaments and it functions as a double-stranded helical polymer (F-actin) (Figure 1.10). F-actin results from the spontaneous polymerization of G-actin at physiological salt concentration. Actin polymerization starts preferentially from the (+) end of G-actin monomers and is powered by ATP hydrolysis, while depolymerisation occurs at the (-) end. Thus, actin orientation within the sarcomere is the (+) end in the Z-line and the (-) end pointing towards the M-line.

Determination of the structure of actin filaments is of huge interest to scientists. However, this has proven a challenging task. This is because obtaining crystals of long and unequal actin filaments is not possible. In addition, crystallisation of monomeric G-actin was also problematic because monomeric actin (G-actin) polymerise in the presence of salt which are generally used to drive the formation of protein crystals. The first crystal structure of G-actin (monomeric form) was obtained in 1990 (Kabsch *et al.*, 1990) from the complex of skeletal muscle G-actin with bovine pancreatic DNase I in the presence of ATP (resolution of 2.8 Å) and ADP (resolution of 3 Å). In this structure, G-actin has four

domains (1-4) (Kabsch *et al.*, 1990). The inner (large) domain, can be divided to subdomain 1 and subdomain 2, and the outer (small) domain, is divided into subdomain 3 and subdomain 4 (figure 1.11). The inner and outer domains are linked longitudinally by a cleft. The crystal structure of uncomplexed actin in the ADP state have been published in 2001 by Ludovic R el at (Otterbein *et al.*, 2001). Although, the two crystal structures of G-actin are very similar, there are some differences between them. For example, the orientation of subdomains 2 and 4 are slightly different in the two actin structures. The DNase binding loop within subdomain 2, is folded as an α -helix in the G-actin-DNase structure but in the other structure it is either disordered or folded as a β - turn. Additionally, in subdomain 1 at the opposite side of the molecule TMR binds in a hydrophobic pocket near the COOH-terminus (Otterbein *et al.*, 2001). Functionally, the outer domain contains the S1 binding sites and the N terminal and C terminal regions of actin. The ATP and Ca^{2+} binding sites are located in the cleft at the center of the actin molecule (Galkin *et al.*, 2015; Yanagida *et al.*, 2010).

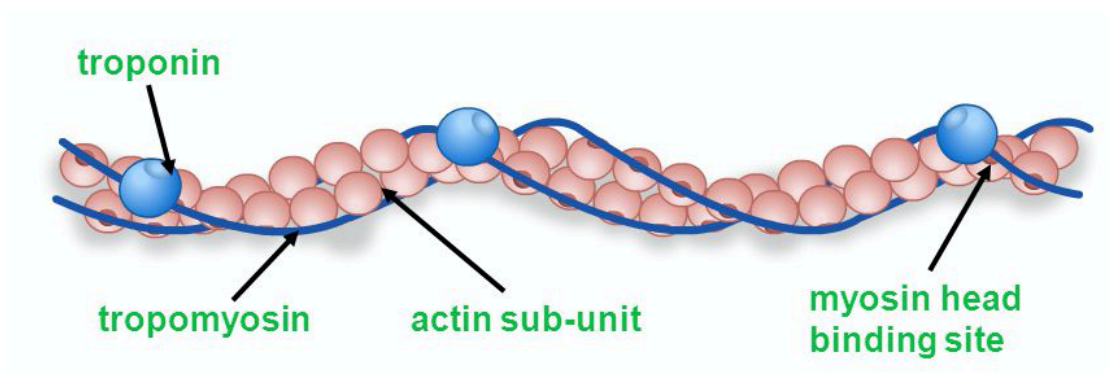


Figure 1.10: Thin filament structure.

The cartoon shows the structure of thin filament. Pink circle represented G-actin (formed as F-actin), blue line represents tropomyosin, and blue circle represent troponin complex.

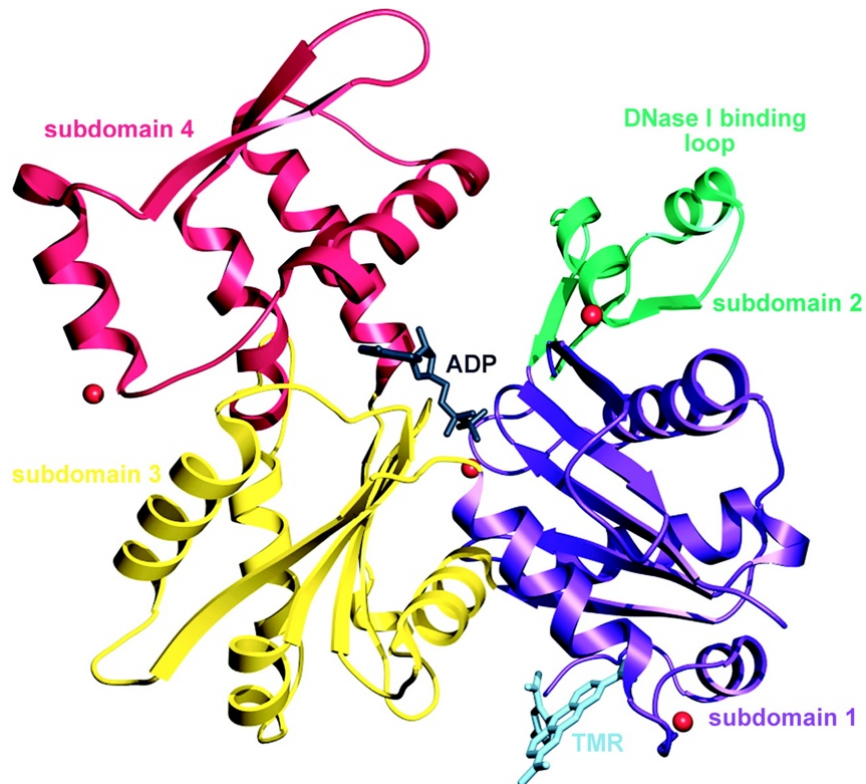


Figure 1.11: Structure of G-actin.

Ribbon display the structure of uncomplexed actin in the ADP state. Each colour represents a subdomain of actin: subdomains 1 (purple), 2 (green), 3 (yellow), and 4 (red). ADP is bound at the centre of the molecule, where the four actin subdomains meet. Four Ca^{2+} ions bound to the actin monomer represented in red spheres. Tetramethylrhodamine-5-maleimide (TMR), which is covalently attached to Cys374, binds in a hydrophobic pocket near the COOH-terminus in actin subdomain 1 (Otterbein et al., 2001)

In most instances, F-actin (a polymer) is the functional form of actin, hence, understanding the function of actin requires an understanding of the structure and dynamics of the actin filament. For this reason, and because of the fact that F-actin cannot be crystallized, cryo-electron microscopy (cryo-EM) (Yanagida *et al.*, 2010) and x-ray fiber diffraction (Holmes *et al.*, 1990; Oda *et al.*, 2009) have been used to investigate the structure of F-actin. The most recent atomic model of F-actin had been built by Vitold E el at 2016 using a direct electron detector, electron cryo-microscopy and the forces

imposed on actin filaments in thin films to reconstruct one state of the filament at 4.7 Å resolution (figure 1.12)(Galkin *et al.*, 2015).

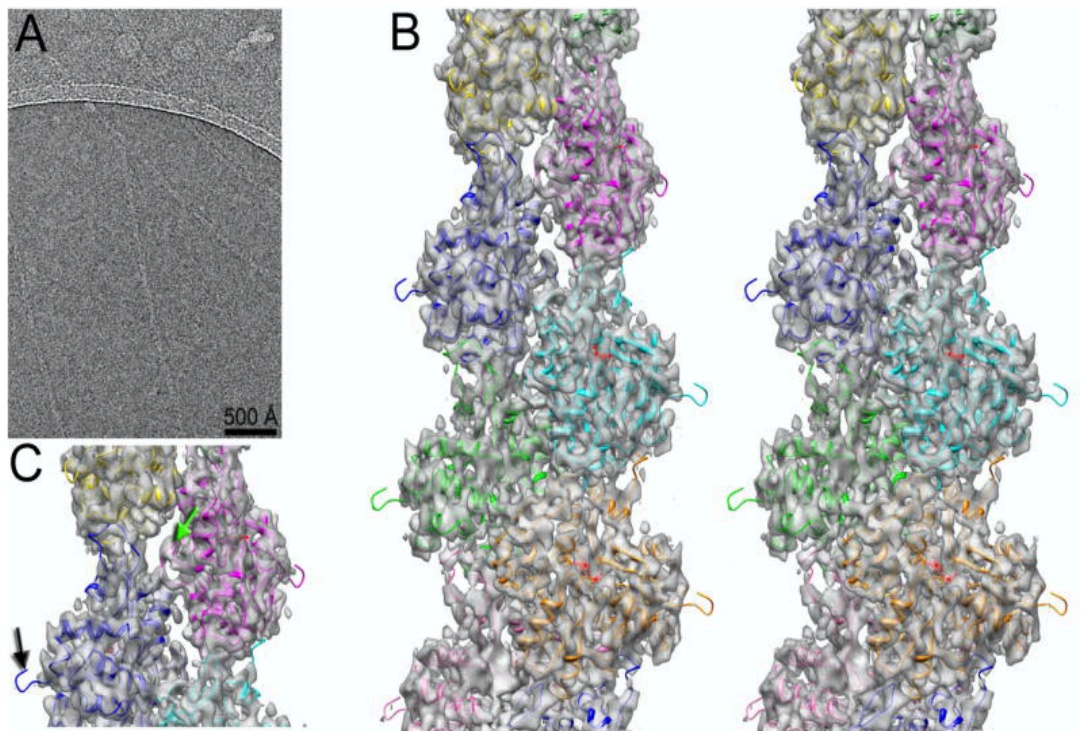


Figure 1.12: Micrograph of actin filaments.

(A) Typical micrograph of actin filaments embedded in thin ice. (B) Stereo view of the 3D-reconstruction at ~ 4.7 Å resolution. (C) The absence of the N-terminal density in the map is indicated with a black arrow, while the hydrophobic plug density is marked with a green arrow (Galkin *et al.*, 2015)

1.4.2.2 Tropomyosin

Tropomyosin is an elongated protein that binds along actin filaments in different positions that depend on the activity of thin filaments as shown in figure 1.13 (El-Mezgueldi, 2014). It is another double-stranded α -helical coiled-coil protein in the thin filament. In Humans, there are four genes that code for more than twenty different Tm isoforms. These genes are TPM1, TPM2, TPM3, and TPM4 (Perry, 2001). TPM1 and TPM2 code the striated muscle tropomyosin (α and β isoforms). Both the α and β isoforms can

be found in the skeletal muscle whereas, in cardiac muscle only α - isoforms can be found (Perry, 2001).

Many basic features of tropomyosin muscle such as the parallel in-register alignment of two chains, length of the molecule, the approximate distance between the N and the C terminal regions, and the presence of bends along the actin molecule (flexibility), and variable pitch length of the supercoil are detected by electron microscopy (Jerry H. Brown *et al.*, 2005; Perry, 2001) . Symmetrically, the two polypeptide chains bind alongside each of the helical strands of filamentous actin (Figure 1.13). On the other hand, biophysical studies demonstrated that tropomyosin is a dynamic protein with domains that fold and unfold independently of one another, reflecting regions of greater and lesser stability (Jerry H. Brown *et al.*, 2005; El-Mezgueldi, 2014).

Tropomyosin plays a critical role in muscle contraction. The actin filament is the universal target of tropomyosin. Binding of Tm to actin and troponin is fundamental to the allosteric switching of the thin filament and modulate the actin-myosin interaction. Tm is also responsible of the cooperativity displayed by thin filaments during contraction and relaxation. Tropomyosin binds end-to-end to form cables along both sides of the helical filament such that the N terminus is oriented towards the pointed, slow-growing end of the filament (towards the M-line in striated muscle sarcomeres). The position occupied by tropomyosin on the actin filament depends on the regulatory state (will be discussed later)

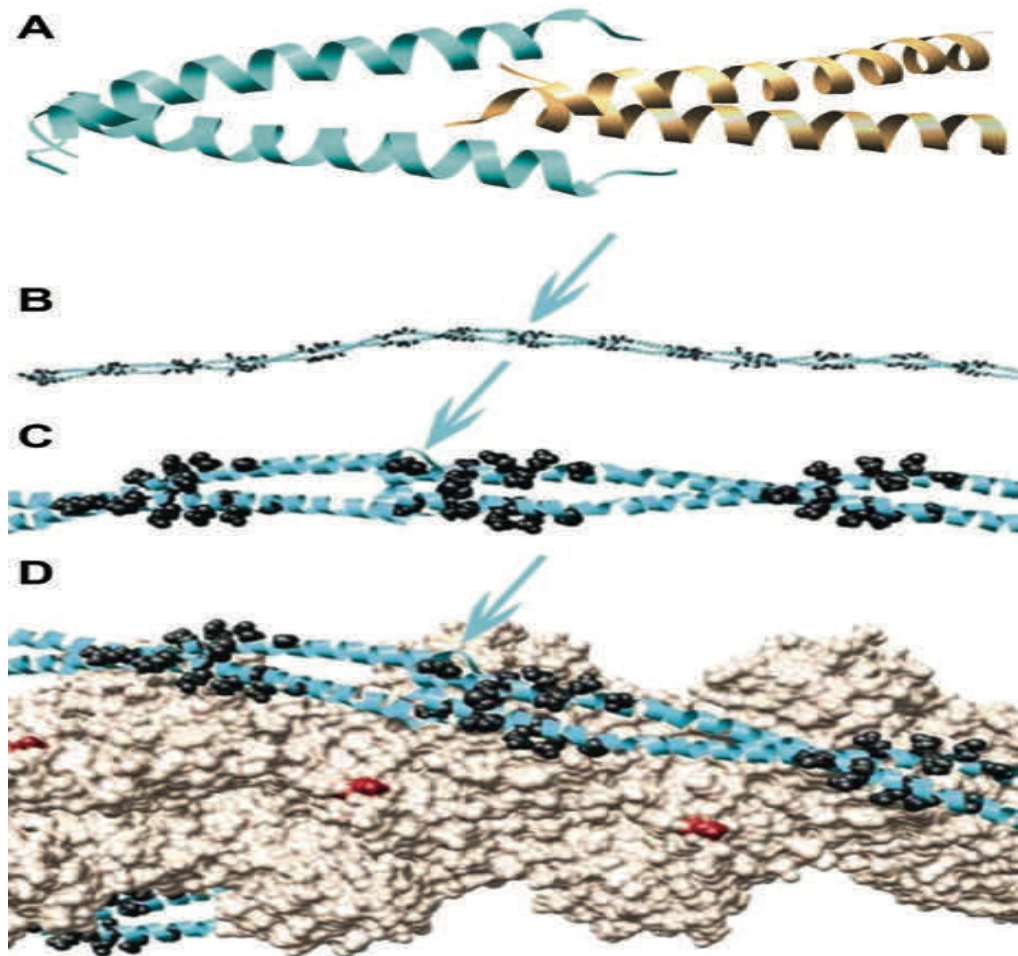


Figure 1.13: crystal structure of tropomyosin.

This figure displays the solution structure of the tropomyosin overlap complex and relationship of actin binding sites to the actin filament. (A) Ribbon diagram of the NMR structure of the striated muscle tropomyosin overlap complex (PDB ID 2G9J). (B) Two molecules of full-length tropomyosin molecules from the 7 Å structure (1C1G) with side-chains of the Phillips consensus actin binding sites shown in black (Phillips 1986). The arrow points to the site of the junction. (C) Detail of the junction between the two molecules in B shows three contiguous actin binding sites. (D) Model of the joined tropomyosin on a model of the actin filament. Residue K238 of actin is shown in red as a position marker. (C) and (D) show the 90° relationship of the two coiled coils in the overlap complex that results in the actin binding sites on either side of the junction having a similar relationship to actin (Greeneld *et al.* 2006)

1.4.2.3 The troponin complex

The Troponin complex (Tn) is a heterotrimeric complex identified as the regulatory unit of the thin filament by Ebashi *et al* (1967). It is the Ca^{2+} -based regulator of striated muscle contraction. It is a 78 kDa protein complex comprised of three subunits named according to their function, Troponin C (TnC) is the Ca^{2+} binding subunit, Troponin I (TnI) is the inhibitory subunit, and troponin T (TnT) is the tropomyosin binding subunit. The Troponin complex (Tn) and the tropomyosin dimer (Tm) together with actin monomers are considered as the major components of thin filaments (figure 1.10). Each one Tn complex is associated to one Tm molecule and both bind to seven actin monomers.

The main role of the troponin complex is to regulate the motor function of the actomyosin complex following a change in intracellular calcium concentration. At low calcium, troponin inhibits the actomyosin ability to hydrolyze ATP and the subsequent power stroke while at high calcium it activates the actomyosin chemomechanical function. The inhibition of contractile interaction of actomyosin by troponin-tropomyosin (in the absence of Ca^{2+}) is due to the inhibitory action of troponin I. Troponin C neutralize this inhibition by troponin I irrespective of Ca^{2+} concentrations when troponin T is absent. This neutralization becomes sensitive to Ca^{2+} only in the presence of troponin T such that the Ca^{2+} dependent inhibition and activation of thin filaments require the presence of all 3 subunits Tn C, I and T (Ohtsuki *et al.*, 1986). This regulatory function is driven by an elegant set of dynamic interactions among the troponin T, I, and C subunits. The structure and function of each subunit will be discussed later.

Data from several electron microscopy and low-resolution X-ray crystallographic studies divided Tn into two domains TnT1 a long α -helical domain or tail and a core domain containing most of the regulatory function of the troponin complex (Franz *et al.*, 2001;

Takeda *et al.*, 1997). In 2003, Takeda *et al* published the first crystal structure for the core domain of cardiac troponin complex in the Ca^{2+} saturated form (Takeda *et al.*, 2003). According to this structure the core domain of cardiac troponin complex can be subdivided into two structurally distinct sub-domains: the regulatory head and the IT arm (figure 1.14). The regulatory head comprise the N-terminal lobe of cTnC (cNTnC) which holds the Ca^{2+} binding site and the binding site of the switch peptide of cTnI. The IT arm is approximately 80Å long and is a long α -helical coiled-coil formed by interaction between two cTnI and cTnT α -helices, the C-terminal lobe of cTnC (cCTnC) as the sandwich between cTnI and cTnT as shown in figure 1.15. The structure and function of each subunit will be discussed in more details in the next section.

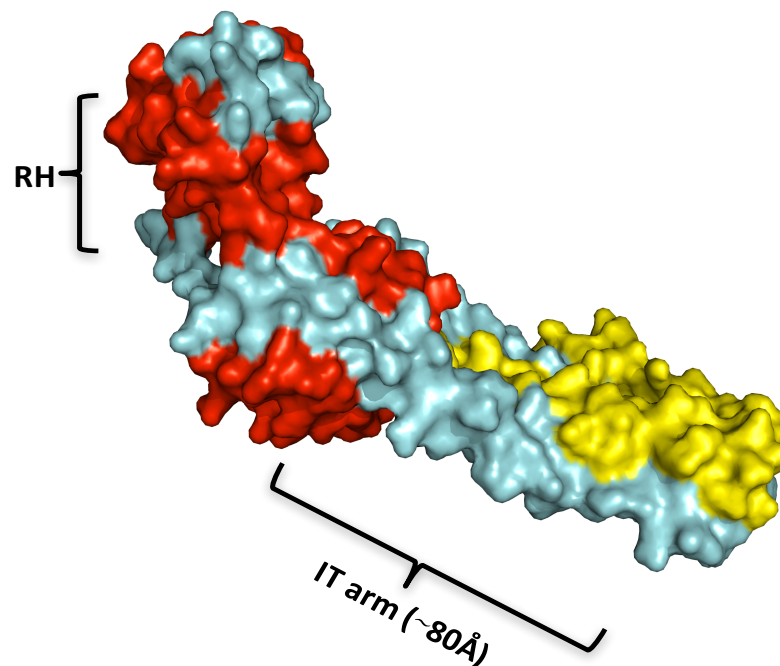


Figure 1.14: Space-filling model of cardiac troponin complex.

RH represent the regulatory head, TnC in red, TnI in cyan, and TnT in yellow. This figure was generated using PyMOL.

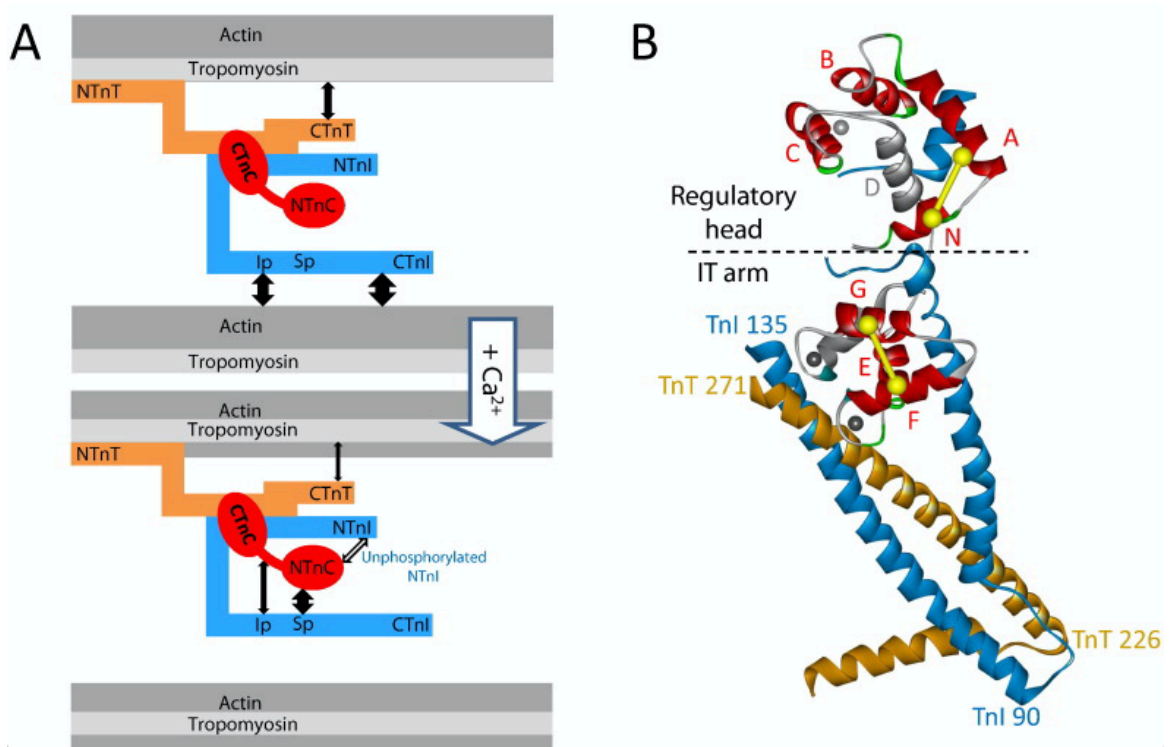


Figure 1.15: The interaction between the components of cardiac thin filament (A) and structure of troponin complex (B).

Panel A, represents the Ca^{2+} dependent interactions between TnT, TnI, TnC and actin which shown in solid double-headed arrows. TnI inhibitory peptide (Ip), TnI switch peptide (S). B, shows structure of the cardiac Tn core complex contains TnC (red, grey) and parts of TnI (blue) and TnT (gold). Bifunctional rhodamine (BR) probes cross-linked cysteines along either the N, A, B, C, E, F or G helix of TnC (red). BR probes cross-linking cysteines across either N and A, or F and G helices are shown in yellow dumbbells. D helix which is inaccessible is in grey (Sevrieva *et al.*, 2014)

1.4.2.3.1 Troponin T (TnT)

Troponin T is the largest troponin subunit and a central player in the calcium dependent regulation by the Tn complex. There are three different isoforms of troponin T encoded by three homologous genes. Slow skeletal muscle which is encoded by TNNT1, cardiac muscle which is encoded by TNNT2, and fast skeletal muscle which is encoded by TNNT3. TnT is expressed in the heart as four isoforms, one is expressed in adult while the other three isoforms are expressed in the foetus. This mean, TnT is subjected to substantial alternative splicing which leads to the expression of several TnT isoforms (Anderson *et al.*, 1995).

TnT is an asymmetric protein that plays a crucial role in anchoring the cTn complex on the thin filament by interacting with Tm. More importantly, Troponin T plays an important role in the Ca^{2+} dependent regulation by the troponin complex. Structurally, cTnT contains two functional domains (TnT1 and TnT2)(Ohtsuki, 1979; Wei & Jin, 2011). TnT1 represents the N-terminus of cTnT, which controls the modulation of the overall molecular conformation and function of TnT, and the middle region of TnT which binds to the head-tail junction of Tm to anchor the Tn complex independently of Ca^{2+} (figure 1.15 A and B). TnT2 represents the C-terminus of cTnT which is responsible for linking the rest of the troponin complex and the middle region of tropomyosin in a Ca^{2+} sensitive manner (Figure 1.15-A).

To date there is no crystal or NMR structure for the whole cTnT. The high-resolution structure of whole Tn complex only includes the regions interacting with TnI and TnC (Takeda 2003) displayed in figure 1.16. This structure showing that the α -helical coiled-coil formed between TnI-TnT corresponding to Leu₂₂₄-Val₂₇₄ of human cardiac TnT (Vinogradova *et al.*, 2005a). This form an intertwined structure made of a parallel α -helical coiled-coil formed between the H2 helix of cTnT and the H2 helix of cTnI together with a second α -helical coiled-coil formed between H1 helix of cTnT and H1 of cTnI. Ertz-Berger *et al* studied part of T1 (residues 70-170) and computationally built up an α -helix structure for this region (He *et al.*, 2007). In 2011 Manning *et al.* used this structure to dock onto a known Tm structure and performed large scaled computational modeling studies (Manning *et al.*, 2011). Two binding sites between Tm and TnT have been demonstrated by protein binding studies. The first interaction between Tm and T1 region of TnT has been mapped to a 39-amino acid segment at the N-terminal of TnT. The second interaction between Tm and T2 region of TnT mapped to a 25-amino acid segment

at the beginning of the T2 fragment (Jin & Chong, 2010). In general, cTnT has essential physiological roles in holding all Tn subunit and to bind to the thin filament.

1.4.2.3.2 Troponin I (TnI)

Troponin I TnI is a 24 kDa protein responsible for inhibiting the activity of the actomyosin ATPase and holding the troponin complex bound to the actin. Troponin I is encoded by three different genes: cardiac troponin I (cTnI), fast skeletal troponin I (fsTnI) and slow skeletal troponin I (ssTnI). The main difference between the cardiac isoform and skeletal form is the cardiac form has 32 amino acids as an N terminal extension.

The main function of TnI is driven by its binding to actin in the absence of calcium (responsible for actomyosin inhibition) and the dissociation from actin upon binding to troponin C in the presence of Ca^{2+} . In the absence of Ca^{2+} , troponin I forms a stable complex with troponin C. The action of Ca^{2+} on troponin C induces changes in the interaction of troponin C with troponin I and then troponin I is dissociated from actin-tropomyosin. When troponin I is complexed with troponin C, it binds to actin-tropomyosin so weakly that troponin I cannot exert its inhibitory activity even in the absence of Ca^{2+} .

As shown in figure 1.16 the N terminal extension of cardiac troponin I (cTnI) including residues 1-11 represents the single turn of a helix and residues 12-18 (a polyproline helix). In between these two helices the helix C (residues 19-30) which contains the bisphosphorylation motif (Sadayappan *et al.*, 2008). There is no crystal structure for the N-terminal extension of cTnI (residues 1-32). However, NMR spectroscopy has been used to define the structures of both the non-phosphorylated and bis-phosphorylated forms of the N-terminal region of TnI. The data obtained from this study suggested that the N-

terminus extension is less structured, and is associated with the NcTnC. While, upon the bis-phosphorylation of Ser-23 and Ser-24, the helix C (residues 21-30) is stable. As a consequence, the interaction between the cTnI (residues 1-32) and NcTnC is weak allowing it to be more mobile and to potentially interact with other regions of cTn complex. Sadayappan *et al.* showed also that the rest of cTnI is divided into four regions. The first region is the IT-arm (residue 40-136), having two helices (H1 and H2) interacting with TnC and TnT2 respectively. The IT-arm primarily plays a structural role in anchoring the troponin complex onto the thin filament by forming a helical coiled-coil with the C-terminal domain of TnT. The second region is the inhibitory region (residues 137-146) which has been considered to be responsible for inhibition of the interactions between actin and myosin heads via binding to the inhibitory region of TnI to actin at low Ca^{2+} concentration (Sadayappan *et al.*, 2008). The inhibitory region is the second missing part in the troponin complex crystal structure published by Takeda (Takeda *et al.*, 2003) whereas, in the crystal structure of skeletal muscle troponin this region is well order (Vinogradova *et al.*, 2005b). On the other hand, the NMR structure of cTnI₁₂₈₋₁₄₇ with cTnC₈₉₋₁₆₁ reported that cTnI₁₃₄₋₁₃₉ formed an alpha-helical structure, and that cTnI₁₄₀₋₁₄₇ displayed an extended conformation that might be associated with the C-lobe of cTnC. According to Takeda's structure, the C-terminus of troponin I cTnI (residues 164-210), which is considered as the second actin-Tm binding site (Solaro, 2010; Burkeen *et al.*, 2004), is mobile, alpha-helical and is free of interaction with either cTnC or cTnT. Between these two inhibitory regions (cTnI₁₃₇₋₁₄₆ and cTnI₁₆₄₋₂₁₀) lies the switch peptide of cTnI (residues 147-163). This region is thought to control the binding of the inhibitory region of cTnI to actin depending on the concentration of Ca^{2+} (Campbell *et al.*, 1993; Månsson, 2014). In addition, the switch peptide is an essential region in cTnI required to stabilize

NcTnC in the open conformation. The structure of the binary complex of the NcTnC and cTnI₁₄₈₋₁₆₃ complex in Ca²⁺-saturated state has been determined by NMR (Oleszczuk *et al.*, 2010b). The result of the NMR studies are in good agreement with the Takeda crystallographic study in term of the orientation and conformation of switch-peptide with respect to the NcTnC.

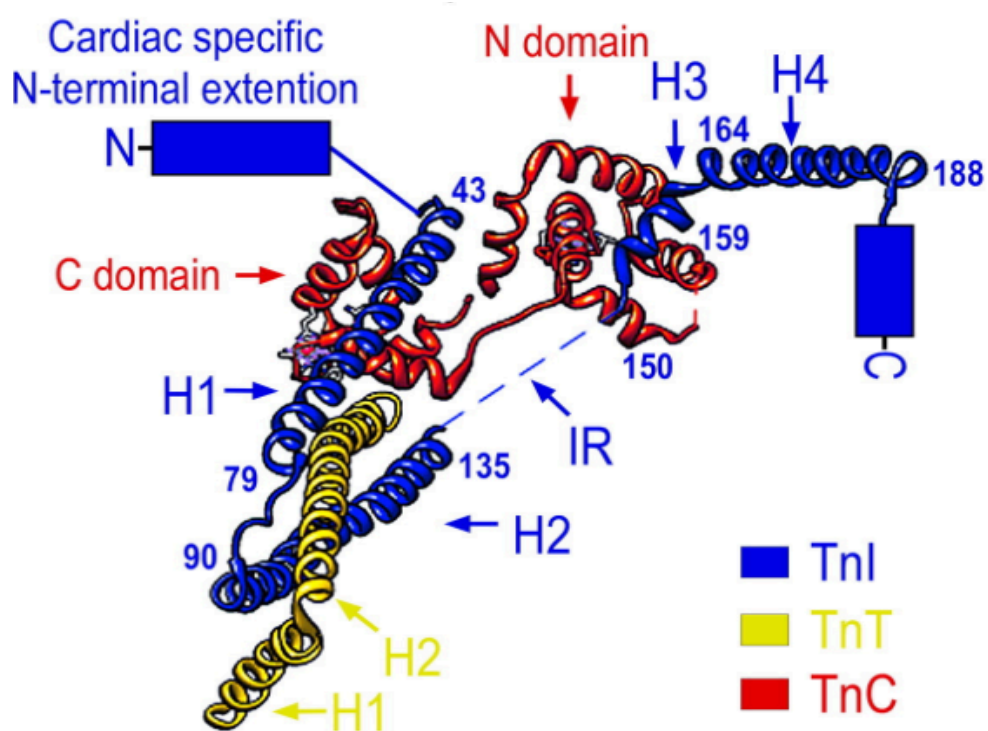


Figure 1.16: The position of cTnI in the crystal structure of troponin complex.

The structure represented the crystal structure of cardiac troponin complex in Ca²⁺ saturated state (PDB 1J1E) (Takeda *et al.*, 2003). The structure shows functional segments of TnI and the interactions with TnC and TnT. There are six functional segments in cTnI, specific cardiac N-terminal extension (residues 1-30), the N-terminal conserved region (residues 42–65) which is the amphiphilic portion of H1 α -helix and binds the C domain of TnC, the TnT-binding region which forms a coiled-coil interface with TnT (residues 66–136, H1 and H2), the inhibitory region (residues 137–148), the switch region (residues 148–163, H3), and the C-terminal mobile domain (residues 164–210, H4) (Sheng & Jin, 2016).

A major physiological mechanism for alteration of myofilament properties is driven by phosphorylation of Ser-23/ Ser-24 residues on cTnI by several different kinases (Metzger & Westfall, 2004). Several studies have suggested that human heart failure is associated with a low level of thin-filament protein phosphorylation (Hamdani *et al.*, 2008; van der Velden *et al.*, 2006; van der Velden *et al.*, 2003c). However, it has also been shown that very small increases in troponin phosphorylation can have a big impact on ventricular function (Kirk *et al.*, 2009). Moreover, recent studies suggested that the different responses to chronic pressure overload observed in heart failure patients are reflective of changes in both contractile protein phosphorylation (in particular of TnI and MLC2) and changes in phosphatase expression (Walker *et al.*, 2013). Consequently, cTnI phosphorylation could play an important role in the pathophysiology of hypertrophic and dilated cardiomyopathies associated with mutations in troponin subunits. Indeed, HCM associated mutations in troponin T have been shown to suppress the modulation of Ca²⁺-sensitivity by troponin I phosphorylation (Messer *et al.* 2016).

1.4.2.3.3 The calcium binding subunit troponin C (TnC)

Troponin C (TnC) belongs to the family of EF hand Ca²⁺ binding proteins which is a family of protein ubiquitously distributed in eukaryotic cells. However, TnC is muscle specific. There are two genes of troponin C, one gene is expressed in fast skeletal muscle while the second gene is expressed in both cardiac and slow skeletal muscles (Zot *et al.*, 1987). TnC is an 18 kDa dumbbell-shaped molecule. It is a highly acidic protein because it has a high content of aspartate and glutamate residues.

1.4.2.3.3.1 Troponin structure

Troponin C consists of an N-terminal regulatory lobe (cNTnC) and C-terminal structural lobe (cCTnC) connected by a single alpha helical linker. The regulatory lobe contains five alpha helices, helix N (residues 5-11), helix A (residues 14-27), helix B (residues 41-46), helix C (residues 54-63), and helix D (residues 75-86). The structural lobe contains four alpha helices, helix E (residues 95-105), helix F (residues 116-124), helix G (residues 131-141), and helix H (residues 151-158) (Slupsky & Sykes, 1995). In addition, there are four binding metal sites. Two sites in the N terminal domain (I and II) and two sites in the C terminal domain (III and IV) (figure 1.17).

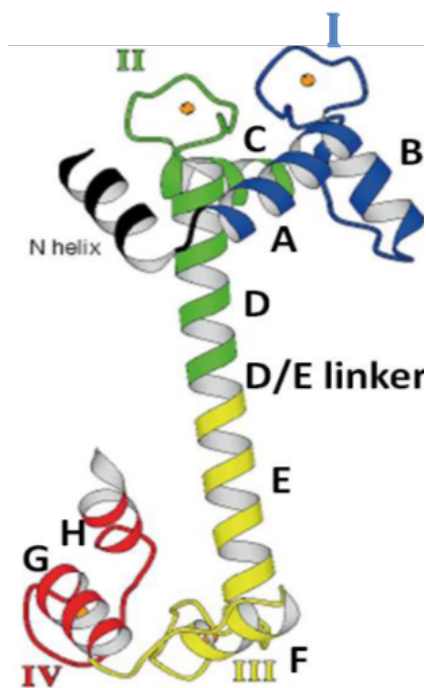


Figure 1.17: A ribbon diagram of the TnC structure.

The TnC composed of two lobes connected by an α -helical linker. Helices A-H and N are shown. The N lobe (that contains calcium binding sites I and II) is connected to C lobe (that contains metal binding sites III and IV) by the D/E linker (Houdusse et.al., 1997).

Calcium binds to the troponin complex in specific sites in TnC. The antiparallel beta sheet in the N terminal domain of cTnC, which consists of residues (36-38 and 72-74), and the antiparallel beta sheet in the C terminal domain of cTnC (residues 112-114 and 148-150), together with the helices form four helix-loop-helix calcium binding sites, (figure 1.17) (Slupsky & Sykes, 1995). The binding of Ca^{2+} is seven-coordinated to the 12-residue loop via oxygen result in pentagonal bipyramidal arrangement (EF-hands) (figure 1.18-C). The positions of the six residues in the loop sequences provide ligand groups. These loops always contain Asp residue in position 1 and Glu in position 12th) (figure 1.18 A and B).

Cardiac TnC has three active binding metal sites compared to the skeletal which has four sites. In the N-terminal domain of cardiac TnC, site I is defunct because of amino acid substitutions (figure 1.18). In contrast site II is highly specific for Ca^{2+} (McFarlane-Parrott, 2013). In the C-terminal domain (cCTnC) there are two high affinity $\text{Ca}^{2+}/\text{Mg}^{2+}$ binding site (III and IV). The affinity of Ca^{2+} for these sites is higher than for Mg^{2+} (10^7 M^{-1} and 10^3 M^{-1} respectively) (McFarlane-Parrott, 2013). In the resting state of the cardiac muscle, these two sites (III and IV) mostly bind Mg^{2+} because the intracellular level of Mg^{2+} is (0.5-5 mM) and the intracellular level of Ca^{2+} is $< 100\text{nM}$. Upon cardiomyocytes stimulation, the intracellular Ca^{2+} concentration increases to about 1-10 μM (during the cardiac twitch) (E Bittar & T Keh, 1980). As shown in figure 1.18-B the loops of metal binding site have a specific sequence. The change in these sequences alter the function of cTnC. For example, mutant cTnC in which both sites I and site II bind Ca^{2+} , have an increased Ca^{2+} sensitivity of contraction in comparison to the wild type (*Mutagenesis, Structure-Function*. 2009). Moreover, it has been noticed when cTnC is engineered with an active site I and an inactive site II, TnC does not restore the ability of Ca^{2+} to activate force generation. This observation suggests that site II is more essential for the regulatory function of cTnC than

site I (*Mutagenesis, Structure-Function*. 2009). Furthermore, many mutations in these loops have been linked to cardiomyopathies (figure 1.18-B).

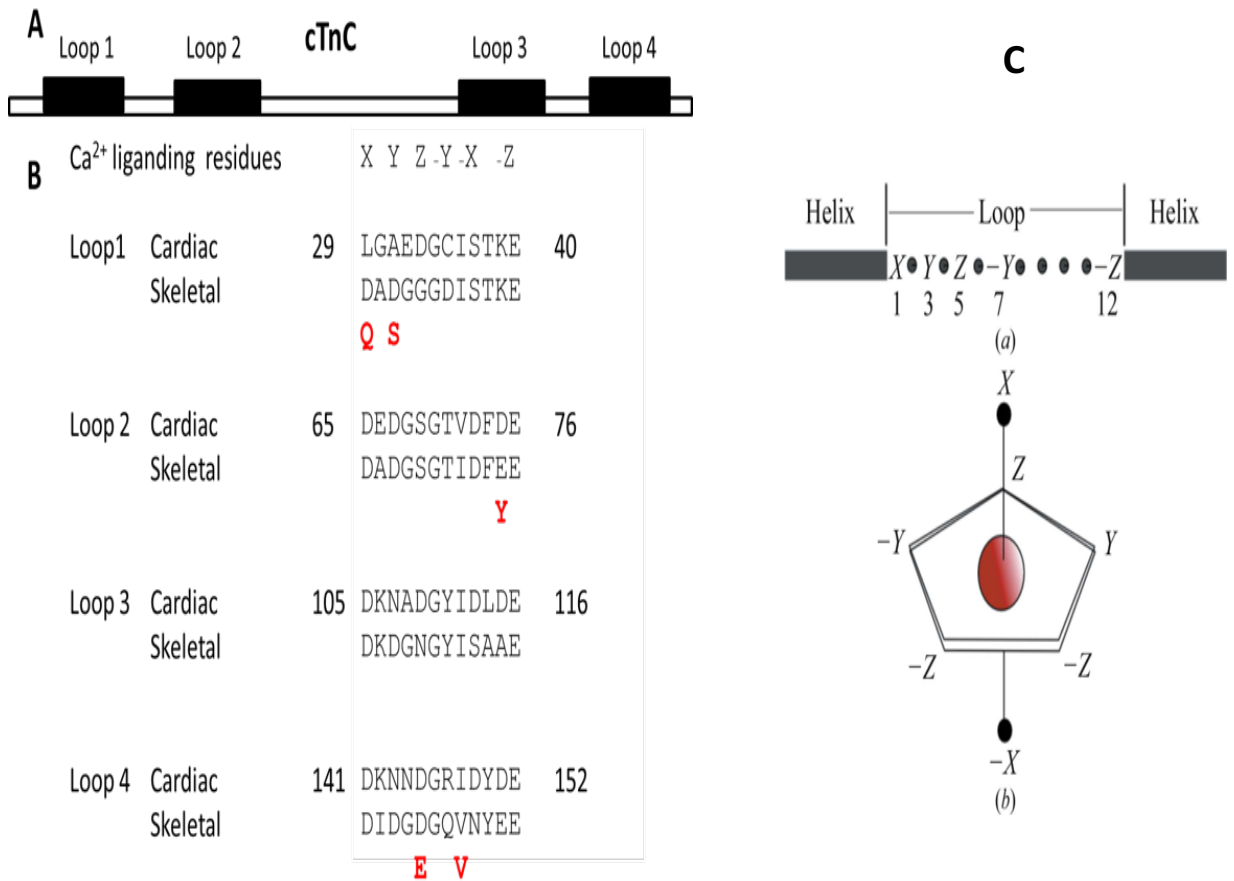


Figure 1.18: Troponin C structure.

The cartoon shows (A) the whole cTnC and boxes represent the Ca²⁺ binding sites loop (B) shows the sequence of each loop in cardiac and skeletal muscle, and C shows the pentagonal bipyramid complex of Ca²⁺. Red colour represents the mutations on the cTnC

1.4.2.3.3.2 Function of troponin C

Functionally, in cTnC the N-domain primarily plays a regulatory role in initiating thin filament activation and the subsequent generation of force and contraction whereas the C-domain (cTnC) mostly plays a structural role in anchoring TnC within firstly the whole Tn complex and secondly the thin filament. Determination of the structure of the

regulatory part of cTnC is fundamental to understanding how Ca^{2+} binding to site II initiates the signaling process leading to thin filament activation. Therefore, many studies determined the structure of the regulatory domain of TnC in both states, Ca^{2+} -saturated and Ca^{2+} -free, and also in complex with the switch peptide of TnI (Oleszczuk *et al.*, 2010a). The results of these studies have shown that in the Ca^{2+} -free state (the apo state) most of the hydrophobic residues of cNTnC are buried and the regulatory domain stays in a closed conformation (Oleszczuk *et al.*, 2010). The binding of Ca^{2+} to the regulatory domain (cNTnC) induces an opening of a hydrophobic patch and leads to an increase in the interaction with TnI. Remarkably, the change in the structure of the N-terminal of cTnC (cNTnC) induced by Ca^{2+} binding to site II is much smaller than the change induced in the N-terminal domain of skeletal TnC. Thus, most of the hydrophobic patch residues remain un-exposed. Therefore, in cardiac muscle both the binding of Ca^{2+} to site II and interaction with the cTnI switch-peptide are required to keep NcTnC in a stable open state (Oleszczuk *et al.*, 2010; Sheldahl *et al.*, 2003) (figure 1.19-B). In support of this idea, previous NMR studies showed an interaction between cNTnC and the cTnI region 147-163 in both the apo Ca^{2+} -free state and the Ca^{2+} -saturated state (Li *et al.*, 1999; Spyrapoulos *et al.*, 1997). These studies confirmed that the conformation in the cNTnC state upon Ca^{2+} binding is similar to the conformation of the apo state.

Troponin C interacts with both TnI, the inhibitory subunit, and TnT the tropomyosin binding subunit, on the actin-tropomyosin thin filament (Figure 1.16). According to Gaele *et al.* 2000, the cTnC-cTnI interaction is extensive involving six interaction sites, which are affected by Ca^{2+} . A stable binary complex is formed by the antiparallel interaction of the C-terminal domain of cardiac troponin C (cTnC) comprising residues 81-161 and the N-terminal domain of cardiac troponin I (cTnI) comprising residues 33-80 (Frank *et al.*, 1992),

and the NH₂-domain of cTnC has been shown to interact with cTnI (147-163). The interactions between TnC and TnI contribute to stabilizing the open conformation of cNTnC by interfering with the AB helical interface resulting in a series of conformational changes in the troponin complex that plays a key role in the regulation of muscle contraction (Figure 1.19 A and B) (Li et al.1999). In term of interaction of troponin C with Troponin T, two TnT peptides containing residues 160–193 and 228–260, bind to the C domain of cTnC (Blumenstein et al.2001). This study also suggested that there is a competition between TnT and TnI inhibitory region, to bind TnC. while the first 40 residues of TnI bind to TnC simultaneously with TnT-(160–193).

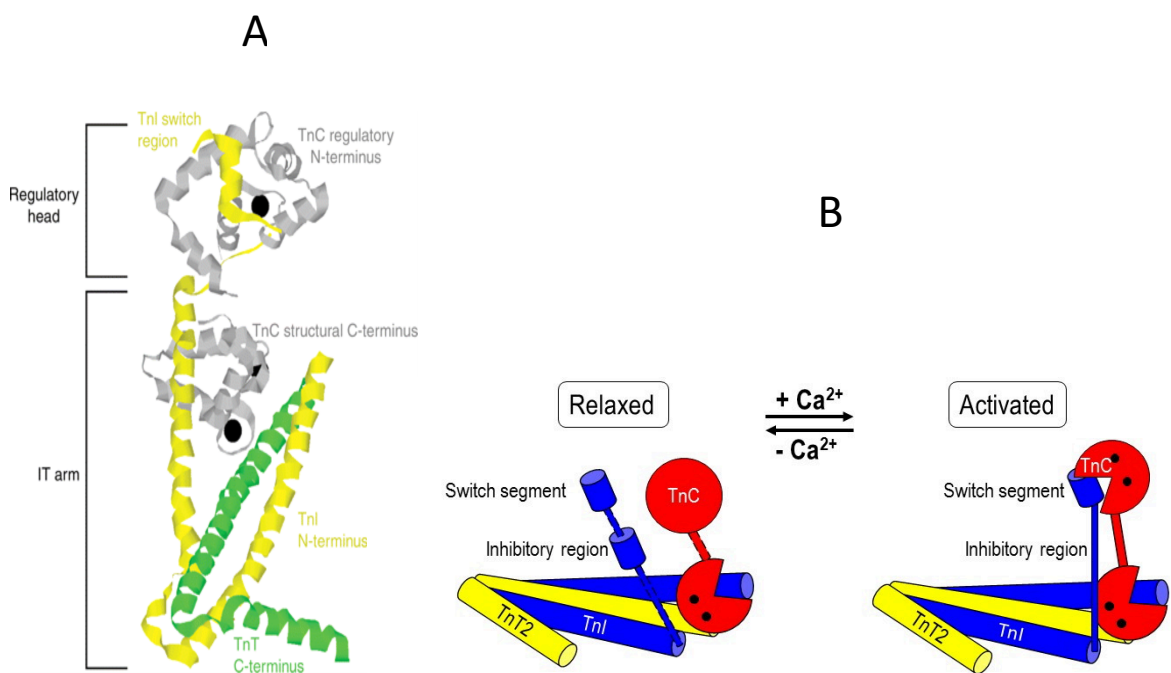


Figure 1.19: Ribbon structure of troponin (A) and conformational change of troponin upon Ca²⁺ activation (B).

Panel A represents the ribbon structure of troponin complex. TnC is shown in grey, TnI in yellow, and TnT in green. (B) The cartoon illustrates the conformational changes occurring in the troponin complex upon Ca²⁺ binding. TnI is shown in blue, TnC in red and TnT in yellow. Ca²⁺ is shown in black. Figure modified from the model proposed by (Sevrieva *et al.*, 2014).

1.5 The molecular basis of regulation of striated muscle contraction

1.5.1 The mechanism of striated muscle contraction

In striated muscle, regulation is achieved by long range conformational rearrangements in the various components of the thin filament that are propagated by end-to-end connections between adjacent tropomyosin molecules along the muscle thin filament. There are three factors that control this process. Firstly Ca^{2+} concentration, secondly the troponin macromolecular complex and thirdly the myosin cross-bridge that binds to the thin filament.

It is generally assumed that the thin filament system equilibrates very fast with Ca^{2+} (much faster than the mechanical events of contraction and relaxation). Therefore, it must bind with fast Ca^{2+} association and dissociation rates (Chalovich, 2002). Moreover, the binding of Ca^{2+} to TnC plays a significant role in modulating the rate of myofilament inactivation and force generation in both skeletal and cardiac muscle (Chalovich, 2002). Ca^{2+} controls the activation and relaxation of cardiac myofilaments and coordinate interactions between the thin and thick filaments. The thin filament is activated when Ca^{2+} binds to cardiac troponin C (cTnC). Consequent interactions between troponin (Tn) subunits result in an increase mobility of tropomyosin and an increase of the probability of myosin interaction with actin (A. M. Gordon *et al.*, 2000). In cardiac muscle, strong myosin binding to actin moves tropomyosin and raises Ca^{2+} binding affinity to troponin (Geeves & Lehrer, 1994; Holmes *et al.*, 1990). This mechanism is essential for rapid thin filament activation and force development in cardiac muscle.

In the most basic sense, the metal dependent interaction between cTnC and cTnI plays a critical structural and functional role in the regulation of muscle contraction. Cardiac

troponin C has a binary function in the contraction of the heart muscle. Its interaction with cTnI is responsible for the release of ATPase inhibition whereas, its interaction with cTnT is responsible for the activation of ATPase. The interaction between cTnC and cTnI is enhanced by the binding of Ca^{2+} to N-terminal domain (the regulatory sites). This interaction leads to the dissociation of the main inhibitory region of the cTnI. Because of that the binding of Ca^{2+} to TnC neutralizes the inhibition of the actin-activated myosin Mg^{2+} -ATPase activity and trigger other interactions of TnI with TnT and Tm · actin. The two actin-binding sites, located on the C-terminal domain of TnI has been shown to act as a molecular Ca^{2+} -sensitive switch during muscle contraction since they move between Tm · actin and TnC in response to Ca^{2+} (Vassilyev *et al.*, 1998; Stone *et al.*, 1998). There are three type of interactions that take place between cTnC and cTnI in an antiparallel manner. The binding between the C-terminus of TnC and the N-terminus of TnI, which interacts with TnT as well, depends on having Ca^{2+} or Mg^{2+} bound to the Ca^{2+} - Mg^{2+} sites of TnC (site III and IV in cTnC). The second interaction is metal independent. The last interaction is the Ca^{2+} dependent between the N-terminus of TnC and the C-terminus of TnI and is the key interaction in the regulatory role of troponin. It depends on having Ca^{2+} in the specific Ca^{2+} binding site of the N-terminal of TnC (site II in cTnC). A conformational change occurs in TnC during this binding lead to the binding of the switch region of the C-terminal of TnI subsequently and results in the activation of the thin filament. As a consequence, Ca^{2+} control the interaction of the inhibitory regions of TnI which either interacts with actin and inhibits the actomyosin ATPase activity or interacts with TnC, releasing the inhibition and initiating contraction.

The myosin head region S1 is the molecular motor that associates with actin in thin filaments in a cyclic pattern to form cross-bridges and generate force (Corrie *et al.*, 1999).

In each cycle, myosin motor undergoes a series of conformational changes that result in myosin binding to actin and the subsequent power stroke. This cycle is powered by ATP hydrolysis. The binding of ATP to the actomyosin complex leads to the myosin dissociation from actin. In cardiac muscle, it is believed that the release of ADP follows the power stroke and that ADP should be released before another ATP can associate and induces the detachment of myosin (Nyitrai & Geeves, 2004; Gordon *et al.*, 2001). These studies are in good agreement with another study which showed that the rise in the concentration of ADP results in a slower rate of relaxation (Poggesi *et al.*, 2005). Thus, Ca^{2+} dissociation from the regulatory unit troponin C and cross-bridge detachment from actin together induce muscle relaxation.

1.5.2 Regulation of muscle contraction

1.5.2.1 The role of calcium in the regulation

Contraction and relaxation cycle of the heart is regulated by intracellular calcium. This cycle is controlled by calcium release/uptake by the sarcoplasmic reticulum in response to changes in membrane action potential. The changes in concentration of Ca^{2+} are relatively modest from around 0.1 micromolar at rest to few micromolar upon calcium release from the sarcoplasmic reticulum. The binding of Ca^{2+} to TnC (one of calcium receptors) initiates a set of conformational changes on thin filament that ultimately lead to the activation of muscle (as measured by change in actomyosin ATPase or force) (Gordon *et al.*, 2000). The Ca^{2+} sensitivity (the relationship between the concentration of Ca^{2+} and various contractile parameters such as actomyosin ATPase, force, *in vitro* motility...) is sigmoidal allowing full activation to take place over this narrow change in calcium concentration. This sigmoidal shape is a signature that thin filament acts as a cooperative allosteric

system. This behavior implies cooperation between subunits of a multimeric macromolecular complex following initial activation. This has been explained by the existence of two conformations. An OFF conformation that has a low biological activity and an ON conformation that has a high biological activity. Although this model was successfully able to explain the equilibrium binding however it was not able to define the effect of troponin-tropomyosin on the kinetics of S1 binding to actin (Hill et al., 1980).

1.5.2.2 Thin filament switches between three different states

Muscle contraction is controlled by tropomyosin-troponin on-off switching mechanism. This mechanism is a complex cooperative and dynamic process with highly nonlinear behavior. McKillop and Geeves explained the dual inhibitory and potentiating effects of tropomyosin on actin-activation of myosin ATPase in part by the ability of thin filaments to exist in equilibrium between three different functional states: a blocked state, a closed state and an open state. In this model, relative occupancy of these states is biased by the respective effects of troponin, Ca^{2+} binding and myosin-interactions. Kinetic modeling of this process suggested that the blocked state is obtained when both myosin and Ca^{2+} are released from thin filament. While the closed state is promoted by Ca^{2+} binding to the troponin complex and releasing the inhibition induced by troponin I. In this state, S1 is able to bind weakly with actin because the troponin-tropomyosin complex moves to the groove, between the inner and outer domains of actin. However, the actomyosin ATPase is still inhibited and the muscle is in a relaxed state. Finally, the open state is induced by myosin head strong binding to actin and the subsequent movement of the troponin-tropomyosin complex to the inner domain of actin exposing all the S1 binding sites (figure 1.20). Consequently, the actomyosin ATPase is activated and the muscle is in a contracted

state. This process is characterized by the coupling of tropomyosin and myosin binding to actin which could accentuates the cooperativity since each may enhance the affinity of the other.

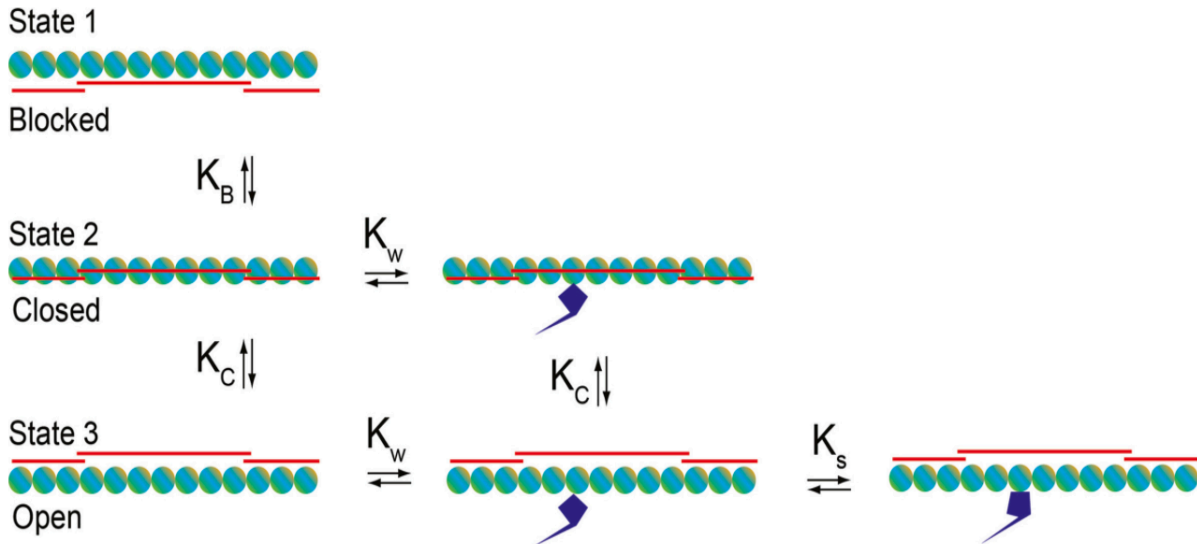


Figure 1.20: Schematic diagram of the McKillop-Geeves three-state regulatory model of the thin filament.

Thin filament regulatory units represented by a single line depicting tropomyosin (red) over seven circles representing actin (aquamarine/tan); myosin is drawn as blue S1-like objects. Thin filaments are shown in three states: Blocked, closed and open states. The dynamic equilibrium between states is illustrated as a movement of tropomyosin on actin and an isomerization of myosin into a strongly attached configuration. K_B and K_C correspond to the equilibrium constants between blocked and closed states and closed and open states respectively. K_W and K_S represent equilibria for initial weak and then strong myosin binding steps on actin

1.5.2.3 The role of troponin C in the contraction heart muscle

Under physiological conditions, the binding of Ca^{2+} to the regulatory unit troponin C functions as a gatekeeper for contraction of muscle. Many interactions among the subunits of troponin complex are controlled by Ca^{2+} . These interactions include the binding between cTnI and actin, cTnT and Tm for stabilizing the cTn complex onto thin

filament. A decrease of the Ca^{2+} concentration results in Tm covering the myosin head binding sites on the actin. At low $[\text{Ca}^{2+}]$ or in other words when Ca^{2+} dissociates from cTnC the cTnT1 and the two-inhibitory regions on cTnI controls the movement of Tm to cover the myosin head binding sites on thin filament. On the other hand, the cTnC lobe, which represent the regulatory domain of cTn complex and is connected to the rest of cTn complex by D/E-linker, search to bind the switch peptide of cTnI₁₄₇₋₁₆₃ by turning around its center D-helix and its binding to cTnI₁₄₇₋₁₆₃ throws the hydrophobic surface of the N-terminal of cTnC. Binding of Ca^{2+} to the cTnC alone is not able to switch the N terminal of cTnC to the open state. Both cTnI switch peptide binding to cTnC and Ca^{2+} are needed to stabilize the open state.(Li *et al.*, 1999). In support of this idea, NMR studies showed that the binding of Ca^{2+} to N regulatory lobe in site II leads to an opening of this site partially. The fully open state is reached when the C-terminal of TnI bind to the N-terminal of cTnC. As a consequence, cTnC would switch the inhibitory region and cTnI from their actin binding inhibitory sites. Troponin-tropomyosin will move to the grooves between inner and outer domains of actin. As a result of all these conformational changes in thin filaments, myosin binds actin weakly (Lehman *et al.*, 2000). Strong binding between actin and S1 to generate force accrues when S1 binding pushes the troponin-tropomyosin further more to the inner domain of actin (Kobayashi *et al.*, 2008; Stehle *et al.*, 2007; Solaro *et al.*, 2008). It is clear that the conformational dynamics of the cTnC upon Ca^{2+} -activation plays a critical role in the regulation of cardiac muscle contraction. On the other hand, the IT arm of cTn complex is fixed during activation. This fact suggests that the C-terminal of cTnC and coiled-coil helices of cTnT and cTnI function as a scaffold holding cTnC and actin binding regions of cTnI.

Kinetic studies showed that dysfunction of TnC results of altered Ca^{2+} binding properties. Evidence for this is supported by the fact that mutations in TnC which can result in cardiomyopathies affect Ca^{2+} sensitivities (Liu *et al.*, 2012). Thus, the rate of Ca^{2+} dissociation from TnC dominates the modulation of the rate of cardiac muscle relaxation. In contrast, it is not clear if cTm or actin in absence or presence of myosin can have an impact on the kinetics of the Ca^{2+} dissociation from TnC (Tomoyoshi Kobayashi & R. John Solaro, 2006; ROBINSON *et al.*, 2004).

1.5.2.4 The role of TnC in the relaxation of the heart

In the physiological context of the heart, the relaxation phase (diastole) is the process of returning of active heart muscle to its initial conditions of the load and length. Relaxation initiates with the active removal of the cytosolic Ca^{2+} by pumped Ca^{2+} back into the SR by SERCA and pumped out of the cell by NCX (Bers & Ginsburg, 2007). The decline in the concentration of Ca^{2+} result in dissociation of Ca^{2+} from TnC and then inactivate the thin filament. The inactive filament result of intracellular processes leading to reducing the Ca^{2+} concentration from 10^{-5}M to 10^{-7}M and dissociation of actomyosin cross bridges. As previously mention, Ca^{2+} dissociation from TnC and cross-bridge detachment from actin control the inactive thin filament (Stehle & Iorga, 2010; Janssen *et al.*, 2002; Brittsan & Kranias, 2000). The decline of the intracellular of Ca^{2+} concentration result in dissociation of Ca^{2+} from TnC and leading to reduce the binding between TnC and TnI. As a result of that TnI rebind actin and this rebinding inhibits the movement of Tm and holds Tm in the blocked state (Chalovich, 2002). On the other hand, during the process of inactivation of thin filament myosin continues to progress through the cross-bridge cycle to maintain pressure once the cross-bridge has dissociated from actin and the intracellular Ca^{2+} concentration is decreased, the myosin cross-bridge cycle is tentatively disconnected

because of the inability of myosin to bind actin. Therefore, myosin binding to actin is inhibited by the inactivation of thin filament.

Rapid and complete relaxation is prerequisite for keeping the heart functioning properly. Modulation of the rate of relaxation could be affected by loading conditions, inotropic stimulation, and heart rate. For example, a reduction of the rate of relaxation means the heart would not be able to fill with an adequate volume of blood before the next contraction. The rate of relaxation is limited by the rate of Ca^{2+} dissociation from troponin C and Tn-Tm interaction with actin crossbridge properties (the number of and kinetic of function cross bridges) (Chemla *et al.*, 2000). The rate of Ca^{2+} dissociation is controlled by the affinity of troponin C for Ca^{2+} , Ca^{2+} up take back into the SR, $\text{Na}^+/\text{Ca}^{2+}$ exchange, sarcolemmal Ca^{2+} ATPase, and Ca^{2+} buffer. It is clear from above that the modulation on TnC either by alter the Ca^{2+} binding properties (Ca^{2+} dissociation rate under conditions of physiological regulation) or alter the protein-protein interaction of TnC with the binding partners in thin filament has crucial role in organization the relaxation of the heart muscle.

1.6 TnC mutations

Recently, genetic studies have shown that genetic cardiomyopathies (HCM and DCM) are caused by mutations in the cTnC gene. Cardiomyopathies disease's association with mutations in cTnC points to the key role played by cTnC in the heart. The question that remain to be answered is how the cTnC mutations can alter the function of troponin C. Alterations in the contractile function because of these mutations may result by two ways (figure 21). Firstly, change in the intramolecular dynamic of cTnC and this change could cause either from changes in the size or duration of the Ca^{2+} transient (The rate of Ca^{2+}

dissociation from cTnC) and/or changes in myofilament response to Ca^{2+} . Secondly, alteration of the interaction of cTnC with its binding partners. Thus, how these mutations affect cTnC structure, function, and role in the activation and relaxation of cardiac thin filaments are important for a full understanding of the onset and progression of these diseases.

In next section, we discuss the eight cTnC mutation linked to HCM and DCM and investigated in this project. These mutations classified into two groups, those located in the Ca^{2+} binding sites (A31S, D75Y, D145E, I148V) and those outside of the Ca^{2+} binding sites (Y5H, A8V, E59D, C84Y). Figure 1.22 shows the location of these eight mutations in the troponin C structure.

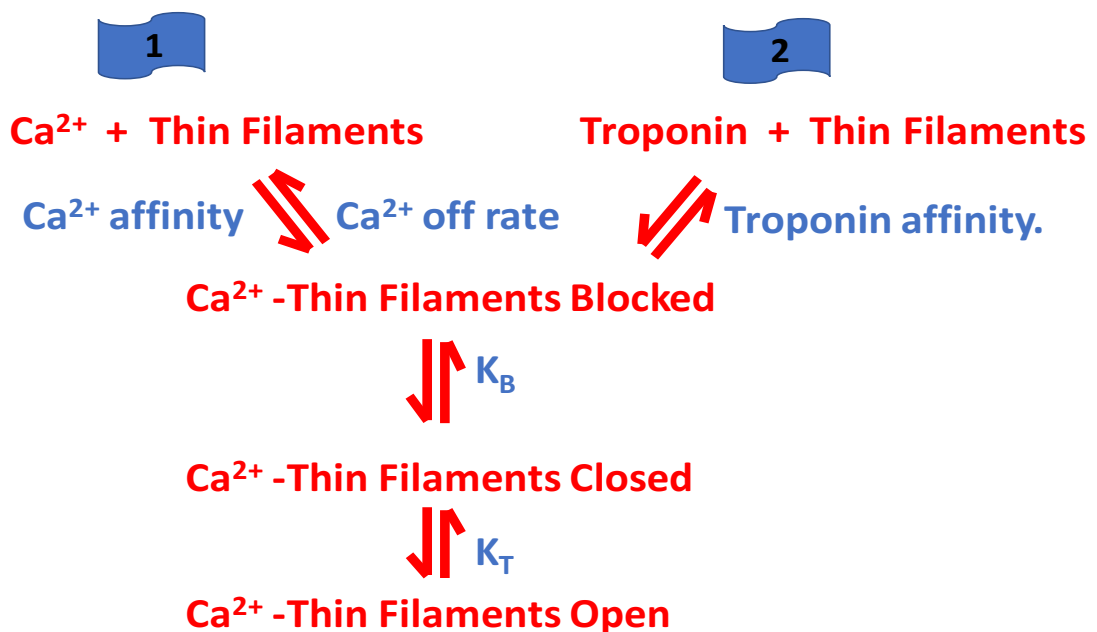


Figure 1.21: A diagram illustrating the various steps in thin filament cooperative allosteric activation that could be affected by TnC mutations.

Diagram representation of the elementary steps (millisecond timescale) alteration in contractile could be affected by cTnC mutations. Mutations on cTnC could possibly affect the function of troponin by two ways. (1) change intramolecular dynamic of cTnC and this change could cause alterations in the Ca^{2+} binding affinity of cTnC or Ca^{2+} dissociation off rate. (2) Alter the interactions of the TnC with its binding partners.

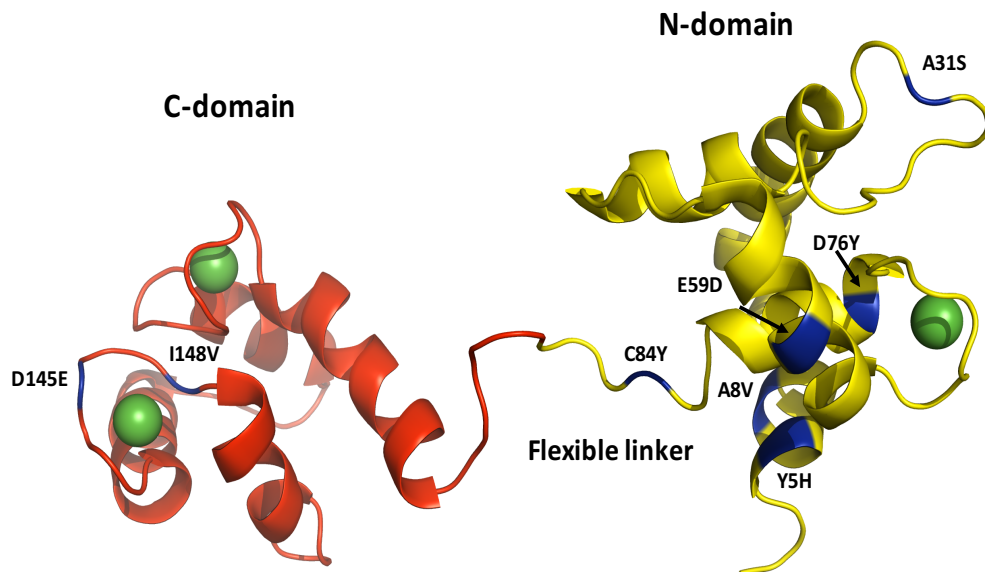


Figure 1.22: Location of cTnC mutations in the 3D structure of troponin C.

The NMR structure of Ca^{2+} saturated cardiac troponin C of *Gallus gallus* (1AL0). The mutations (blue) are spread through the N-domain (yellow) and C-domain (red), green spheres depicted Ca^{2+} binding sites loops and figure generated by using PyMOL.

1.6.1 Y5H

The TnC Y5H mutation was found in a patient that developed heart failure. This mutation is situated at the N-domain of TnC at helix N as shown in figure 1.22. (Pinto et al., 2011b; Hershberger et al., 2010). Several biochemical, biophysical and mechanical studies have been performed on this mutation. Experiments using skinned porcine cardiac fibers found that fibers reconstituted with Y5H showed decreased Ca^{2+} sensitivity of force development in comparison with TnC WT fibers (pCa50 values of 5.53 and 5.61 respectively). However, upon PKA phosphorylation, both fibers showed a similar Ca^{2+} sensitivity of force development, suggesting that Y5H did not respond to PKA to the same extent as the WT (-0.07 and -0.12 respectively). On the other hand, the activation and inhibition of the actomyosin ATPase activity is not affected by Y5H. From a structural point of view, Y5H appears to be different compared to the WT because circular

dichroism, in the apo, Mg²⁺ and Ca²⁺/Mg²⁺ states showed that Y5H had reduced alpha-helical content compared to the WT (Pinto et al., 2011).

1.6.2 A8V

The TnC A8V mutation was discovered in 2008 in a patient with 18 mm left ventricular wall thickness (Landstrom *et al.*, 2008). A8V is located in the N helix at a region essential for the structural stability of Tn complex and for the Ca²⁺ affinity of TnC (Figure 1.22). Reconstituted porcine cardiac fibres, demonstrated that fibres containing A8V mutant had higher Ca²⁺ sensitivity of force development than fibres which reconstituted by WT human cTnC (pCa₅₀ 6.02 and 5.66 respectively) (Pinto *et al.*, 2009). This is in agreement with ATPase experiments where A8V reconstituted thin filaments had increased Ca²⁺ sensitivity compared to WT TnC (+0.51) (Pinto *et al.*, 2009). Moreover, the reconstituted thin filaments containing A8V mutant were not significantly different from the filaments containing WT in inhibiting the actomyosin ATPase activity in the absence of Ca²⁺ (Pinto *et al.*, 2009; Albury *et al.*, 2012a). Furthermore, Swindle and Tikunova showed that this mutation had no effect on Ca²⁺ binding at the C-terminal sites III and IV compared to the WT (Swindle & Tikunova, 2010a). Additionally, this study measured the rate of Ca²⁺ dissociation from C-terminal sites using stopped-flow methodology and the measurement showed that A8V had no impact on Ca²⁺ dissociation rate constant compared to WT (Swindle & Tikunova, 2010). The Ca²⁺ affinity of A8V was similar to Ca²⁺ affinity of WT at the N-terminal site at high [Ca²⁺] and at low [Ca²⁺] A8V showed a small reduction in Ca²⁺ affinity at the C-terminal sites compared to WT while the Ca²⁺ affinity of A8V within the Tn complex and within the thin filament showed a significant increase in comparison to

thin filaments reconstituted with WT TnC (6.27 vs. 6.13 respectively)(Pinto *et al.*, 2009). This study is in good agreement with the last study in 2017 (Charles M. Stevens *et al.*, 2017) which demonstrated that the Ca^{2+} affinity of A8V TnC measured by ITC is close to WT TnC. Moreover, a recent NMR report measuring the paramagnetic relaxation enhancement derived distances showed that A8V affect the Ca^{2+} binding mechanism and lead to a more open conformation compared to WT in both the apo and holo states (Charles M. Stevens *et al.*, 2017). Furthermore, A8V has significant effect on the TnC-TnI interaction according to Henry G.Zot et al 2016 (Zot *et al.*, 2016). They illustrated that the A8V cause a delay in the rate of Ca^{2+} dissociation from TnC and this result in altering the interaction between TnC and TnI.

1.6.3 A31S

The TnC A31S mutation was discovered in a five years old boy with episodes of ventricular fibrillation and with a negative family history for HCM or sudden cardiac death. The genetic study showed he had a G > T mutation at nucleotide 91 in the TNNC1 gene (Parvatiyar *et al.*, 2012). A31S is located in the Ca^{2+} binding site I (the non-functional site in cTnC) at the N-terminal domain (figure 1.22) and as shown in figure 1.17-B, it is one of the Ca^{2+} coordination sites (A31) in position (+Y) (figure 1.18-C). Mechanical studies showed that Ca^{2+} sensitivity of force development increased in porcine fibers reconstituted with A31S (+0.17 pCa units) compared to WT TnC. Additionally, A31S reconstituted in thin filaments in the presence of Ca^{2+} increased the activation of the actomyosin ATPase compared to filaments containing WT TnC while in absence of Ca^{2+} the inhibition of the actomyosin ATPase was similar to WT. Moreover, A31S thin filament increases the Ca^{2+} sensitivity of ATPase activity by +0.38 pCa units in comparison to WT

(Parvatiyar *et al.*, 2012). Furthermore, Parvatiyar *et al.* 2012 illustrated that the Ca^{2+} affinity increased for A31S reconstituted in isolated TnC ($\Delta\text{pCa}_{50} +0.17$), A31S reconstituted in Tn complex ($\Delta\text{pCa}_{50}+0.27$), A31S reconstituted in thin filament ($\Delta\text{pCa}_{50} +0.54$), or A31S reconstituted in thin filament and in presence of S1 ($\Delta\text{pCa}_{50} +0.21$) (Parvatiyar *et al.*, 2012). These data are in disagreement with a recent study in 2017 (Charles M. Stevens *et al.*, 2017) which tested the Ca^{2+} affinity for A31S reconstituted in isolated TnC using isothermal titration calorimetry (ITC) and the results showed that the Ca^{2+} affinity for N-TnC mutant with A31S was close to N-TnC WT (K_d 11.8 μM and 14.9 μM respectively). Structurally, the biochemical characterization showed that the A31S has no impact on the structure of TnC. The result of ITC showed that the Apo, Mg^{2+} bound, and $\text{Mg}^{2+}/\text{Ca}^{2+}$ bound states A31S are similar to WT cTnC (Parvatiyar *et al.*, 2012). The effect of A31S on the interactions between TnC and TnI tested using Molecular Dynamics (MD) simulation suggests that A31S had a pronounced impact on the contacts between the N-terminal region of TnI_{sw} and the N-helix of TnC than WT (Charles M. Stevens *et al.*, 2017)

1.6.4 E59D

TnC E59D was found in a DCM patient (Lim *et al.*, 2008). This mutation is located in helix C near the Ca^{2+} binding site II in the regulatory domain of cTnC (figure 1.22). This region is important in fine tuning Ca^{2+} binding to the regulatory site (Leblanc *et al.*, 2000). The contractility of electrically stimulated E59D transfected myocytes was observed by video-edge detection and the results showed that the number of cell shortening decreased significantly compared to WT transfected myocytes (1.5 vs. 3.2)(Lim *et al.*, 2008). Moreover, Lim *et al.* 2008 showed that the skinned porcine cardiac fibers reconstituted with E59D have a decreased Ca^{2+} sensitivity of force development (by 0.3 pCa units) compared to

WT (Lim *et al.*, 2008). Furthermore, cardiac myofibrils reconstituted with E59D have reduced Ca^{2+} sensitivity of ATPase activity. In spite of the fact that E59D reconstituted in thin filament had no impact on the inhibition of ATPase activity in the absence of Ca^{2+} it activated the actomyosin ATPase activity in the presence of Ca^{2+} to lower levels compared to the WT controls (Dweck *et al.*, 2010). The Ca^{2+} binding affinity of the regulatory site of for E59D reconstituted with TnI, TnI and TnT, and in fully reconstituted thin filament had been tested by Dweck et al. 2010. The results showed that in all three complexes the Ca^{2+} binding affinity has been reduced in comparison to WT (ΔpCa_{50} -0.65, ΔpCa_{50} -0.9, and ΔpCa_{50} -0.36 respectively) (Dweck *et al.*, 2010). The structural effect of E59D has been examined using NMR spectroscopy and the data showed that E59D produced NMR spectra very similar to WT.

Baryshnikova et al. 2008a showed that E59D-TnC binds TnI₁₄₇₋₁₆₃ tighter than WT-TnC (60 vs. 154 μM) (Baryshnikova *et al.*, 2008). However, the affinity binding of E59D with TnI₁₄₇₋₁₆₃ increased by 4.8-fold in comparison to WT when in complex with the dP-TnI₁₋₂₉, while in the presence of P-TnI₁₋₂₉ peptide the binding affinity decreased and the K_d increased by 13.8-fold compared to WT (Baryshnikova *et al.*, 2008).

1.6.5 D75Y

TnC D75Y was found in a DCM patient (Lim *et al.*, 2008). It is very similar to E59D in term of the effect of this mutation on the function of TnC. D75 is located in the Ca^{2+} binding site II (figure 1.22). TnC D75Y also reduces the Ca^{2+} sensitivity of force development producing a rightward shift of the Force-pCa curves by 0.3 pCa unit in comparison to WT, reduces the Ca^{2+} sensitivity of ATPase activity with pCa_{50} value 5.95, and activates the actomyosin ATPase activity in the presence of Ca^{2+} to lower levels compared to the WT

but in absence of Ca^{2+} it has no impact on the inhibition of the actomyosin ATPase activity (Dweck *et al.*, 2010). Moreover, the Ca^{2+} binding affinity of the regulatory site has been reduced for D75Y in complex with TnI, TnI and TnT, and fully reconstituted thin filament in comparison to WT (ΔpCa_{50} -0.65, ΔpCa_{50} -0.9, and ΔpCa_{50} -0.36 respectively)(Dweck *et al.*, 2010). This study also measured the Ca^{2+} binding to the low and high Ca^{2+} affinity sites using IAANS labelled TnC at both Cys (35 and 84) and the result showed that the Ca^{2+} binding affinities of D75Y were reduced for both sites compared to WT (by a ΔpCa_{50} -0.18 for both sites). Furthermore, structurally D75Y is similar to WT, both of them produced very similar NMR spectra (Baryshnikova *et al.*, 2008).

On the basis of the location of D75Y, which is in the Ca^{2+} binding site II and that might be the direct cause of lowering the Ca^{2+} binding affinity in site II, and as a consequence affect the TnC-TnI interaction. Therefore, many studies measure the binding affinity between the switch region of TnI and TnC. According to Baryshnikova *et al.* the titration of TnI₁₄₇₋₁₆₃ with D75Y-TnC produced similar chemical shift changes as binding to the WT-TnC suggesting that the peptide bound in similar manner to the same site. However, the binding affinity of TnI₁₄₇₋₁₆₃ higher than WT by 2.6-fold (Baryshnikova *et al.*, 2008). Recently, Sukriti Dewan *et al.* showed that the rate of Ca^{2+} dissociation of NcTnC-D75Y was significantly reduced by more than 50-fold in comparison to WT (5×10^6 M.s and 3.1×10^8 M.s respectively) (Dewan *et al.*, 2016). Since the intramolecular conformational changes triggered by Ca^{2+} binding and result in association of the cTnI switch peptide it is critical to investigate the kinetics of the opening and closing of the cTnC hydrophobic patch. The best description of the degree of opening of the hydrophobic patch is the interhelical angle between helices A and B (Wang *et al.*, 2002). Sukriti Dewan *et al.* have used microsecond molecular dynamics simulation to clarify the hydrophobic patch opening

behavior of NcTnC-D75Y. The qualitative analysis showed that NcTnC-D75Y had similar behavior to the NcTnC-WT with an open conformation ($\sim 150^\circ$) (Dewan *et al.*, 2016). However, the A/B interhelical angle, determined experimentally was around 90° . In the same time this study (Dewan *et al.*, 2016) demonstrated that D75Y causes opening to A/B interhelical angles between 110° and 130° then the WT.

1.6.6 C84Y

TnC C84Y was initially detected in a 17 years old patient associated with 19 mm left ventricular wall thickness and with the symptom of syncope on exertion (Landstrom *et al.*, 2008). C84Y is situated at the N-terminal domain of cTnC at the end of Helix D and at the beginning of the central helix (Figure 1.22). Based upon this position C84Y might play an essential role in the stabilization of the open conformation of cTnC when bound to cTnI (Li & Hwang, 2015) and could alter the function of the critically important positioning of the cTnC N-domain (Hwang *et al.*, 2014). Biochemical studies have shown that C84Y increased the Ca^{2+} sensitivity of force development (Landstrom *et al.*, 2008). This result is in excellent agreement with a recent study (Jose R. Pinto *et al.*, 2017). Furthermore, Jose R. Pinto *et al.*, 2017 reported that reconstituted cTnC- C84Y in bovine myofibrils have a reduced ATPase activity at high $[\text{Ca}^{2+}]$. This study is in disagreement with the previous study showed that the activation and inhibition of actomyosin filaments contacting TnC- C84Y was similar to actomyosin filaments contacting TnC-WT (Hershberger *et al.*, 2010). Although, isolated C84Y reduce the Ca^{2+} affinity at the C-terminal sites with pCa_{50} values of 6.92 compared to WT with 7.06 values, C84Y has no impact on the Ca^{2+} binding affinities for the N-domain site II (Hershberger *et al.*, 2010). However, a recent study showed that the Ca^{2+} affinity of NcTnC-C84Y, as measured by ITC increase by 3-fold

compared to NcTnC-WT (Charles M. Stevens *et al.*, 2017). On the other hand, The Ca^{2+} sensitivity of the actomyosin ATPase activity of reconstituted myofilaments either containing 100% C84Y mutant protein or a 50:50 mixture of C84Y and WT cTnC increased significantly producing a shift by +0.56 pCa units to the left of the ATPase-pCa curve (Hershberger *et al.*, 2010) .

Structural changes of cTnC due to C84Y were measured using Circular dichroism (CD). The CD results showed that the C84Y mutant reduced the α -helical content in comparison to the WT whereas there was no significant difference between C84Y and WT TnC in the Mg^{2+} bound or the $\text{Mg}^{2+}/\text{Ca}^{2+}$ bound states (Hershberger *et al.*, 2010).

1.6.7 D145E

TnC D145E was found in a patient diagnosed with 22 mm of left ventricular wall thickness and a family history of HCM. D145E is located at the C-terminal domain of cTnC (figure 1.22), in the binding pocket of site IV and it is one of the Ca^{2+} coordination sites (D145) at position (+Z) (figure 1.18). Many studies have shown that D145E produces a great impact on either the function of TnC or TnC-D145E reconstituted in Tn complex. According to Landstrom *et al.* 2008, D145E reconstituted in porcine cardiac fibers shift the force pCa curve to the left in comparison to WT by a ΔpCa_{50} of +0.24 (pCa_{50} values being 5.898 and 5.657 respectively). Moreover, D145E fibers increase the force recovery percentages (70.3%) compared to WT (59.1) (Landstrom *et al.*, 2008). Furthermore, Pinto *et al.* 2009 showed that there is a significant increase in the Ca^{2+} - sensitivity of ATPase activity of the thin filament reconstituted with D145E mutant compared to WT TnC (Pinto *et al.*, 2009). Pinto *et al.* 2009 also showed that this mutation lead to an increase in the ATPase-pCa curve compared to the WT, with Hill coefficients of 3.99 and 2.14 respectively.

Interestingly, the result above were similar whether they used a 50:50 mixture of WT and D145E TnCs or a protein solution containing 100% of D145E. This suggests that the D145E has a dominant effect.

In agreement with the previous studies Baxley et al. showed that D145E increases the Ca^{2+} affinity and modify the distribution of regulated actin states (Baxley *et al.*, 2017). These authors suggested that TnC D145E stabilizes the Open state of regulated actin. Thus, the stabilization of the open state produce by D145E can explain the increase of the affinity of TnC-D145E for Ca^{2+} . Moreover, Pinto et al. 2011a determined the Ca^{2+} dissociation rates (k_{off}) from TnC D145E reconstituted in Tn complex and incorporated in thin filament using stopped flow methodology. TnC D145E incorporated in the Tn complex has a reduced Ca^{2+} -dissociation rate constant in comparison to the WT (14.6 s^{-1} and 18.95 s^{-1} respectively while, incorporation of TnC D145E in thin filaments increased the Ca^{2+} -dissociation rate constant when compared to the WT (129 s^{-1} vs. 96 s^{-1}) (Pinto *et al.*, 2011).

Circular dichroism experiments (CD) showed differences in the structure of cTnC D145E is comparison to WT. The CD data showed that D145E decrease the alpha-helical content in its Apo and $\text{Mg}^{2+}/\text{Ca}^{2+}$ bound states, in comparison to WT. Swindle and Tikunova 2010 monitored the affinity of D145E and WT TnC for a TnI₁₂₈₋₁₈₀ peptide (both the switch and the inhibitory regions) by titrating the cTnI₁₂₈₋₁₈₀ peptide into IANBD labelled TnCs at Cys53 and the result showed that D145E decreased the affinity for the TnI peptide by 8-fold compared to WT. However, the interaction of TnC with cTnI₁₂₈₋₁₈₀ is Ca^{2+} -dependent and, as mentioned before D145E had different Ca^{2+} binding properties. As a consequence, TnC D145E had different binding affinity for the TnI peptide when compared to the WT.

1.6.8 I148V

A patient diagnosed with DCM since childhood was subjected to genetic testing, which revealed that DCM was inherited from the mother caused by the I148V mutation in cTnC (Hershberger *et al.*, 2010) . This residue is located in the $\text{Ca}^{2+}/\text{Mg}^{2+}$ binding site IV at the C-domain of TnC as shown in NMR structure in figure 1.22 and it is one of the Ca^{2+} coordination sites (I148) at position (-Z) as shown in figure 1.18-B and C.

Structurally, I148V appears different compared to WT because the CD result showed that I148V decrease the alpha-helical content compared to WT in its apo and Mg^{2+} states. However, in the $\text{Ca}^{2+}/\text{Mg}^{2+}$ -bound state TnC I148V was not significantly different in comparison to WT. Moreover, the previous study showed that the fibers reconstituted with I148V reduce the Ca^{2+} sensitivity of force development in comparison to fibres reconstituted with WT. On the other hand, I148V activates and inhibits the actomyosin ATPase activity to the same level with the WT (Pinto *et al.*, 2011a) . Furthermore, I148V had no impact on the Ca^{2+} sensitivity of force development.

1.7 Aim of study

Previous work in our laboratory has investigated mutations in the troponin I (Sameeh Al-Sarayreh, PhD thesis, University of Leicester) and troponin T (Zimna Wazeer, PhD thesis, University of Leicester) linked to hypertrophic and dilated cardiomyopathy. In this project, I aimed to study mutations in troponin C associated with hypertrophic and dilated cardiomyopathies.

I used transient kinetics to assess the impact of cTnC mutations on single step reactions that take place during activation or de-activation of myofilament. The mutations studied in this project were classified into two types.

- I. A group of mutations located in the Ca²⁺ binding sites (A31S, D75Y, D145E, I148V)
- II. A group of mutations located outside the Ca²⁺ binding sites (Y5H, A8V, E59D, C84Y)

In TnC there are four loops for Ca²⁺ binding. Each loop contains 12 residues. The residues at positions 1,3,5,7 and 12 provide seven oxygen atoms in pentagonal bipyramidal geometry that serve as ligand for Ca²⁺ binding (figure 1.18). I hypothesised that the mutation located in the Ca²⁺ binding site I (A31S) may activate this Ca²⁺ binding site and consequently may increase cTnC Ca²⁺ affinity and cardiac thin filament Ca²⁺ sensitivity. (figure 1.18-A). D75Y which is located in loop 2, could affect the Ca²⁺ affinity and Ca²⁺ dissociation rate constant because it is in EF- hand loop even if it is not in a coordinating position for Ca²⁺ binding (figure 1.18-B).

Although in the mutant D145E the difference in chemical properties of the amino acids is not big, many studies identified them to cause heart diseases. We expect that the change from an aspartic acid to a glutamic acid could affect the structure of pentagonal bipyramidal arrangement. Glutamic acid residues contribute both of their side chain oxygen atoms to Ca²⁺ coordination while aspartic acid residues provide only their carbonyl oxygen atom. Consequently, we expect that D145E might increase cTnC Ca²⁺ affinity. On the other hand, the mutant C84Y, which is located in the D helix of the N-terminal regulatory lobe of troponin C, could affect the stability of troponin C because the N-terminal regulatory lobe is connected to the C-terminal structural lobe by a single alpha helical linker (Vinogradova et al., 2005) (Figure 1.22). This mutation could affect the hydrophobic interaction with other proteins.

The aim of this project is to understand, at the molecular level, how the above discussed mutations in TnC that caused cardiomyopathies alter the regulation of the cardiac

contractile cycle. The relationship between the Tm.Tn-controlled on/off state change of the thin filament as modulated by and the binding of myosin heads to actin, which occurs in two steps. In order to fully understand the significance of cardiovascular diseases associated mutation in TnC, an in depth study combining structural, kinetic and thermodynamic studies is needed. Therefore, we have chosen to study eleven TnC mutations in two ways:

- 1- Using transient kinetics and thermodynamics to assess the impact of TnC mutations on single step reactions that take place during activation or de-activation of myofilament.
- 2- Using NMR spectroscopy to study the effect of the mutations on the structure of troponin C.

Chapter 2

Materials and methods

2.1 Design the mutations

2.1.1 Primer Design

DNA mutations were introduced in primers chemically synthesized commercially and used in PCR reaction using the human cardiac TnC as template. The complete nucleotide sequence of human cardiac troponin C has been used to design the primers for each mutant. We designed forward primers and reverse primers for the mutations A31S, E59D, D75Y, C84Y. Only forward primers have been designed for the mutations at the start of the sequence Y5H and A8V while for the mutations at the end of the sequences, D145E and I148V, only reverse primers were designed. In addition, we designed wild type forward and reverse primers.

2.1.2 PCR

Human cardiac troponin C mutants were formed by overlapping extension PCR using hcTnC cDNA. Overlap extension PCR was carried out by Dr. Xiaowen Yang at the University of Leicester. Two primary PCR reactions were performed using either the forward wild type primer, the reverse mutant primer and the cTnC template or the reverse wild type primer, the forward mutant primer and the cTnT template for each mutant. The PCR products of this primary PCR reaction were used in a secondary PCR reaction for A31S, E59D, D75Y, C84Y, using the forward wild type primer and reverse wild type primer for each mutant. The product of this secondary PCR represented the cTnC mutants cloned into the bacterial expression vector (PLEICS-05).

2.1.3 Transformation

All troponin clones: human cardiac troponin T (cTnT), human cardiac troponin I (cTnI), and human cardiac troponin C (cTnC) wild type and cTnC mutants were transformed in competent cells BL21(DE3) pLysS and Top10. In sterile Eppendorf tubes about 2-4 μ l of

desirable construct DNA was transformed into 50µl competent cells. Then the tube flicked gently for mixing few times and incubated for 30 minutes in ice. The cells were heat shocked at 42 °C for 60 seconds without shaking and immediately the tube put back in ice for 2 minutes. The transformed cells were diluted in 250µl of autoclaved LB media and incubated at 37 °C with shaking at 220 rpm for 60-90 minutes. About 100µl of cell culture was then spread on LB agar plate with ampicillin antibiotic and incubated at 37 °C overnight.

2.1.4 Plasmid Mini Preps

A Wizard® Plus Miniprep kit (Promega) was used to purify troponin subunits wild type and TnC clones. From 1-10 ml, overnight cell culture was pelleted in a micro-centrifuge by spinning down for 5 minutes at 13,000 rpm at room temperature. The supernatant discarded and the pellet was then re-suspended in the various buffers as described in the protocol provided in the kit. The DNA was stored at -80 °C.

2.2 Protein purification from tissues

Sheep heart muscle was used as a source of cardiac muscle actin, tropomyosin, troponin, myosin, and myosin subfragment-1 (S1).

2.2.1 Cardiac myosin preparation

The method of Margossian and Lowey (Margossian and Lowey 1982) was used to prepare cardiac muscle myosin. Rabbit heart was dissected, cut, and placed at 4 °C. The muscle was minced and a double volume of Guba-Straub buffer (0.3 M KCl, 1 mM EDTA, 0.1 M K₂HPO₄, and 0.05 M KH₂PO₄) was added. This mixture was centrifuged at 6,000 rpm, using SLC 6000 rotor for 20 minutes. The supernatant was used for myosin preparation and the pellet kept to prepare an acetone powder. 14 volumes of cold water were added

slowly and with stirring to precipitate the myosin. The mixture was left overnight at 4 °C to allow the myosin to settle as a sediment. Water was sucked away and the remaining solution that contained the myosin was spun down at 5,000 rpm, using SLC 6000 rotor for about 10 minutes. The pellets were weighed and dissolved in 0.25 volume of (3 M KCl, 30 mM imidazole, pH 7.0). An equal volume of cold water was slowly added with stirring to precipitate the actomyosin. The mixture was spun down at 5,000 rpm, using SLC 6000 rotor for about 10 minutes (an extra cycle of precipitation might have needed if the size of the pellet was not small). To precipitate the myosin eight volumes of cold water were added to the supernatant and the mixture was spin down at 5,000 rpm, using SLC 6000 rotor for 10 minutes. The pellet was weighed and dissolved in 1.5 volumes of 3 M KCl, 2.5 mM DTT, 30 mM imidazole, pH 7.0. Then the Lowry method was used to determine the concentration of myosin. Then myosin was diluted with an equal volume of glycerol, thoroughly mixed and stored at -20 °C.

2.2.2 Preparation of sheep cardiac muscle acetone powder

Pardee's method was used to prepare the muscle acetone powder (Pardee 1982). The first pellets (3.5.1 Cardiac myosin preparation) have been washed by different water, sodium carbonate and acetone solutions. In each washing step, the pellet was stirred, filtered through a fine nylon mesh, and squeezed as dry as possible. The pellets were washed consecutively at 4 °C as follow: two times in ten volumes of cold water, one time in four volumes of 0.4% NaHCO₃, and finally four times with four volumes of cold acetone. Then the acetone powder was dried overnight at room temperature in the fume hood. The dry powder was weighed and stored at -20 °C.

2.2.3 Cardiac F-actin preparation

Sheep heart acetone powder was used to prepare cardiac F-actin (Spudich and Watt 1971). To each 1g of acetone powder was added 20ml of G-actin buffer (2mM Tris-HCl pH 8.0, 0.2mM ATP, 0.1mM CaCl₂, 0.5mM DTT, and 1 mMNaN₃). The mixture was stirred for 20 minutes at 4°C. Then it was spun down at 18,000 rpm for 20 minutes. The supernatant was taken and the pellets were re-extracted by another equal volume of G-actin buffer. After a second centrifugation at 18,000 rpm for 20 min, the supernatant was combined with the first supernatant and polymerisation was induced by addition of 0.1 volume of 10 x KME buffer (100mM Tris-HCl pH 8.0, 500 mM KCl, 25mM MgCl₂, 10mM EGTA, and 10 mM NaN₃). The solution was incubated at 30 °C in a water bath for one hour. After that the F-actin solution was brought to 0.8 M KCl and stirred gently for about 30 minutes. The F-actin was pelleted by spinning down at 100000g for 2 hours in an ultracentrifuge. The F-actin pellets were washed and soaked in a small volume of ATPase buffer (Usually 2-4 ml). The concentration of F-actin was measured and the F-actin solution was stored at 4 °C and used within 3 weeks.

2.2.3.1 Preparation of N-(1-pyrenyl)-iodoacetamide-labelled cardiac F-actin

For labelling Actin Cys-374 with N-(1-pyrenyl) iodoacetamide (PIA) the method of Kouyama and Mihashi (Kouyama and Mihashi 1981) was used. Firstly, cardiac F-actin was prepared as mentioned previously in (2.2.4). The final F-actin pellets were dissolved in labelling buffer containing (25 mM Tris-HCl pH 7.5, 100 mM KCl, 2 mM MgCl₂, 3 mM NaN₃, and 0.3 mM ATP) and dialysed against the same buffer overnight. N-(1-pyrenyl) iodoacetamide were added at a ratio of 7 moles of pyrene per mole of F-actin. Then the mixture was incubated in dark at room temperature for 3 hours with slow stirring. To

precipitate any free pyrene, the mixture was spun down at low speed of 10,000 rpm using an SS34 rotor for 10 minutes. The supernatant was taken and spun down again at 100000g, in an ultracentrifuge for two hours. The pellets were dissolved in G-buffer (at about 5-5.5 mg/ml) and dialyzed against G-buffer for 2 days. The N-(1-pyrenyl) iodoacetamide G-actin was spun down at 100000g, in an ultracentrifuge using T-1250 rotor for two hours and the supernatant was filtered and loaded onto gel filtration column (Sepharyl S200 or S300) that had been equilibrated with G-buffer. Fractions of 4 ml were collected and the absorbance of the various fractions was read at 290 nm. 12% SDS gel was used to check the purity of N-(1-pyrenyl) iodoacetamide G-actin. The pure fractions were pooled, polymerized by 0.1 volume of 10xKME buffer, and incubated at 30 °C for 45 minutes. The PIA F-actin was pelleted by spinning down at 100000g in an ultracentrifuge for two hours. The pellets were soaked and resuspended in ATPase buffer and kept in ice and used within a week. The degree of pyrene labelling was determined from the ratio of pyrene concentration over actin concentration and was usually around 0.8-0.9 pyrene/actin. The actin concentration in μM , was determined using the following formula $((\text{Absorbance at } 290 - (\text{Absorbance at } 344 * 0.127)) * 38.5)$. The concentration of pyrene in μM , was determined using the following formula: $(\text{Absorbance at } 344 * 45.5)$.

2.2.4 Preparation of cardiac troponin complex

The Troponin complex was extracted from sheep heart acetone powder. 30 g of sheep heart acetone powder was extracted in 20 volumes of extraction buffer (1 M KCl, 20 mM TES pH 7 and 15 mM β - mercaptoethanol) by continuous stirring overnight at 4 °C (Potter, 1982). The suspension was centrifuged at 14,000 rpm for 20 minutes at 4 °C using an SS-34 rotor. The pellet was discarded and the supernatant was adjusted to pH 8.0 with 1 M potassium hydroxide and brought to 30% ammonium sulphate. The ammonium

sulphate was added slowly over 1 hour at 4 °C with a continuous gentle stirring. During addition of ammonium sulphate, the pH was maintained between 7 and 8. The solution was spun down at 12,000 rpm for 20 minutes at 4 °C using an SLA 1500 rotor. The 30% supernatant was then brought to 42.5% ammonium sulphate by gentle addition of ammonium sulphate over 1 hour to precipitate the troponin complex. The troponin complex solution centrifuged at 12,000 rpm for 20 minutes at 4 °C using an SLA 1500 rotor. The 42.5% supernatant was kept for tropomyosin preparation later and the pellet was dissolved in ATPase buffer (10 mM MOPS pH 7, 150 mM KCl, 3.5 mM MgCl₂, 1 mM DTT, and 1 mM NaN₃) and dialysed against the same buffer overnight. Aggregated proteins were removed by centrifugation at 10,000 rpm for 10 minutes using an SS34 rotor. The clear protein solution was loaded onto a DEAE column which was pre-equilibrated with the same buffer. The troponin complex was eluted with a linear gradient of KCl in the same buffer (50-600 mM KCl). 5 ml fractions were collected and monitored at 280 nm. The purity of troponin complex was checked using SDS gel electrophoresis.

2.2.5 Preparation of cardiac tropomyosin (cTm)

Tropomyosin was purified from the 42.5% supernatant obtained during the preparation of a cardiac troponin complex (section 2.2.4). The ammonium sulphate concentration was raised to 65% by slow addition of ammonium sulphate over 1 hour at 4 °C with a continuous gentle stirring. The new solution was spun down to pellet the tropomyosin at 12,000 rpm for 20 minutes in the SLA rotor at 4 °C. The 65% pellet which contained the tropomyosin was dissolved in (10 mM MOPS pH 7.2, 50 mM KCl, 3.5 mM MgCl₂, 1 mM DTT, and 1 mM NaN₃) and dialysed against the same buffer overnight. A DEAE column was used to purify the tropomyosin, which had been equilibrated with the same dialysis

buffer. The tropomyosin was eluted by applying a linear gradient of 50-500 mM KCl. 5 ml fractions were collected and monitored at 280 nm. The purity of tropomyosin was checked by running 15% SDS gel. The fractions with pure cardiac Tm were pooled, concentrated and stored at -80 °C.

2.3 Expression and purification of human troponin complex

Fully functional human cardiac troponin complexes (hcTn) were reconstituted from individual troponin subunits human cardiac troponin T (hcTnT), human cardiac troponin I, (hcTnI), and human cardiac troponin C or troponin C mutants (hcTnC). Each troponin subunit has been expressed and purified separately before reconstitution into the ternary troponin complex.

2.3.1 Purification of troponin T (TnT) and troponin I (TnI)

Human cardiac troponin T (hcTnT) and human cardiac troponin I (hcTnI) clones were over expressed in *Escherichia coli* strain BL21 (DE3) plys (Studier et al., 1990). BL21 (DE3) plys cells were transfected with hcTnT or hcTnI constructs cloned into a pLEICS-05 were grown in LB broth medium at 37 °C in the presence of ampicillin. When the absorption of the culture reached 0.6-0.8 (exponential growth phase) at 600 nm, the induction was achieved by the addition of IPTG (isopropyl-1-thio- β -D-galactopyranoside) to the medium of growing cells and incubated overnight at 20 °C. The bacterial solution was spun down and the pellets were frozen. TnT and TnI were purified using a modified protocol as previously reported by (Krüger et al., 2003). The frozen bacterial pellets were dissolved in a lysis buffer (40 mM Tris-HCl, pH 8, 1 mM DTT), at 10 ml/g and the cells were broken by a French press. The protein solution was centrifuged at 40000g for 20 minutes. The pellet

resuspended in (20mM Tris pH 8, 6M urea, 1mM EDTA, 1mMDTT) and dialysed against the same buffer overnight and loaded in the CM-Sephrose column. TnT and TnI were eluted using a NaCl gradient of 0-0.6M NaCl.

2.3.2 Purification of troponin C (TnC)

Frozen Bacterial pellets containing TnC were resuspended in a buffer containing 50 mM Tris pH7.5, 1 mM DTT. The cells Broken by a French press and the solution centrifuged at 40000g for 20 min. The solution containing troponin C was loaded onto a phenyl sepharose column after addition of CaCl₂ to the supernatant to bring it to a final concentration of 10 mM. TnC was eluted using the following buffer: 50 mM Tris pH 7.5, 1 mM DTT, 0.2 M NaCl, 10 mM EDTA.

2.3.3 Reconstitution of troponin complex

The purified troponin subunits were reconstituted to form a functional troponin complex by mixing 50 µM of each subunit in (25 mM MOPS pH 7.0, 0.2 M NaCl, 0.5 M CaCl₂, 1 mM DTT and 8 M urea). The solution was incubated for one hour and dialysed against the same buffer with a stepwise decrease in the concentration of urea and NaCl were decreased using the following buffers (2 M Urea, 1 M NaCl for the first dialysis buffer, 0.75 M NaCl for the second dialysis buffer, and 0.5 M KCl for the last dialysis buffer). Aggregated proteins were removed by centrifugation at 14,000 rpm for 10 minutes at 4 °C. The troponin complex sample was then concentrated to a minimum volume using a centrifugal filter unit (30,000 MWCO). The troponin solution was purified using a Sephacryl S-200 gel filtration column pre-equilibrated with 25 mM MOPS pH 7.0, 0.2 M NaCl, 0.5 M CaCl₂, 1 mM DTT. The column was calibrated with a set of proteins of known molecular weight and the position of the troponin complex peak was monitored to

confirm that the troponin complex corresponds to a ternary 1:1:1 complex of troponin I, T and C. The purity of the troponin complex was also confirmed by SDS-PAGE.

2.4 General assays

2.4.1 The Actomyosin ATPase assay

A Mixture of actin, tropomyosin and troponin (molar ratio 7:1:1) and myosin sub-fragment 1 (S1) was incubated in a final volume of 200 μ l of ATPase buffer (10 mM MOPS pH 7, 3.5 mM $MgCl_2$, 1 mM DTT). The assay was performed with the troponin complex containing either cTnC WT or mutated cTnC. A blank containing S1 only was also included. The ATPase reaction was started by addition of 10 μ l of 100 mM MgATP and the mixtures were incubated for 5 minutes at 30 °C. The reaction was stopped by addition of 0.5 ml of 10% Trichloroacetic acid to give a final volume of 700 μ l. The new solution was centrifuged at 13,000 rpm for 5 minutes. 500 μ l of the supernatant was taken and placed in a test tube. The method of Taussky and Schorr (UMEDA et al., 1965) was used to determine the free inorganic phosphate (Pi). 1 ml of 1% ammonium molybdate in 0.5 M H_2SO_4 was added into each tube and mixed, then 0.5 ml of freshly prepared (10 g $FeSO_4$ dissolved in 25 ml 0.5 M H_2SO_4) was added and mixed. The solution was left for 5 minutes for the blue color to develop. Standards containing 0, 65 and 130 nmoles of inorganic phosphate were processed in the same way.

The concentration of inorganic phosphate was determined by measurement of absorbance at 700 nm using spectrophotometer. Standard buffer contained zero nmoles of inorganic phosphate was used as a blank buffer. The OD at 700 nm was read for all samples and standard buffers. The equation below was used to work out the optical density per nmole of Pi.

Average OD per nmoles of Pi = [(OD700 for 100µl of Pi/65nmoles of Pi) + (OD700 for 200µl of Pi/130nmoles of Pi)] / 2

A control with S1 in the absence of actin was carried out for every ATPase reaction. The OD determined for S1 only and its contribution to the total Pi release was subtracted from the acto-S1 OD. This remaining difference was divided by the average OD per nmole of Pi to determine the amount of Pi created from the acto-S1 ATPase. 7/5 volume correction was made because the OD measured was for a 0.5 ml reaction as opposed to the actual total quenching volume of 0.7 ml. To determine the rate at which ATP was hydrolyzed, the amount of Pi nmoles produced was divided by the total reaction time in seconds.

2.4.2 Determination of the secondary structure of cTnC mutants by Circular Dichroism

A Jasco -J715 spectropolarimeter was utilized to measure, firstly the secondary structure of cTnC WT and cTnC mutants alone or reconstituted with cTnI and cTnT to form the cardiac troponin complex (cTn). The spectra were collected between 190-300 nm in the far UV region. The path length of the cell was 0.1 cm and a bandwidth of 1nm at a speed of 50 nm per min at a resolution of 1 nm and measurements was at 4 °C and 25 °C in a 10 mM sodium phosphate, pH 7.0 and 0.3 M NaF solution. 5 scans were averaged at concentrations 10 µM for cTnC and 5 µM for cTn.

The molar ellipticity of cTn solutions at 222 nm as a function of temperature in a buffer containing 0.3 M NaF, 10 mM sodium phosphate, pH 7.0, was used to measure the thermal stability of cTnC alone or reconstituted with cTnI and cTnT. The Data were collected at 1.0 °C intervals from 15 to 85 °C using the same protein concentration.

2.4.3 Isothermal titration calorimetry (ITC)

Isothermal titration microcalorimetry (ITC) was used to measure the binding between TnC and TnI, Tn complex and Tm and Tn complex with actin-Tm in thin filament. All three experiments were performed using a VP-ITC Microcal LLC, Northampton, MA, USA at 25 °C. Proteins were dialyzed extensively against ATPase buffer (140 mM KCl, 10 mM Mops pH 7.2, 3.5 mM MgCl₂, 0.1 mM DTT, 1 mM NaN₃, and 500 μM CaCl₂). Protein samples were centrifuged at 13,000 rpm for 10 min at 4 °C using a bench centrifuge. In the titration of cTnC with cTnI, the cell was filled with 1.4 ml of 7 μM cTnI and titrated with 300 μl of 70 μM hcTnC WT or hcTnC mutants at 240 sec intervals with stirring at 300 rpm. The injection volume was 15 μl.

Titration of Tm with Tn complex was performed by filling the cell with 1.4 ml of 7 μM hcTnC WT or hcTnC mutants reconstituted in troponin complex and titrated with 300 μl of 70 μM Tm at 240 sec intervals with stirring at 300 rpm and an injection volume of 15 μl for each single point. The last titration was used to study Tn complex binding to the actin-Tm complex. In this titration, the cell filled with pre-incubated actin-Tm mixture (35 μM and 6 μM respectively) and titrated with 50-60 μM of troponin complexes reconstituted with hcTnI, hcTnT and hcTnC WT or hcTnC mutants. Control titration of buffer with each of hcTnI, Tm and actin-Tm indicated that heats of dilution were small and constant. All binding isotherms data were analyzed using Origin ITC data analysis software (Microcal Inc.).

2.5 Transient State Kinetic Measurements

The kinetic parameters were measured using Hi-tech Scientific SF61 stopped flow apparatus equipped with a 100 watt Xe/Hg lamp. KinetAsyst software package was used for the interpretation and analysis of the kinetic data. Single mixing modes were used in this project. The manual set up was used to select the desired excitation wavelength and to maximize the signal. To maximize the signal; the Live Display was utilized by adjusting the photomultiplier voltage. The excitation wavelength is set up and the signal optimized, Acquire Control Panel was used to adjust the run time and the channel.

2.5.1 Kinetics of Myosin subfragment-1 (S1) Binding to PIA-actin thin filament was used to determine the equilibrium constant between thin filament blocked and closed states

The Kinetics of Myosin subfragment-1 (S1) binding to PIA-actin-Tm-Tn (7:1:1) in the presence and absence of Ca^{2+} was used to determine the equilibrium constant between thin filament blocked and closed states, K_B (Head et al., 1995). This assay was performed by mixing a large excess of PIA-labelled actin (alone or with Tm and/or troponin complexes in the presence and absence of Ca^{2+}) in one syringe and S1 (at a concentration $1/10^{\text{th}}$ to actin) in the second syringe. The pyrene iodoacetamide fluorescence was excited at 364 nm and emission of fluorescence was monitored through a 400nm cut-off filter (GG400 filter). Experimental conditions were as follows: 25 °C, 10 mM Mops, pH 7.2, 140 mM KCl, 4 mM MgCl_2 , 1 mM DTT, 1 mM NaN_3 . The average of 5 to 9 transients data was fitted to one exponential equation by a nonlinear least square curve fit using the Fit Control Panel of the Fit Asystant and the observed rate constant (k_{obs}) of S1 binding to actin was determined. The values of k_{obs} were plotted as a function of actin

concentration and the obtained curves were fit to a linear equation. The slopes of the curves obtained for actin alone and for the regulated actin (i.e. in the presence of Tm or hcTn complexes with or without Ca^{2+}) were used to calculate the value of the equilibrium constant between blocked and closed states K_B according to the following question:

$$k_{\text{obs}} (\text{for regulated actin}) / k_{\text{obs}} (\text{actin alone}) = K_B / (1 + K_B)$$

2.5.2 Calcium Dissociation Kinetics Measurements

The Ca^{2+} dissociation kinetics of TnC and Tn complex was measured using a chase experiment where one syringe contained Actin.Tm.Tn.S1 and CaCl_2 while the other syringe contained Quin-2. Mixing the 2 solutions lead to Ca^{2+} binding to Quin-2 and an increase in the fluorescence of Quin-2. The excitation wavelength used is 334 nm and the emission was monitored with a GG455 cut-off filter. In these experiment, the free Ca^{2+} bind instantaneously to Quin-2 with no observed transient. The observed transient are due to Quin-2 binding to Ca^{2+} which is limited by its rate of dissociation from TnC. The experimental conditions were as follows: 25°C, 140 mM KCl, 4 mM MgCl_2 , and 50 mM MOPS pH 7.2. Actin.Tm.Tn.S1 were present in the following concentration of 7:1.3:1.3:2.7 μM , CaCl_2 was present at 50 μM and Quin-2 was present at 150 μM . The average of 3 to 6 transients was fitted to one and two exponentials by a non-linear least-squares method and the observed rate constants recorded.

2.6 NMR Spectroscopy

2.6.1 Preparation of minimal media

In a 2.5 L Erlenmeyer flask the following chemicals were added in the described order: 1.0 g of $(\text{NH}_4)_2\text{SO}_4$ (N^{15}), 100ml of 10X stock of PO_4/NaCl (17g Na_2HPO_4 , 7.5g KH_2PO_4 , 1.25g NaCl and the solution was completed to 250ml with water before 1ml of 0.3M Na_2SO_4 (1000X stock) was added and 4.26g in Na_2SO_4 . To this mixture was added 10ml 100X stock solution of EDTA trace elements which have the following elements

- 1g EDTA
- Dissolving in 160 ml water and adjust to pH 7 with NaOH
- 0.32g MnCl_2
- 0.1g FeCl_3
- 0.01g ZnCl_2
- 0.002 CoCl_2
- 0.002g H_3BO_3
- Water was added to bring the solution to 200ml and the pH was adjusted to 7.0.

After mixing these ingredients, water was added to give the final volume of 975ml. After that this solution was divided into two 2.5L baffles and then autoclaved. Once these flasks cooled the following materials were added: 1ml of 1000X filter sterilised MgSO_4 (1M), 1ml of 1000X filter sterilised CaCl_2 (0.3M), 1ml of 1000X filter sterilised d-Biotin, 1ml of 1000X filter sterilised Thiamine (1mg/ml), and 20ml of 50X autoclaved glucose to get final concentration 4g/l.

2.6.2 Expression of troponin C ^{15}N

cTnC WT and mutant constructs (prepared in 2.1) were added to chemically competent *E. coli* BL21 (DE3) cells with selection for transformation achieved by plating on LB agar

containing 100 µg/ml ampicillin. Starter cultures prepared by using single colonies to inoculate a 50ml LB media containing 100 µg/ml ampicillin and incubated at 37 °C overnight. The starter cultures centrifuged at 1800g for 12 minutes and the pellet re-suspended in 1ml minimal media and this solution was used to inoculate a 1 L minimal media in a 2.5 L baffled flask in the presence of 100 µg/ml ampicillin and incubated at 37 °C, 200 rpm until the OD reached 0.6-0.9 at 600nm. Subsequently, 0.5 mM IPTG was used to induce protein expression and the bacterial culture was incubated at 20 °C overnight. Finally, the bacterial culture was centrifuged at 4000g for 10 minutes and the pellets were stored at -20 °C prior to protein extraction and purification.

The bacterial pellets of cTnC WT and mutants N¹⁵ labelled were used to extract and purify cTnC WT and mutants each one separately using the method described in 2.3.2 (purification of troponin C). Sephacryl S-200 gel filtration column had been used for further purification. The pure N¹⁵ cTnC WT and mutants were concentrated and dialysed against NMR buffer (10mM bis-Tris pH 6.8, 0.1M KCl, 4mM CaCl₂, 1mM DTT, 3mM Na₃N) and used in HSQC experiments.

Chapter 3

Purification and reconstitution of
cardiomyopathy associated troponin C
mutants into a stable and functional troponin
ITC ternary complex.

3.1 Introduction

Cardiac muscle contraction represents the product of a cascade of molecular events involving several protein-protein interactions coupled to specific and coordinated structural changes. Any slight upset in these molecular events is likely to affect cardiac function. Over the last 25 years, a number of mutations in genes encoding contractile proteins including titin, actin, myosin, tropomyosin, and all three subunits of cardiac troponin (cTn) have been associated with HCM and DCM cardiomyopathies (Kalyva *et al.*, 2014). There is a sustained research effort to understand how these mutations affect the biochemical properties of these proteins.

Cardiac troponin (cTn) is a heterotrimeric complex comprised of a Ca^{2+} binding subunit TnC, an inhibitory subunit troponin I, and an elongated troponin T. The study of cTnC is particularly interesting in that it represents a key player in the allosteric transitions induced in thin filament upon Ca^{2+} binding or dissociation. The binding of regulatory Ca^{2+} to specific sites in troponin C is the initial step in the activation of muscle contraction and its dissociation is a pre-requisite to muscle relaxation. Ca^{2+} binding/ dissociation triggers a set of coordinated allosteric transitions that leads to muscle activation/relaxation.

In order to investigate the functional and structural effect of troponin C mutations, the expression of sufficient amount of TnC mutants and reconstitution with TnI and TnT into a functional troponin complex is crucial. In the current chapter, we describe the cloning and mutagenesis to obtain the constructs of the mutated hcTnC cDNA in an expression vector, the induction of protein expression, the purification of the various mutants and their reconstitution into a ternary complex with hcTnI and hcTnT and their initial structural and biochemical characterisation. The HcTnC-cDNA was used as a template to produce the

specific mutants which include the following mutations: Y5H, A8V, A31S, E59D, D75Y, C84Y, D145E, I148V. Once the constructs were produced, they were sequenced to verify that sequences were correct prior to expression and purification. All these mutations were expressed, purified and reconstituted with TnI and TnT into a functional troponin complex. Circular dichroism was used to assess the effect of TnC mutations on the secondary structure of troponin C and troponin complex. In addition, circular dichroism was used to evaluate the thermal stability of TnC mutations and TnC mutations reconstituted in Tn complex. Finally, we wanted to assess the ability of these complexes to bind actin-tropomyosin and to perform their allosteric regulatory function. To this end, we analyzed the effect of TnC mutations on the ability of Tn complex to activate and inhibit the actomyosin ATPase activity in the presence or absence of Ca^{2+} respectively.

3.2 Results

3.2.1 Mutagenesis

The first step for this project was designing the primers for each mutation and producing cDNA of hcTnC in which the different mutations were carried out using the overlap extension PCR method. Two primers were designed (a forward and a reverse primer) for each of the mutations A31S, E59D, D75Y, C84Y, M103I, and E134D. For the mutants H5Y and A8V, the mutations were inserted in the forward 5' primer while for D145E and I48V the mutation were inserted in the forward 3' primer. A single PCR was used to obtain the cDNA for the mutants H5Y, A8V, D145G, and I148V. For hcTnC mutants A31S, E59D, D75Y, C84Y, M103I, and E134D two PCR reactions were used to obtain the final hcTnC mutants. The products of a PCR using the 5' and 3' hcTnC primers were analysed by Agarose gel and the results are shown in figure 3.1. The gel shows a single band corresponding to a size approximately 500 bp which is the expected size for the cDNA of the hcTnC.

All TnC generated constructs were verified by sequencing (Appendix 1). Moreover figure 3.2 shows the PCR products run on an agarose gel after DNA purification (miniprep). All lanes show a band at the predicted size of 500 bp.

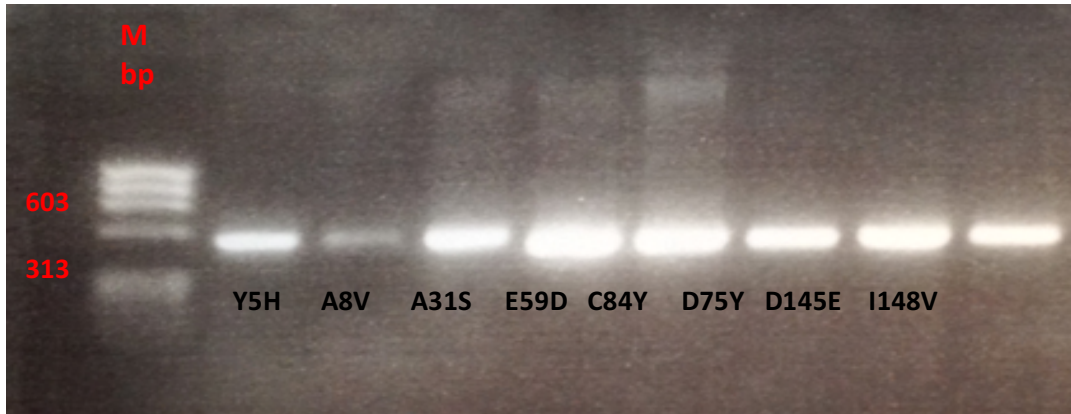


Figure 3.1: Agarose gel of the products of a PCR reaction using the various hcTnC clones.

Agarose gel of the PCR products of hcTnC mutants obtained by the overlap extension method. Each lane represented the product of one human construct as labelled. The DNA ladder lane (M) represents a marker of molecular weight (carried out by Dr Xiaowen Yang at the University of Leicester).

3.2.2 Test expression

We tested the level of expression of the various constructs of hcTnC. Cell lysates were analyzed by SDS-gels and we monitored the time dependent increase in intensity of the troponin C band at 18 KDa molecular weight (Figure 3.3). SDS gel electrophoresis reveals a number of protein bands in every lane including the 0 lane (i.e. before induction). These bands correspond to bacterial proteins. In contrast after addition of IPTG which used to induce the expression of proteins carried in a plasmid, we observe the appearance of a band around 17 kDa which corresponds to hcTnC. Expression of hcTnC is already prominent 1 hour after the addition of IPTG. The highest level for expression was obtained after three hours of induction by IPTG. The gel shows that there is no significant increase in the level of expression after three hours.

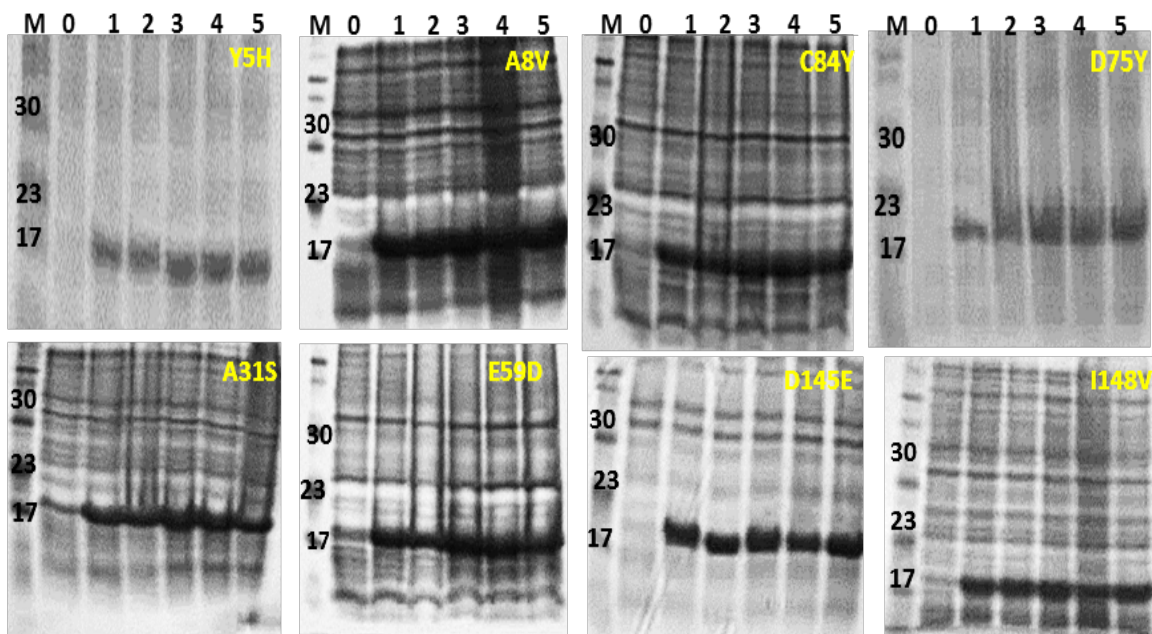


Figure 3.2: SDS gel electrophoresis analysis of the results of test expressions.

Test expressions of cTnC mutants: Y5H, A8V, C84Y, D75Y, A31S, E59D, D145E, I148V. Lanes: 0, before induction of protein expression with IPTG. ; lanes 1, 2, 3, 4 and 5 correspond to 1, 2, 3, 4 and 5 hours incubation after addition of IPTG.

3.2.3 Reconstitution of Troponin complex

In order to get pure and functional troponin complex, each hcTn subunit was purified separately and then reconstituted with hcTnI and hcTnT to form the troponin complex.

Figure 3.3 shows the results of the purification of hcTnT. The gel shows a single band at just above 37kDa which correspond to the MW of hcTnT. Figure 3.4 shows the results of the purification of hcTnI. The gel shows a single band at around 25 kDa which correspond to the MW of hcTnI. Troponin C was purified by using affinity column (phenyl Sepharose) as shown in figure 3.5. All three subunits are highly pure. The purified troponin T, I, and C subunits were reconstituted by mixing the three subunits in a denatured state and re-folding the mixture by a step-wise decrease in the concentration of the denaturing agent in the presence of a high concentration of salt (Krüger *et al.*, 2003). Although the troponin subunits were purified from bacterial proteins another purification was performed after reconstitution using gel filtration (figure 3.6). The aim of this purification is to separate

the non-reconstituted subunits and potential binary (IC or IT) or quaternary troponin complexes. This step was used to purify the ternary troponin complex (1:1:1) which was eluted in fractions that correspond to a MW of 78 kDa. Fractions of peak 1 (figure 3.6: B) show a protein pattern containing only the troponin subunits TnT, TnI, and TnC because the mixture of protein eluted at 40-50 ml. The only combination of troponin subunits that give the molecular weight 80 kDa is the trimeric TnT-I-C complex with (1:1:1).

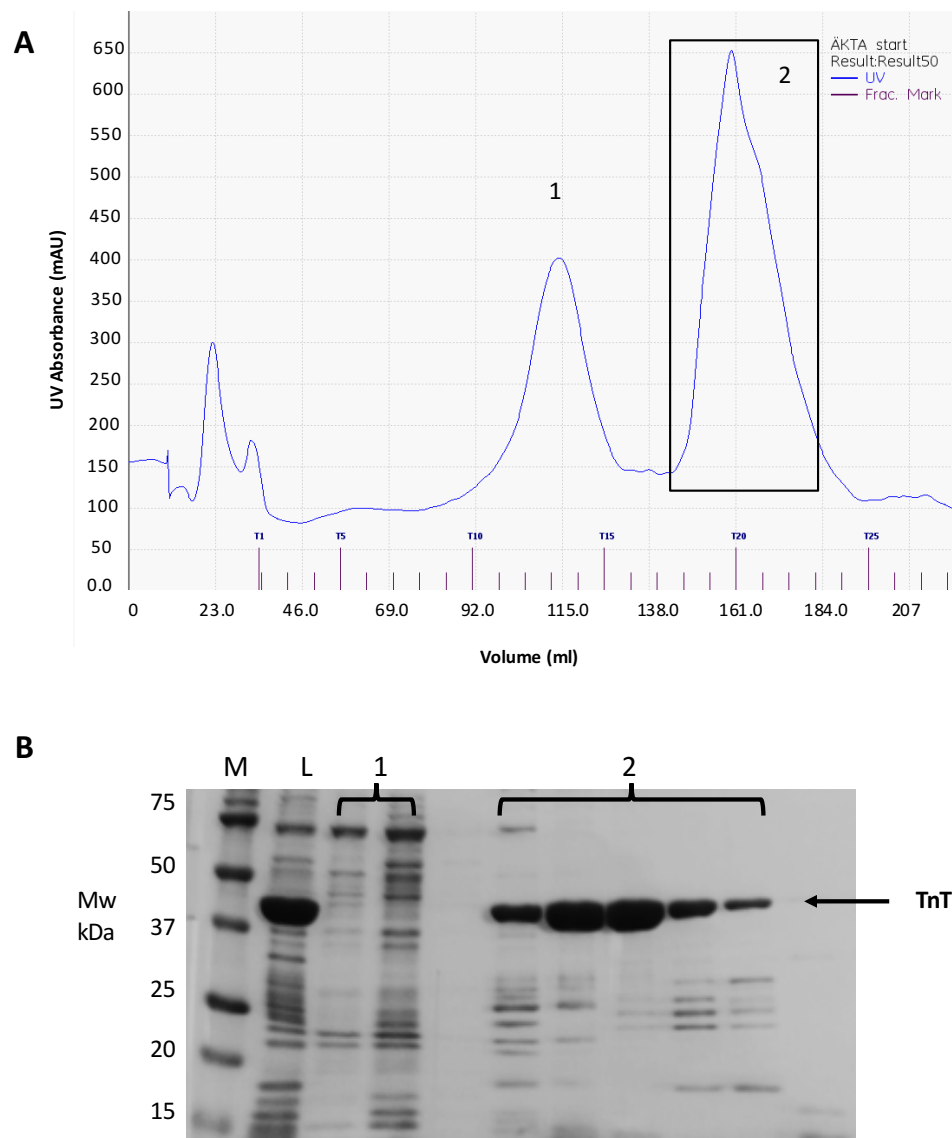
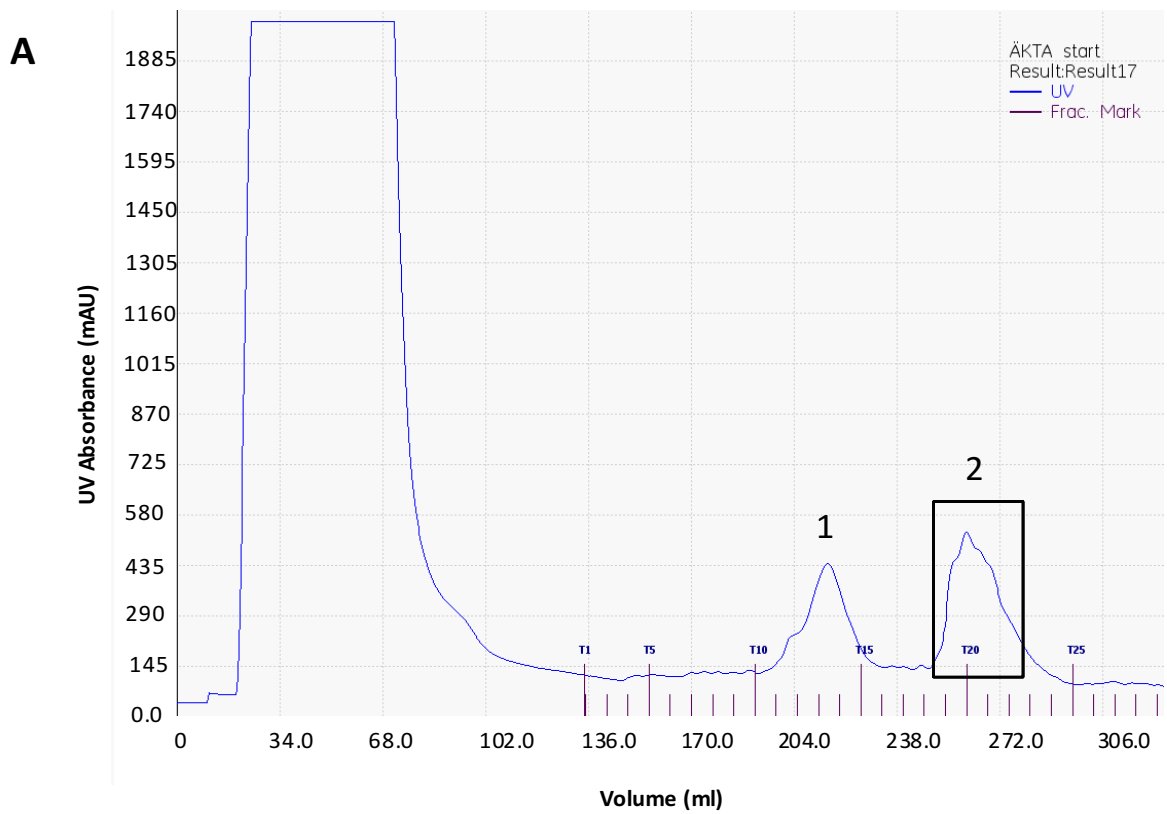


Figure 3.3: TnT purification.

The chromatogram (A) shows a single eluted peak (2) during a linear NaCl gradient from 0-0.6M from SP sepharose column. (B) Shows the SDS PAGE. Bands in the fractions from eluted peak (2) are consistent with troponin T (TnT)



B

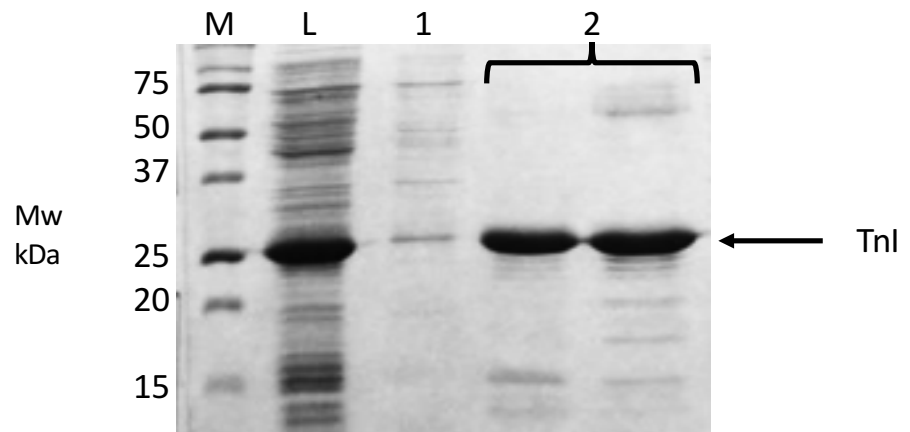


Figure 3.4: Tnl Purification.

The chromatogram (A) shows a single eluted peak (2) during a linear NaCl gradient from 0-0.6M from SP sepharose column. (B) shows the SDS PAGE. Bands in the fractions from eluted peak (2) are consistent with troponin T (Tnl).

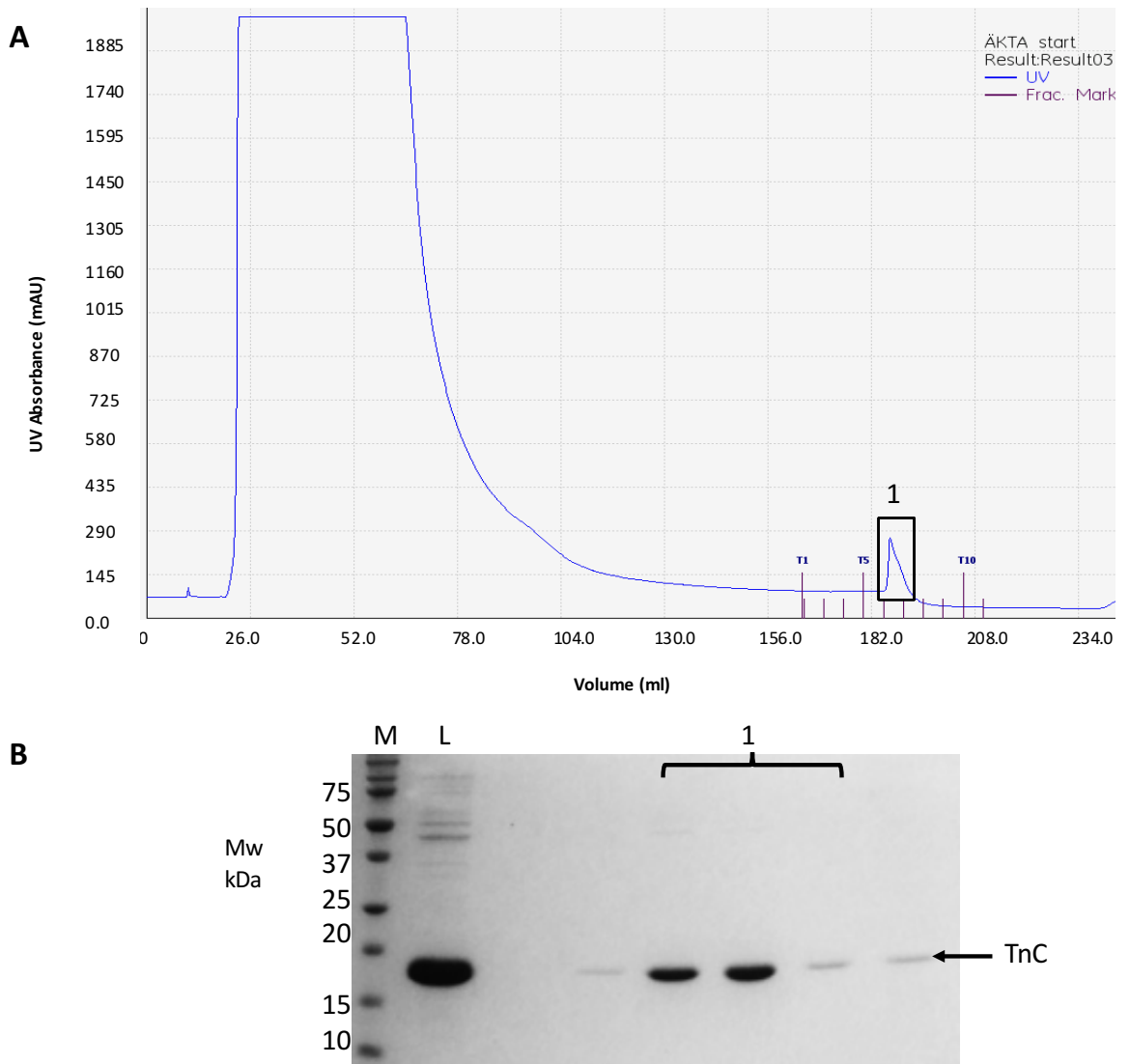


Figure 3.5: TnC purification.

The chromatogram (A) shows a single peak (1) for TnC eluted from phenyl Sepharose column with buffer 50mM Tris pH7.5, 1mM DTT, 0.2M NaCl, 10mM EDTA. (B) shows the SDS PAGE. Bands in the fractions from eluted peak (1) are consistent with troponin C (TnC).

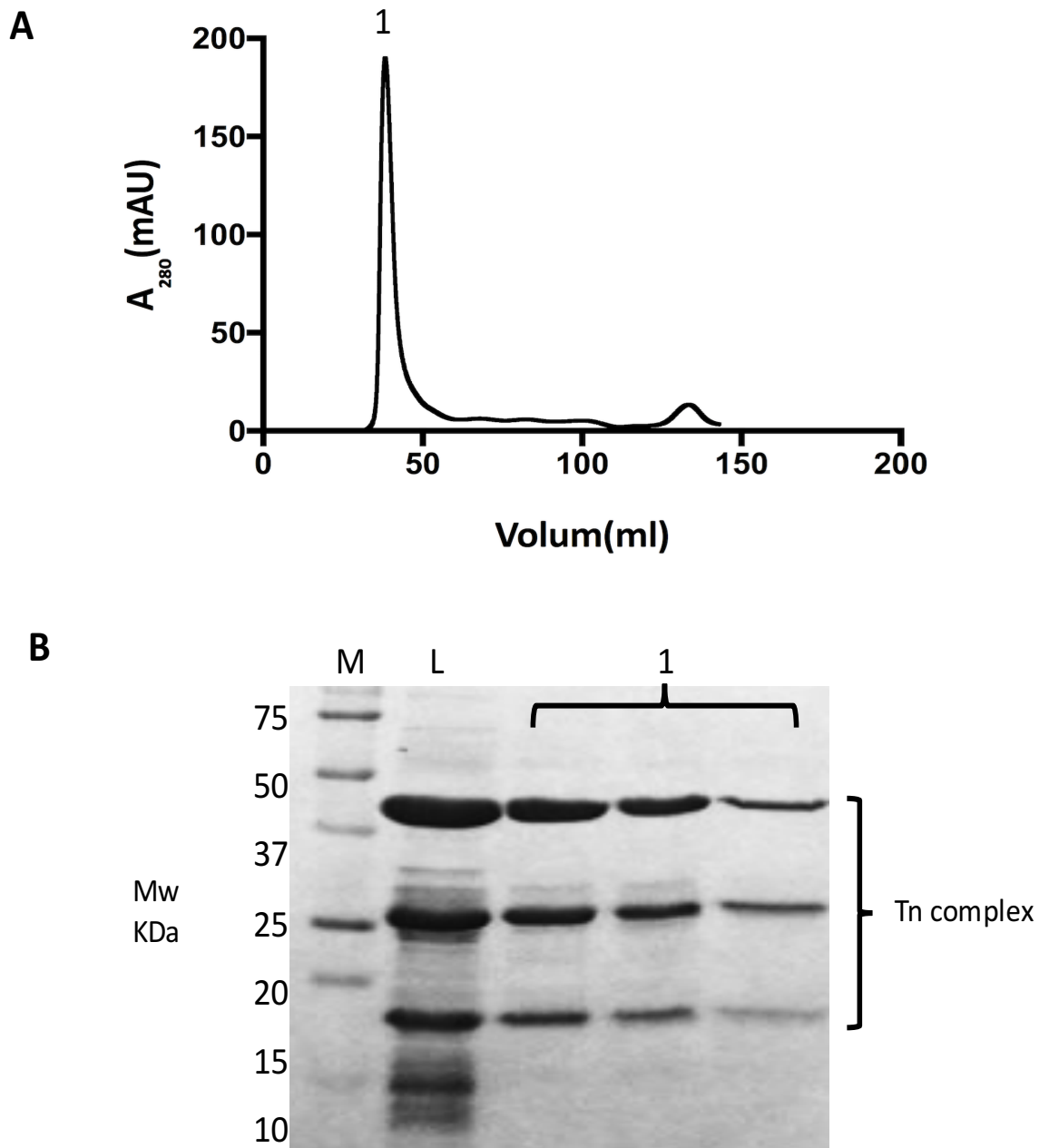


Figure 3.6: Size exclusion chromatography of the reconstituted troponin complex.

The chromatogram (A) shows a single eluted peak after loading Tn complex on a S200 gelfiltration column. SDS PAGE analysis (B) confirmed that only Tn complex (79 KDa) was present.

3.2.4 Circular Dichroism of TnC mutations

3.2.4.1 Effect of troponin C mutations on the secondary structure of troponin C

Circular dichroism (CD) is a structural method widely used for a rapid assessment of the impact of mutations on the overall structure of proteins and in particular on the secondary structure elements such as α -helices and β -sheets. CD relies on the unequal absorption of left-handed and right-handed circularly polarized light since in the far UV spectral region (190-250nm) the peptide bond absorption is affected by its environment (Greenfield 2006). Different secondary structure motifs such as random coil, α -helices and β -sheets produce spectra with very different shape and characteristics. For example, α -helices produce clear minima at 208 nm and 222 nm. CD can also be used to characterize the thermally induced unfolding of the protein and assess the effect of mutations on this process which is used as an indication of structural stability.

In this project, we aimed to evaluate the effect of hcTnC mutations on the secondary structure of isolated hcTnC, hcTnC reconstituted in a ternary troponin complex and the impact of T⁰C induced unfolding. Figure 3.7 and 3.8 display the spectra of hcTNC WT and mutants. The CD spectra of hcTnC mutants (shown in red) are very similar to the CD spectra of the WT hcTnC indicating that the mutations of TnC in general do not affect the secondary structure of troponin C. There are small differences in the amplitude of the CD signal which are likely due to differences in the protein concentrations.

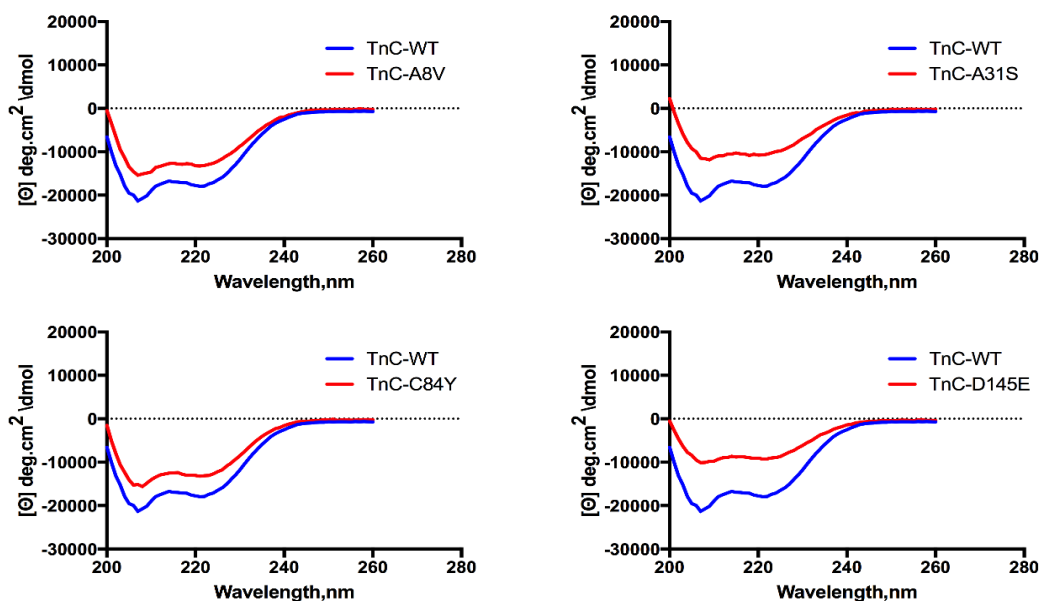


Figure 3.7: Characterization of secondary structure of TnC DCM mutants by circular dichroism.

CD spectra of the troponin C using the TnC WT (blue) and different TnC mutants (red) were measured in the presence of 10 mM NaH_2PO_4 , pH 7.0 and 0.3 M NaF. All samples were used at a concentration of 10 μM . Each data point is an average of three experiments.

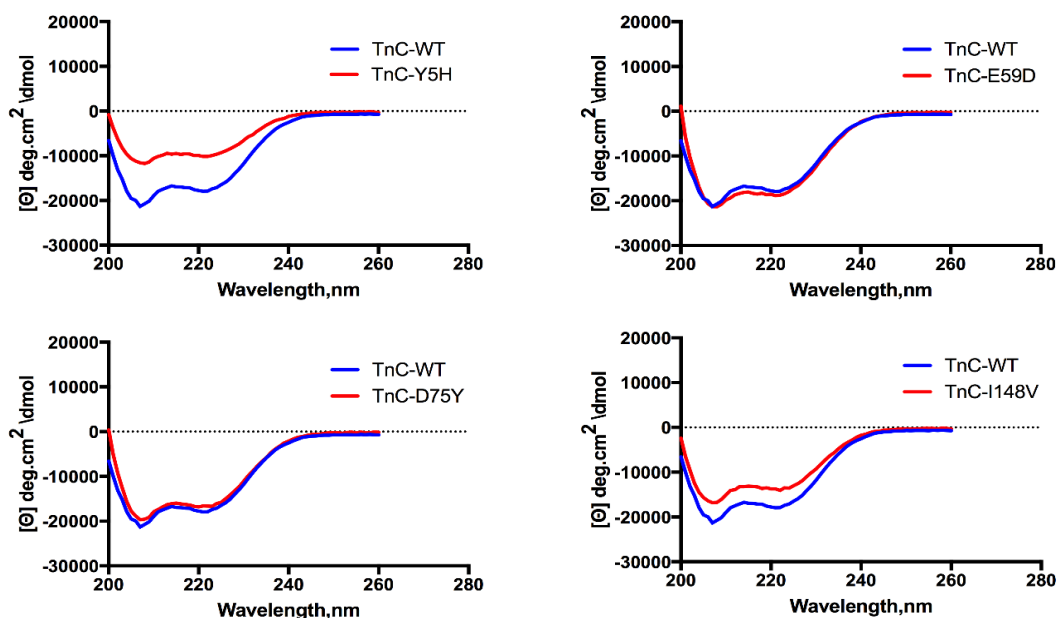


Figure 3.8: Characterization of secondary structure of TnC HCM mutants by circular dichroism.

CD spectra of the troponin C using the TnC WT (blue) and different TnC mutants (red) were measured in the presence of 10 mM NaH_2PO_4 , pH 7.0 and 0.3 M NaF. All samples were used at a concentration of 10 μM . Each data point is an average of three experiments.

Fig 3.9 shows the results of the temperature induced unfolding of troponin monitored by changes in ellipticity at 222nm. The Observed change has been normalized and plotted as percentage. The data are fit using the Jackson analysis software and the melting points (Temperature that gives half maximal value) are compared between the different hcTnC mutants. Our results suggest that the mutations E59D, D75Y and D145E in isolated TnC reduced the thermal stability (reduce the melting point). As shown in table 3.1 the melting point of TnC WT is 55.14 ± 1.38 and 50.09 ± 0.82 for E59D; 51.28 ± 0.13 for D75Y and 50.07 ± 2.62 for D145E.

Table 3.1 Melting point temperature (mid-point) of troponin C mutation in isolated troponin C.

Troponin C	Melting point
WT	55.14 ± 1.38
Y5H	58.39 ± 6.91
A8V	52.64 ± 1.31
A31S	56.51 ± 2.22
E59D	50.09 ± 0.82
D75Y	51.28 ± 0.13
C84Y	57.10 ± 0.2
D145E	50.07 ± 2.62
I148V	61.33 ± 5.09

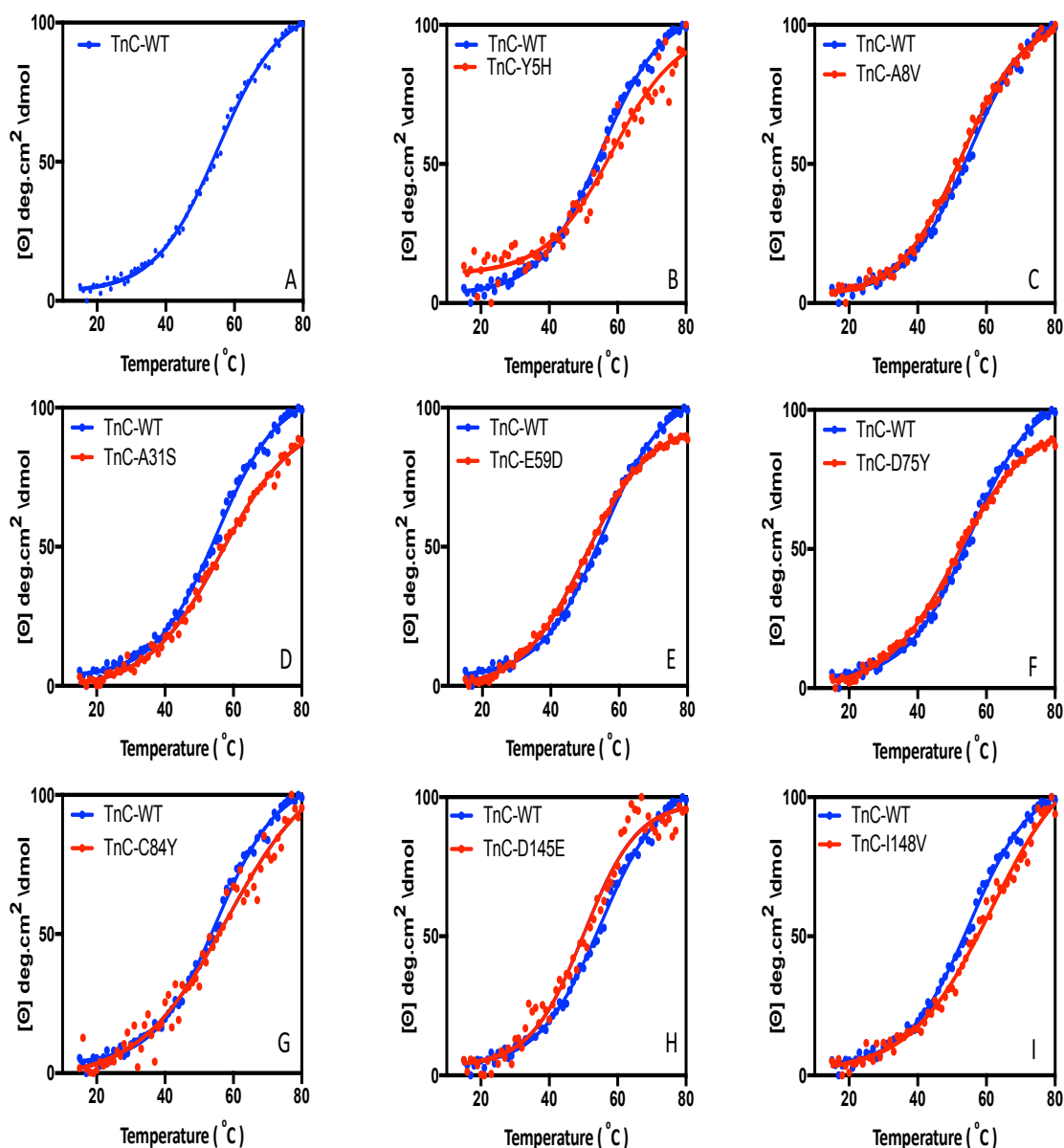


Figure 3.9: Thermal denaturation of TnC WT, HCM, and DCM mutations.

Effect of TnC mutations on hcTnC thermal unfolding measured as changes in ellipticity at 222nm at a constant heating rate of 1 °C/min between 15-80°C. The individual data points display the ellipticity measured at 222nm and the lines display the curve fit for WT (blue line) and each mutant (red line). (A) WT, (B) WT and Y5H, (C) WT and A8V, (D) WT and A31S, (E) WT and E59D, (F) WT and D75Y, (G) WT and C84Y, (H) WT and D145E, and (I) WT and I148V. All samples were in 10 mM NaH₂PO₄, pH 7.0 and 0.3 M NaF.

3.2.4.2 Effect of TnC mutations on the secondary structure of troponin complex

The previous section showed that all hcTnC mutations studied in this project did not have a major impact on the structure of isolated TnC. We have also used CD to monitor the impact of mutations in hcTnC on the structure of the reconstituted troponin complexes. Figure 3.10 shows the CD spectra for the DCM troponin C mutations and figure 3.11 shows the CD spectra for HCM troponin C mutations. The CD data indicate that both the HCM mutations and DCM mutations have no effect on secondary structure of the troponin complexes reconstituted with the various TnC mutations. All these mutations gave the same shape of the CD spectra compare to the WT except for a slight decrease in the amplitude.

Figure 3.12 shows the data obtained from the thermal unfolding of troponin plotted as change in the ellipticity at 222nm as a function of increasing temperature. To evaluate the effect of cTnC mutations on the melting point the normalized plots of ellipticity versus temperature were used to calculate the melting point (table 3.2). We have also used a first derivative to visualize the observed changes (figure 3.13). In this case, one transition of cooperative thermal unfolding for all TnC mutations. The highest temperature transition (from 50 °C to 60 °C) were very similar for all TnC mutations (figure 3.12 panel C). Thus, the above data demonstrated that the Y5H, A8V, A31S, E59D, C84Y, and I148V have no big impact on the thermal stability of troponin complex (figure 3.12 and 3.13 and table 3.2). On the other hand, D75Y and D145E reduce the melting point. These results indicate that the effect observed for isolated hcTnC D75Y and D145E was still present when these mutants were reconstituted with hcTnI and hcTnT.

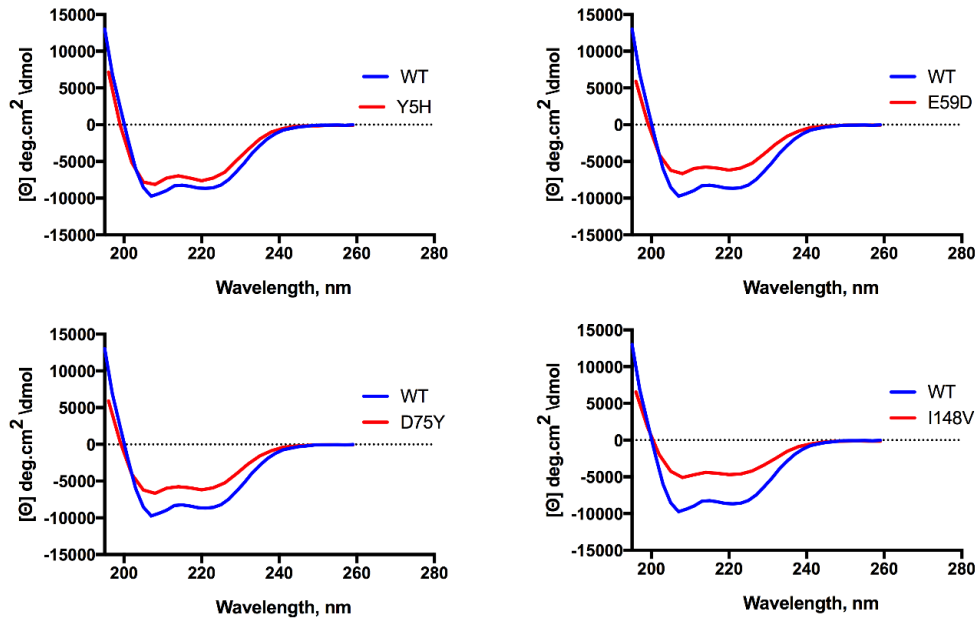


Figure 3.10: Characterization of secondary structure of TnC WT and DCM mutants reconstituted in troponin complex.

CD spectra of the troponin C using the TnC WT (blue) and different TnC mutants (red) reconstituted in troponin complex were measured in the presence of 10 mM NaH_2PO_4 , pH 7.0 and 0.3 M NaF. All samples were used at a concentration of $5\mu\text{M}$. Each data point is an average of three experiments.

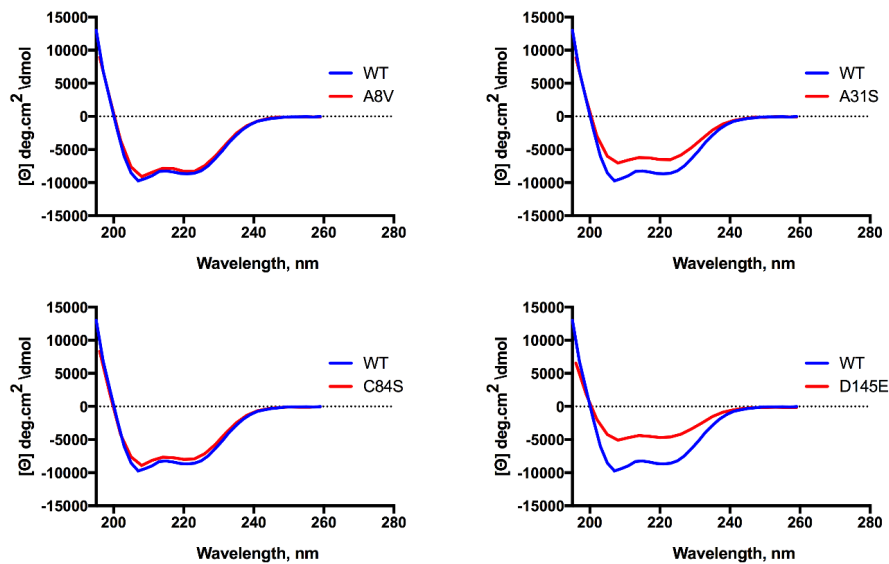


Figure 3.11: Characterization of secondary structure of TnC WT and HCM mutants reconstituted in troponin complex.

CD spectra of the troponin C using the TnC WT (blue) and different TnC mutants (red) reconstituted in troponin complex were measured in the presence of 10 mM NaH_2PO_4 , pH 7.0 and 0.3 M NaF. All samples were used at a concentration of $5\mu\text{M}$. Each data point is an average of three experiments.

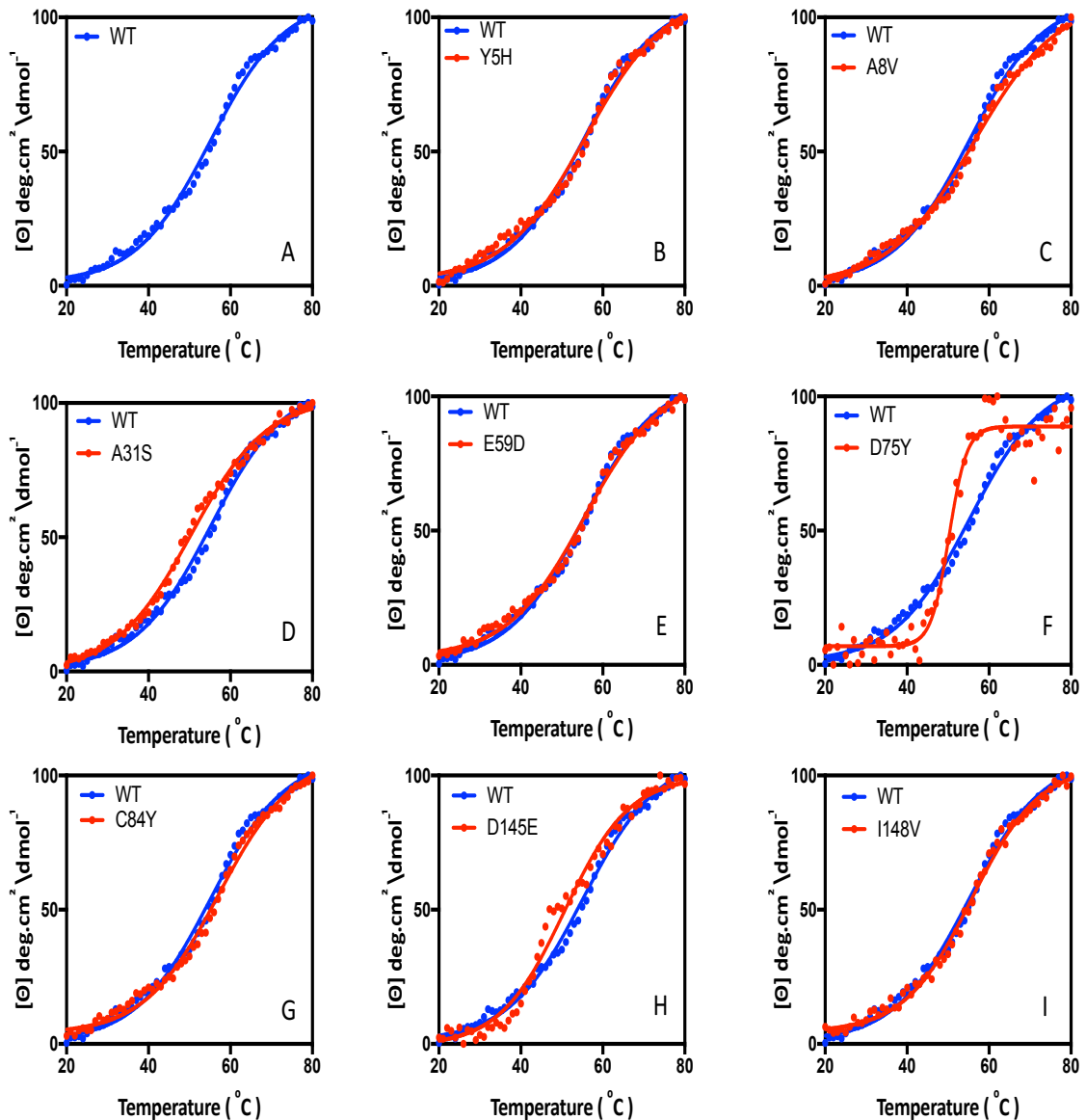


Figure 3.12: CD measurements of the thermal denaturation of TnC WT and DCM mutants reconstituted in troponin complex.

Effect of TnC mutations on the thermal unfolding of the whole hcTn complex measured as changes in ellipticity at 222nm at a constant heating rate of 1 °C/min between 15-80°C. The individual data points display the ellipticity measured at 222nm and the lines display the curve fit for WT (blue line) and each mutant (red line). (A) WT, (B) WT Y5H, (C) WT and A8V, (D) WT and A31S, (E) WT and E59D, (F) WT and D75Y, (G) WT and C84Y, (H) WT and D145E, and (I) WT and I148V. All samples were in 10 mM NaH₂PO₄, pH 7.0 and 0.3 M NaF.

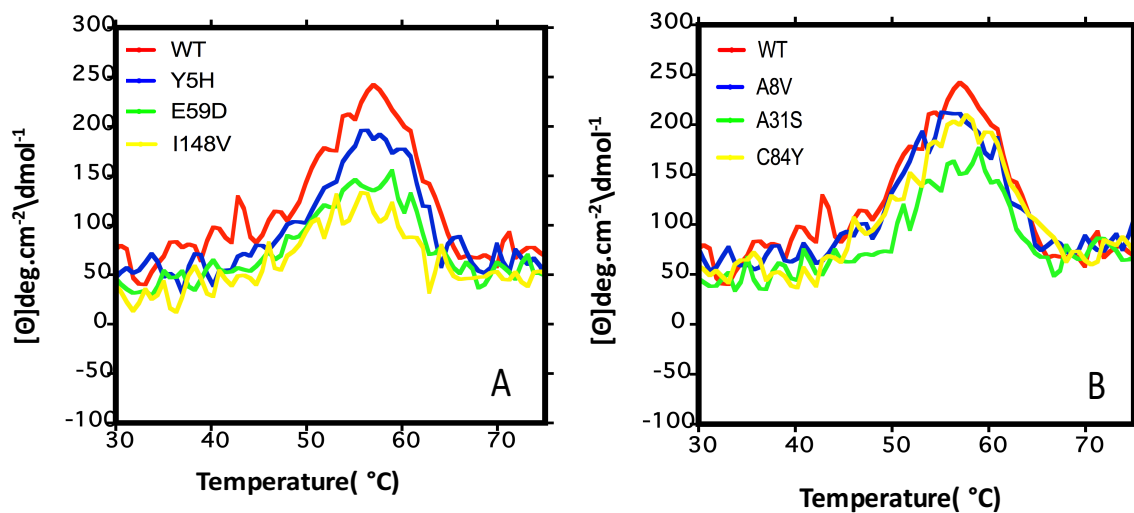


Figure 3.13: First-derivative profiles for CD data measurements of thermal denaturation of TnC WT and HCM mutants reconstituted in troponin complex. Panel A: DCM mutations, panel B: HCM mutations). The peaks indicate the melting point.

Table 3.2: Melting point temperature (mid-point) of troponin C mutation reconstituted in troponin complex

Troponin complex	Melting point
WT	55.1±0.3
Y5H	55.8±0.1
A8V	56.4±0.3
A31S	57.6±0.2
E59D	55.5±0.2
D75Y	50.2±0.4
C84Y	57.1±0.2
D145E	50.0±0.1
I148V	55.7±0.4

3.2.5 Effect of hcTnC mutations on the activation and inhibition of the actomyosin ATPase by the troponin complex.

To detect the effect of TnC mutations on the troponin complex activation and inhibition of the actomyosin ATPase, we measured the impact of increasing troponin concentration on the actin-Tm-activated myosin ATPase in the absence and presence of Ca^{2+} . The ATPase is plotted as percentage of uninhibited ATPase (i.e. actin-tm activation of myosin ATPase). In presence of Ca^{2+} , increasing amount of hcTn induces the activation of the actomyosin ATPase up to a maximum of 300% (Figure 3.14) while in the absence of Ca^{2+} increasing the hcTn concentration induces an inhibition of the actomyosin ATPase up to a maximum of 50% (Figure 3.15). Mutations Y5H, A8V, C84Y, D145E, and I148V gave maximal activation of actomyosin comparable to the WT (figure 3.14). ATPase rate in presence of Ca^{2+} of actomyosin for wild type was $288 \pm 11.979\%$ (table 3.1). In contrast, mutations A31S, E59D and D75Y affected troponin regulation of the actomyosin ATPase (figure 3.14 and figure 3.15). In presence of Ca^{2+} , hcTn A31S increased the activation of reconstituted thin filament to 447.180 ± 23.872 when compared to hcTn WT. On the other hand, E59D and D75Y reduced the activation of reconstituted thin filament to 217 ± 39.174 and 174 ± 25.239 respectively. Finally, none of the hcTnC mutations affected the inhibitory ability of the reconstituted troponin complexes in the absence of calcium (figure 3.15 and table 3.1).

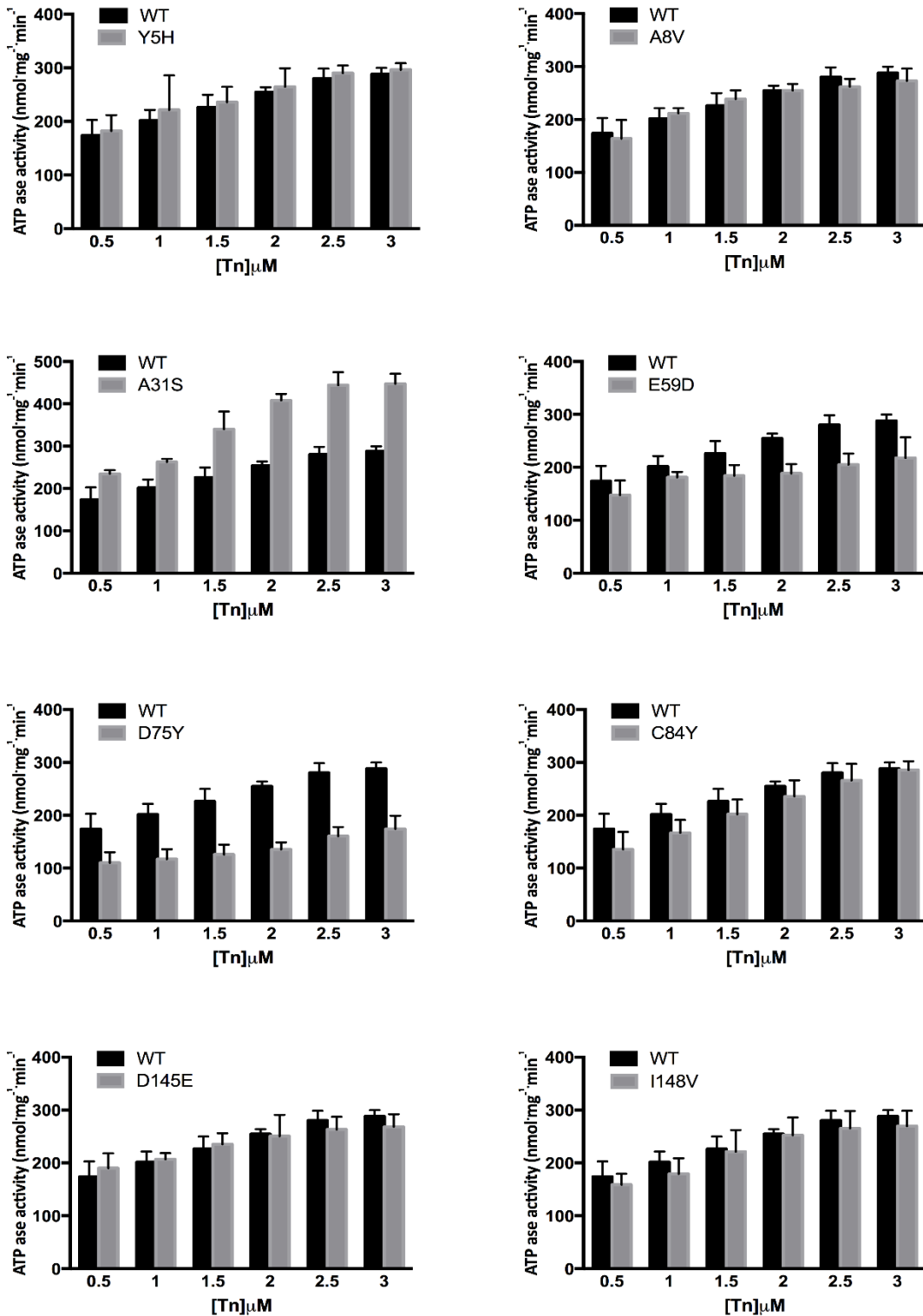


Figure 3.14: Effect of the HCM and DCM cTnC mutations on the ability of the troponin complex to activate the Actin-Tm activated Myosin-S1 ATPase in presence of Ca²⁺.

ATPase assays were performed in the presence of 0.2mM CaCl₂ and 0-3 μM troponin. The assay consisted of 7 μM cardiac actin, 2 μM cardiac Tm, and 1 μM skeletal S1 (low S1 concentration) at 37 °C in low salt ATPase buffer (10 mM KCl, 10 mM MOPS pH 7.2, 3.5 mM MgCl₂, 1 mM DTT, and 1 mM NaN₃). 3-4 experiments were carried out and are expressed as an average

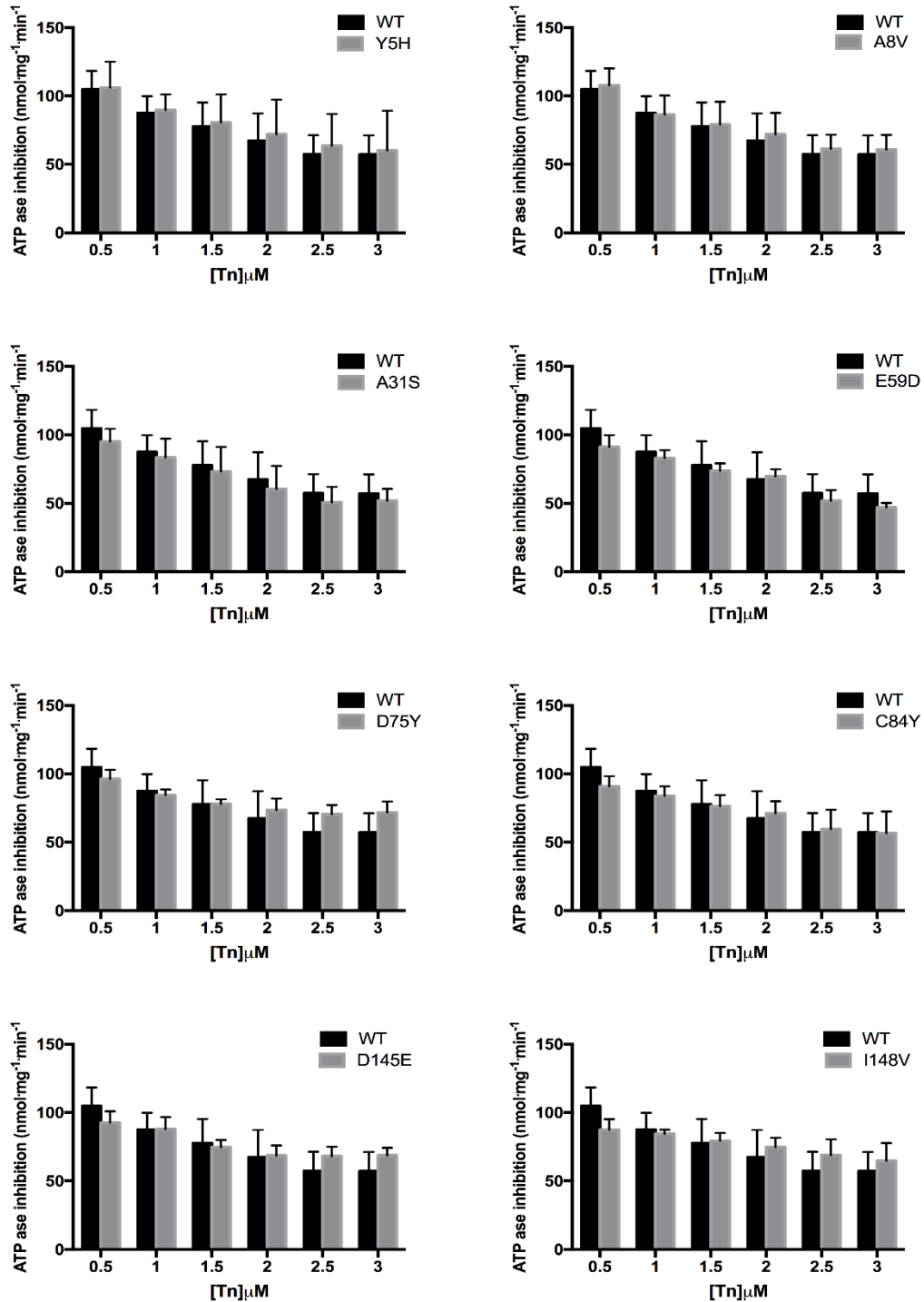


Figure 3.15: Effect of the HCM and DCM cTnC mutations on the ability of the troponin complex to inhibit the Actin-Tm activated Myosin-S1 ATPase in absence of Ca²⁺.

ATPase assays were performed in the presence of 1mM EGTA and 0-3 μM troponin. The assay consisted of 7 μM cardiac actin, 2 μM cardiac Tm, and 1 μM skeletal S1 (low S1 concentration) at 37 °C in low salt ATPase buffer (10 mM KCl, 10 mM MOPS pH 7.2, 3.5 mM MgCl₂, 1 mM DTT, and 1 mM NaN₃). 3-4 experiments were carried out and are expressed as an average

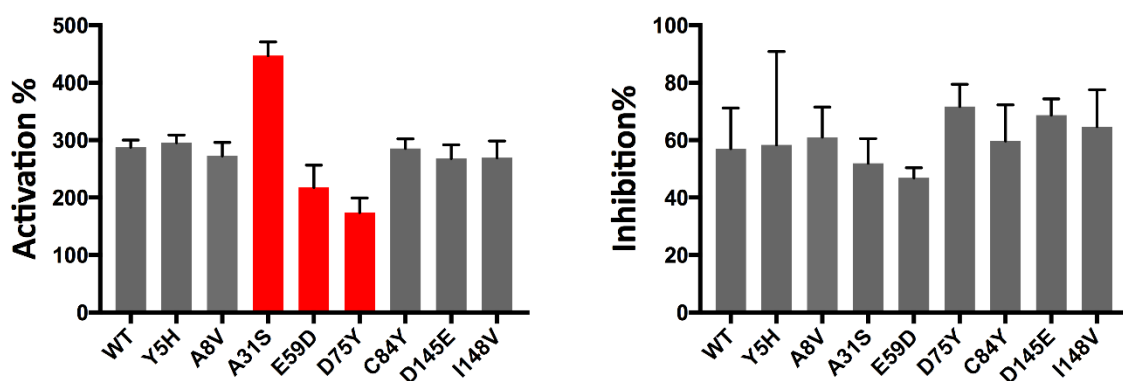


Figure 3.16: The maximal activation and inhibition obtained for each troponin complex obtained by reconstitution with each hcTnC mutant.

The data shows the percentage of ATPase activation or inhibition using the last point in figure 3.14 and 3.15. The level of both activation and inhibition is set as 100% by measure the actomyosin ATPase activity in absence of troponin complex concentration.

Table 3.3: A table displaying the % of maximal activation and inhibition obtained for each troponin complex obtained by reconstitution with each hcTnC mutant.

Maximal activation and inhibition for WT and TnC mutation reconstituted in troponin complex by using 3µM troponin complex. The data show as mean of three experiments and SD. For each parameter*indicates significant difference from WT (p<0.05) and parameter** indicates difference from WT (p<0.0001)

Troponin complex	Maximal activation %	Maximal inhibition %
WT	288 ± 11.979	57 ± 14.177
Y5H	292 ± 12.410	60 ± 29.002
A8V	272 ± 23.506	61 ± 10.774
A31S	447 ± 23.872**	52 ± 8.561
E59D	217 ± 39.170*	47 ± 3.46
D75Y	174 ± 25.239**	72 ± 7.932
C84Y	268 ± 24.042	57 ± 15.788
D145E	268 ± 24.042	69 ± 5.593
I148V	269 ± 28.991	65 ± 12.906

3.3 Discussion

In this chapter, we describe the obtain of cTnC mutant proteins, the characterization of their secondary structure, their reconstitution with cTnI and hcTnT into a troponin complex that folds and function in a comparable manner to the wild type troponin complex. We cloned the troponin cDNA into the pLEICS-05 vector (a vector designed for high yield protein expression). The following troponin C single amino acid mutants were produced (Y5H, A8V, A31S, E59D, D75Y, C84Y, D145E, I148V). First, we established a reliable method for the expression and purification of cTnC mutations in order to deliver reasonable amounts of highly pure troponin C reconstituted in functional troponin complex. The level of the expression of these mutations were comparable to WT (10-15 mg/L of LB media). The WT and cTnC mutations were purified using affinity column in presence of Ca^{2+} and then reconstituted with relatively pure TnI and TnT subunits. We also used the gel filtration column to purify the Tn complex and to assess the stoichiometry of troponin complex (1:1:1). Another aim was to assess their secondary structure by circular dichroism and their function by an actomyosin ATPase assay. Overall, we have shown that we can obtain pure WT and cTnC mutants and reconstitute them in trimeric TnT-I-C complex with a 1:1:1 stoichiometry as shown in figure 3.6. Moreover, since transient kinetic rely on the use of a large amount of protein a large effort was dedicated to get sufficient amount of proteins. Thus, we can characterize fully the impact of four HCM (A8V, A31S, C84Y, and D145E) and four DCM (Y5H, D59E, D75Y, and I148V) on the functional properties, biochemical, kinetic, and structure of cTnC.

3.3.1 The effect of HCM and DCM on the secondary structure

3.3.1.1 The effect of HCM and DCM on the secondary structure of TnC

It has been established that all TnC mutants were able to combine with the two other troponin subunits in a trimeric complex, we aimed to uncover if any mutation had a big impact on the secondary structure of troponin C and troponin complex. The data obtained from the CD spectra of TnC mutants suggest that the HCM and DCM mutations on the cardiac TnC gene have no impact on the secondary structure of troponin C (figure 3.7 and figure 3.8). Our results from the mutations Y5H, A31S, E59D, D75Y, and I148V are in agreement with previous studies (Pinto *et al.*, 2011; Pinto *et al.*, 2009; Parvatiyar *et al.*, 2012) except for Y5H, A8V, and D145E. Pinto *et al.* showed that Y5H and D145E reduce the α -helical content in comparison to WT (Pinto *et al.*, 2009; Pinto *et al.*, 2011). Moreover, Pinto *et al.* 2009 showed that A8V increases the α -helical content in comparison to WT. It is important to note that calculation of the exact content of secondary structure by CD is notoriously difficult because it requires high protein purity, high accuracy in protein concentration and can be affected by problems such as aggregation. Overall, our CD results indicated that D75Y and D145E impact was still present when these mutants were reconstituted in a troponin complex. Moreover, these two mutations reduce the melting point of isolated TnC which suggest that they destabilize the troponin C structure.

3.3.1.2 The effect of the HCM and DCM on the structure of troponin complex

The impact of mutations on secondary structure of the troponin C subunit (or lack of impact) does not preclude the fact that different effect on the secondary structure can be obtained in the whole trimeric troponin complex. Because of that we measured the CD spectra of TnC mutations reconstituted in the troponin complex and assessed the thermally induced unfolding of the troponin complexes.

The Circular dichroism was used to assess whether hcTn complex secondary structure was perturbed by the HCM and DCM TnC mutations. Our findings show that Y5H, A8V, A31S, E59D, C84Y, and I148V did not change the CD spectra of reconstituted troponin complexes. In contrast, D75Y and D145E produced CD spectra slightly different in comparison to WT (figure 3.10 and figure 3.11).

In addition, HCM mutations (A8V, A31S, and C84Y) affected the thermal stability of troponin complex in presence of these mutations (figure 3.13 C), while DCM mutations (Y5H, E59D, and I148V) did not affect the thermal stability of troponin complex in presence of these mutations (figure 3.12:C). In the same time, the globular effect of TnC mutations on the stability of troponin complex was by presence of the mutations D75Y and D145E.

Overall CD spectroscopy demonstrated that the overall shape and fold of the TnC and the reconstituted troponin complex is not affected by mutations in cTnC in agreement with the gel filtration data which showed that the troponin complex reconstituted with the mutated hcTnC is eluted at the same point in the elution profile as the WT.

3.3.2 The effect of the TnC mutations on the steady state actomyosin ATPase

Troponin is the calcium-based regulator of striated muscle contraction. Ca^{2+} controls the activation and relaxation of cardiac myofilaments and coordinates interactions between the thin and thick filaments. The thin filament is activated when Ca^{2+} binds to cardiac troponin C (cTnC). Complex interactions between troponin (Tn) subunits result in increased mobility of tropomyosin and increase the probability of myosin interaction with actin (Gordon *et al.*, 2001). In cardiac muscle, strong myosin binding to actin moves tropomyosin and also affect Ca^{2+} binding to troponin (Geeves & Lehrer, 1994). This mechanism is essential for rapid thin filament activation and force development in cardiac muscle.

To investigate the impact of TnC mutations Y5H, A8V, A31S, E59D, D75Y, C84Y, D145E, and I148V on the ability of troponin complex to regulate thin filaments biochemical activity, the ATPase assays were carried out in the presence of increasing concentration of troponin complex in the presence and absence of Ca^{2+} . Firstly, the WT and all TnC mutations showed a clear activation and inhibition of ATPase which suggest that the overall structure and biochemical properties of these troponin complexes are preserved in agreement with the CD results. Secondly, all mutations in hcTnC in the absence of Ca^{2+} had little effect on the inhibition of the actomyosin ATPase. This is not surprising since the primary role of hcTnC is to bind Ca^{2+} but it does suggest that the inhibition by troponin I is not affected by mutations in the TnC subunit.

In the presence of Ca^{2+} , Y5H, A8V, C84Y, D145E, AND I148V showed similar activation to the WT. In contrast A31S induced an increase in the level of activation while D75Y induced a decrease in the level of activation. These data are in agreement with several

previous studies (Albury *et al.*, 2012; Pinto *et al.*, 2011). Pinto *et al.* (2011) showed that the double mutants E59D and D75Y, located in helix C, failed to activate the thin filament to the levels of WT actomyosin ATPase in presence of calcium, but the inhibition of ATPase activity in absence of calcium was similar to WT. The results we obtained with A31S is consistent with a previous report which found that A31S increases the activation of ATPase in the presence of Ca^{2+} in comparison to WT (Parvatiyar *et al.*, 2012) .

In conclusion, we have produced fully functional hcTnC and hcTn complexes containing several hcTnC mutations and we have shown that these complexes can be incorporated in thin filaments and regulate the biochemical activity of thin filaments. It is therefore important to study in details the dynamics and kinetics of activation and inhibition using more robust approaches such as transient kinetics.

Chapter 4

Effect of cTnC mutations on the kinetics of Ca^{2+} binding and on the dynamics of thin filaments

4.1 Introduction

In striated muscle, contraction results by the cyclic association and dissociation of crossbridges formed between thick and thin filament accompanied by ATP hydrolysis. The interaction between actin and myosin is regulated by a multimeric protein complex made of troponin (TnI, T and C) and tropomyosin (Tm).

Ca²⁺ plays a major role in myofilaments activation and inhibition and every contractile parameter displays a characteristic dependence on the Ca²⁺ concentration named Ca²⁺ sensitivity. Changes in Ca²⁺ sensitivity have been reported in the majority of HCM and DCM associated mutations in contractile proteins. In addition, dissociation of Ca²⁺ from troponin is a prerequisite for cardiac relaxation and it is believed that the rate of Ca²⁺ dissociation from thin filaments limits the rate of muscle relaxation. Several models have been put forward to explain the mechanism of the Ca²⁺ dependent switch. The model of Hill and co-workers suggested two thin filament states of different affinity for myosin heads (Hill, Eisenberg et al.1980). In Lehrer and Morris (Lehrer and Morris 1982), ATPase studies have shown that Ca²⁺ alone cannot activate the thin filament and this led to the development of a three states model in which tropomyosin occupies a third non-blocking position at high concentration of myosin S1. The role of Ca²⁺ is to facilitate the binding of myosin heads leading to the active state and dissociation of Ca²⁺ is a pre-requisite for full relaxation.

Functionally, TnC is the Ca²⁺ binding subunit of the troponin complex that acts as an allosteric activator. When intracellular calcium concentration is high during systole, Ca²⁺ binds to TnC which then binds to TnI with a high affinity, thereby releasing it from its inhibitory site of actin. This Ca²⁺-induced allosteric transitions also leads to a change in

the position of Tm on the actin filament, which results in turning actin filaments to the active state. Relaxation is initiated when $[Ca^{2+}]$ falls to diastolic level which then in a reverse process, returns the thin filament to the relaxed state.

Recent studies have shown that genetic cardiomyopathies are caused by mutations in cardiac TnC and that these mutations affect thin filament sensitivity to Ca^{2+} . To fully understand the significance of cardiovascular diseases associated mutation in TnC, it is necessary to understand the mechanism behind shifts in Ca^{2+} sensitivity and also determine the impact of these mutations on the rate of Ca^{2+} dissociation. Our hypothesis in this chapter is that HCM and DCM associated mutations in cTnC are likely to alter the kinetics of Ca^{2+} binding and the consequent transitions in thin filaments between an active and inactive states. Therefore, we used the fluorophore Quin-2 to investigate the effect of HCM and DCM cTnC mutations on the rate constant of Ca^{2+} dissociation from TnC, Tn complex, thin filament, and thin filament + rigor myosin heads. Moreover, we try to understand, at the molecular level, how the mutations in TnC which caused cardiomyopathies alter the regulation of the cardiac contractile cycle, the relationship between the Tm-Tn-controlled on/off state change of the thin filament. Therefore, we investigated the effect of HCM and DCM cTnC mutations on the dynamics of thin filament switching by using transient kinetics.

In this chapter, we investigated the effect of HCM and DCM mutations associated with TnC protein on the dynamics of thin filament switching including three parameters: the rate of Ca^{2+} dissociation, the equilibrium constant between blocked and closed states and the binding of troponin to thin filaments.

4.2 Result

4.2.1 Impact of HCM and DCM cTnC mutations on the kinetics of calcium dissociation.

One of the most important biochemical steps in the regulation of muscle contraction is the rate of calcium dissociation from cTnC. To understand how DCM and HCM cTnC mutations can affect the rate constant of Ca^{2+} dissociation from troponin C alone or associated with other thin filaments proteins we used a chase experiment that relies on the rapid reaction between Ca^{2+} and a fluorophore Quin-2 with a parallel increase in its fluorescence. In order to study the effect of TnC mutations on the calcium dissociation rate of troponin complex we measured the Ca^{2+} dissociation rate of troponin C, troponin complex, troponin complex with Actin-Tm, and troponin complex with actin-Tm thin filament in presence of myosin head using stopped flow based transient kinetics. The normalised transient are displayed for Ca^{2+} dissociation from troponin C WT and TnC mutations alone (figure 4.1), reconstituted in a trimeric troponin complex (Figure 4.2), reconstituted in a full thin filament (Actin-Tm-Tn, Figure 4.3) and thin filament in the presence of rigor myosin head (Figure 4.4). The transient of troponin C and the troponin complex are fit for one exponential and gave one observed rate constant as shown in table 4.1. The transient of thin filament and thin filament with rigor myosin head clearly show two phases: a fast phase and slow phase (table 4.1). The traces were fit to two exponentials with two rate constants. The results are summarized in table 4.1.

For troponin C alone the rate constant of Ca^{2+} dissociation was not affected by any of the studied mutations except I148V. The rate constant for this mutation was higher than WT by 2-fold.

When hcTnC is reconstituted into a troponin complex with hcTnI and hcTnT, the rate constant of Ca²⁺ dissociation is increased substantially (a weakening of the affinity of troponin for Ca²⁺). Four mutations including Y5H, D75Y, C84Y and D145E increased this rate constant above the WT level (From 90 s⁻¹ to 111-149 s⁻¹). While three mutations including A8V, A31S and I148V decreased the rate constant of Ca²⁺ dissociation (from 90 s⁻¹ to 56-80 s⁻¹). It is important to note that A8V is located at N-terminal domain.

When hcTnC is reconstituted into a troponin complex and then into a thin filament (with actin and Tm), the rate constant of Ca²⁺ dissociation is further increased (a further weakening of the affinity of troponin for Ca²⁺). All mutations but Y5H reduced the rate constant of Ca²⁺ dissociation.

In contrast when this thin filament was reconstituted with myosin head, the rate constant of Ca²⁺ dissociation was decreased and the pattern of change was different. All mutations but I148V increased the rate constant of Ca²⁺ dissociation.

Table 4.1: The rate of Ca²⁺ dissociation.

The effect of cTnC mutation on the Ca²⁺ dissociation rate of cTnC and troponin complex by 2-Quin.

TnC mutations	TnC Rate(s ⁻¹)	Tn-complex Rate (s ⁻¹)	Thin filament Rate (s ⁻¹)		Thin filament +S1	
			Fast	Slow	Fast	Slow
WT	1.95±0.071	90.5±2.121	217±05.657	3±0.0	97±26.5	5±1
Y5H	1.8±0.14	115.5±4.95	214±17.678	3±0.0	164±39.598	6±3
A8V	1.65±0.07	66±2.828	140±52.326	6±3	103±49.497	5±2
A31S	1.65±0.071	56±0.00	119±22.627	4±0.0	74±7.778	4±1
E59D	2.25±0.212	91.5±2.121	116±13.435	4±2	122±38.185	4±1
D75Y	1.7±0.14	149±9.192	179±17.678	4±0.0	146±15.555	4±1
C84Y	1.75±0.212	120±19.092	165±38.184	3±1	117±12.728	3±1
D145E	1.8±0.14	111±1.414	179±01.414	3±0.0	107±9.899	3±2
I148V	4±1.414	80.5±2.121	135.5±10.607	3±1	80±1.414	3±2

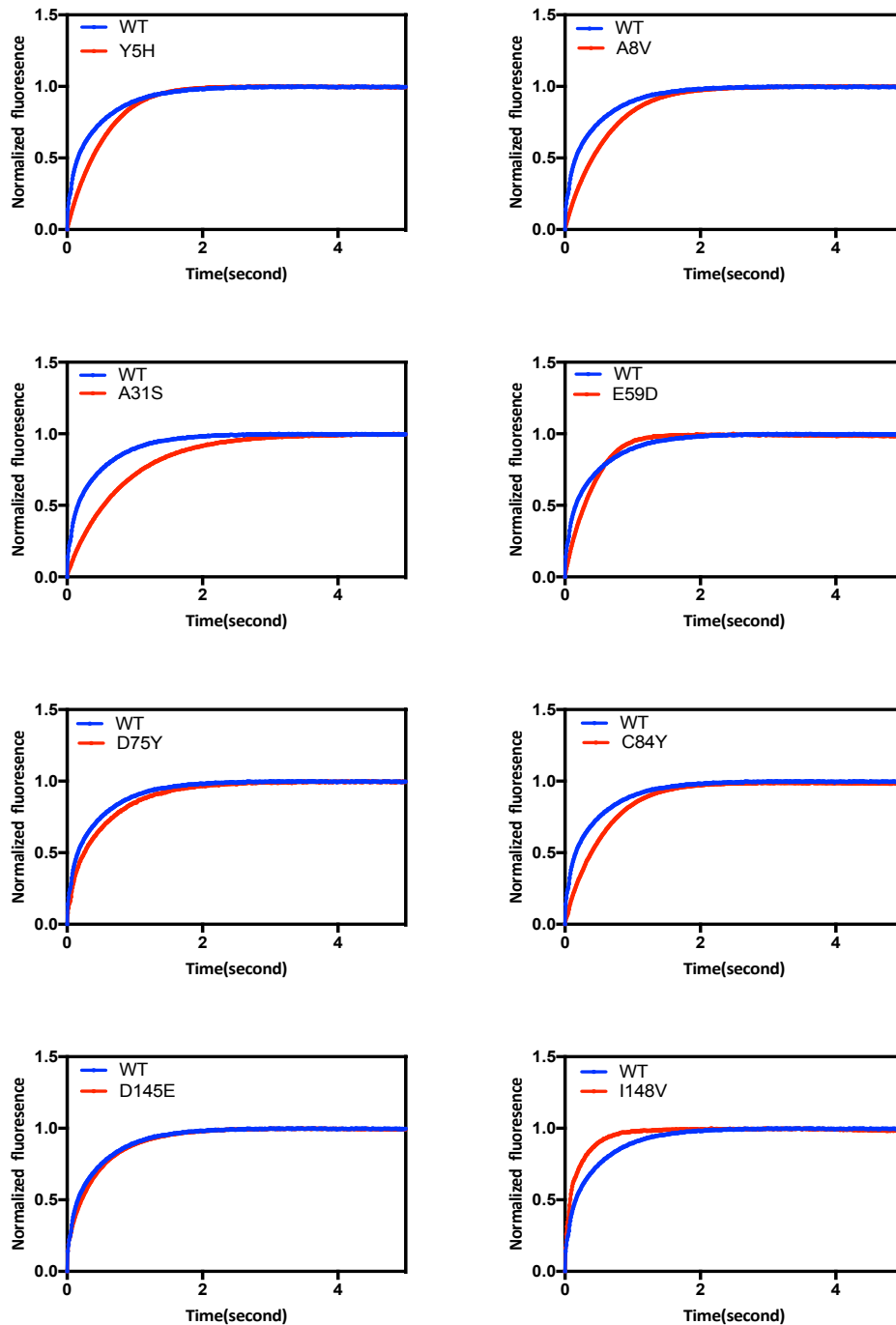


Figure 4.1: Normalised Ca²⁺ dissociation transients from troponin C.

Ca²⁺ dissociation normalised fluorescence from TnC WT (blue) and HCM and DCM mutants (red). Each trace obtained by using 18 μM of troponin C in 50 mM MOPS pH 7.2, 140 mM KCl, and 4 mM MgCl₂, and 60 μM CaCl₂. The experiment don at 25° and Quin-2 concentration 150 μM .

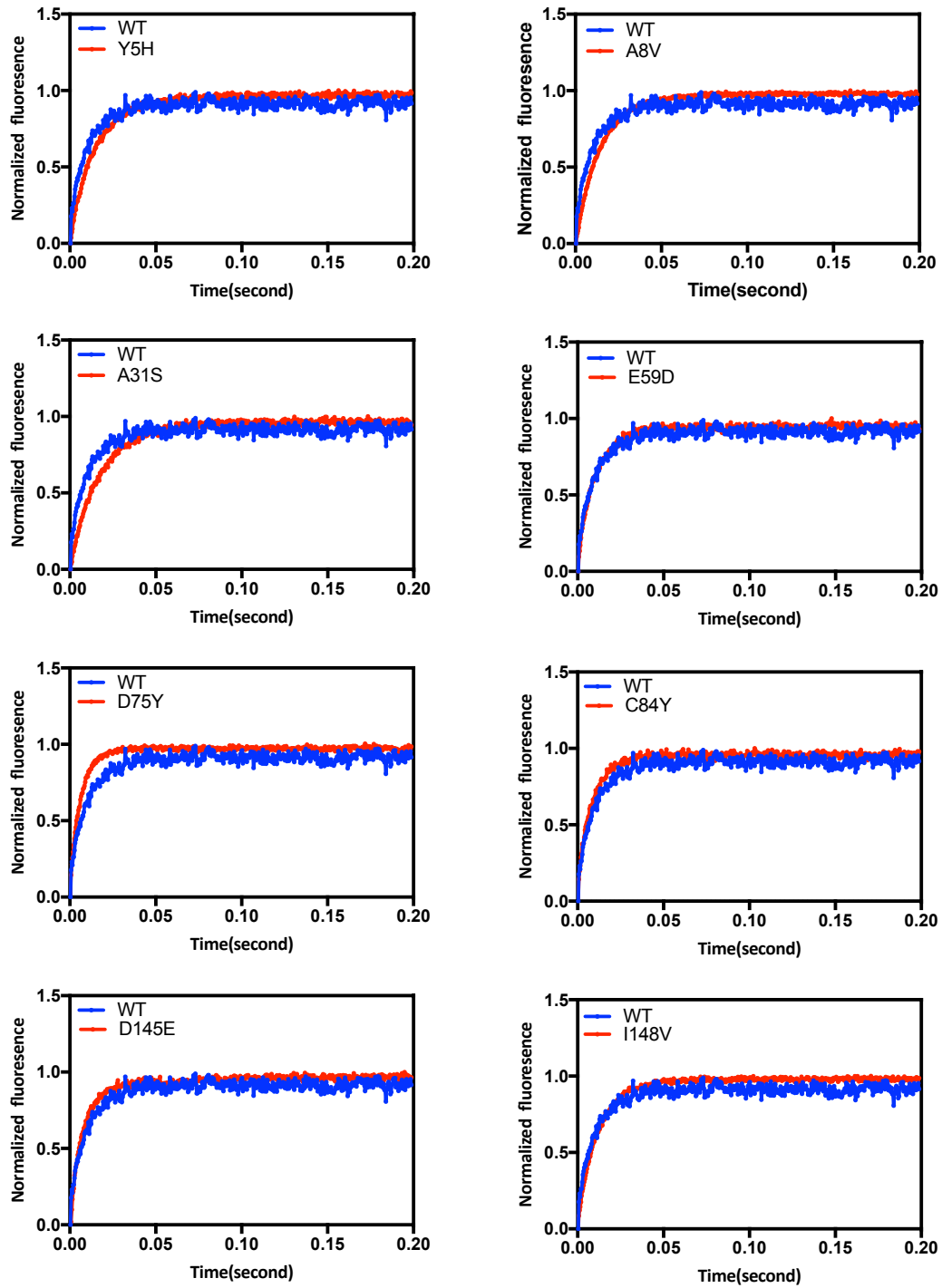


Figure 4.2: Normalised Ca^{2+} dissociation transients from troponin complex.

Ca^{2+} dissociation normalised fluorescence from TnC WT (blue) and HCM and DCM mutants (red) reconstituted in troponin complex. Each trace obtained by using 18 μM of troponin complex in 50 mM MOPS pH 7.2, 140 mM KCl, and 4 mM MgCl_2 , and 60 μM CaCl_2 . The experiment done at 25°C and Quin-2 concentration 150 μM .

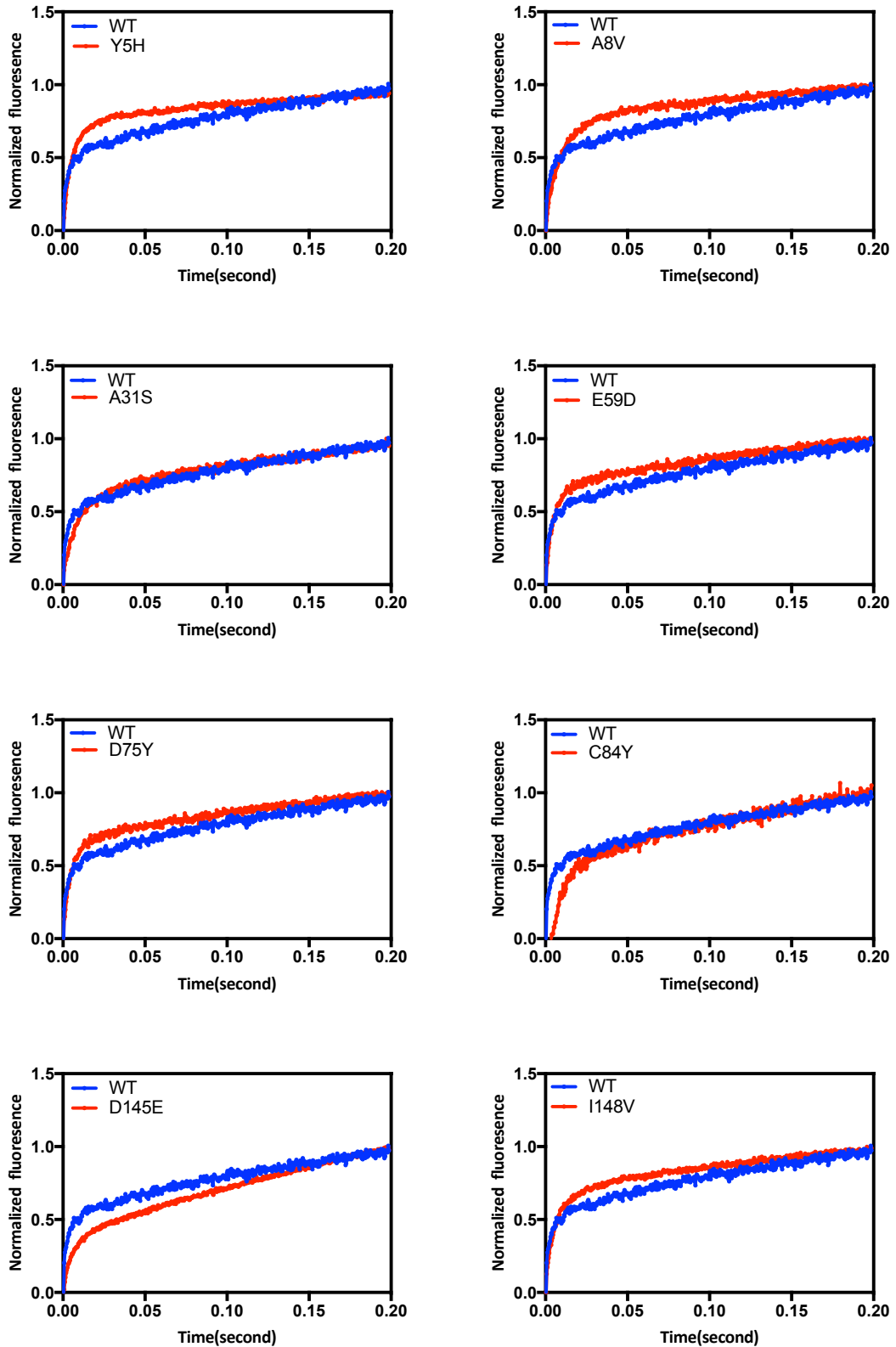


Figure 4.3: Normalised Ca²⁺ dissociation transients from thin filament.

Ca²⁺ dissociation normalised fluorescence from TnC WT (blue) and HCM and DCM mutants (red) reconstituted in troponin complex with Actin-Tm. Each trace obtained by using 18 μ M of troponin complex in 50 mM MOPS pH 7.2, 140 mM KCl, and 4 mM MgCl₂, and 60 μ M CaCl₂. The experiment don at 25°C and Quin-2 concentration 150 μ M.

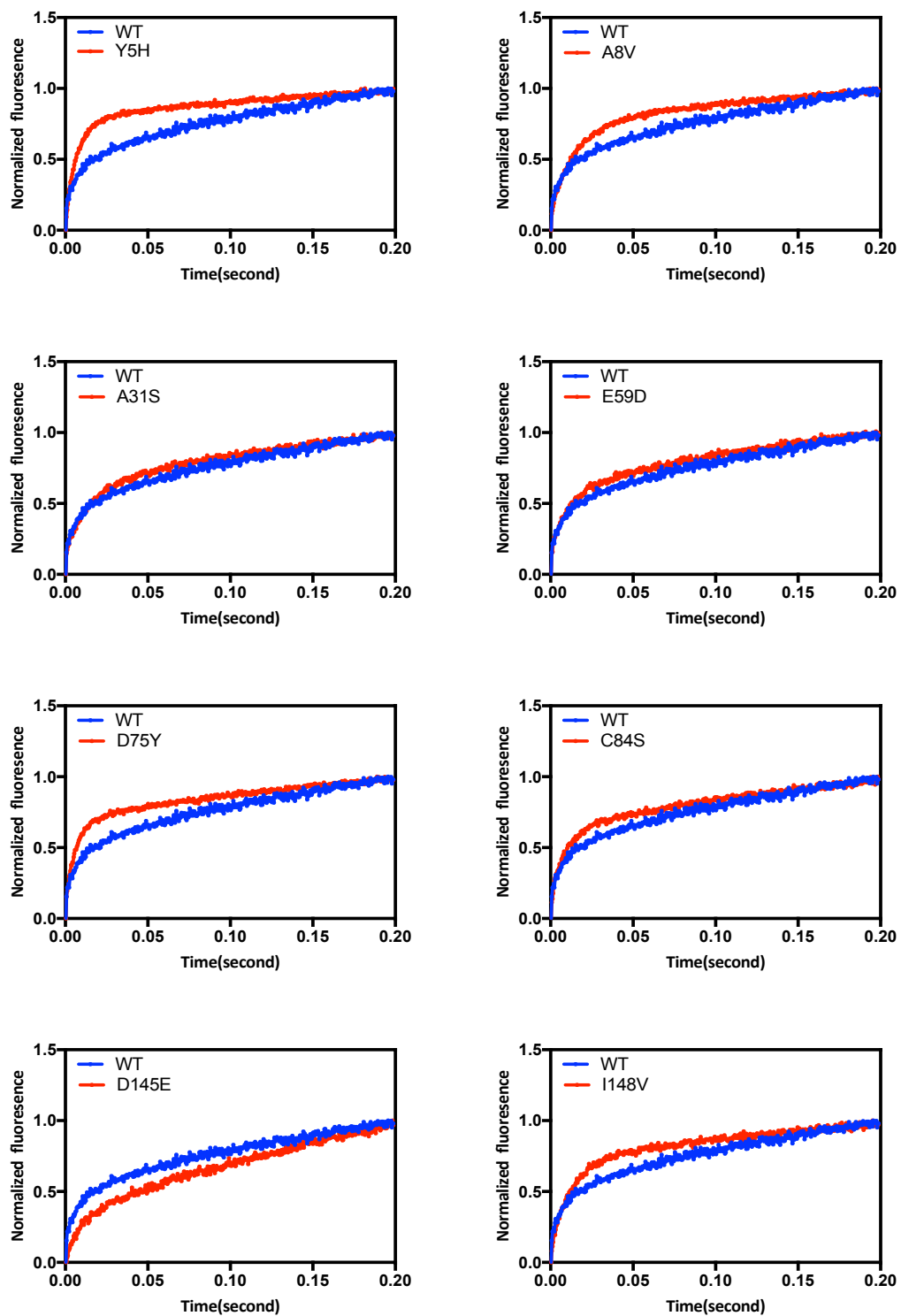


Figure 4.4: Normalised Ca^{2+} dissociation transients from thin filament in presence of S1.

Ca^{2+} dissociation normalised fluorescence from TnC WT (blue) and HCM and DCM mutants (red) reconstituted in troponin complex. Each trace obtained using 18 μM of troponin complex in 50 mM MOPS pH 7.2, 140 mM KCl, and 4 mM MgCl_2 , and 60 μM CaCl_2 . The experiment don at 25 $^\circ\text{C}$ and Quin-2 concentration 150 μM

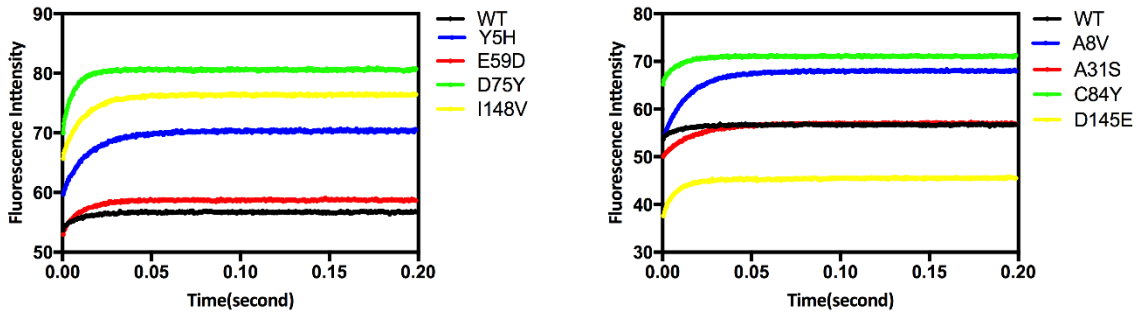


Figure 4.5: Ca²⁺ dissociation fluorescence transients from troponin C.

Each trace obtained by using 8 μM troponin complex, in 50 mM MOPS pH 7.2, 140 mM KCl, and 4 mM MgCl₂, and 60 μM CaCl₂. The experiment was done at 25 °C and Quin concentration 150 μM.

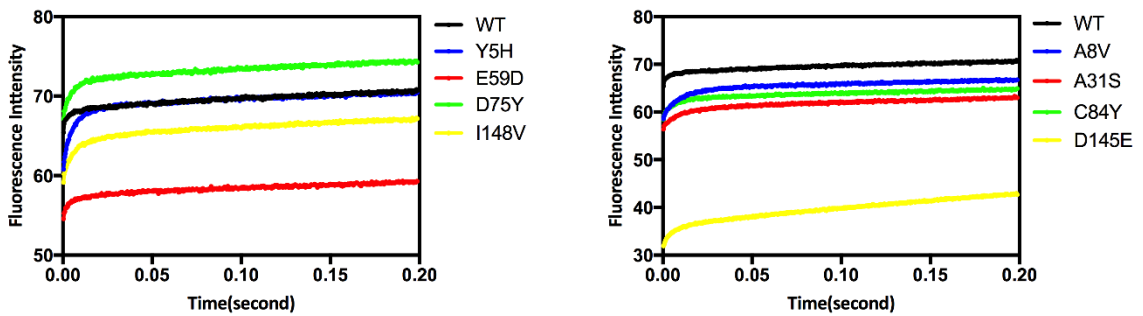


Figure 4.6: Ca²⁺ dissociation fluorescence transients from troponin complex.

Each trace obtained by mixing 47,8, 8, μM of actin, tropomyosin, and troponin complex, in 50 mM MOPS pH 7.2, 140 mM KCl, and 4 mM MgCl₂, and 60 μM CaCl₂. The experiment was done at 25 °C and Quin concentration 150 μM.

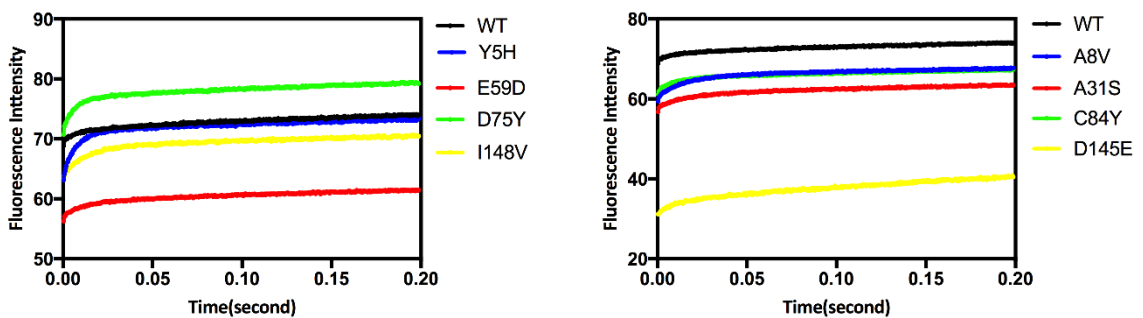


Figure 4.7: Ca²⁺ dissociation fluorescence transients from thin filaments.

Each trace obtained by mixing 47,8, 8, 12 μM of actin, tropomyosin, troponin complex, and rigor myosin heads respectively in 50 mM MOPS pH 7.2, 140 mM KCl, and 4 mM MgCl₂, and 60 μM CaCl₂. The experiment was done at 25 °C and Quin concentration 150 μM.

4.2.1.1 Effect of TnC mutations on the thin filament-switch between blocked and closed states

The equilibrium constants K_B characterizes the transition between the blocked state (thin filament unable to bind to the myosin head) and the closed state (myosin head able to bind to actin weakly). K_B is an allosteric constant that describes an important transition during the cooperative-allosteric activation and inactivation of thin filaments secondary to Ca^{2+} binding/dissociation. Since Ca^{2+} binding to hcTnC is an allosteric effector, it is critical to assess the effect of the troponin C mutations on K_B . PIA-labeled actin was mixed with a small amount of S1 (1/10th), and the kinetics of binding of S1 to PIA-actin. Tm.Tn (7:1:1) in the presence and absence of Ca^{2+} (Head et al., 1995) was followed. The measurements were carried out in ATPase buffer (10 mM Mops, pH 7.2, 140 mM KCl, 4 mM $MgCl_2$, 1 mM DTT, 1 mM NaN_3) at 25 °C. Then the average data was fitted to a single exponential. The exponential change in fluorescence was used to determine the observed rate constant of S1 binding to thin filaments. In Figure 4.8, k_{obs} is plotted versus increasing thin filament concentration. The k_{obs} obtained in both the presence and absence of calcium as well as actin alone are linearly dependent upon actin concentration over the range 2-10 μ M. The slope of each curve is divided by the slope of the curve obtained for actin alone to determine K_B according to the following equation:

$$K_{obs} (\text{regulated actin}) / k_{obs} (\text{actin alone}) = K_B / (1+K_B)$$

Where k_{obs} is the observed rate constant (for regulated actin or for actin alone), and K_B is the equilibrium constant between blocked and closed states (figure 4.8).

Table 4.2 summaries the results of the K_B parameter in presence and absence of Ca^{2+} for each HCM and DCM cTnC mutation. It is apparent from this table that all HCM and DCM

mutations had no impact on the K_B in presence of Ca^{2+} . On the other hand, the result suggested that there is clear effect of TnC mutations on the kinetics of S1 binding to the thin filament in absence of Ca^{2+} except Y5H. The A8V, A31S, E59D, D75Y, D145E and I148V show that they have big impact on the K_B equilibrium constant in absence of Ca^{2+} compared to WT (figure 4.9). The K_B for D145E mutations was higher than WT by 3.2-fold in absence of calcium (1.25 ± 0.07 and 0.39 ± 0.07 respectively). Moreover, the K_B of D75Y and C84Y higher than the K_B of WT by 2.6-fold in absence of Ca^{2+} . The less effect on the kinetics of S1 binding to the thin filament in absence of Ca^{2+} was obtained from the mutations I148V, A31S, and A8V. The K_B of I148V in absence of Ca^{2+} higher than the WT by 1.5-fold (0.58 ± 0.07 and 0.39 ± 0.07 respectively) while A31S and A8V higher than WT by 1.6-fold.

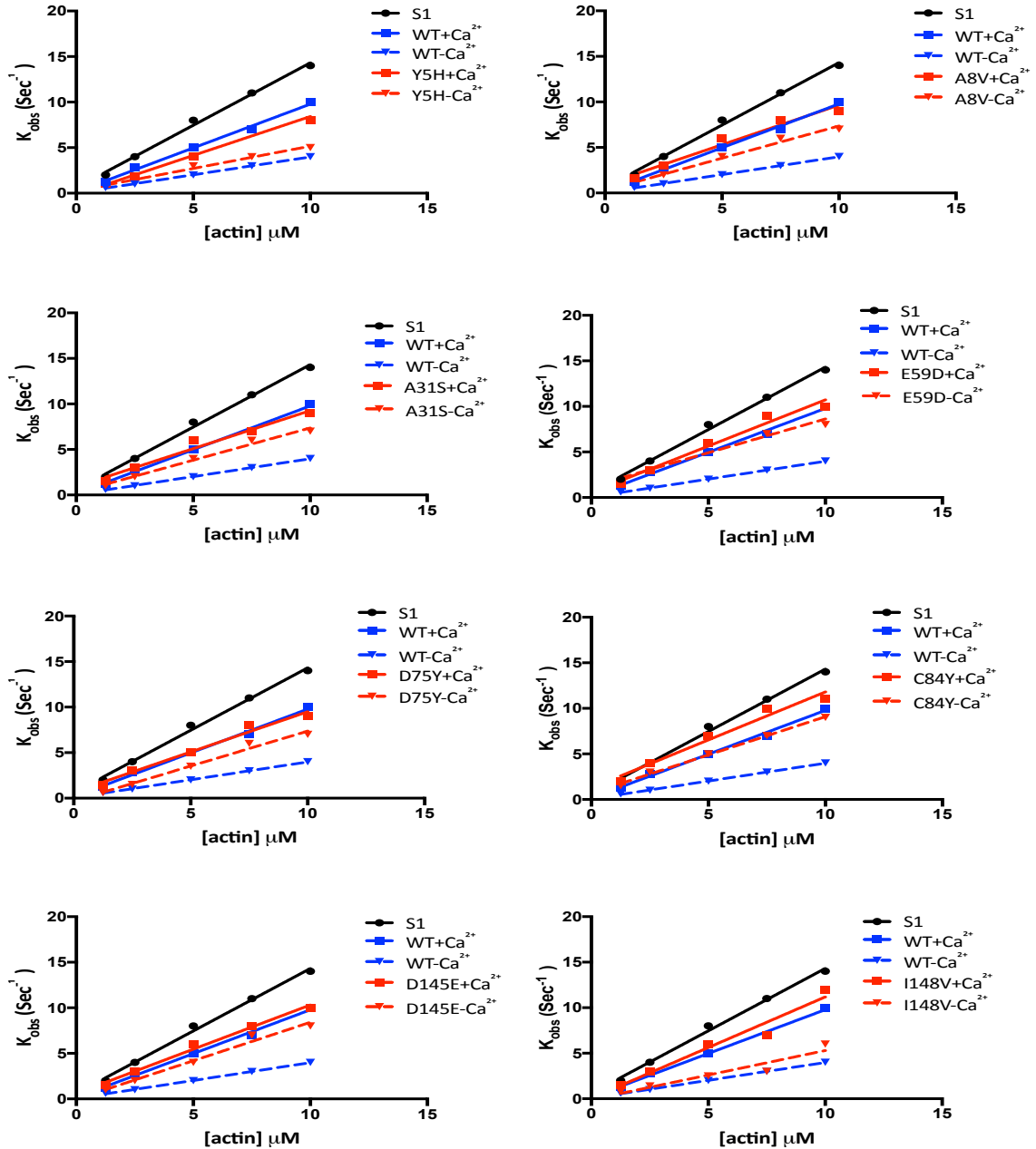


Figure 4.8: Determination of KB of HCM and DCM cTnC mutations reconstituted in troponin complex.

The binding of S1 to PIA-Actin-Tm-Tn in the presence and absence of calcium for the HCM and DCM cTnC mutation. The conditions of experiment were 140 mM KCl, 10 mM Mops pH 7.2, 4 mM MgCl₂, 1 mM DTT, 0.5 mM CaCl₂ or 1 mM EGTA, at 25 °C. the black line represent PIA-S1, the red line represent troponin complex WT (+Ca²⁺) and (-Ca²⁺) with PIA-S1, and blue line represent each troponin C mutations (+Ca²⁺) and (-Ca²⁺)

Table 4.2 a Summary of K_b values for thin filaments reconstituted with hcTnC mutants.

K_B of cTnC WT and HCM and DCM reconstituted in troponin complex. For each parameter*indicates significant difference from WT ($p<0.05$) and parameter** indicates difference from WT ($p<0.0001$)

TnC mutations	K_b+Ca^{2+}	K_b-Ca^{2+}	Number of experiments
WT	>1	0.39 ± 0.07	7
Y5H	>1	0.35 ± 0.16	3
A8V	>1	$0.62\pm 0.03^*$	3
A31S	>1	$0.62\pm 0.04^*$	4
E59D	>1	$0.80\pm 0.17^*$	3
D75Y	>1	$1.05\pm 0.06^*$	3
C84S	>1	$1.03\pm 0.25^*$	3
D145E	>1	$1.25\pm 0.07^{**}$	3
I148V	>1	$0.58\pm 0.07^*$	3

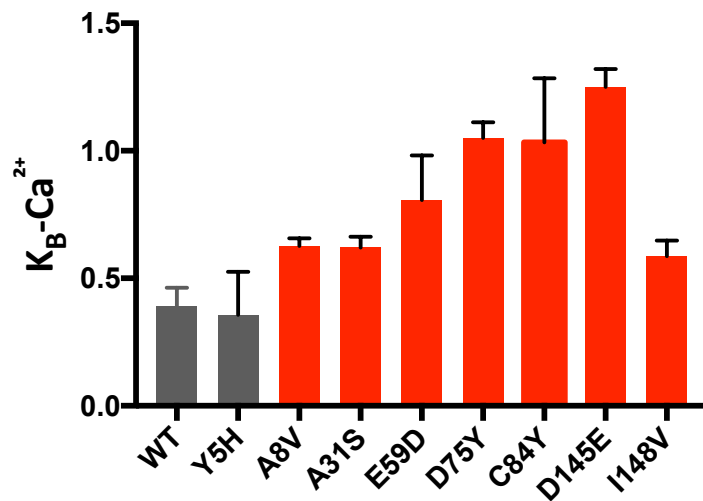


Figure 4.9: Comparison of thin filament switching parameter K_B of cTnC mutations.

The Block state parameter K_B of cTnC WT and HCM and DCM mutation reconstituted in troponin complex in absence of Ca^{2+} .

4.2.2 Effect of TnC mutations on Troponin binding to tropomyosin and actin-tropomyosin.

The regulatory properties of the troponin complex depend on a set of complexes interactions in thin filaments that involve interactions between troponin and tropomyosin and troponin and actin. Changes in the biochemical properties such as K_b and the rate constant of Ca^{2+} dissociation could be due to changes in the interactions of troponin with its partners. Isothermal titration microcalorimetry (ITC) was used to monitor the interaction of the troponin complex to tropomyosin, troponin complex to thin filament, and TnC to TnI.

4.2.2.1 Effect of TnC mutations on the TnC-TnI binding

Troponin C interacts with TnI, the inhibitory subunit, and TnT the tropomyosin binding subunit, on the actin-tropomyosin thin filament. According to (Gaelle et al, 2000) the cTnC-cTnI interaction involved a complex interface with as much as six interaction sites, that are either Ca^{2+} dependent or independent. A stable binary complex is formed by antiparallel interaction of C-terminal domain of cardiac troponin C (cTnC) comprising residues 81-161 and the N-terminal domain of cardiac troponin I (cTnI) comprising residues 33-80 (Frank et al, 1992), and the NH₂-domain of cTnC has been shown to interact with cTnI (147-163). To obtain a more comprehensive picture about how TnC mutations can affect the TnC binding to TnI we used ITC. The experiment was carried out in the following conditions: 25°C, 140 mM KCl, 10 mM Mops pH 7.2, 3.5 mM MgCl₂, 0.1 mM DTT, 1 mM NaN₃, and 1 mM CaCl₂, injection volume 15 μM, volume of TnC in syringe 0.5 ml at 70 μM, and 1.4ml 7 μM TnI. Origin ITC data analysis software (Microcal Inc.) was applied to analyze all binding isotherms.

Figures 4.10-4.13 present the experimental data obtained from titration of cTnI with cTnC WT and HCM and DCM mutations. Traces of these titrations of TnC with TnI showed negative peaks which mean the interactions are exothermic. In each case the stoichiometric ratio(n) of TnI binding to TnC was 1:1 as shown in table 4.3 which summarized all the binding parameters for complexation between cTnI and cTnC. The stoichiometry (n), dissociation constant K_d , and the enthalpy binding (ΔH), entropy (ΔS) and the change in Gibbs free energy (ΔG) which calculated according to following equation.

$$\Delta G = -RT \ln K_d = \Delta H - T\Delta S$$

As shown in table 4.3 and figure 4.10 the dissociation constant of binding between cTnC and cTnI for WT is $1.4 \pm 0.2 \mu\text{M}$ and this K_d were slightly higher for C84Y, Y5H, A31S and D75Y than WT while for E59D and I148V K_d for TnI-TnC interaction was higher than WT by 2.8 fold.

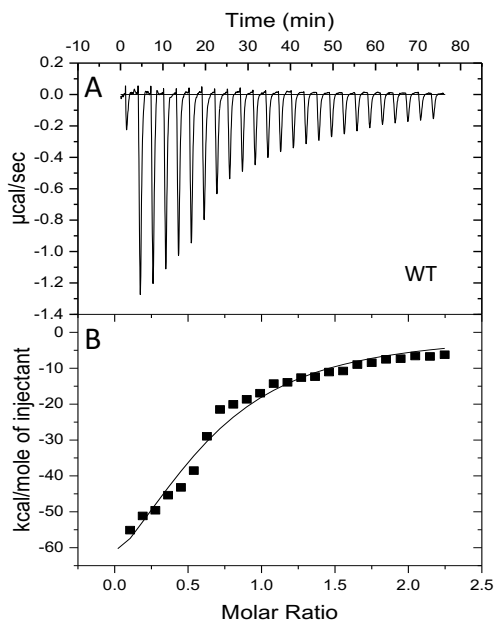


Figure 4.10: TnC binding to TnI in the presence of 1mM CaCl₂ measured by isothermal titration calorimetry (ITC). (A) The trace of titration obtained by 25 injections of TnC into TnI at 25 °C, 140mM KCl, 10mM MOPS PH 7.2, 3.5 MgCl₂. (B) Integrated heats for each injection versus the molar ratio of tropomyosin to troponin and solid line is the data fitting using 1:1 binding mode.

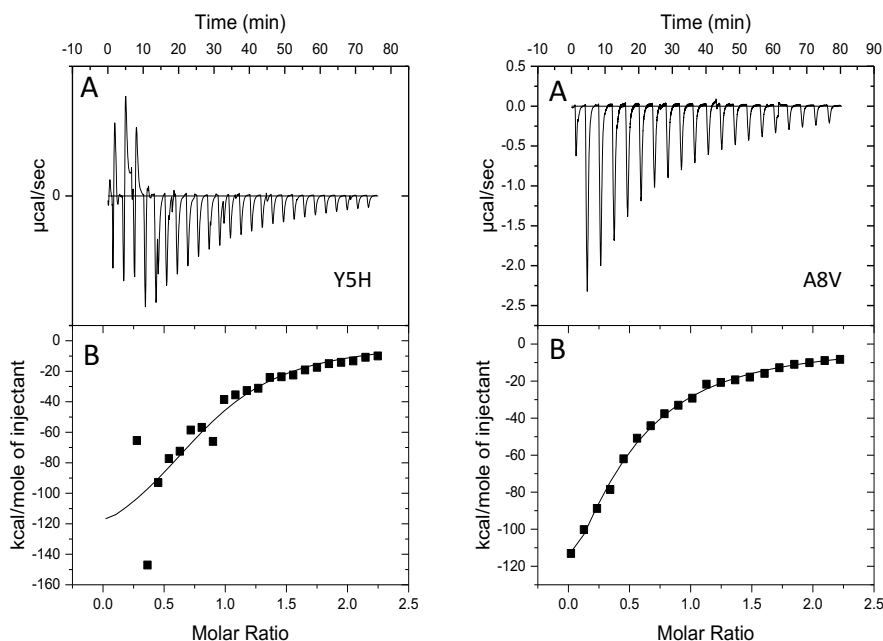


Figure 4.11: TnC binding to TnI by isothermal titration calorimetry (ITC). Titration of Troponin C mutations (Y5H, A8V) with troponin I in presence 1mM CaCl₂. (A) The trace of titration obtained by 25 injections of TnC into TnI at 25 °C, 140mM KCl, 10mM MOPS PH 7.2, 3.5 MgCl₂. (B) Integrated heats for each injection versus the molar ratio of tropomyosin to troponin and solid line is the data fitting using 1:1 binding mode.

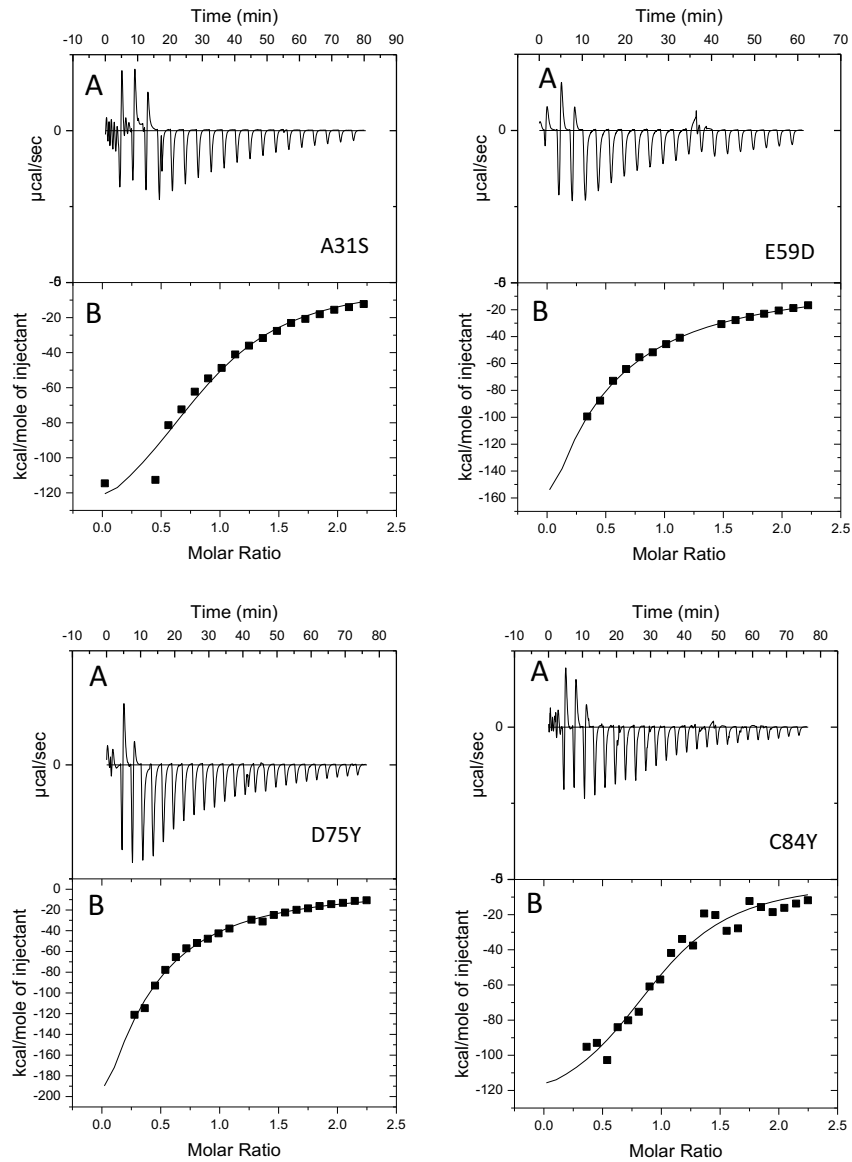


Figure 4.12: TnC binding to TnI by isothermal titration calorimetry (ITC). Titration of Troponin C mutations (D75Y, C84Y, A31S, E59D) with troponin I in presence 1mM CaCl_2 . (A) The trace of titration obtained by 25 injections of TnC into TnI at 25 $^{\circ}\text{C}$, 140mM KCl, 10mM MOPS PH 7.2, 3.5 MgCl_2 . (B) Integrated heats for each injection versus the molar ratio of tropomyosin to troponin and solid line is the data fitting using 1:1 binding model.

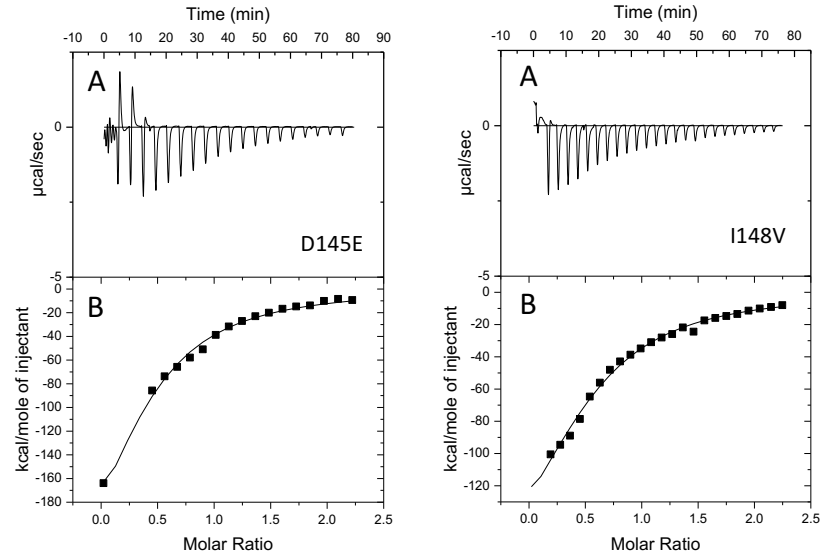


Figure 4.13: TnC binding to TnI by isothermal titration calorimetry (ITC). Titration of Troponin C mutations (D145E, I148V) with troponin I in presence 1mM CaCl₂. (A) The trace of titration obtained by 25 injections of TnC into TnI at 25 OC, 140mM KCl, 10mM MOPS PH 7.2, 3.5 MgCl₂. (B) Integrated heats for each injection versus the molar ratio of tropomyosin to troponin and solid line is the data fitting using 1:1 binding model.

Table 4.3 Binding parameters between troponin C WT and HCM and DCM mutations and cTnI.

For each parameter*indicates significant difference from WT ($p < 0.05$) and parameter** indicates difference from WT ($p < 0.0001$)

cTnC	K_d μ M	Stoichiometry (n)	ΔH (kcal/mole)	ΔS (kcal/mole)	ΔG (kcal/mole)
WT	1.4 \pm 0.20	0.9 \pm 0.12	-5.9e4 \pm 1.1e4	-172 \pm 4.7	-6.3e4 \pm 1.4e3
Y5H	1.5 \pm 0.20	0.9 \pm 0.20	-1.5e5 \pm 4.9e4*	-467 \pm 5.80**	-2.7e4 \pm 1.5e3*
A8V	3.5 \pm 0.03**	1.0 \pm 0.45	-2.6e5 \pm 2.8e4	-865 \pm 19.7**	-4.7e4 \pm 2.1e3*
A31S	1.8 \pm 0.1*	0.9 \pm 0.06	-1.5e5 \pm 1.4e4*	-497 \pm 14.6**	-2.7e4 \pm 1.2e3**
E59D	4.0 \pm 0.02**	1.1 \pm 0.26	-1.0e5 \pm 3.8e4	-260 \pm 6.40	-1.8e4 \pm 1.7e3**
D75Y	1.6 \pm 0.44	0.8 \pm 0.03	-1.4e5 \pm 1.0e4*	-456 \pm 7.9**	-2.5e4 \pm 1.2e3**
C84Y	1.0 \pm 0.34	0.9 \pm 0.07	-1.3e5 \pm 1.5e4*	-426 \pm 2.9**	-2.4e4 \pm 9e3**
D145E	4.0 \pm 0.25**	0.6 \pm 0.02	-2.6e5 \pm 1.4e4	-845 \pm 7.4**	-4.7e4 \pm 1.7e3*
I148V	2.8 \pm 0.02*	0.9 \pm 0.05	-2.2e5 \pm 2.5e4	-688 \pm 3.5**	-3.9e4 \pm 882**

4.2.2.2 Effect of TnC mutations on the troponin tropomyosin binding

These experiments were performed at 25 °C on a VP-ITC instrument (Microcal LLC, Northampton, MA, USA). Troponin complex and tropomyosin were dialyzed extensively against ATPase buffer (140 mM KCl, 10 mM Mops pH 7.2, 3.5 mM MgCl₂, 0.1 mM DTT, 1 mM NaN₃, and 50 μM CaCl₂). The sample cell was filled with 1.4 ml of tropomyosin, 7 μM and titrated with 300 μl of 70 μM wild type and TnC mutations combined into troponin complexes. The injection size was 15 μl, with duration of 14 sec., at 240 sec intervals with a stirring at 300 rpm. Control titration of buffer with troponin and buffer with tropomyosin indicated that heats of dilution were small and constant.

Figures 4.14-4.17 show the result of titration of Tm with cTnC WT and HCM and DCM mutations reconstituted in troponin complex by ITC. These graphs display the integrated heats for each tropomyosin injection. Each negative peak represents heat released by troponin complex binding to tropomyosin. The result of ITC suggested that the molar ratio of the binding between troponin and tropomyosin is around 1 in agreement with the physiological ratio of one troponin/tropomyosin. All the mutations gave a stoichiometry close to the wild type. On the other hand, the result of ITC showed that there is effect on the affinity of the binding between troponin and tropomyosin. As can be seen from the table 4.4 the dissociation constants (K_d) of WT is 1.1 ± 0.15 . The K_d of A8V, D75Y, and I148V were very close to K_d of WT (1.3 ± 0.34 , 1.4 ± 0.62 , 1.1 ± 0.55 respectively). Mutations A31S and E59D increased the K_d of TnI-TnC interaction by 8.8-fold and 2.9-fold (9.7 ± 0.25 and 3.2 ± 0.46 respectively). Interestingly Y5H, D145E and C84Y strengthened the binding of TnC to TnI (Decrease of K_d to 0.6 ± 0.01 and 0.8 ± 0.14 and 0.4 ± 0.3 respectively).

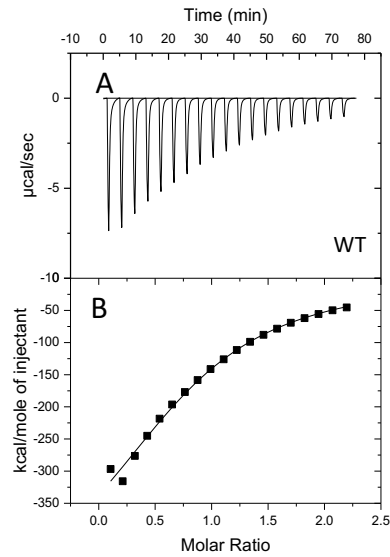


Figure 4.14: Troponin complex binding to Tropomyosin by isothermal titration calorimetry (ITC). Titration of Troponin C WT and mutations reconstituted in troponin complex with tropomyosin in presence 1mM CaCl_2 . (A) The trace of titration obtained by 20 injections of $70\mu\text{M}$ tropomyosin into $7\mu\text{M}$ troponin complex at 25°C , 140mM KCl, 10mM MOPS PH 7.2, 3.5 MgCl_2 . (B) Integrated heats for each injection versus the molar ratio of tropomyosin to troponin and solid line is the data fitting using 1:1 binding model.

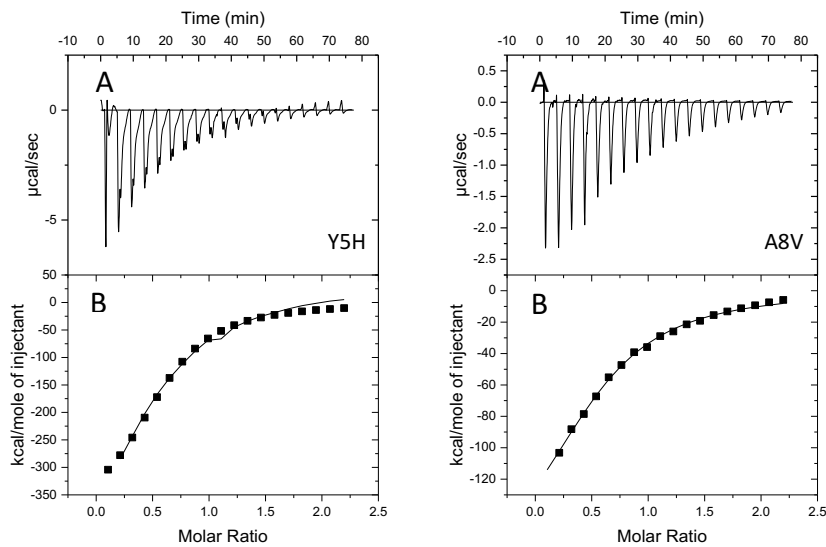


Figure 4.15 Troponin complex binding to Tropomyosin by isothermal titration calorimetry (ITC): Titration of Troponin C mutations (Y5H and A8V) reconstituted in troponin complex with tropomyosin in presence 1mM CaCl_2 . (A) The trace of titration obtained by 20 injections of $70\mu\text{M}$ tropomyosin into $7\mu\text{M}$ troponin complex at 25°C , 140mM KCl, 10mM MOPS PH 7.2, 3.5 MgCl_2 . (B) Integrated heats for each injection versus the molar ratio of tropomyosin to troponin and solid line is the data fitting using 1:1 binding model.

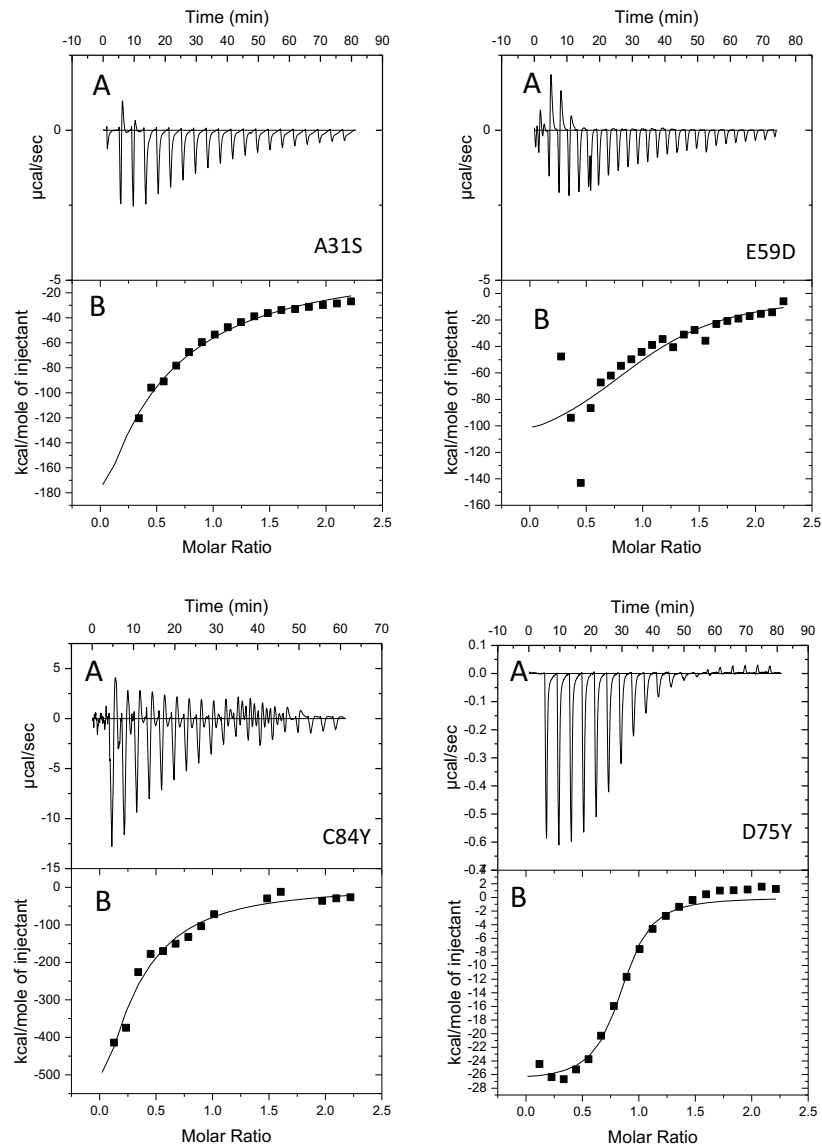


Figure 4.16: Troponin complex binding to Tropomyosin by isothermal titration calorimetry(ITC).

Titration of Troponin C mutations (A31S, E59D, D75Y, C84Y) reconstituted in troponin complex with tropomyosin in presence 1mM CaCl_2 . (A) The trace of titration obtained by 20 injections of $70\mu\text{M}$ tropomyosin into $7\mu\text{M}$ troponin complex at 25°C , 140mM KCl, 10mM MOPS PH 7.2, 3.5 MgCl_2 . (B) Integrated heats for each injection versus the molar ratio of tropomyosin to troponin and solid line is the data fitting using 1:1 binding model.

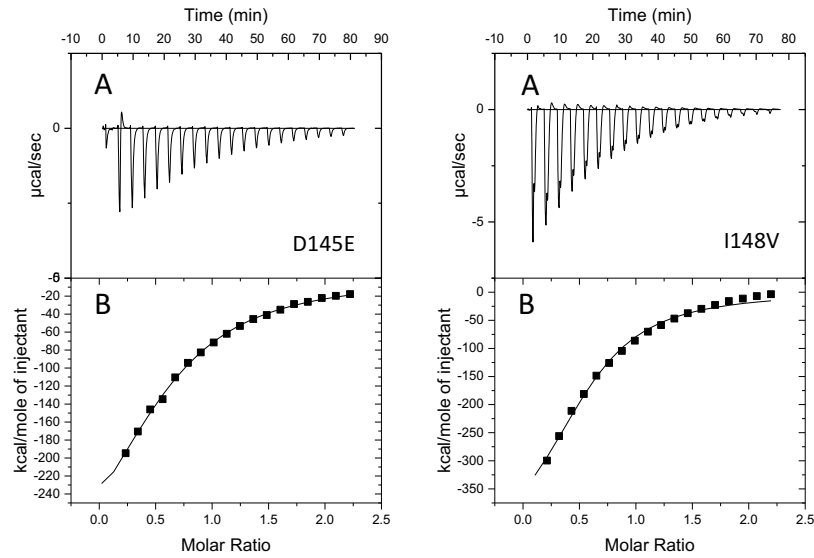


Figure 4.17: Troponin complex binding to Tropomyosin by isothermal titration calorimetry(ITC).

Titration of Troponin C mutations (D145E and I148V) reconstituted in troponin complex with tropomyosin in presence 1mM CaCl₂. (A) The trace of titration obtained by 20 injections of 70µM tropomyosin into 7µM troponin complex at 25 °C, 140mM KCl, 10mM MOPS PH 7.2, 3.5 MgCl₂. (B) Integrated heats for each injection versus the molar ratio of tropomyosin to troponin and solid line is the data fitting using 1:1 binding mode

Table 4.4: Binding parameters of troponin to tropomyosin.

Binding parameters between troponin C WT and HCM and DCM mutations reconstituted in troponin complex and tropomyosin. For each parameter*indicates significant difference from WT (p<0.05) and parameter** indicates difference from WT (p<0.0001)

Troponin complex	K _d (µM)	Stoichiometry (n)	ΔH (kcal/mole)	ΔS (kcal/mole)	ΔG (kcal/mole)
WT	1.1±0.15	1.2±0.15	-5.2e5±4.5e4	-1.7e3±88.2	-5.6e5±5e3
Y5H	0.6±0.01*	0.8±0.04	-2.4e5±3.3e4*	-786±10.7*	-2.5e5±1e4*
A8V	1.3±0.34	0.7±0.10	-1.4e5±1.0e4**	-445±7.9*	-1.5e5±5e3*
A31S	9.7±0.25**	0.7±0.09	-3.6e5±2.2e4**	-1.2e3±88.2	-3.9e5±5e3*
E59D	3.2±0.46*	1.2±0.19	-1.4e5±3.9e4*	-462±6.6*	-1.5e5±1e4*
D75Y	1.4±0.62	0.8±0.02	-2.7e4±786*	-59.1±3.2**	-2.8e4±1.5e3**
C84Y	0.4±0.35*	0.7±0.11	-1.7e5±1.9e4**	-5.9e3±272*	-1.7e5±2.5e4*
D145E	0.8±0.14*	1.0±0.09	-1.9e5±2.7e4**	-630±17.3*	-2.1e5±1.5e4*
I148V	1.1±0.55	0.7±0.03	-3.7e5±2.5e4*	-2.2e3±115*	-3.7e5±1.5e3*

4.2.2.3 Effect of TnC mutations on the binding of troponin complex to thin filaments.

Finally, we used ITC to understand how the troponin C mutations can affect the binding of troponin complex to actin-Tm thin filament. Actin and tropomyosin were mixed as 7:1 and incubated in ice for one hour and then dialyzed against ATPase buffer (140 mM KCl, 10 mM Mops pH 7.2, 3.5 mM MgCl₂, 0.1 mM DTT, 1 mM NaN₃, and 50 μM CaCl₂). The syringe was filled with 300 μl of troponin complex, 60μM and titrated with 1.4ml of 40 μM actin with 6μM tropomyosin. The injection size was 15 μl, with duration of 14sec, at 240 sec intervals with a stirring at 300 rpm. Control titration of buffer with troponin and buffer with actin tropomyosin indicated that heats of dilution were small and constant.

Figure 4.18 shows the trace and integrated heat of titration of troponin complex WT and actin-Tm thin filament and figures 4.19 to 4.21 present the data of titration of cTnC mutation reconstituted in troponin complex and actin-Tm thin filament. Overall this titration was not easy because the binding ratio between troponin complex and actin-Tm thin filament is 1:7 and the interaction of troponin complex and actin-Tm thin filament is complex. We obtained a stoichiometry of 0.11 (1:7) for WT and the K_d of the troponin complex WT to actin-Tm was 1.3±0.5 and these data strongly agree with the data obtained from (Al-Sarayreh S. 2011). In general, the data obtained from this experiment demonstrated that cTnC mutations have impact on the binding between troponin complex and actin-Tm thin filament to different levels. Table 4.5 provides all binding parameters of troponin complex and actin-Tm titration (K_d, stoichiometry, ΔH, ΔS, and ΔG). From the table above we can see that the K_d of Y5H, E59D, D145E, and I148V slightly higher than WT and the K_d of A8V and A31S, less than WT by 4.3 and 2.6-fold respectively.

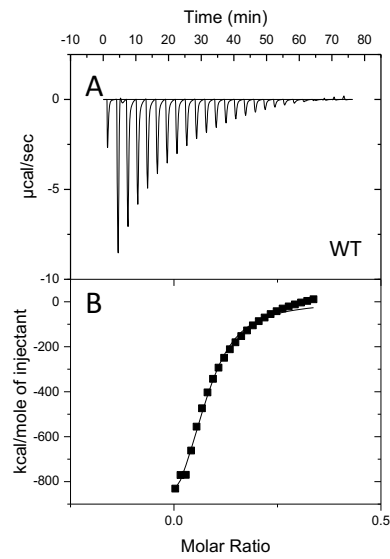


Figure 4.18 Troponin complex binding to actin-Tm thin filament by isothermal titration calorimetry (ITC). Titration of Troponin C WT and TnC mutations reconstituted in troponin complex (Y5H, A8V) with tropomyosin in presence 1mM CaCl_2 . (A) The trace of titration obtained by 25 injections of $50\mu\text{M}$ troponin complex into $40\mu\text{M}$ actin, $6\mu\text{M}$ tropomyosin at 25°C , 140mM KCl, 10mM MOPS PH 7.2, 3.5MgCl_2 . (B) Integrated heats for each injection versus the molar ratio of tropomyosin to troponin and solid line is the data fitting using 1:1 binding model.

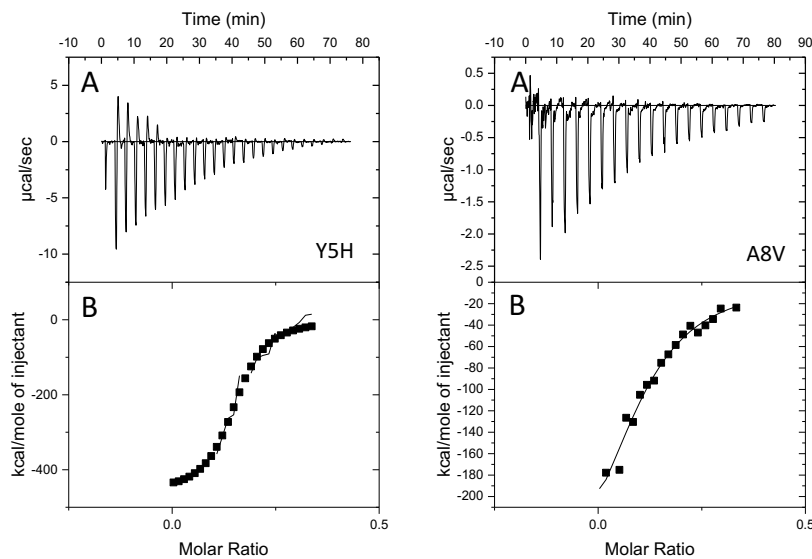


Figure 4.19: Troponin complex binding to actin-Tm thin filament by isothermal titration calorimetry (ITC). Titration of Troponin C WT and TnC mutations reconstituted in troponin complex (Y5H, A8V) with tropomyosin in presence 1mM CaCl_2 . (A) The trace of titration obtained by 25 injections of $50\mu\text{M}$ troponin complex into $40\mu\text{M}$ actin, $6\mu\text{M}$ tropomyosin at 25°C , 140mM KCl, 10mM MOPS PH 7.2, 3.5MgCl_2 . (B) Integrated heats for each injection versus the molar ratio of tropomyosin to troponin and solid line is the data fitting using 1:1 binding model.

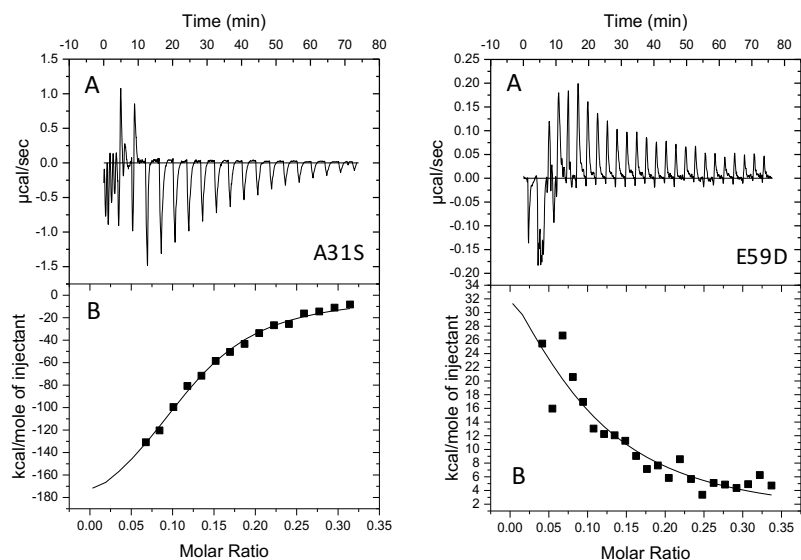


Figure 4.20 Troponin complex binding to actin-Tm thin filament by isothermal titration calorimetry (ITC).

Titration of Troponin C WT and TnC mutations reconstituted in troponin complex (Y5H, A8V) with tropomyosin in presence 1mM CaCl_2 . (A) The trace of titration obtained by 25 injections of $50\mu\text{M}$ troponin complex into $40\mu\text{M}$ actin, $6\mu\text{M}$ tropomyosin at 25°C , 140mM KCl, 10mM MOPS PH 7.2, 3.5 MgCl_2 . (B) Integrated heats for each injection versus the molar ratio of tropomyosin to troponin and solid line is the data fitting using 1:1 binding model.

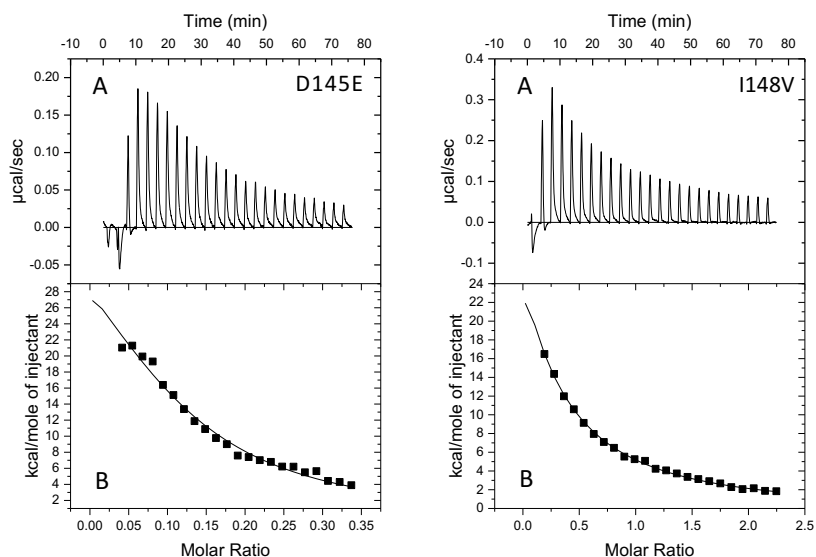


Figure 4.21: Troponin complex binding to actin.Tm thin filament by isothermal titration calorimetry (ITC).

Titration of Troponin C WT and TnC mutations reconstituted in troponin complex (Y5H, A8V) with tropomyosin in presence 1mM CaCl_2 . (A) The trace of titration obtained by 25 injections of $50\mu\text{M}$ troponin complex into $40\mu\text{M}$ actin, $6\mu\text{M}$ tropomyosin at 25°C , 140mM KCl, 10mM MOPS PH 7.2, 3.5 MgCl_2 . (B) Integrated heats for each injection versus the molar ratio of tropomyosin to troponin and solid line is the data fitting using 1:1 binding model

Table 4.5: Binding parameters of troponin to thin filament

Binding parameters between troponin C WT and HCM and DCM mutations reconstituted in troponin complex and actin-Tm thin filament. For each parameter*indicates significant difference from WT ($p < 0.05$) and parameter** indicates difference from WT ($p < 0.0001$)

Troponin complex	K_d (μM)	Stoichiometry	ΔH (kcal/mole)	ΔS (kcal/mole)	ΔG (kcal/mole)
WT	1.3 ± 0.5	0.11 ± 0.04	$-3.1e5 \pm 2.0e5$	$-1.0e3 \pm 150$	$-3.3e5 \pm 1.5e4$
Y5H	1.8 ± 0.8	0.15 ± 0.01	$-4.6e5 \pm 2.0e4$	$-1.5e3 \pm 150$	$-4.9e5 \pm 4.0e4$
A8V	$0.3 \pm 0.3^*$	0.18 ± 0.03	$-2.1e5 \pm 1.7e4$	-686 ± 5.5	$-2.2e5 \pm 1.5e4$
A31S	0.5 ± 0.4	0.11 ± 0.01	$-2.1e5 \pm 2.6e4$	-686 ± 5.5	$-2.2e5 \pm 1.5e4$
E59D	1.8 ± 0.3	0.09 ± 0.06	$6.5e5 \pm 5.0e4^*$	$246 \pm 4.5^*$	$6.5e5 \pm 2.5e4^{**}$
D145E	1.8 ± 0.8	0.12 ± 0.02	$4.9e4 \pm 1.0e4^*$	$191 \pm 2.0^*$	$4.9e5 \pm 3.5e4^*$
I148V	$2.2 \pm 0.1^*$	0.10 ± 0.07	$2.9e5 \pm 2.4e4^*$	$1.02e3 \pm 100^{**}$	$3.1e5 \pm 2.0e4^*$

4.3 Discussion

Cardiac contraction muscle process is a consequence of interactions of the myosin head with the actin filaments. This process is regulated by troponin complex together with tropomyosin and Ca^{2+} dependent. Binding of Ca^{2+} to the regulatory domain of troponin C (N-terminal) leads to structural and dynamic changes in troponin complex. Between helices A and B of cTnC there is exposure of hydrophobic residues on the surface when Ca^{2+} bind to troponin C. This binding results in a strong association with the switch peptide region of cTnI and lead to a reduction in the interaction between the inhibitory peptide of cTnI and actin. This increase the mobility of tropomyosin and allows myosin to bind actin strongly and contraction (Anson *et al.*, 1996; Araujo & Walker, 1996). It is clear that troponin C is a key regulator of the contractile cycle. Many studies have been shown that familial hypertrophic and dilated cardiomyopathies are cause by mutations in genes encoding sarcomeric proteins including hcTnC. TnC mutations can cause contractile alterations in the molecular mechanisms in different steps. In this chapter, we aimed to determine the impact of several hcTnC mutations on the affinity of calcium binding of troponin C, the rate constant of Ca^{2+} dissociation from troponin C, the interaction of hcTnC with other components of thin filaments including hcTnI, and the interaction of reconstituted troponin complexes with tropomyosin and thin filament and the allosteric transitions between the different regulatory states.

4.3.1 Cardiac troponin C mutations alter the Ca²⁺ binding affinity.

Although Ca²⁺ plays a pivotal role in heart contraction, it is only a messenger and as previously described, Ca²⁺ needs TnC (as a receptor) to bind and deliver its message. In addition, Ca²⁺ levels in the cytoplasm of cardiomyocytes are tightly controlled by various Ca²⁺ channels and Ca²⁺ binding proteins that act as buffers. The high concentrations of troponin C in cardiomyocytes make this protein play a fundamental role in intracellular Ca²⁺ buffering in these cells. Consequently, measuring the rate of the Ca²⁺ dissociation from Tn C and Tn complex is an important tool to study the effect of TnC mutations on the Ca²⁺ dissociation rate and potentially on the cTnC Ca²⁺ buffering capacity.

The rate of Ca²⁺ dissociation from TnC WT measured using Quin-2 was 1.95 ± 0.071 (Table 4.1). This is in agreement with Susan. J and Paul J. (1990) findings which showed the rate of Ca²⁺ dissociation from TnC is 1.6 s^{-1} ('Susan & P J E,). In this experiment, E59D and I148V TnC were found to cause increase the Ca²⁺ dissociation rate compare to WT. A possible explanation for this increase is the location of these mutations. E59D could modify Ca²⁺ affinity indirectly because it is located in helix C which has been shown to be essential in fine tuning Ca²⁺ binding to the regulatory site (Leblanc *et al.*, 2000). I148V is located in Ca²⁺/Mg²⁺ binding site IV and it is one of the Ca²⁺ coordination sites (I148). Thus, I148V could directly modify Ca²⁺ coordination even if there is no big difference structurally between Isoleucine and Valine. On the other hand, Y5H, A8V, A31S, D75Y, C84Y, and D145E slightly affect the Ca²⁺ dissociation rate. Our result obtained with A8V is in good agreement with previous study (Swindle & Tikunova, 2010b). However, our data

are in disagreement with a previous study which showed that E59D and D75Y decrease the Ca^{2+} dissociation rate of cTnC (Dewan *et al.*, 2016)

Since TnC works in concert with the other proteins of the thin and thick filament measuring the Ca^{2+} dissociation rate of TnC in isolation is insufficient to explain the pathophysiology of these mutations. Hence Ca^{2+} dissociation rate was measured from the troponin complex, and the troponin complex reconstituted in thin filament, and in presence of S1 for each mutation. Our findings showed that A8V, A31S, and I148V incorporated in the Tn complex had slower Ca^{2+} dissociation rate compared to WT. A31S and I148V are in the Ca^{2+} binding sites I and IV respectively and these positions can explain why these mutations can affect the Ca^{2+} binding properties. The effect of A8V on the Ca^{2+} dissociation rate was unexpected. This result support previous study that showed that A8V affect the metal binding affinity of sites III and IV in the C-domain (Cordina *et al.*, 2013). On the other hand, Y5H, D75Y, C84Y, and D145E incorporated in the Tn complex had faster Ca^{2+} dissociation rate compared to WT. Our findings are in good agreement with a recent study that showed that A8V, A31S, and C84Y indirectly modify the affinity of Ca^{2+} by altering the interaction between N-cTnC and the TnI_{sw} (Charles M. Stevens *et al.*, 2017). Overall it seems that hcTnC mutations can alter the Ca^{2+} binding kinetics regardless of whether they are spatially near or far from the regulatory Ca^{2+} binding sites of cTnC.

4.3.2 Impact of TnC mutations on the transition between the blocked and closed state

Regulation of cardiac muscle contraction depends on a set of allosteric and cooperative transitions in thin filaments. Geeves and co-workers (Geeves & Lehrer, 1994) have

suggested a model in which thin filament can exist in three biochemical states: blocked, closed and open. The blocked state is obtained in the absence of calcium. In this state, the thin filament is unable to bind S1 and Tn-Tm complex is positioned on the outer domain of actin. In the closed state, the S1 binds the thin filament weakly. This weak binding is permitted by the movement of the troponin-tropomyosin to the groove (between inner and outer domain of actin). Thus most but not all myosin binding sites on actin is exposed. This state is obtained in the presence of calcium. Finally, S1 binds actin strongly in open state. To monitor the transition between the blocked and closed states (k_B) the large fluorescence change of PIA-labelled actin upon S1 myosin heads binding had been used (Head et al., 1995;(Mustapha Alahyan *et al.*, 2006) . In the blocked state (in absence of Ca^{2+}) K_B is expected to be less than 1 when the thin filaments are predominantly in the blocked state and this is an indication of the relaxed state. While the K_B is predicted to be more than 1 when thin filaments are predominantly in the closed state. $K_B=1$ is obtained for a 50:50 distribution of closed and blocked states. The kinetics of S1 binding to pyrene actin method of determination of K_B is accurate for values around 1. But when K_B is very small i.e. lower than 0.2 or very high i.e. higher than 2 the calculations are not accurate (since small changes in the slopes give large changes in K_B). The most interesting finding was E59D, D75Y, and D145E increased K_B in the absence of Ca^{2+} to nearly 1. This suggests that these mutations may interfere with relaxation in the absence of Ca^{2+} . These results can explain why Tn complex reconstituted weather with E59D or D75Y reduce the ATPase activity in comparison to WT. In the other hand, A8V and A31S increase the K_B in absence of Ca^{2+} (0.62) in compare to WT (0.39).

4.3.3 cTnC mutations affect the binding between TnC and the partners

Cardiac troponin C is an allosteric effector in muscle thin filaments. Its complex network of interaction with other components of thin filaments such as tropomyosin (Tm) and troponin I and T regulate the interaction between actin and myosin sub fragment (S1) in vertebrate striated muscle. Structural changes are induced in troponin complex when calcium binds to the troponin C. This binding lead to strong association of cTnC with the switch peptide region of cTnI (Kobayashi et al., 2008; Stehle et al., 2007). Therefore, HCM and DCM cTnC mutations could alter the interactions of cTnC with its binding partners. For this purpose, we performed three experiment to study the effect of cTnC mutations on the binding between cTnC and TnI, Tm, and actin.Tm thin filament by using ITC.

The result of the first titration between the cTnC WT and HCM and DCM cTnC mutations and TnI showed that A8V, E59D, D145E and I148V cTnC mutations bind weaker to cTnI than WT (Table 4.3). Furthermore, the titration of HCM and DCM mutation reconstituted in the Tn complex with Tm give more comprehensive picture of impact of the cTnC mutations on the binding properties of Tn. Our data showed that Y5H, C84Y, and D145E bind Tm stronger than WT while A8V and I148V bind Tm slightly weaker than WT. The most interesting finding that the A31S and E59D bind Tm weaker than WT by 8.8-fold and 2.9 respectively.

The titration of cTn-complex and reconstituted thin filaments was the biochemical system of choice because they maintain the geometric structure of the contractile proteins at the stoichiometric proteins ratios 1:1:7. The result of this titration has been shown that all TnC mutations gave the stoichiometric ratio 0.1 (1:1:7) which is very closed to WT. The

affinity binding between Tn-complex and actin.Tm thin filament slightly affected by Y5H, E59D, and D145E. On the other hand, A8V and A31S bind actin.Tm thin filament strong than the WT (less K_d). Moreover, I148V reduce the binding affinity of Tn to actin.Tm thin filament by 1.7-fold. Overall these binding studies demonstrate changes in the interaction networks in thin filaments but since we do not have a clear picture of the structural changes during the allosteric transitions it is hard to pinpoint an exact mechanism for these changes.

Chapter 5

Investigation of the effect of Cardiac Troponin C mutations on troponin C structure using NMR spectroscopy

5.1 Introduction

In previous chapters, we have measured the impact of the TnC mutations on the thermodynamics and kinetics of Ca²⁺ dependent thin filament regulatory transitions. However, kinetics and thermodynamic methods cannot unravel the mechanism of action of these mutations. Knowledge of the changes induced by the mutations in the structure of troponin C are required. Nuclear Magnetic Resonance spectroscopy is a method of choice for studying protein structure and dynamics in solution. NMR is particularly suitable for assessing the impact of mutations on highly dynamic proteins such as troponin and for unravelling changes in the local structure. If a protein is well folded and suitable for structural studies, the ¹⁵N-HSQC spectrum which represents the “fingerprint” of a protein is typically the first experiment of an NMR based investigation. Change in ¹⁵N-HSQC a good indication of either change in protein structure or change in dynamic processes such as chemical exchange. In addition, the ¹⁵N-HSQC experiment forms the basis of many other three- and four-dimensional NMR experiments. Finally, measuring several ¹⁵N-HSQC spectra over a prolonged time can be used to assess protein stability. In the ¹⁵N-HSQC spectrum each peak corresponds to an amide residue in proteins, with the exception of proline, contains at least one amide (i.e. the amide in the peptide bond) that gives rise to one peak. However, ¹⁵N-HSQC experiments require an assignment, a process aimed at identifying which amide gives rise to which peak in the spectrum. This process requires additional experiments. We have collected HSQC spectra for TnC wild type and the various mutants but unfortunately, we did not have the time to perform the additional experiments required for the assignment. Fortunately, there are several published HSQC spectra of cTnC and we used these as a basis of our data analysis. In this

chapter, we used a chemical shift perturbation (CSP) analysis. This technique is a simple and powerful technique which allows the measurement of chemical shift in small and medium size proteins. In order to test the impact of HCM and DCM cTnC mutations on the structure of cTnC we measured minimal chemical shift between the ^{15}N -HSQC spectrum of cTnC WT and cTnC mutation using CcpNmr AnalysisAssign Version-3 software which was developed recently by Luca Mureddu and Geerten W. Vuister.

5.2 Results

5.2.1 Preparation of NMR sample

In this chapter, we used ^{15}N -HSQC as a starting point to study the effect of the cTnC mutations on the structure of cTnC. The production of isotope labelled cTnC WT and mutations for ^{15}N -HSQ experiment achieved by recombinant cTnC expression in a bacterial system cultured in a minimal medium containing ^{15}N cTnC ammonium sulphate as a nitrogen source. cTnC was purified as described previously (section 2.3.2) using phenyl sepharose purification followed by gel filtration as a final purification step and to confirm the molecular weight of TnC. TnC was eluted in single peak at the correct approximate elution volume (figure 5.1). The yield of purified cTnC WT or cTnC mutations was approximately 10 mg/l culture.

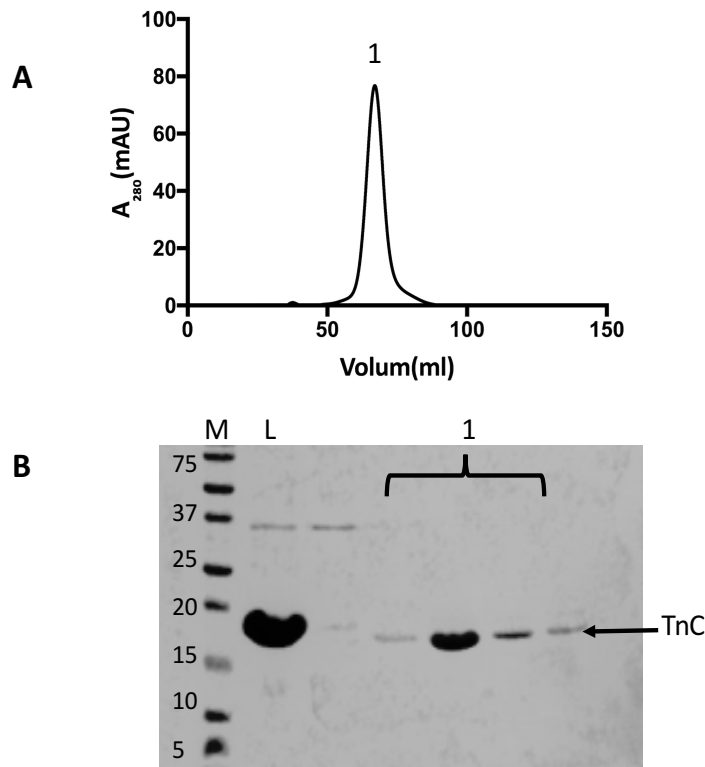


Figure 5.1: size exclusion chromatography of cardiac troponin C.

The chromatogram (A) shows a single eluted peak after loading Tn C on a S200 gelfiltration column. SDS PAGE analysis (B) confirmed that only Tn C (18 KDa) was present.

5.2.2 Effect of the cTnC mutations on the troponin C structure

5.2.2.1 HSQC experiment

Cardiac troponin C is highly α -helical and comprise two domains (the N- and C-domains) connected by a highly conserved nine-residue linker. The first solution NMR of full-length of cardiac troponin C was published by Nicole M in 2012. In addition, the conformation of each domain of cTnC has been thoroughly characterized through NMR studies involving either the isolated N-domain (N-cTnC) or C-domain (C-cTnC). In contrast, little attention has been paid to the range of interdomain orientations possible in full-length cTnC. These NMR studies suggest the feasibility of NMR investigations of structural questions in TnC.

In this study, Full-length cTnC either WT or cTnC mutations were used in ^{15}N -HSQC NMR experiment. NMR experiments were performed using typically 350-400 μl of 100-150 μM ^{15}N -labelled hcTnC in 5mm Shigemi tubes. Buffer condition were 10mM bis-Tris pH 6.8, 0.1M KCl, 4mM CaCl_2 , 1mM DTT, 3mM NaN_3 . All of the 2D $\{^1\text{H}, ^{15}\text{N}\}$ HSQC NMR spectra were obtained at 30°C using an 800-MHz spectrometer. Two-dimensional (2D) $\{^1\text{H}, ^{15}\text{N}\}$ HSQC NMR spectroscopy was used to monitor the changes in NMR spectra produced by eight cTnC mutation (Y5H, A8V, A31S, E59D, D75Y, C84Y, D145E, AND I148V) in comparison with NMR spectra of cTnC WT (figure 5.2). Figure 5.2 HSQC spectra show a number of peaks that are well dispersed. These spectra are very close to previously determined HSQC spectra. The spectra are also compatible with a small and well folded protein.

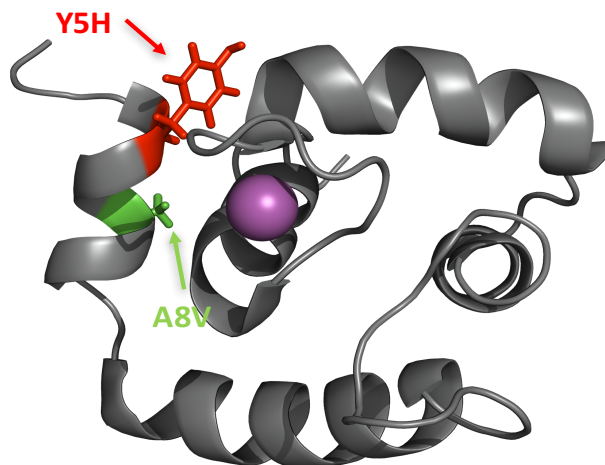


Figure 5.3: Location of Y5H and A8V in the structure of hcTnC.

Location of Y5H and A8V residues in the 3D structure of TnC using the NMR structure of cardiac TnC saturated with Ca^{2+} (PDP 1A0). Y5H displayed in red and A8V displayed in blue. The sphere corresponds to Ca^{2+} .

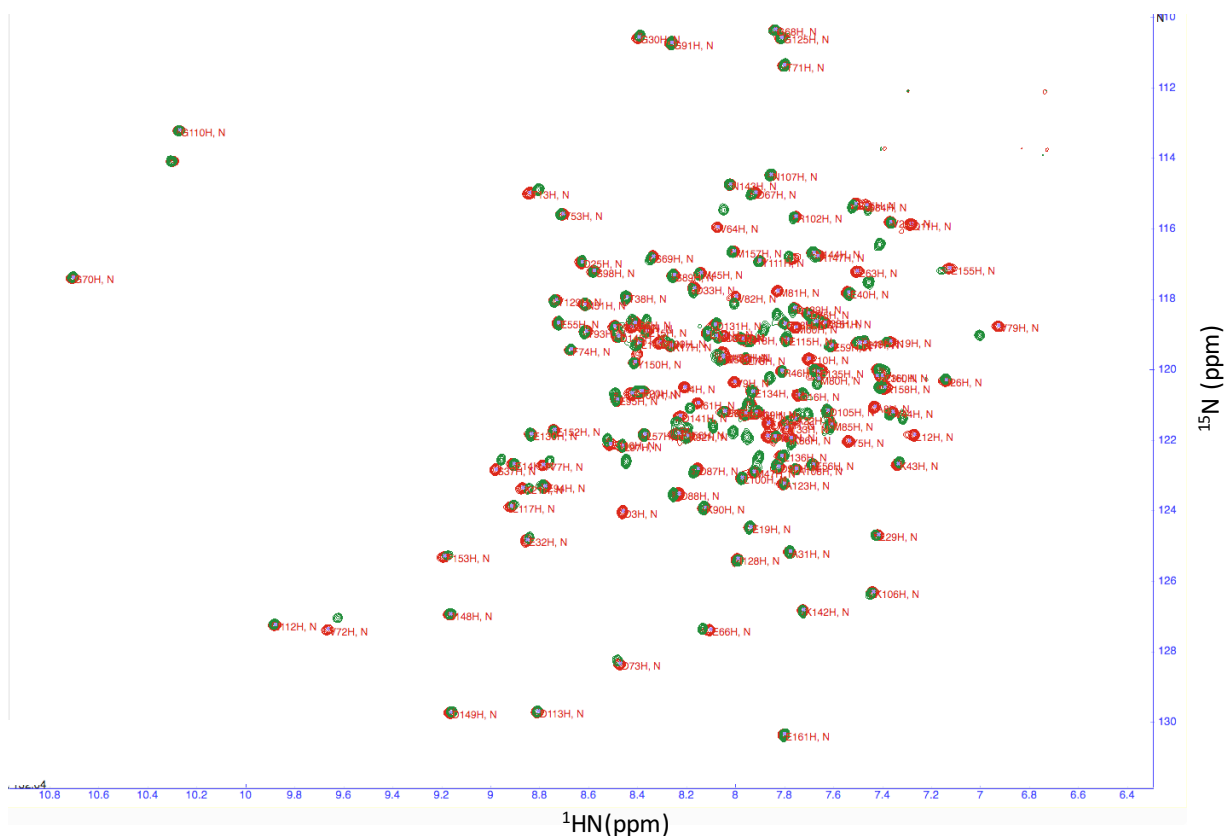


Figure 5.4: 2D ^1H - ^{15}N HSQC NMR spectra of cardiac TnC-Y5H.

The figure display the ^{15}N -HSQC overlays of cTnC-WT (red) and cTnC-Y5H (green). Both hcTnC variants are in the Ca^{2+} loaded state.

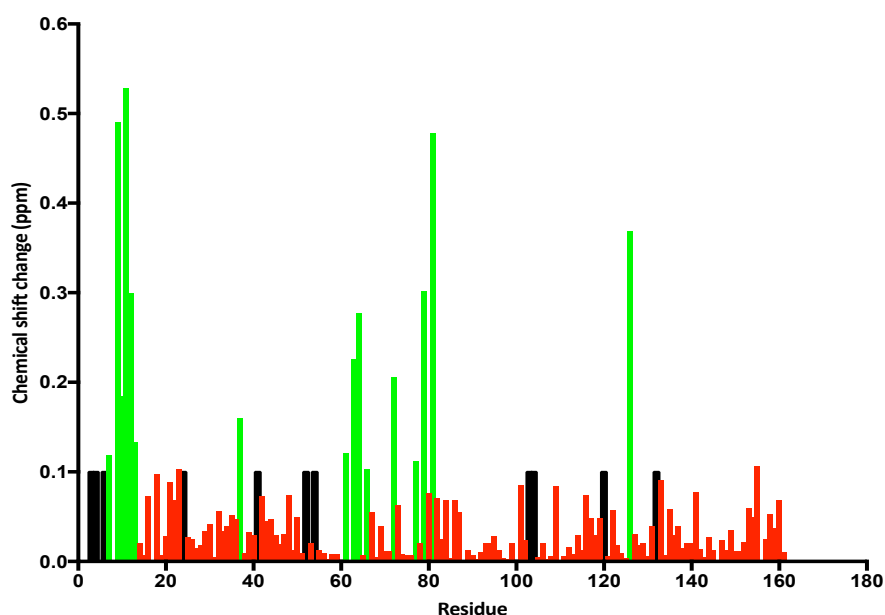


Figure 5.5: Chemical shift differences between TnC-Y5H and TnC-WT

Combined backbone amide (N and HN) chemical shift changes between TnC-WT and TnC-Y5H in Ca^{2+} loaded state. Residues marked in red indicate no or little chemical shift. Residues marked in green indicate a chemical shift perturbation above the threshold limit of 0.1. The black bars indicate that assignments are available for these residues in TnC-WT form but not in the TnC-Y5H form. The automated analysis in which all the peaks were accurately matched, was done by Luca Mureddu. CSPi values are calculated for each residue.

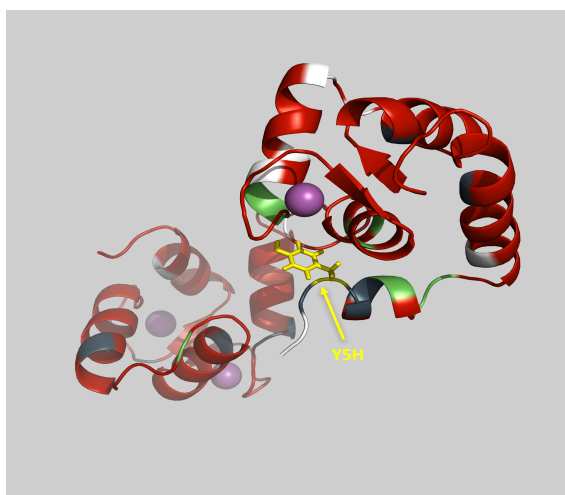


Figure 5.6: Mapping Chemical Shift Perturbations induced by Y5H mutation in hcTnC.

The ribbon representation of TnC shown in red. Residues with a chemical shift difference with the WT above the threshold 0.1 ppm are shown in green. Black residues indicate that assignments are available for these residues in TnC-WT form but not in the TnC-Y5H form. The figure was created using the solution structure of the Ca^{2+} saturated cTnC (PDB 1AJ4).

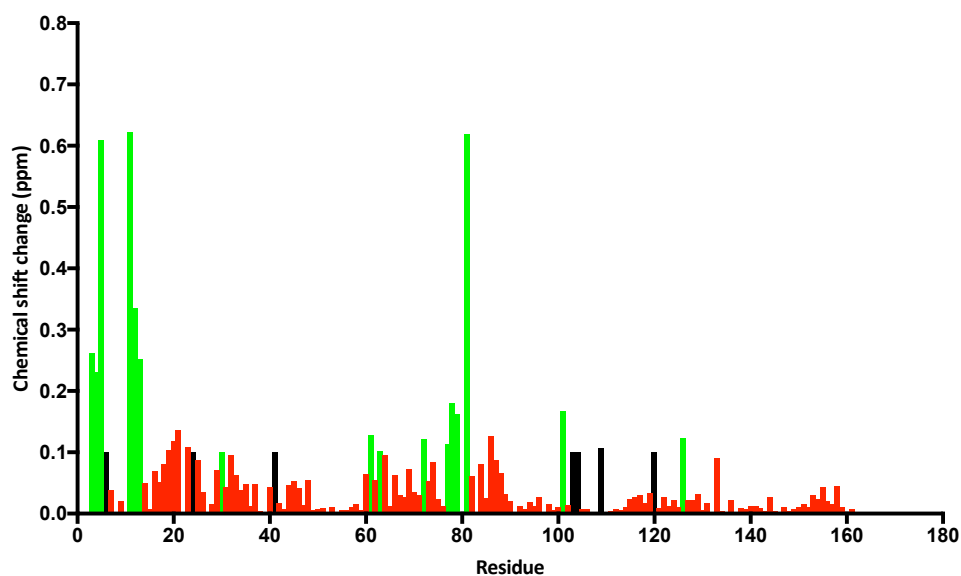


Figure 5.8: Mapping of TnC-A8V on the TnC-WT

Combined backbone amide (N and HN) chemical shift changes between TnC-WT and TnC-A8V in Ca^{2+} loaded state. Residues marked in red indicate no or little chemical shift. Residues marked in green indicate a chemical shift perturbation above the threshold limit of 0.1. The black bars indicate that assignments are available for these residues in TnC-WT form but not in the TnC-A8V form. The automated analysis in which all the peaks were accurately matched, was done by Luca Mureddu. CSPi values are calculated for each residue.

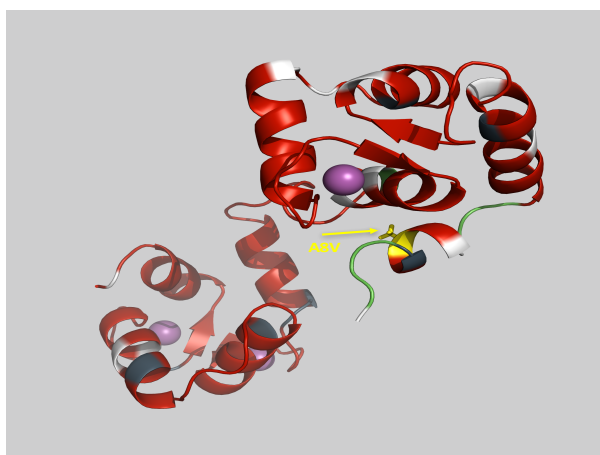


Figure 5.9: Mapping Chemical Shift Perturbations induced by A8V mutation in hcTnC.

The ribbon representation of TnC shown in red. Residues with a chemical shift difference with the WT above the threshold 0.1 ppm are shown in green. Black residues indicate that assignments are available for these residues in TnC-WT form but not in the TnC-A8V form. The figure was created using the solution structure of the Ca^{2+} saturated cTnC (PDB 1AJ4).

5.2.2.3 Mutations located in the Ca²⁺ binding sites

Ca²⁺ binding to the EF hand motif in each of the Ca²⁺ binding sites requires a precise geometry (the pentagonal bipyramidal) and chemistry. Mutations in the Ca²⁺ binding sites could possibly affect either the geometry or the nature of the chemical group and consequently alter Ca²⁺ binding. Mutations A31S and D75Y are located in the Ca²⁺ sites (site I and site 2) as shown in figure 5.10. Residue A31 is located in the inactive Ca²⁺ binding sites of cTnC. The overlay of ¹⁵N-HSQC spectra of A31S and WT is shown in figure 5.11. Analysis of the chemical shift change between TnC-WT and TnC-A31S showed that mutation A31S induces changes in the following positions (1, 8, 11, 20, 49, 13, 21, 35, 16, 18, 19, 15, 22, 14, 24) as illustrated in figure 5.12 and 5.13.

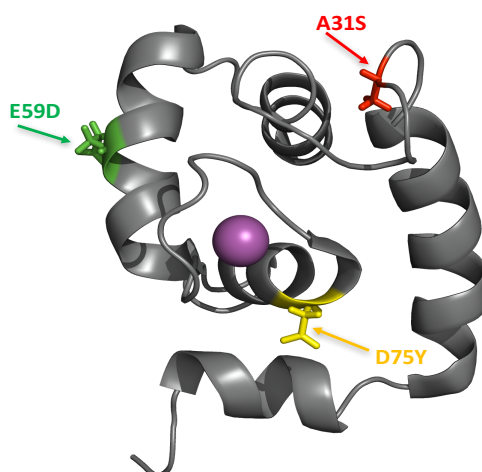


Figure 5.10: Location of A31S, E59D and D75Y in the structure of hcTnC.

Location of A31S, E59D and D75Y residues in the 3D structure of TnC using the NMR structure of cardiac TnC saturated with Ca²⁺ (PDP 1AL0). A31S is displayed in red, E59D is displayed in green and D75Y is displayed in yellow. The sphere corresponds to Ca²⁺.

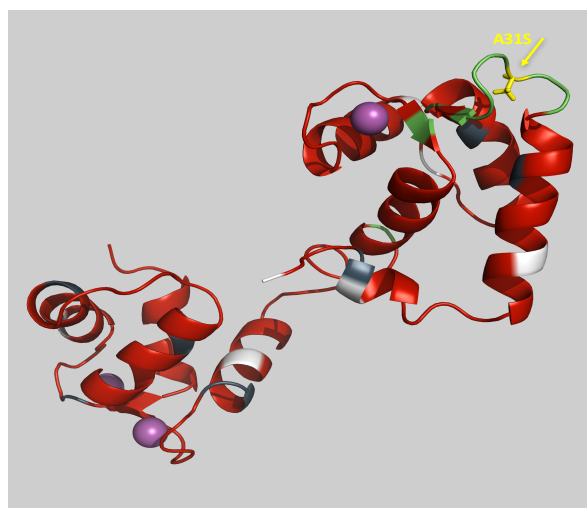


Figure 5.13: Mapping Chemical Shift Perturbations induced by A31S mutation in hcTnC.

The ribbon representation of TnC shown in red. Residues with a chemical shift difference with the WT above the threshold 0.1 ppm are shown in green. Black residues indicate that assignments are available for these residues in TnC-WT form but not in the TnC-A31S form. The figure was created using the solution structure of the Ca^{2+} saturated cTnC (PDB 1AJ4).

The ^{15}N -HSQC spectra of E59D which is located in helix C, did not show significant difference with the spectra of the hcTnC WT. As shown in figure 5.14, chemical shift changes produced by cTnC-E59D are located in residues (55, 56, 58, 60, 62, 61, 114 and 139). This suggests that mutation E59D had only a local effect around residue E59.

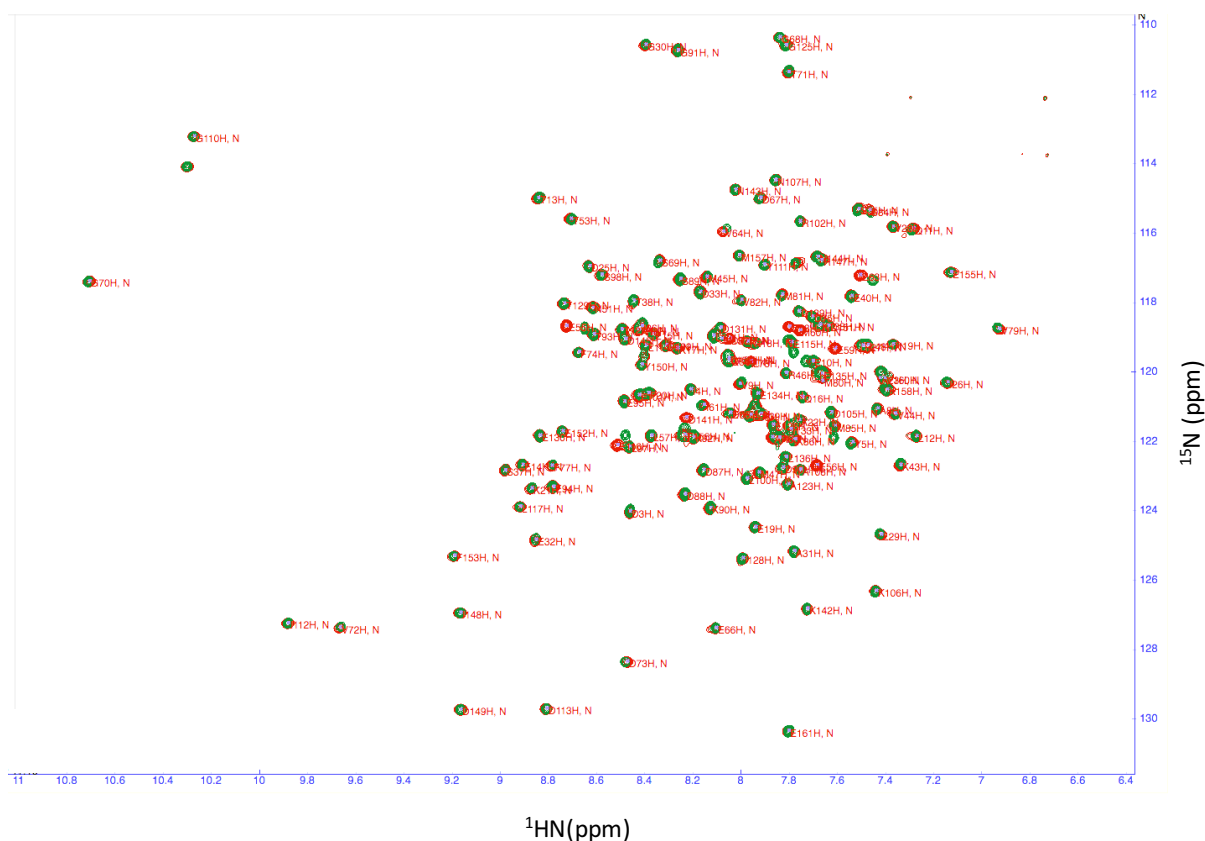


Figure 5.14: 2D ^1H - ^{15}N HSQC NMR spectra of cardiac TnC-E59D.

The figure displays the ^{15}N -HSQC overlays of cTnC-WT (red) and cTnC-E59D (green). Both hcTnC variants are in the Ca^{2+} loaded state.

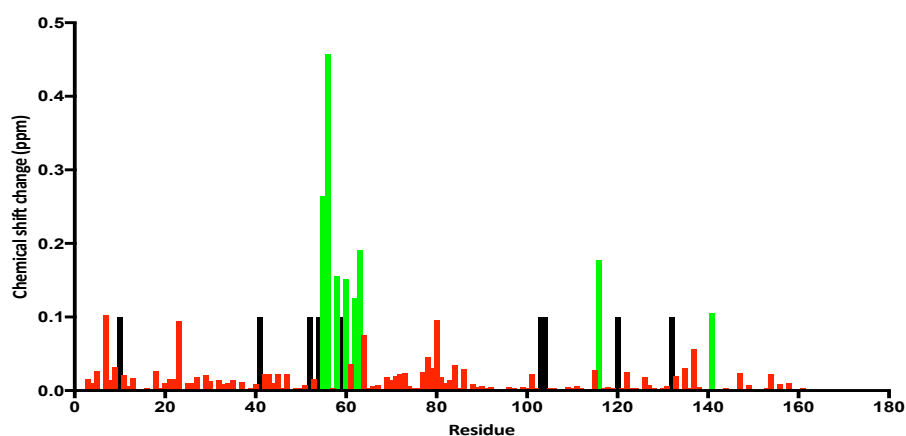


Figure 5.15: Mapping of TnC-E59D on the TnC-WT

Combined backbone amide (N and HN) chemical shift changes between TnC-WT and TnC-E59D in Ca^{2+} loaded state. Residues marked in red indicate no or little chemical shift. Residues marked in green indicate a chemical shift perturbation above the threshold limit of 0.1. The black bars indicate that assignments are available for these residues in TnC-WT form but not in the TnC-E59D form. The automated analysis in which all the peaks were accurately matched, was done by Luca Mureddu. CSPi values are calculated for each residue.

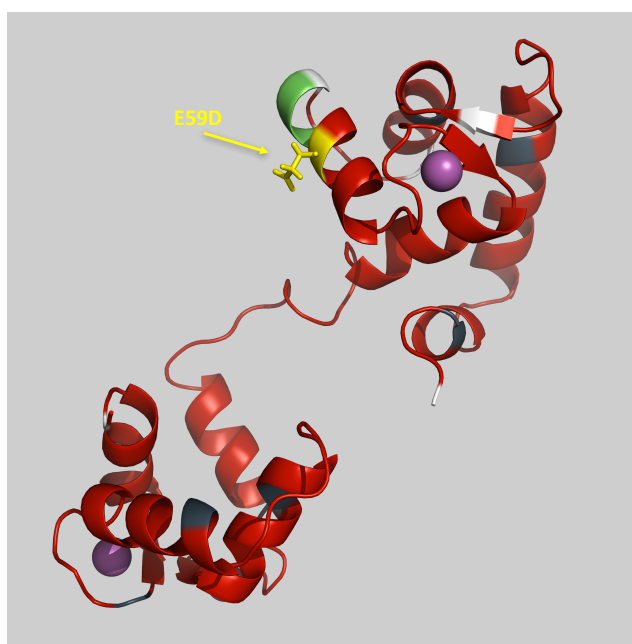


Figure 5.16: Mapping Chemical Shift Perturbations induced by E59D mutation in hcTnC.

The ribbon representation of TnC shown in red. Residues with a chemical shift difference with the WT above the threshold 0.1 ppm are shown in green. Black residues indicate that assignments are available for these residues in TnC-WT form but not in the TnC-E59D form. The figure was created using the solution structure of the Ca^{2+} saturated cTnC (PDB 1AJ4).

The ^{15}N -HSQC spectra of D75Y which is located in the Ca^{2+} binding sites II, produced a spectra with noticeable difference from the WT (figure 5.17). Analysis of the differences in chemical shift showed differences in the following residues (3-5, 7, 12,18, 21-23, 25, 27, 29, 30, 32-35, 37, 43, 47-48, 61-70, 72-74, 79-82, 101, 107) (Figure 5.18 and 5.19). These changes correspond to the region around residue 75 but interestingly also in the N-terminal region particularly between residues 20 and 40.

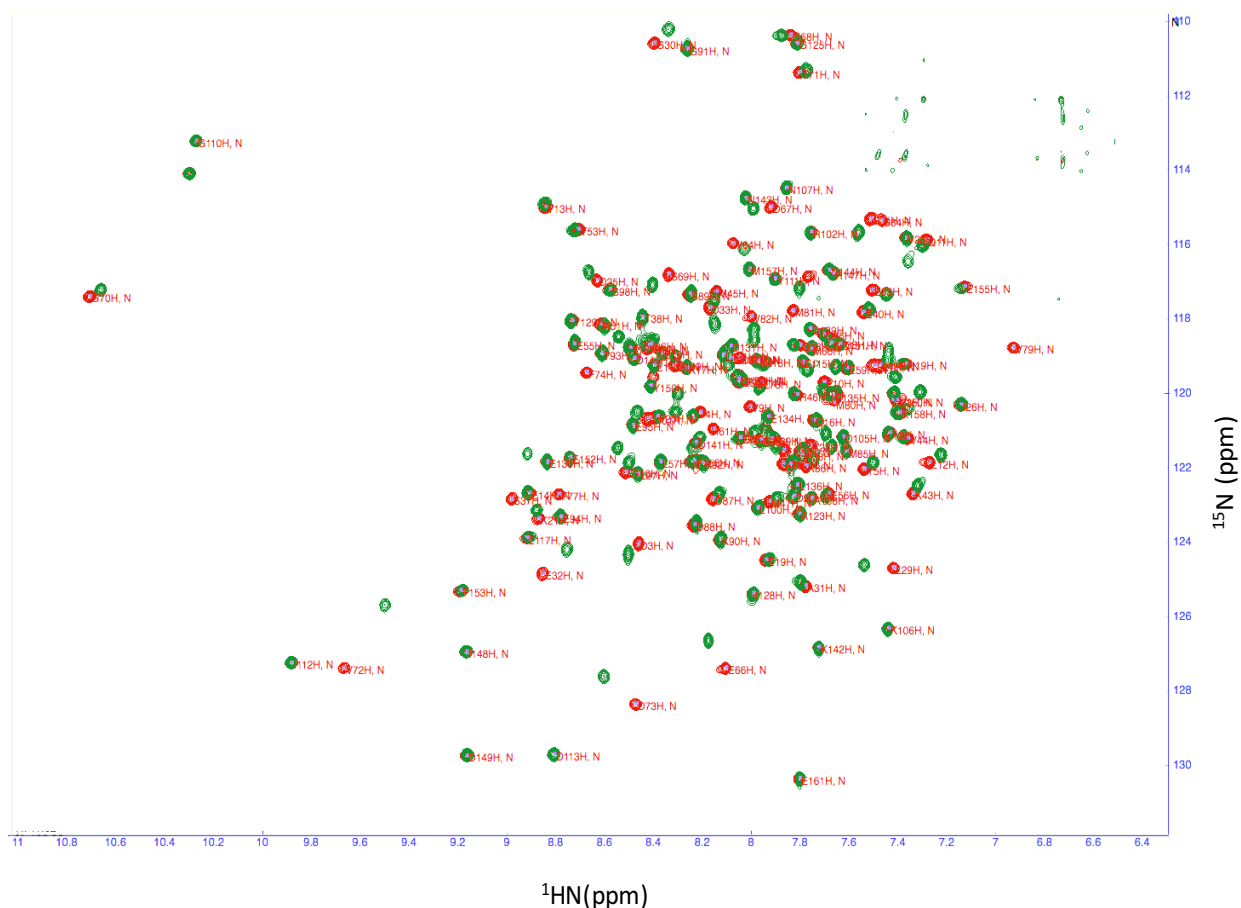


Figure 5.17: 2D ^1H - ^{15}N HSQC NMR spectra of cardiac TnC-D75Y.

The figure displays the ^{15}N -HSQC overlays of cTnC-WT (red) and cTnC-D75Y (green). Both hcTnC variants are in the Ca^{2+} loaded state.

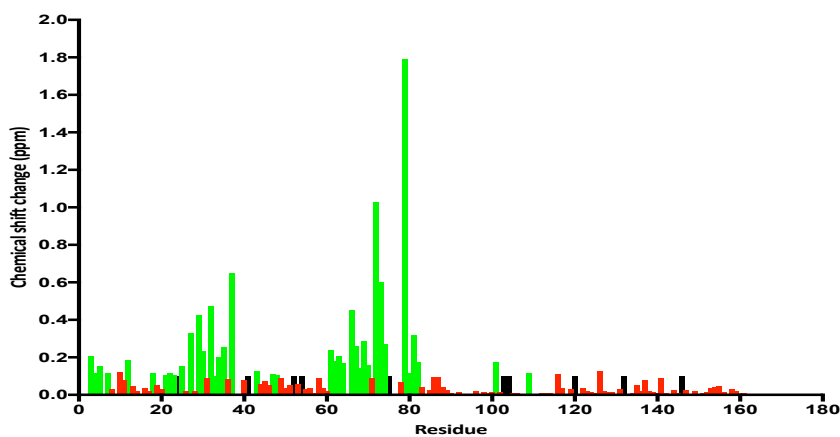


Figure 5.18: Mapping of TnC-D75Y on the TnC-WT

Combined backbone amide (N and HN) chemical shift changes between TnC-WT and TnC-D75Y in Ca^{2+} loaded state. Residues marked in red indicate no or little chemical shift. Residues marked in green indicate a chemical shift perturbation above the threshold limit of 0.1. The black bars indicate that assignments are available for these residues in TnC-WT form but not in the TnC-D75Y form. The automated analysis in which all the peaks were accurately matched, was done by Luca Mureddu. CSPi values are calculated for each residue.

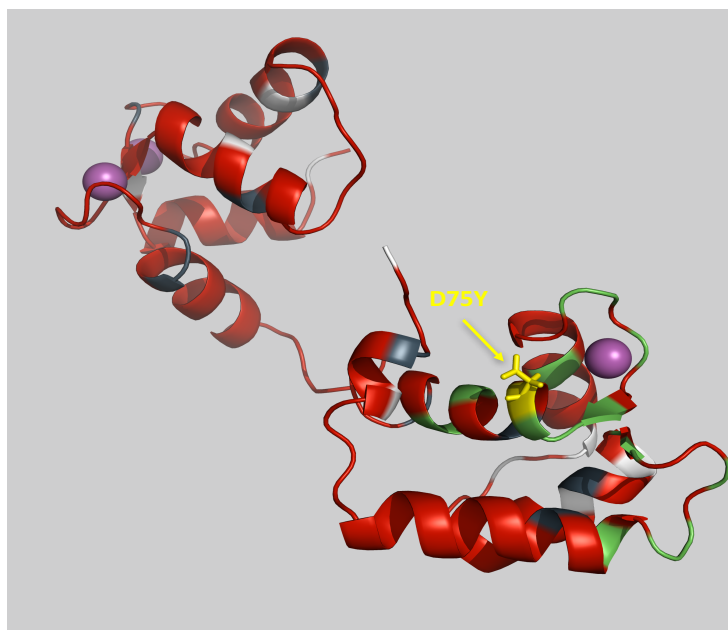


Figure 5.19: Mapping Chemical Shift Perturbations induced by D75Y mutation in hcTnC.

The ribbon representation of TnC shown in red. Residues with a chemical shift difference with the WT above the threshold 0.1 ppm are shown in green. Black residues indicate that assignments are available for these residues in TnC-WT form but not in the TnC-D75Y form. The figure was created using the solution structure of the Ca^{2+} -saturated cTnC (PDB 1AJ4).

5.2.2.4 Flexible linker mutation

Cardiac troponin C consists of two domains (N and C-domains) connected by a flexible linker which is crucial for effective regulatory function of troponin. The linker region [residues 86-94] changes conformation substantially upon Ca^{2+} binding. Residue C84 (mutated in DCM) is located in this region (figure 5.20). When the ^{15}N -HSQC spectra of cTnC-WT with cTnC-C84Y are overlaid, the result showed that C84Y produced changes in the chemical shift nearly across the TnC structure (figure 5.21 and 5.22) and in particular in the N-terminal region. Differences were assigned to the following residues (3-5, 8-10, 13, 18, 21, 23, 25, 26, 29, 36, 37, 40, 45, 55, 58, 60-63, 64-68, 70, 71, 75-77, 79, 80, 85-88, 116, 135, 141) (figure 5.22 and 5.23).

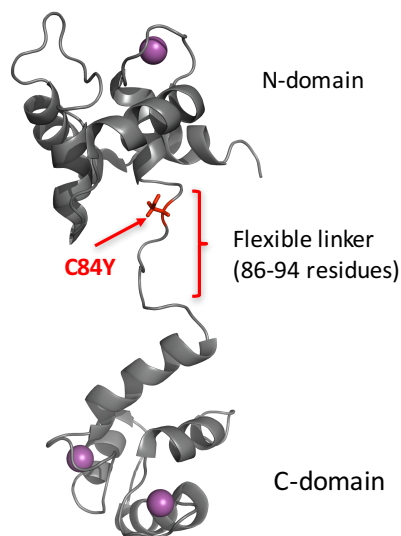


Figure 5.20: Location of C84Y in the structure of hcTnC.

Location of C84Y residue in the 3D structure of TnC using the NMR structure of cardiac TnC saturated with Ca^{2+} (PDP 1A0). C84Y is displayed in red. The spheres correspond to Ca^{2+} .

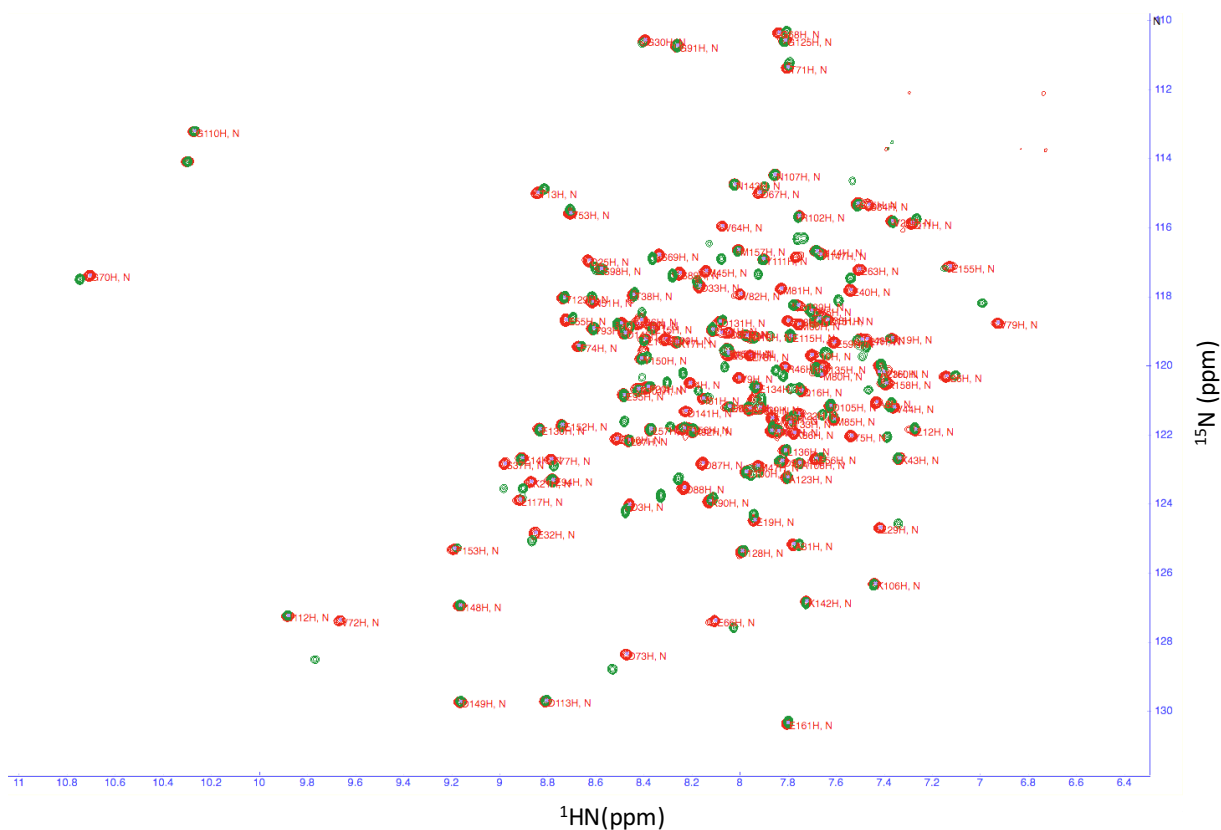


Figure 5.21: 2D ^1H - ^{15}N HSQC NMR spectra of cardiac TnC-C84Y.

The figure display the ^{15}N -HSQC overlays of cTnC-WT (red) and cTnC-C84Y (green). Both hcTnC variants are in the Ca^{2+} loaded state.

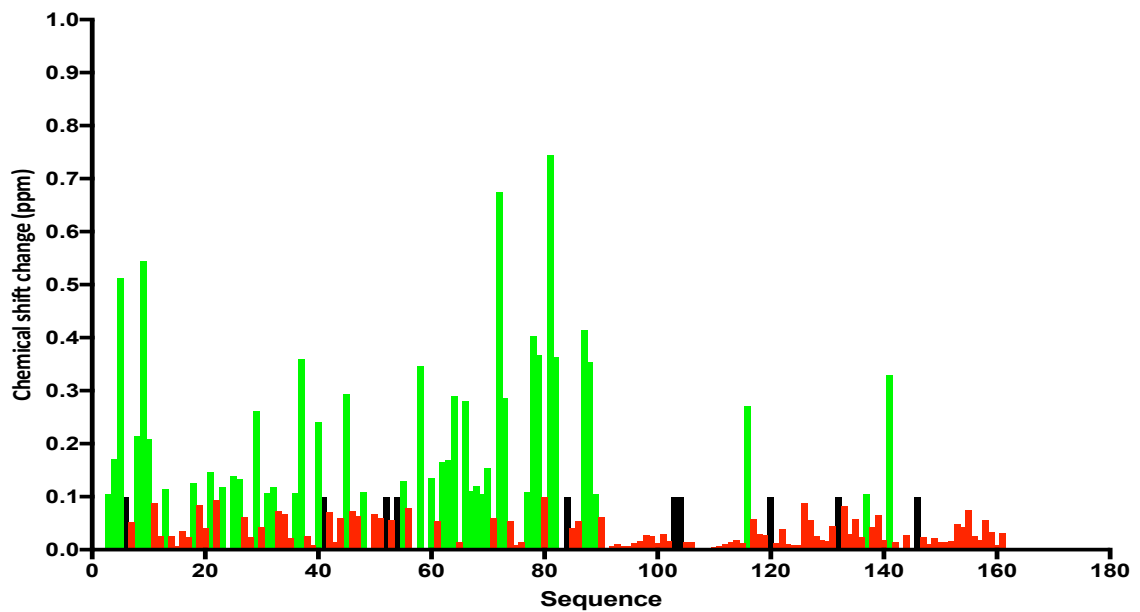


Figure 5.22: Mapping of TnC-C84Y on the TnC-WT

Combined backbone amide (N and HN) chemical shift changes between TnC-WT and TnC-C84Y in Ca^{2+} loaded state. Residues marked in red indicate no or little chemical shift. Residues marked in green indicate a chemical shift perturbation above the threshold limit of 0.1. The black bars indicate that assignments are available for these residues in TnC-WT form but not in the TnC-C84Y form. The automated analysis in which all the peaks were accurately matched, was done by Luca Mureddu. CSPi values are calculated for each residue.

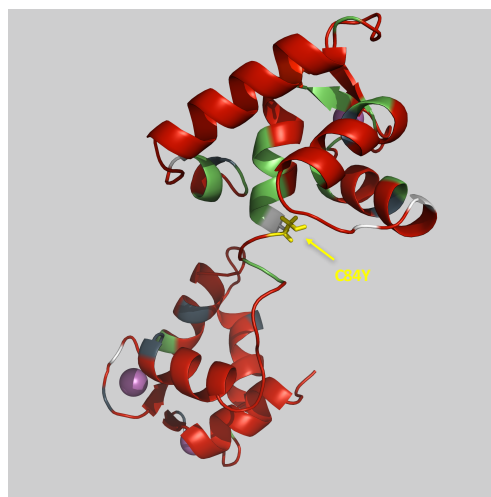


Figure 5.23: Mapping Chemical Shift Perturbations induced by C84Y mutation in hcTnC.

The ribbon representation of TnC shown in red. Residues with a chemical shift difference with the WT above the threshold 0.1 ppm are shown in green. Black residues indicate that assignments are available for these residues in TnC-WT form but not in the TnC-C84Y form. The figure was created using the solution structure of the Ca^{2+} saturated cTnC (PDB 1AJ4).

5.2.2.5 Mutations located in Ca²⁺ and Mg²⁺ binding sites

Troponin C has two metal binding sites (site III and site IV), which bind Ca²⁺ or Mg²⁺ with high affinity in the structural C-domain. D145E and I148V are located in the binding pocket of site IV and both of them are involved in the coordination of Ca²⁺ (figure 5.24). D145E induced changes in the ¹⁵N-HSQC spectra that affected primarily the C-domain residues including (97, 104, 108-112, 115, 117, 122-123, 126-129, 136, 139, 140, 143-145, 147, 150-153, 155-157, 159). In the N-domain only few residues (28, 38, 65, 75, 76, 85) were affected.

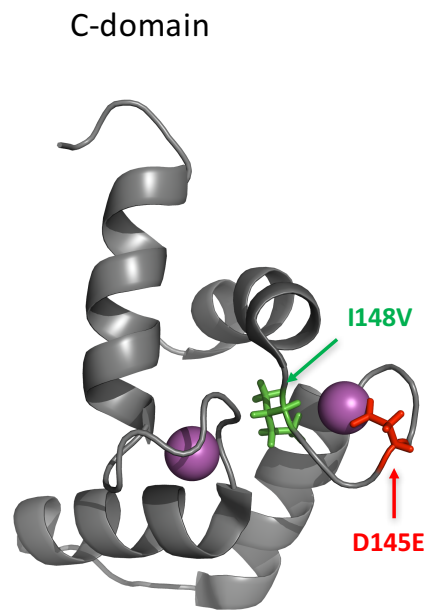


Figure 5.24: Location of D145E and I148V in the structure of hcTnC.

Location of D145E and I148V residues in the 3D structure of TnC using the NMR structure of cardiac TnC saturated with Ca²⁺ (PDP 1AL0). D145E is displayed in red while I148V is displayed in green. The spheres correspond to Ca²⁺.



Figure 5.25: 2D ^1H - ^{15}N HSQC NMR spectra of cardiac TnC-D145E.

The figure displays the ^{15}N -HSQC overlays of cTnC-WT (red) and cTnC-D145E (green). Both hcTnC variants are in the Ca^{2+} loaded state.

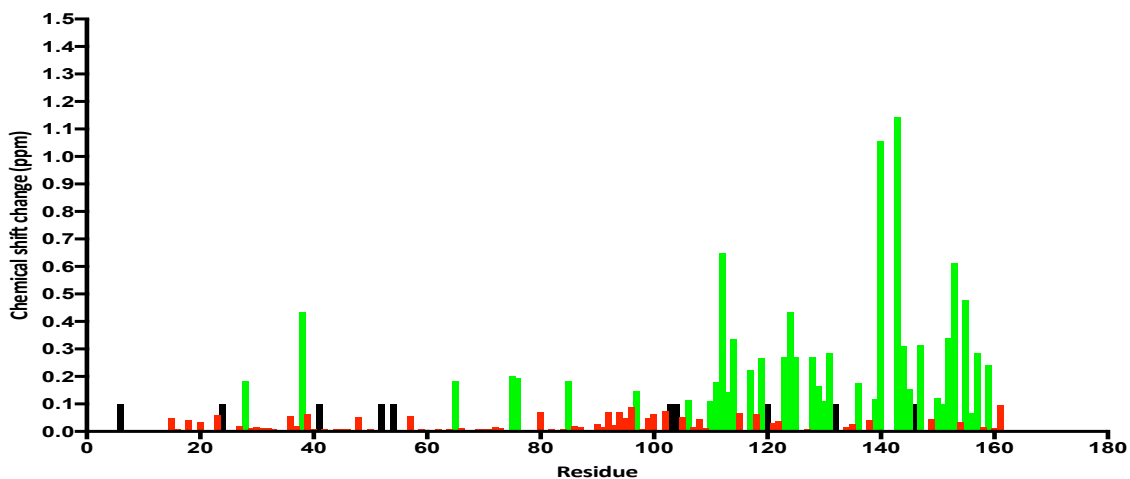


Figure 5.26: Mapping of TnC-D145E on the TnC-WT

Combined backbone amide (N and HN) chemical shift changes between TnC-WT and TnC-D145E in Ca^{2+} loaded state. Residues marked in red indicate no or little chemical shift. Residues marked in green indicate a chemical shift perturbation above the threshold limit of 0.1. The black bars indicate that assignments are available for these residues in TnC-WT form but not in the TnC-D145E form. The automated analysis in which all the peaks were accurately matched, was done by Luca Mureddu. CSPi values are calculated for each residue.

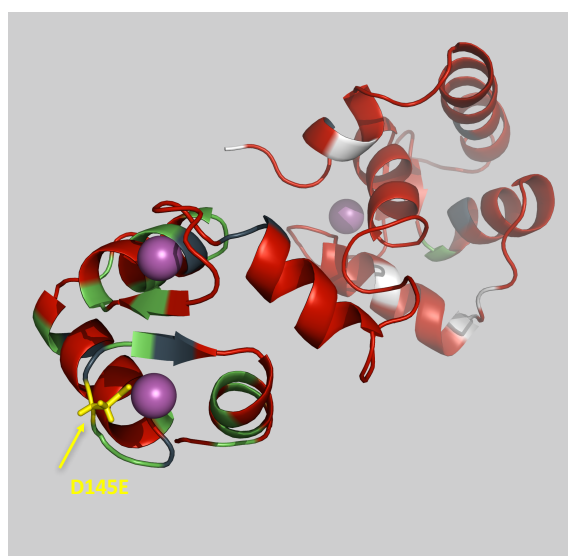


Figure 5.27: Mapping Chemical Shift Perturbations induced by D145E mutation in hcTnC.

The ribbon representation of TnC shown in red. Residues with a chemical shift difference with the WT above the threshold 0.1 ppm are shown in green. Black residues indicate that assignments are available for these residues in TnC-WT form but not in the TnC-D145E form. The figure was created using the solution structure of the Ca²⁺ saturated cTnC (PDB 1AJ4).

I148V is located in the binding pocket of site IV also showed big shifting in C-domain when overlay on the TnC-WT (figure 5.28). Figure 5.29 and 5.30 illustrates the minimal chemical shift perturbation mapping produced by TnC-I148V. Figure 5.29 showed that mutation I148V induced changes in the ¹⁵N-HSQC spectra primarily in the C-domain including residues (97, 102, 106, 111, 112,119, 123-125, 130,138, 140, 145, 147, 148, 150, 151, 155, and 158). Only residues 17, 38, and 85 in the N-domain were affected.

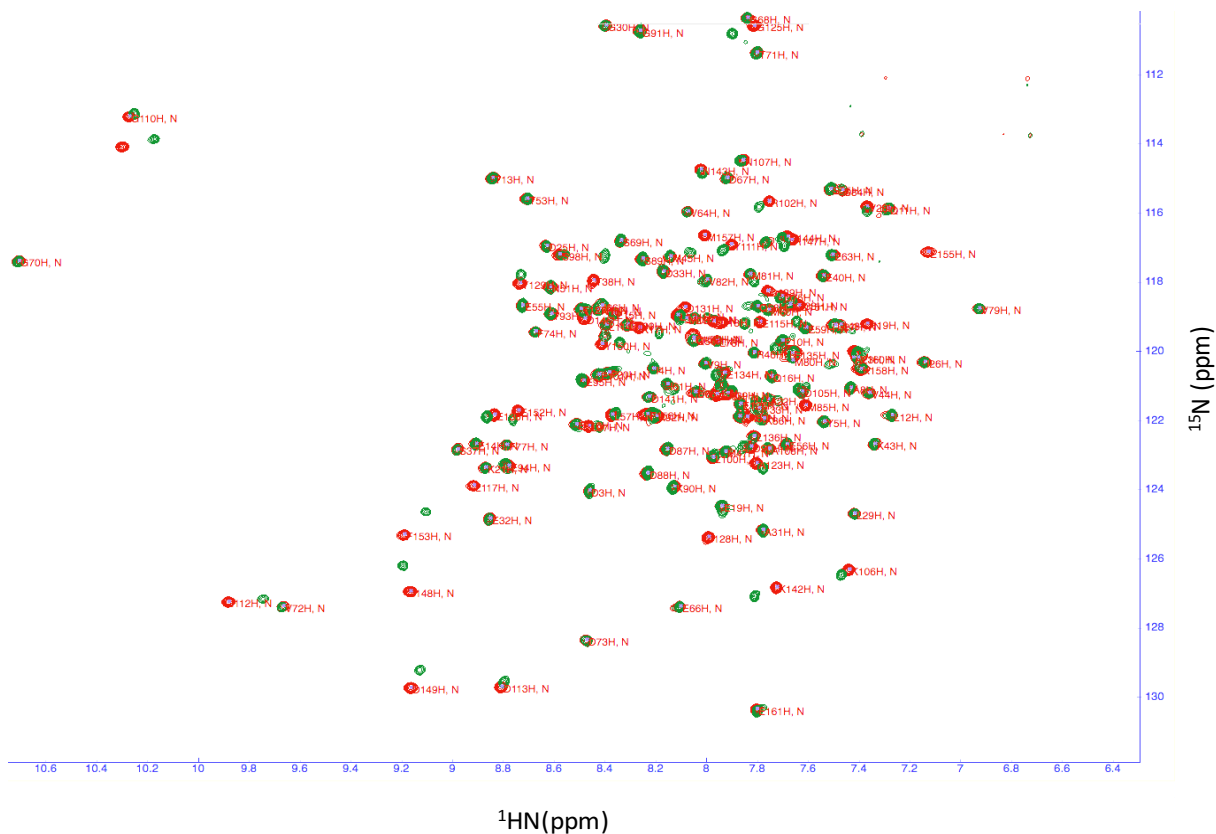


Figure 5.28: 2D ^1H - ^{15}N HSQC NMR spectra of cardiac TnC-I148V.

The figure displays the ^{15}N -HSQC overlays of cTnC-WT (red) and cTnC-I148V (green). Both hcTnC variants are in the Ca^{2+} loaded state.

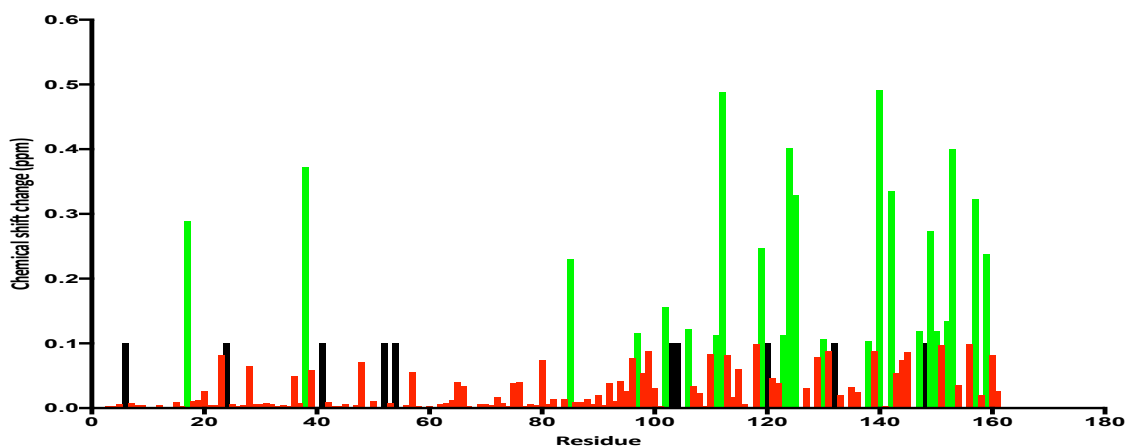


Figure 5.29: Mapping of TnC-I148V on the TnC-WT.

Combined backbone amide (N and HN) chemical shift changes between TnC-WT and TnC-I148V in Ca^{2+} loaded state. Residues marked in red indicate no or little chemical shift. Residues marked in green indicate a chemical shift perturbation above the threshold limit of 0.1. The black bars indicate that assignments are available for these residues in TnC-WT form but not in the TnC-I148V form. The automated analysis in which all the peaks were accurately matched, was done by Luca Mureddu. CSPi values are calculated for each residue.

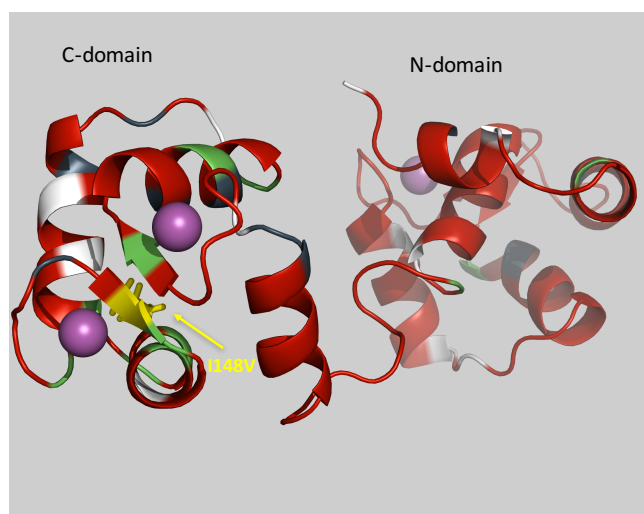


Figure 5.30: Mapping Chemical Shift Perturbations induced by I148V mutation in hcTnC.

The ribbon representation of TnC shown in red. Residues with a chemical shift difference with the WT above the threshold 0.1 ppm are shown in green. Black residues indicate that assignments are available for these residues in TnC-WT form but not in the TnC-I148V form. The figure was created using the solution structure of the Ca^{2+} -saturated cTnC (PDB 1AJ4).

5.3 Discussion

NMR spectroscopy was used to determine the changes in the structure of troponin C induced by HCM and DCM associated mutations. Chemical shift perturbation is very useful as a simple tool to elucidate the effect of HCM and DCM mutations on the structure of troponin C. Chemical shift perturbation analysis has been used to calculate minimal chemical shift perturbations. Thereafter the Chemical shift perturbation results were mapped and visualized on TnC structure. The overall structure was not drastically changed by any of the DCM or HCM cTnC mutations, resulting in a well dispersed spectra that correspond to a folded protein in agreement with the CD and Biochemical studies (Chapters 3 and 4). However, when the ^1H - ^{15}N HSQC of cTnC-WT and each of eight cTnC mutations were overlaid (Y5H, A8V, A31S, E59D, D75Y, C84Y, D145E, and I148V) mutation specific changes were found. Different mutations induced different amide chemical shift perturbations in the ^1H - ^{15}N HSQC spectrum of cTnC. Because 2D HSQC NMR spectroscopy

provides information of individual nuclei in the protein, we able to identify specific residues that were affected by each mutation. Chemical shift perturbation analysis was used to determine the extent of differences in the chemical shift of each residue. We used a threshold of 0.1ppm as a benchmark for significant differences in line with several NMR research groups. Accumulation of the chemical shift perturbation for the residues that display significant difference revealed the extent of chemical shift perturbation for each hcTnC mutant (figure 5.31).

Overall the NMR spectra of troponin C showed that all TnC mutations have an impact on the local structure of troponin C (near the site of the mutation) as expected. E59D had the lowest total CSP difference (around 2) which suggests that this mutation had little effect on the structure of the TnC beyond residues in the vicinity of E59. In addition, to these local effects on the structure of TnC, several mutations induce changes at a long range from the mutation and interestingly the region around residues 75 showed changes in the chemical shift in all mutations but E59D. Finally, mutations C84Y, D145E and I148V induced chemical shifts in most of the residues in the domain where they are located (C84Y led to changes in the N-terminal domain while D145E and I148V led to changes in the C-domain) and the total CSP difference is above 10. This suggest that these mutations induced substantial changes in the domain where they are located. In addition, all mutations induced changes (although limited) in the second domain (the domain where they are not located) which suggest that there is communication between the two domains of TnC.

Finally, the structural basis of the allosteric transitions in TnC are not well understood and consequently it is difficult to correlate the observed structural differences in the mutations with the kinetic and thermodynamic data.

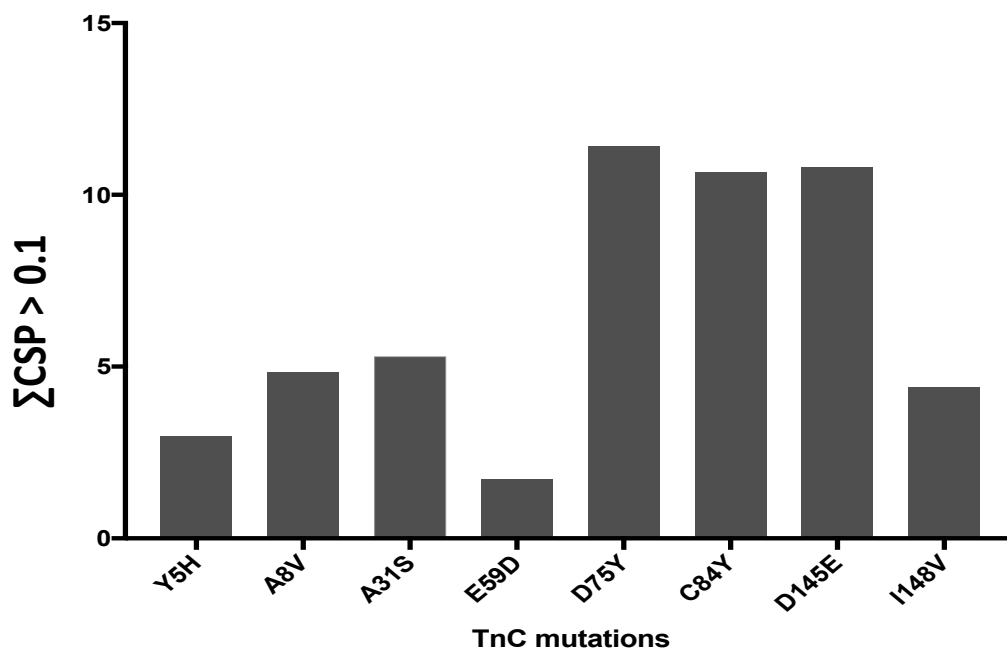


Figure 5.31: Sum of the residues with a Delta shifts above the threshold of 0.1ppm.

The figure represents the comparison of observed and calculated sum of the residues with a Delta shifts above the threshold of 0.1ppm for each TnC mutations.

Chapter 6

General discussion

6.1 Introduction

Genetic hypertrophic and dilated cardiomyopathies are characterized by changes in the morphology and physiology of the heart. The genetics of these cardiomyopathies have been established and many mutations were found in the contractile proteins including the troponin subunits I, T and C. Although great effort has been made to unravel how mutations in these proteins can alter their function and lead to pathological states, the biochemical basis of these diseases is poorly understood. The primary aims of this study is to understand, at the molecular level, how mutations in TnC, which cause cardiomyopathies, alter the regulation of the cardiac contractile cycle.

Contraction of cardiac muscle consists of a cascade of events involving several protein structural changes and protein-protein interaction. Troponin C plays a central role in the cardiac contractile cycle since it interacts with Ca^{2+} , the second messenger used by cardiomyocytes to initiate contractions and relaxations. Mutations in hcTnC can potentially lead to abnormal myofilament behaviour which can lead to contractile dysfunction. Numerous mutations in hcTnC have been identified in patients with DCM and HCM (Hoffmann et al, 2001 & Tardiff et al, 2011). In this thesis, we use a variety of structural, biochemical and functional techniques to shed light on the impact of four HCM and four DCM mutations on the cardiac troponin C gene on the structure and function of cTnC (table 6.1). We cloned, expressed and purified these 9 TnC variants, the WT and 8 mutants. We also purified a number of other contractile proteins required for the various assays used in this project including hcTnI, hcTnT, Tm, actin and myosin head. The methods used in this project namely ITC, stopped flow based transient kinetics and NMR spectroscopy are all methods that require lots of proteins and this led to both the commitment of substantial amount of time to these tasks and the acquisition of good

skills in protein expression and purification. We investigated the effect of TnC mutations on hcTnC structure by CD and NMR spectroscopy. We assessed the impact of these mutations on interaction between hcTnC and hcTnI and between Tn complexes and Tm or actin-Tm. Finally, we investigated the impact of these mutations on kinetic parameters including the rate constant of Ca²⁺ dissociation, the equilibrium constant between the blocked and closed states and the activation and inhibition of the actomyosin ATPase.

6.2 Investigation of the effects of troponin C mutations on the structure of troponin C and the troponin complex.

Structural investigations of mutated proteins are important for two reasons: i) First they are used to determine if the mutations have a major impact on structure to the point that it may change the fold of the protein and since the function depends on the fold of the protein, major changes are likely to affect protein function in a non-specific manner. ii) Secondly, high resolution structural studies can be combined with kinetic and thermodynamic investigations to define the mechanism by which a mutation may have affected the function of a protein.

Overall our CD measurements showed that the secondary structure of cTnC or cTn complex was not drastically changed. NMR spectroscopy showed that hcTnC mutants were still folded and had a fairly similar structure to the WT. These findings suggest that the mutations did the structure of cTnC or cTn complex was not drastically changed. This warrant biochemical of functional investigations. There are however several small changes that may explain the observed differences in the biochemical properties of the mutants. In general, the position of the troponin C mutation in the primary sequence of cTnC affect the nature and the extent of change in the structure of TnC. Mutations in the

EF hand motifs (A31S, D75Y, , C84Y, D145E, and I148V) produced big chemical shift changes in ^{15}N -HSQC spectra of the WT. It is not surprising since binding of Ca^{2+} to EF hand induces structural changes. The other mutations (Y5H, A8V and E59D) showed only small change around the mutated residues. However HSQC spectra are only a first step and more advanced NMR experiments are necessary to understand the nature of the structural changes and their impact on troponin dynamics (an important determinant of troponin regulatory proteins).

6.3 Effect of troponin C mutations on the interaction between the components of the thin filament macromolecular complex.

In cardiac muscle, the thin filaments are made of actin, tropomyosin and the troponin complex. Ca^{2+} binding/dissociation results in the activation/inhibition of thin filaments and is mediated by a set of elegant allosteric transitions that starts at Ca^{2+} binding to regulatory site of TnC and travels via TnI, TnT and Tm to the actin filament inducing a conformational change in the structure of thin filament. The nature of these interactions and in particular in relation to their role in these allosteric transitions are not well understood. Interaction of Tn with both actin and Tm are key to these allosteric transitions. Therefore, it is important to measure the impact of cTnC mutations on these interactions. Our data revealed that cTnC mutations affected various interactions between thin filament components including the interaction of troponin complex with tropomyosin and actin-tropomyosin. Several mutations decreased the interaction of TnC with TnI. Since TnC and actin compete for interaction with TnI, one would deduce that these mutations will increase the interaction of the reconstituted troponin complexes with actin. This is indeed the case for two mutations (A8V and A31S) but not for the other

mutations. This indicates the complexity of the network of interactions in thin filaments. Several mutations decreased the binding affinity to tropomyosin of the troponin complexes reconstituted with the hcTnC mutants (for example A31S, E59D, C84Y and D145E). These effects are likely due to allosteric effects (Distant effects) since the primary site of interaction with tropomyosin is located in TnT.

6.4 Effect of mutations on the kinetics of Ca^{2+} dissociation and the transition between the blocked and closed states.

Relaxation of cardiac muscle requires the dissociation of Ca^{2+} and the transition from the closed state to the blocked state. The rate constant of Ca^{2+} dissociation is an important determinant of the rate of cardiac relaxation. Consequently, assessing the impact of hcTnC mutations on the rate constant of Ca^{2+} dissociation and on the equilibrium constant between the closed and the blocked state is a pre-requisite to understand the impact of cTnC mutations on the relaxation process. We have measured the rate constant of Ca^{2+} dissociation from isolated hcTnC, Tn complex, thin filaments and thin filaments with bound rigor. We found a decrease in the rate constant of Ca^{2+} dissociation from thin filament for all TnC mutation. In addition, we found that all TnC mutations decreased the proportion of thin filament in the blocked state in the absence of Ca^{2+} . Taken together these two findings we suggest that these mutations are likely to affect the rate and the amplitude of cardiac muscle relaxation.

Table 6.1: Summary of biochemical characterisation of cTnC mutations in this thesis (N/A no data available).

TnC mutations	Structural change		Thermal stability		Actomyosin ATPase		Ca ²⁺ dissociation rate constant				Kb		Troponin affinity for		
	TnC	Tn	TnC	Tn	activation	inhibition	TnC	Tn	Thin filament	Thin filament + S1	+Ca ²⁺	-Ca ²⁺	TnI	Tm	Actin.Tm
Y5H	Similar to WT	Similar to WT	Similar to WT	Similar to WT	Similar to WT	Similar to WT	Similar to WT	Increase	Similar to WT	Increase	Similar to WT	Similar to WT	Similar to WT	Increase	Similar to WT
A8V	Similar to WT	Similar to WT	Similar to WT	Similar to WT	Similar to WT	Similar to WT	Similar to WT	Decrease	Decrease	Increase	Similar to WT	Increase	Decrease	Similar to WT	Increase
A31S	Similar to WT	Similar to WT	Similar to WT	Similar to WT	Increase	Similar to WT	Similar to WT	Decrease	Decrease	Decrease	Similar to WT	Increase	Decrease	Decrease	Increase
E59D	Similar to WT	Similar to WT	Decrease	Similar to WT	Decrease	Similar to WT	Increase	Similar to WT	Decrease	Increase	Similar to WT	Increase	Decrease	Decrease	Decrease
D75Y	Decrease in the α -helical content	Decrease in the α -helical content	Decrease	Decrease	Decrease	Similar to WT	Similar to WT	Increase	Decrease	Increase	Similar to WT	Increase	Similar to WT	Similar to WT	N/A
C84Y	Similar to WT	Decrease in the α -helical content	Similar to WT	Similar to WT	Similar to WT	Similar to WT	Similar to WT	Increase	Decrease	Increase	Similar to WT	Increase	Similar to WT	Decrease	N/A
D145E	Decrease in the α -helical content	Decrease in the α -helical content	Decrease	Decrease	Similar to WT	Similar to WT	Similar to WT	Increase	Decrease	Increase	Similar to WT	Increase	Decrease	Decrease	Decrease
I148V	Similar to WT	Similar to WT	Similar to WT	Similar to WT	Similar to WT	Similar to WT	Increase	Decrease	Decrease	Decrease	Similar to WT	Increase	Decrease	Similar to WT	Decrease

6.5 Conclusion

We have studied 8 mutations in TnC associated with both HCM (A8V, A31S, C84Y and D145E) and DCM (Y5H, E59D, D75Y and I148V) using structural, kinetic and thermodynamic approaches. We found a number of differences in the interaction networks in thin filaments (Tnl-TnC and Tn complex with Tm and thin filaments). We also found a number of changes in thin filament dynamics (particularly the proportion of thin filaments in the blocked state at low Ca²⁺ and the rate constant of Ca²⁺ dissociation). We also found changes in the local structure. Many of the differences observed in these mutations are possible starting points for HCM and DCM, however our studies are performed with 100 % mutant protein in our experiments, while all HCM and DCM diseases investigated here are dominant negative which imply that the level of the mutant is likely to be less than 50% of the total amount of TnC present in cardiomyocytes. In addition, it will be desirable to input the changes in kinetic and thermodynamic parameters in contractile models of cardiomyocytes and assess how they will modify cardiomyocyte contraction and relaxation. Finally, cell and animal models of these mutations will likely help to validate our in vitro findings. In a sense this project represents a small contribution in the quest to understand the molecular basis of diseases as complex as HCM and DCM.

References

- A. M. Gordon, E. Homsher, M. Regnier, 2000. Regulation of Contraction in Striated Muscle. *Physiological Reviews*. **80**, 853-924.
- Albury, A.N.J., Swindle, N., Swartz, D.R., Tikunova, S.B., 2012a. Effect of hypertrophic cardiomyopathy-linked troponin C mutations on the response of reconstituted thin filaments to calcium upon troponin I phosphorylation. *Biochemistry*. **51**, 3614.
- Albury, A.N.J., Swindle, N., Swartz, D.R., Tikunova, S.B., 2012b. Effect of hypertrophic cardiomyopathy-linked troponin C mutations on the response of reconstituted thin filaments to calcium upon troponin I phosphorylation. *Biochemistry*. **51**, 3614.
- Anderson, P.A., Greig, A., Mark, T.M., Malouf, N.N., Oakeley, A.E., Ungerleider, R.M., Allen, P.D., Kay, B.K., 1995. Molecular basis of human cardiac troponin T isoforms expressed in the developing, adult, and failing heart. *Circulation Research*. **76**, 681-686.
- Anson, M., Geeves, M.A., Kurzawa, S.E., Manstein, D.J., 1996. Myosin motors with artificial lever arms. *The EMBO Journal*. **15**, 6069-6074.
- Ashrafian, H., McKenna, W.J., Watkins, H., 2011. Disease pathways and novel therapeutic targets in hypertrophic cardiomyopathy. *Circulation Research*. **109**, 86-96.
- Arad, M., Seidman, J.G., Seidman, C.E., 2002. Phenotypic diversity in hypertrophic cardiomyopathy. *Human Molecular Genetics*. **11**, 2499-2506.
- Araujo, A. & Walker, J.W., 1996. Phosphate release and force generation in cardiac myocytes investigated with caged phosphate and caged calcium. *Biophysical Journal*. **70**, 2316-2326.
- Ashrafian, H. & Watkins, H., 2007. Reviews of translational medicine and genomics in cardiovascular disease: new disease taxonomy and therapeutic implications cardiomyopathies: therapeutics based on molecular phenotype. *Journal of the American College of Cardiology*. **49**, 1251-1264.
- Baryshnikova, O.K., Li, M.X., Sykes, B.D., 2008. Modulation of cardiac troponin C function by the cardiac-specific N-terminus of troponin I: influence of PKA phosphorylation and involvement in cardiomyopathies. *Journal of Molecular Biology*. **375**, 735-751.
- Baudenbacher, F., Schober, T., Pinto, J.R., Sidorov, V.Y., Hilliard, F., Solaro, R.J., Potter, J.D., Knollmann, B.C., 2008. Myofilament Ca²⁺ sensitization causes susceptibility to cardiac arrhythmia in mice. *The Journal of Clinical Investigation*. **118**, 3893-3903.
- Baxley, T., Johnson, D., Pinto, J.R., Chalovich, J.M., 2017. Troponin C Mutations Partially Stabilize the Active State of Regulated Actin and Fully Stabilize the Active State When Paired with Delta14 TnT. *Biochemistry*. **56**, 2928-2937.
- Becker, K.D., Gottshall, K.R., Hickey, R., Perriard, J.C., Chien, K.R., 1997. Point mutations in human beta cardiac myosin heavy chain have differential effects on sarcomeric structure and assembly: an ATP binding site change disrupts both thick and thin filaments, whereas

- hypertrophic cardiomyopathy mutations display normal assembly. *The Journal of Cell Biology*. **137**, 131-140.
- Behrmann, E., Müller, M., Penczek, P.A., Mannherz, H.G., Manstein, D.J., Raunser, S., 2012. Structure of the rigor actin-tropomyosin-myosin complex. *Cell*. **150**, 327-338.
- Bers, D.M. & Ginsburg, K.S., 2007. Na:Ca stoichiometry and cytosolic Ca-dependent activation of NCX in intact cardiomyocytes. *Annals of the New York Academy of Sciences*. **1099**, 326-338.
- Bers, D.M., 2002. Cardiac excitation-contraction coupling. *Nature*. **415**, 198-205.
- Bonne, G., Carrier, L., Richard, P., Hainque, B., Schwartz, K., 1998. Familial hypertrophic cardiomyopathy: from mutations to functional defects. *Circulation Research*. **83**, 580-593.
- Bonnemann, C.G. & Laing, N.G., 2004. Myopathies resulting from mutations in sarcomeric proteins. *Current Opinion in Neurology*. **17**, 529-537.
- Brittsan, A.G. & Kranias, E.G., 2000. Phospholamban and cardiac contractile function. *Journal of Molecular and Cellular Cardiology*. **32**, 2131-2139.
- Burkeen, A.K., Maday, S.L., Rybicka, K.K., Sulcove, J.A., Ward, J., Huang, M.M., Barstead, R., Franzini-Armstrong, C., Allen, T.S., 2004. Disruption of *Caenorhabditis elegans* Muscle Structure and Function Caused by Mutation of Troponin I. *Biophysical Journal*. **86**, 991-1001.
- Campbell, K.B., Taheri, H., Kirkpatrick, R.D., Burton, T., Hunter, W.C., 1993. Similarities between dynamic elastance of left ventricular chamber and papillary muscle of rabbit heart. *AJP - Heart and Circulatory Physiology*. **264**, H1941.
- Chalovich, J.M., 2002. Regulation of striated muscle contraction: a discussion. *Journal of Muscle Research and Cell Motility*. **23**, 353-361.
- Chaponnier, C. & Gabbiani, G., 2004. Pathological situations characterized by altered actin isoform expression. *The Journal of Pathology*. **204**, 386-395.
- Charles M. Stevens, *et al*, 2017. Changes in the Dynamics of the Cardiac Troponin C Molecule Explain the Effects of Ca²⁺ Sensitizing Mutations.
- Chemla, D., Coirault, C., Hebert, J.L., Lecarpentier, Y., 2000. Mechanics of Relaxation of the Human Heart. *News in Physiological Sciences: An International Journal of Physiology Produced Jointly by the International Union of Physiological Sciences and the American Physiological Society*. **15**, 78-83.
- Cirino, A.L. & Ho, C., 1993. Hypertrophic Cardiomyopathy Overview. In Pagon, R. A., Adam, M. P., Ardinger, H. H., Wallace, S. E., Amemiya, A., Bean, L J H, Bird, T. D., Ledbetter, N., Mefford, H. C., Smith, R J H and Stephens, K., eds, *GeneReviews(R)*. Seattle (WA): University of Washington, Seattle. GeneReviews is a registered trademark of the University of Washington, Seattle. All rights reserved.
- Cordina, N.M., Liew, C.K., Gell, D.A., Fajer, P.G., Mackay, J.P., Brown, L.J., 2013. Effects of calcium binding and the hypertrophic cardiomyopathy A8V mutation on the dynamic

equilibrium between closed and open conformations of the regulatory N-domain of isolated cardiac troponin C. *Biochemistry*. **52**, 1950-1962.

Cordina, N.M., Liew, C.K., Gell, D.A., Fajer, P.G., Mackay, J.P., Brown, L.J., 2012. Interdomain orientation of cardiac troponin C characterized by paramagnetic relaxation enhancement NMR reveals a compact state. *Protein Science : A Publication of the Protein Society*. **21**, 1376-1387.

Corrie, J.E., Brandmeier, B.D., Ferguson, R.E., Trentham, D.R., Kendrick-Jones, J., Hopkins, S.C., van der Heide, U A, Goldman, Y.E., Sabido-David, C., Dale, R.E., Criddle, S., Irving, M., 1999. Dynamic measurement of myosin light-chain-domain tilt and twist in muscle contraction. *Nature*. **400**, 425-430.

Dewan, S., McCabe, K.J., Regnier, M., McCulloch, A.D., Lindert, S., 2016. Molecular Effects of cTnC DCM Mutations on Calcium Sensitivity and Myofilament Activation-An Integrated Multiscale Modeling Study. *The Journal of Physical Chemistry. B*. **120**, 8264.

Downloaded from <http://rspb.royalsocietypublishing.org/> on July, 1 8 and 2017, Downloaded from <http://rspb.royalsocietypublishing.org/> on July 18, 2017.

Du, C.K., Morimoto, S., Nishii, K., Minakami, R., Ohta, M., Tadano, N., Lu, Q.W., Wang, Y.Y., Zhan, D.Y., Mochizuki, M., Kita, S., Miwa, Y., Takahashi-Yanaga, F., Iwamoto, T., Ohtsuki, I., Sasaguri, T., 2007. Knock-in mouse model of dilated cardiomyopathy caused by troponin mutation. *Circulation Research*. **101**, 185-194.

Dweck, D., Reynaldo, D.P., Pinto, J.R., Potter, J.D., 2010. A dilated cardiomyopathy troponin C mutation lowers contractile force by reducing strong myosin-actin binding. *The Journal of Biological Chemistry*. **285**, 17371-17379.

E E Bittar & T Keh, 1980. An investigation of myoplasmic magnesium adenosine triphosphate in barnacle muscle fibres with the firefly method. *The Journal of Physiology*. **302**, 73-88.

Effect, R., Force-Interval Relations of Twitches and Cold Contractures in Rat Cardiac Trabeculae.

Eisner, D.A., Caldwell, J.L., Kistamas, K., Trafford, A.W., 2017. Calcium and Excitation-Contraction Coupling in the Heart. *Circulation Research*. **121**, 181-195.

El-Mezgueldi, M., 2014. Tropomyosin dynamics. *Journal of Muscle Research and Cell Motility*. **35**, 203-210.

Franz, W., Müller, O.J., Katus, H.A., 2001. Cardiomyopathies: from genetics to the prospect of treatment. *The Lancet*. **358**, 1627-1637.

Galkin, V., Orlova, A., Vos, M., Schröder, G., Egelman, E., 2015. Near-Atomic Resolution for One State of F-Actin. *Structure*. **23**, 173-182.

Geeves, M.A. & Lehrer, S.S., 1994. Dynamics of the muscle thin filament regulatory switch: the size of the cooperative unit. *Biophysical Journal*. **67**, 273-282.

Gomes, A.V., Venkatraman, G., Davis, J.P., Tikunova, S.B., Engel, P., Solaro, R.J., Potter, J.D., 2004. Cardiac troponin T isoforms affect the Ca (2+) sensitivity of force development in the presence of slow skeletal troponin I: insights into the role of troponin T isoforms in the fetal heart. *The Journal of Biological Chemistry*. **279**, 49579-49587.

- Gordon, A.M., Regnier, M., Homsher, E., 2001. Skeletal and cardiac muscle contractile activation: tropomyosin "rocks and rolls". *News in Physiological Sciences : An International Journal of Physiology Produced Jointly by the International Union of Physiological Sciences and the American Physiological Society*. **16**, 49-55.
- Guinto, P.J., Haim, T.E., Dowell-Martino, C.C., Sibinga, N., Tardiff, J.C., 2009. Temporal and mutation-specific alterations in Ca²⁺ homeostasis differentially determine the progression of cTnT-related cardiomyopathies in murine models. *American Journal of Physiology. Heart and Circulatory Physiology*. **297**, 614.
- Gregorio, C.C. & Antin, P.B., 2000. To the heart of myofibril assembly. *Trends in Cell Biology*. **10**, 355-362.
- Hamdani, N., Kooij, V., van Dijk, S., Merkus, D., Paulus, W.J., Remedios, C.D., Duncker, D.J., Stienen, G.J., van der Velden, J., 2008. Sarcomeric dysfunction in heart failure. *Cardiovascular Research*. **77**, 649-658.
- Harada, K. & Morimoto, S., 2004. Inherited cardiomyopathies as a troponin disease. *The Japanese Journal of Physiology*. **54**, 307-318.
- He, H., Javadpour, M.M., Latif, F., Tardiff, J.C., Ingwall, J.S., 2007. R-92L and R-92W Mutations in Cardiac Troponin T Lead to Distinct Energetic Phenotypes in Intact Mouse Hearts. *Biophysical Journal*. **93**, 1834-1844.
- Hershberger, R., Norton, N., Morales, A., Li, D., Siegfried, J., Gonzalez-Quintana, J., 2010. Coding Sequence Rare Variants Identified in MYBPC3, MYH6, TPM1, TNNC1, and TNNI3 From 312 Patients With Familial or Idiopathic Dilated Cardiomyopathy. *Circulation: Cardiovascular Genetics*. **3**, 155-161.
- Holmes, K.C., Popp, D., Gebhard, W., Kabsch, W., 1990. Atomic model of the actin filament. *Nature*. **347**, 44-49.
- Hwang, P.M., Cai, F., Pineda-Sanabria, S.E., Corson, D.C., Sykes, B.D., 2014. The cardiac-specific N-terminal region of troponin I positions the regulatory domain of troponin C. *Proceedings of the National Academy of Sciences of the United States of America*. **111**, 14412-14417.
- Iorga, B., Blaudeck, N., Solzin, J., Neulen, A., Stehle, I., Lopez Davila, A.J., Pfitzer, G., Stehle, R., 2008. Lys184 deletion in troponin I impairs relaxation kinetics and induces hypercontractility in murine cardiac myofibrils. *Cardiovascular Research*. **77**, 676-686.
- Ivan, R., *et al*, Three-Dimensional Structure of Myosin Subfragment- 1: A Molecular Motor.
- Janssen, P.M., Stull, L.B., Marban, E., 2002. Myofilament properties comprise the rate-limiting step for cardiac relaxation at body temperature in the rat. *American Journal of Physiology. Heart and Circulatory Physiology*. **282**, 499.
- Jerry H. Brown, Zhaocai Zhou, Ludmilla Reshetnikova, Howard Robinson, Rama D. Yammani, Larry S. Tobacman, Carolyn Cohen, 2005. Structure of the Mid-Region of Tropomyosin: Bending and Binding Sites for Actin. *Proceedings of the National Academy of Sciences of the United States of America*. **102**, 18878-18883.

- Jin, J.-. & Chong, S.M., 2010. Localization of the two tropomyosin-binding sites of troponin T. *Archives of Biochemistry and Biophysics*. **500**, 144-150.
- Jose R. Pinto, Tiago Veltri, Maicon Landim-Vieira, Michelle S. Parvatiyar, David Gonzalez-Martinez, Karissa M. Dieseldorff Jones, Clara A. Michell, David Dweck, Andrew P. Landstrom, P. Bryant Chase, 2017. Hypertrophic Cardiomyopathy Cardiac Troponin C Mutations Differentially Affect Slow Skeletal and Cardiac Muscle Regulation. *Frontiers in Physiology*. **8**,
- Kabsch, W., Mannherz, H.G., Suck, D., Pai, E.F., Holmes, K.C., 1990. Atomic structure of the actin:DNase I complex. *Nature*. **347**, 37-44.
- Kalyva, A., Parthenakis, F.I., Marketou, M.E., Kontaraki, J.E., Vardas, P.E., 2014. Biochemical characterisation of Troponin C mutations causing hypertrophic and dilated cardiomyopathies. *Journal of Muscle Research and Cell Motility*. **35**, 161-178.
- Kamisago, M., Sharma, S.D., DePalma, S.R., Solomon, S., Sharma, P., McDonough, B., Smoot, L., Mullen, M.P., Woolf, P.K., Wigle, E.D., Seidman, J.G., Seidman, C.E., 2000. Mutations in sarcomere protein genes as a cause of dilated cardiomyopathy. *The New England Journal of Medicine*. **343**, 1688-1696.
- Kampourakis, T., Sun, Y.B., Irving, M., 2016. Myosin light chain phosphorylation enhances contraction of heart muscle via structural changes in both thick and thin filaments. *Proceedings of the National Academy of Sciences of the United States of America*. **113**, 3039.
- Kobayashi, T., Jin, L., de Tombe, P.P., 2008. Cardiac thin filament regulation. *Pflugers Archiv : European Journal of Physiology*. **457**, 37-46.
- Kirk, J.A., MacGowan, G.A., Evans, C., Smith, S.H., Warren, C.M., Mamidi, R., Chandra, M., Stewart, A.F., Solaro, R.J., Shroff, S.G., 2009. Left ventricular and myocardial function in mice expressing constitutively pseudophosphorylated cardiac troponin I. *Circulation Research*. **105**, 1232-1239.
- Kruger, M., Zittrich, S., Redwood, C., Blaudeck, N., James, J., Robbins, J., Pfitzer, G., Stehle, R., 2005. Effects of the mutation R145G in human cardiac troponin I on the kinetics of the contraction-relaxation cycle in isolated cardiac myofibrils. *The Journal of Physiology*. **564**, 347-357.
- Krüger, M., Pfitzer, G., Stehle, R., 2003. Expression and purification of human cardiac troponin subunits and their functional incorporation into isolated cardiac mouse myofibrils. *Journal of Chromatography B*. **786**, 287-296.
- L. M. Delbridge, J. W. Bassani, D. M. Bers, 1996. Steady-state twitch Ca²⁺ fluxes and cytosolic Ca²⁺ buffering in rabbit ventricular myocytes. *American Journal of Physiology - Cell Physiology*. **270**, 192-199.
- Landstrom, A.P., Parvatiyar, M.S., Pinto, J.R., Marquardt, M.L., Bos, J.M., Tester, D.J., Ommen, S.R., Potter, J.D., Ackerman, M.J., 2008. Molecular and functional characterization of novel hypertrophic cardiomyopathy susceptibility mutations in TNNC1-encoded troponin C. *Journal of Molecular and Cellular Cardiology*. **45**, 281-288.

- Lankford, E.B., Epstein, N.D., Fananapazir, L., Sweeney, H.L., 1995. Abnormal contractile properties of muscle fibers expressing beta-myosin heavy chain gene mutations in patients with hypertrophic cardiomyopathy. *The Journal of Clinical Investigation*. **95**, 1409-1414.
- Leblanc, L., Bennet, A., Borgford, T., 2000. Calcium Affinity of Regulatory Sites in Skeletal Troponin-C Is Attenuated by N-Cap Mutations of Helix C. *Archives of Biochemistry and Biophysics*. **384**, 296-304.
- Leblanc, L., Bennet, A., Borgford, T., 2000. Calcium Affinity of Regulatory Sites in Skeletal Troponin-C Is Attenuated by N-Cap Mutations of Helix C. *Archives of Biochemistry and Biophysics*. **384**, 296-304.
- Lehman, W., Hatch, V., Korman, V., Rosol, M., Thomas, L., Maytum, R., Geeves, M.A., Van Eyk, J.E., Tobacman, L.S., Craig, R., 2000. Tropomyosin and actin isoforms modulate the localization of tropomyosin strands on actin filaments. *Journal of Molecular Biology*. **302**, 593-606.
- Li, M.X. & Hwang, P.M., 2015. Structure and function of cardiac troponin C (TNNC1): Implications for heart failure, cardiomyopathies, and troponin modulating drugs. *Gene*. **571**, 153-166.
- Li, M.X., Spyropoulos, L., Sykes, B.D., 1999. Binding of cardiac troponin-I147-163 induces a structural opening in human cardiac troponin-C. *Biochemistry*. **38**, 8289-8298.
- Lim, C.C., Yang, M., Yang, H., Wang, C., Shi, J., Berg, E.A., Pimentel, D.R., Gwathmey, J.K., Hajjar, R.J., Helmes, M., Costello, C.E., Huo, S., Liao, R., 2008. A Novel Mutant Cardiac Troponin C Disrupts Molecular Motions Critical for Calcium Binding Affinity and Cardiomyocyte Contractility. *Biophysical Journal*. **94**, 3577-3589.
- Liu, B., Lee, R.S., Biesiadecki, B.J., Tikunova, S.B., Davis, J.P., 2012. Engineered troponin C constructs correct disease-related cardiac myofilament calcium sensitivity. *The Journal of Biological Chemistry*. **287**, 20027-20036.
- Lyon, R.C., Lange, S., Sheikh, F., 2013. Breaking down protein degradation mechanisms in cardiac muscle. *Trends in Molecular Medicine*. **19**, 239.
- Machackova, J., Barta, J., Dhalla, N.S., 2006a. Myofibrillar remodelling in cardiac hypertrophy, heart failure and cardiomyopathies. *Canadian Journal of Cardiology*. **22**, 953-968.
- Machackova, J., Barta, J., Dhalla, N.S., 2006b. Myofibrillar remodelling in cardiac hypertrophy, heart failure and cardiomyopathies. *Canadian Journal of Cardiology*. **22**, 953-968.
- Manning, E.P., Tardiff, J.C., Schwartz, S.D., 2011. A model of calcium activation of the cardiac thin filament. *Biochemistry*. **50**, 7405.
- Månsson, A., 2014. Hypothesis and theory: mechanical instabilities and non-uniformities in hereditary sarcomere myopathies. *Frontiers in Physiology*. **5**, 350.

- Marian, A., 2008. Utilities and limitations of genetic testing for hypertrophic cardiomyopathy. *Expert Opinion on Medical Diagnostics*. **2**, 539-546.
- Maron, B.J., Gross, B.W., Stark, S.I., 1995. Images in cardiovascular medicine. Extreme left ventricular hypertrophy. *Circulation*. **92**, 2748.
- MB Cannell, H Cheng, WJ Lederer, 1995. The control of calcium release in heart muscle. *Science*. **268**, 1045-1049.
- McFarlane-Parrott, S., 2013. *Muscle Contraction*. [e-book].
- Metzger, J.M. & Westfall, M.V., 2004. Covalent and noncovalent modification of thin filament action: the essential role of troponin in cardiac muscle regulation. *Circulation Research*. **94**, 146-158.
- Mestroni, L., Rocco, C., Gregori, D., Sinagra, G., Di Lenarda, A., Miodini, S., Vatta, M., Pinamonti, B., Muntoni, F., Caforio, A.L., McKenna, W.J., Falaschi, A., Giacca, M., Camerini, 1999. Familial dilated cardiomyopathy: evidence for genetic and phenotypic heterogeneity. Heart Muscle Disease Study Group. *Journal of the American College of Cardiology*. **34**, 181-190.
- Moretti, A., Caron, L., Nakano, A., Lam, J.T., Bernshausen, A., Chen, Y., Qyang, Y., Bu, L., Sasaki, M., Martin-Puig, S., Sun, Y., Evans, S.M., Laugwitz, K.L., Chien, K.R., 2006. Multipotent embryonic isl1+ progenitor cells lead to cardiac, smooth muscle, and endothelial cell diversification. *Cell*. **127**, 1151-1165.
- Mun, J.Y., Kensler, R.W., Harris, S.P., Craig, R., 2016. The cMyBP-C HCM variant L348P enhances thin filament activation through an increased shift in tropomyosin position. *Journal of Molecular and Cellular Cardiology*. **91**, 141-147.
- Mustapha Alahyan, Martin R. Webb, Steven B. Marston, Mohammed EL-Mezgueldi, 2006. The Mechanism of Smooth Muscle Caldesmon-Tropomyosin Inhibition of the Elementary Steps of the Actomyosin ATPase. *Journal of Biological Chemistry*. **281**, 19433-19448.
- Nandi, S.S. & Mishra, P.K., 2015. Harnessing fetal and adult genetic reprogramming for therapy of heart disease. *Journal of Nature and Science*. **1**, e71.
- Nyitrai, M. & Geeves, M.A., 2004. Adenosine diphosphate and strain sensitivity in myosin motors. *Philosophical Transactions of the Royal Society of London. Series B, Biological Sciences*. **359**, 1867-1877.
- Ohtsuki, I., 1979. Molecular arrangement of troponin-T in the thin filament. *Journal of Biochemistry*. **86**, 491-497.
- Oleszczuk, M., Robertson, I.M., Li, M.X., Sykes, B.D., 2010a. Solution structure of the regulatory domain of human cardiac troponin C in complex with the switch region of cardiac troponin I and W7: the basis of W7 as an inhibitor of cardiac muscle contraction. *Journal of Molecular and Cellular Cardiology*. **48**, 925-933.
- Oleszczuk, M., Robertson, I.M., Li, M.X., Sykes, B.D., 2010b. Solution structure of the regulatory domain of human cardiac troponin C in complex with the switch region of cardiac troponin I and W7: The basis of W7 as an inhibitor of cardiac muscle contraction. *Journal of Molecular and Cellular Cardiology*. **48**, 925-933.

- Opie, L.H., Commerford, P.J., Gersh, B.J., Pfeffer, M.A., 2006. Controversies in ventricular remodelling. *Lancet (London, England)*. **367**, 356-367.
- Otterbein, L.R., Graceffa, P., Dominguez, R., 2001. The crystal structure of uncomplexed actin in the ADP state. *Science (New York, N.Y.)*. **293**, 708-711.
- Parvatiyar, M.S., Landstrom, A.P., Figueiredo-Freitas, C., Potter, J.D., Ackerman, M.J., Pinto, J.R., 2012. A mutation in TNNC1-encoded cardiac troponin C, TNNC1-A31S, predisposes to hypertrophic cardiomyopathy and ventricular fibrillation. *The Journal of Biological Chemistry*. **287**, 31845.
- Perrin, B.J. & Ervasti, J.M., 2010. The actin gene family: function follows isoform. *Cytoskeleton (Hoboken, N.J.)*. **67**, 630-634.
- Perry, S.V., 2001. Vertebrate tropomyosin: distribution, properties and function. *Journal of Muscle Research and Cell Motility*. **22**, 5-49.
- Pinali, C., Bennett, H., Davenport, J.B., Trafford, A.W., Kitmitto, A., 2013. Three-dimensional reconstruction of cardiac sarcoplasmic reticulum reveals a continuous network linking transverse-tubules: this organization is perturbed in heart failure. *Circulation Research*. **113**, 1219-1230.
- Pinto, J.R., Parvatiyar, M.S., Jones, M.A., Liang, J., Ackerman, M.J., Potter, J.D., 2009. A functional and structural study of troponin C mutations related to hypertrophic cardiomyopathy. *The Journal of Biological Chemistry*. **284**, 19090-19100.
- Pinto, J.R., Siegfried, J.D., Parvatiyar, M.S., Li, D., Norton, N., Jones, M.A., Liang, J., Potter, J.D., Hershberger, R.E., 2011a. Functional characterization of TNNC1 rare variants identified in dilated cardiomyopathy. *The Journal of Biological Chemistry*. **286**, 34404-34412.
- Pinto, J.R., Reynaldo, D.P., Parvatiyar, M.S., Dweck, D., Liang, J., Jones, M.A., Sorenson, M.M., Potter, J.D., 2011b. Strong Cross-bridges Potentiate the Ca²⁺ Affinity Changes Produced by Hypertrophic Cardiomyopathy Cardiac Troponin C Mutants in Myofilaments: A FAST KINETIC APPROACH. *Journal of Biological Chemistry*. **286**, 1005-1013.
- Poggesi, C., Tesi, C., Stehle, R., 2005. Sarcomeric determinants of striated muscle relaxation kinetics. *Pflugers Archiv : European Journal of Physiology*. **449**, 505-517.
- Richard, P., Charron, P., Carrier, L., Ledeuil, C., Cheav, T., Pichereau, C., Benaiche, A., Isnard, R., Dubourg, O., Burban, M., Gueffet, J.P., Millaire, A., Desnos, M., Schwartz, K., Hainque, B., Komajda, M., EUROGENE Heart Failure Project, 2003. Hypertrophic cardiomyopathy: distribution of disease genes, spectrum of mutations, and implications for a molecular diagnosis strategy. *Circulation*. **107**, 2227-2232.
- Robertson, S.P., Johnson, J.D., Holroyde, M.J., Kranias, E.G., Potter, J.D., Solaro, R.J., 1982. The effect of troponin I phosphorylation on the Ca²⁺-binding properties of the Ca²⁺-regulatory site of bovine cardiac troponin. *The Journal of Biological Chemistry*. **257**, 260-263.
- Robinson, P., Mirza, M., Knott, A., Abdulrazzak, H., Willott, R., Marston, S., Watkins, H., Redwood, C., 2002. Alterations in thin filament regulation induced by a human cardiac troponin T mutant that causes dilated cardiomyopathy are distinct from those induced by

- troponin T mutants that cause hypertrophic cardiomyopathy. *The Journal of Biological Chemistry*. **277**, 40710-40716.
- Robinson, J., Dong, W., Xing, J., Cheung, H., 2004. Switching of troponin I: Ca²⁺ and Myosin-induced Activation of Heart Muscle. *Journal of Molecular Biology*. **340**, 295-305.
- Robinson, P., Griffiths, P., Watkins, H., Redwood, C., 2007. Dilated and Hypertrophic Cardiomyopathy Mutations in Troponin and α -Tropomyosin Have Opposing Effects on the Calcium Affinity of Cardiac Thin Filaments. *Circulation Research*. **101**, 1266-1273.
- Ruegg, C., Veigel, C., Molloy, J.E., Schmitz, S., Sparrow, J.C., Fink, R.H.A., 2002. Molecular Motors: Force and Movement Generated by Single Myosin II Molecules. *Physiology*. **17**, 213-218.
- Sadayappan, S., Finley, N., Howarth, J.W., Osinska, H., Klevitsky, R., Lorenz, J.N., Rosevear, P.R., Robbins, J., 2008. Role of the acidic N' region of cardiac troponin I in regulating myocardial function. *The FASEB Journal*. **22**, 1246-1257.
- Sevrieva, I., Knowles, A.C., Kampourakis, T., Sun, Y.B., 2014. Regulatory domain of troponin moves dynamically during activation of cardiac muscle. *Journal of Molecular and Cellular Cardiology*. **75**, 181-187.
- Sheldahl, C., Xing, J., Dong, W.J., Harvey, S.C., Cheung, H.C., 2003. The calcium-saturated cTnI/cTnC complex: structure of the inhibitory region of cTnI. *Biophysical Journal*. **84**, 1057-1064.
- Sheng, J.J. & Jin, J.P., 2016. TNNI1, TNNI2 and TNNI3: Evolution, regulation, and protein structure-function relationships. *Gene*. **576**, 385-394.
- Slupsky, C.M. & Sykes, B.D., 1995. NMR solution structure of calcium-saturated skeletal muscle troponin C. *Biochemistry*. **34**, 15953-15964.
- Solaro, R.J., Rosevear, P., Kobayashi, T., 2008. The unique functions of cardiac troponin I in the control of cardiac muscle contraction and relaxation. *Biochemical and Biophysical Research Communications*. **369**, 82-87.
- Solaro, R.J., 2010. Sarcomere control mechanisms and the dynamics of the cardiac cycle. *Journal of Biomedicine & Biotechnology*. **2010**, 105648.
- Spudich, J.A., 2014. Hypertrophic and dilated cardiomyopathy: four decades of basic research on muscle lead to potential therapeutic approaches to these devastating genetic diseases. *Biophysical Journal*. **106**, 1236-1249.
- Spyracopoulos, L., Li, M.X., Sia, S.K., Gagne, S.M., Chandra, M., Solaro, R.J., Sykes, B.D., 1997. Calcium-induced structural transition in the regulatory domain of human cardiac troponin C. *Biochemistry*. **36**, 12138-12146.
- Suematsu, N., Satoh, S., Kinugawa, S., Tsutsui, H., Hayashidani, S., Nakamura, R., Egashira, K., Makino, N., Takeshita, A., 2001. Alpha1-adrenoceptor-Gq-RhoA signaling is upregulated to increase myofibrillar Ca²⁺ sensitivity in failing hearts. *American Journal of Physiology. Heart and Circulatory Physiology*. **281**, 637.

- Stehle, R. & Iorga, B., 2010. Kinetics of cardiac sarcomeric processes and rate-limiting steps in contraction and relaxation. *Journal of Molecular and Cellular Cardiology*. **48**, 843-850.
- Stehle, R., Iorga, B., Pfitzer, G., 2007. Calcium regulation of troponin and its role in the dynamics of contraction and relaxation. *American Journal of Physiology. Regulatory, Integrative and Comparative Physiology*. **292**, 1125.
- Stone, D.B., Timmins, P.A., Schneider, D.K., Krylova, I., Ramos, C.H., Reinach, F.C., Mendelson, R.A., 1998. The effect of regulatory Ca²⁺ on the in situ structures of troponin C and troponin I: a neutron scattering study. *Journal of Molecular Biology*. **281**, 689-704.
- 'Susan, J.S. and P J E, The effects of reported Ca²⁺ + sensitisers on the rates of Ca²⁺ + release from cardiac troponin C and the troponin-tropomyosin complex.
- Swindle, N. & Tikunova, S.B., 2010a. Hypertrophic cardiomyopathy-linked mutation D145E drastically alters calcium binding by the C-domain of cardiac troponin C. *Biochemistry*. **49**, 4813.
- Swindle, N. & Tikunova, S.B., 2010b. Hypertrophic cardiomyopathy-linked mutation D145E drastically alters calcium binding by the C-domain of cardiac troponin C. *Biochemistry*. **49**, 4813.
- Szent-Györgyi, A.G., 2004. The early history of the biochemistry of muscle contraction. *The Journal of General Physiology*. **123**, 631-641.
- Takeda, S., Kobayashi, T., Taniguchi, H., Hayashi, H., Maeda, Y., 1997. Structural and functional domains of the troponin complex revealed by limited digestion. *European Journal of Biochemistry*. **246**, 611-617.
- Takeda, S., Yamashita, A., Maeda, K., Maeda, Y., 2003. Structure of the core domain of human cardiac troponin in the Ca(2+)-saturated form. *Nature*. **424**, 35-41.
- Tardiff, J.C., 2005. Sarcomeric proteins and familial hypertrophic cardiomyopathy: linking mutations in structural proteins to complex cardiovascular phenotypes. *Heart Failure Reviews*. **10**, 237-248.
- Tomoyoshi Kobayashi and R. John Solaro, 2006. Increased Ca²⁺ Affinity of Cardiac Thin Filaments Reconstituted with Cardiomyopathy-related Mutant Cardiac Troponin I*.
- Troponin I an, *et al*, The Relationship between Biological Activity and Primary Structure of Troponin I from White Skeletal Muscle of the Rabbit.
- Tsien, R.Y., 1983. Intracellular measurements of ion activities. *Annual Review of Biophysics and Bioengineering*. **12**, 91-116.
- Van Dijk, S.J., Dooijes, D., dos Remedios, C., Michels, M., Lamers, J.M., Winegrad, S., Schlossarek, S., Carrier, L., ten Cate, F.J., Stienen, G.J., van der Velden, J., 2009. Cardiac myosin-binding protein C mutations and hypertrophic cardiomyopathy: haploinsufficiency, deranged phosphorylation, and cardiomyocyte dysfunction. *Circulation*. **119**, 1473-1483.

Vassilyev, D.G., Takeda, S., Wakatsuki, S., Maeda, K., Maeda, Y., 1998. Crystal structure of troponin C in complex with troponin I fragment at 2.3-Å resolution. *Proceedings of the National Academy of Sciences of the United States of America*. **95**, 4847-4852.

Velden, J., Papp, Z., Boontje, N.M., Zaremba, R., de Jong, J.W., Janssen, P.M., Hasenfuss, G., Stienen, G.J., 2003a. The effect of myosin light chain 2 dephosphorylation on Ca²⁺ sensitivity of force is enhanced in failing human hearts. *Cardiovascular Research*. **57**, 505-514.

Velden, J., Papp, Z., Zaremba, R., Boontje, N.M., de Jong, J.W., Owen, V.J., Burton, P.B., Goldmann, P., Jaquet, K., Stienen, G.J., 2003b. Increased Ca²⁺ sensitivity of the contractile apparatus in end-stage human heart failure results from altered phosphorylation of contractile proteins. *Cardiovascular Research*. **57**, 37-47.

Velden, J., Papp, Z., Zaremba, R., Boontje, N.M., de Jong, J.W., Owen, V.J., Burton, P.B., Goldmann, P., Jaquet, K., Stienen, G.J., 2003c. Increased Ca²⁺ sensitivity of the contractile apparatus in end-stage human heart failure results from altered phosphorylation of contractile proteins. *Cardiovascular Research*. **57**, 37-47.

Velden, J., Narolska, N.A., Lamberts, R.R., Boontje, N.M., Borbely, A., Zaremba, R., Bronzwaer, J.G., Papp, Z., Jaquet, K., Paulus, W.J., Stienen, G.J., 2006. Functional effects of protein kinase C-mediated myofilament phosphorylation in human myocardium. *Cardiovascular Research*. **69**, 876-887.

Walker, L.A., Fullerton, D.A., Buttrick, P.M., 2013. Contractile protein phosphorylation predicts human heart disease phenotypes. *American Journal of Physiology. Heart and Circulatory Physiology*. **304**, 1644.

Watkins, H., Seidman, C.E., Seidman, J.G., Feng, H.S., Sweeney, H.L., 1996. Expression and functional assessment of a truncated cardiac troponin T that causes hypertrophic cardiomyopathy. Evidence for a dominant negative action. *The Journal of Clinical Investigation*. **98**, 2456-2461

Mutagenesis, Structure-Function. 2009. [e-book].

DeLano, W. L. The PyMOL Molecular Graphics System, Version 1.8. Schrödinger LLC <http://www.pymol.org> (2014). doi:10.1038/hr.2014.17